Presentation of Specification to TSG RAN

Presentation to:	**TSG RAN Meeting #25**
Document for presentation:	**TR25.895, Version 2.0.0**
Presented for:	**Approval**

Abstract of document:

This document is a technical report titled “Analysis of higher chip rates for UTRA TDD evolution” for the Release 6 study item “Feasibility Study for the analysis of higher chip rates for UTRA TDD evolution”.

Changes since last presentation to TSG RAN:

TR25.895 version 1.0.0 was presented for information to TSG RAN meeting #19. Since that version, the analysis and feasibility sections have been expanded to include link and system level results for HSDPA and voice type bearers and feasibility analyses relating to various topics such as mobility, coexistence with existing releases, impact on specifications and working groups etc. A conclusion section to the TR has also been written.

Outstanding Issues:

No outstanding issues

Contentious Issues:

No contentious issues

3GPP TR 25.895 V2.0.0 (2004-09)

Technical Report

3rd Generation Partnership Project;
Technical Specification Group Radio Access Network;
Analysis of higher chip rates for UTRA TDD evolution;
(Release 6)

Keywords
<keyword[, keyword]>

3GPP

Postal address

3GPP support office address
650 Route des Lucioles - Sophia Antipolis
Valbonne - FRANCE
Tel.: +33 4 92 94 42 00 Fax: +33 4 93 65 47 16

Internet
http://www.3gpp.org

Contents

Foreword

This Technical Report has been produced by the 3rd Generation Partnership Project (3GPP).

The contents of the present document are subject to continuing work within the TSG and may change following formal TSG approval. Should the TSG modify the contents of the present document, it will be re-released by the TSG with an identifying change of release date and an increase in version number as follows:

Version x.y.z

where:

- x the first digit:
  - 1 presented to TSG for information;
  - 2 presented to TSG for approval;
  - 3 or greater indicates TSG approved document under change control.
- y the second digit is incremented for all changes of substance, i.e. technical enhancements, corrections, updates, etc.
- z the third digit is incremented when editorial only changes have been incorporated in the document.

Introduction

This technical report presents the results of the 3GPP system Study Item to analyse the use of higher chip rates for UTRA TDD evolution. This study includes an analysis of the feasibility and potential benefits of higher chip rates for UTRA TDD. This study includes a recommendation to RAN Plenary on a potential standardisation work plan and time frame.

Higher chip rate UTRA TDD is studied in the light of the imminent allocation of considerably more spectrum for 3G in bands other than the IMT-2000 band in which systems are currently being deployed, and the demand for higher burst rates and sector throughputs for data traffic in the wide area. Higher chip rate UTRA TDD may be used to support (for instance) personal, multimedia and broadcast services.

Potential benefits of higher chip rate UTRA TDD include system gains from trunking efficiency, link level gains from an ability to better resolve channel paths, the ability to support more accurate location services, higher possible peak bit rates and cell throughputs and an improved ability to reject narrowband interferers.

1 Scope

The present document contains results of an analysis of the feasibility and potential benefits of higher chip rate UTRA TDD.

The analysis in this document is based on a reference configuration at the reference chip rate of 7.68Mcps. The comparison of this reference system with current UTRA TDD releases allows conclusions to be drawn as to the potential benefits and feasibility of even higher chip rates for UTRA TDD.

The document presents results of an analysis of the reference configuration using channel models appropriate to a higher chip rate system. Link level and system level results are presented. A link budget shows the coverage that can be expected at a higher chip rate. Aspects of UE and UTRAN complexity are considered.

The feasibility of higher chip rate UTRA TDD systems is considered. This document covers aspects such as coexistence, backward compatibility, use in diverse spectrum arrangements and allocations, mobility, application to 3GPP system and services, antenna systems and impacts on signalling, specifications and RAN working groups.

The study of higher chip rate UTRA TDD is based on the assumption that the higher layer protocol architecture for higher chip rate UTRA TDD is unchanged from 3GPP Release 5. It is assumed that higher chip rate UTRA TDD shall be evolved from 3.84Mcps TDD and that the higher chip rate UTRA TDD carrier may exist without the need for a supporting 3.84Mcps TDD carrier.

2 References

The following documents contain provisions which, through reference in this text, constitute provisions of the present document.

- References are either specific (identified by date of publication, edition number, version number, etc.) or non-specific.
- For a specific reference, subsequent revisions do not apply.
- For a non-specific reference, the latest version applies. In the case of a reference to a 3GPP document (including a GSM document), a non-specific reference implicitly refers to the latest version of that document *in the same Release as the present document*.

[1] 3GPP TS 25.301 : “Radio Interface Protocol Architecture (Release 5)”

[2] 3GPP TS 25.401 : “UTRAN Overall Description (Release 5)”

[3] 3GPP TS 25.222 : “Multiplexing and channel coding (Release 5)”

[4] 3GPP TS 25.223 : “Spreading and modulation (Release 5)”

[5] 3GPP TS 25.221 : “Physical channels and mapping of transport channels onto physical channels (TDD) (Release 5)”

[6] 3GPP TS 25.224 : “Physical Layer Procedures (TDD) (Release 5)”

[7] 3GPP TS 25.225 : “Physical layer – Measurements (TDD) (Release 5)”

[8] 3GPP TS 25.102 : “UTRA (UE) TDD; Radio transmission and reception (Release 5)”

[9] 3GPP TS 25.105 : “UTRA (BS) TDD; Radio transmission and reception (Release 5)”

[10] 3GPP TS 25.331 : “Radio resource control (RRC) protocol specification (Release 5)”

[11] Vollmer *et al*, ”Joint-Detection using the Fast Fourier Transforms in TD-CDMA based Mobile Radio Systems”, ICT, Korea, 1999.

[12] S. L. Loyka,”On the Use of Cann’s Model for Nonlinear Behavioral-Level Simulation,” IEE Trans. Vehicular. Technology, vol 49, pp1982-1985, Sept 2000

[13] 3GPP TR25.942 “RF System Scenarios Release 5”

[14] 3GPP TR34.490 “Common Test Environments for UE Conformance Testing”

[15] 3GPP TR25.945 “RF requirements for 1.28 Mcps UTRA TDD option”

3 Definitions, symbols and abbreviations

3.1 Definitions

3.2 Symbols

3.3 Abbreviations

4 Reference Higher Chip Rate Configuration

4.1 High Level Architecture

The high level protocol architecture (MAC, RLC, RRC and other protocol elements higher than the MAC layer) for the higher chip rate UTRA TDD reference configuration is unchanged from 3GPP Release 5 as described in 25.301 [1].

UTRAN architecture for the higher chip rate reference configuration is unchanged from 3GPP Release 5 as described in 25.401 [2]. The system elements that are considered in the reference configuration are the RNC, Node B and UE.

The layer 1 architecture for the higher chip rate reference configuration is based on an evolution of the 3.84Mcps TDD architecture. The frame structure, power control procedures, HSDPA aspects etc. are based on those of 3.84Mcps TDD.

The higher chip rate UTRA TDD system does not require the support of a 3.84Mcps TDD carrier (a cell may support only the higher chip rate).

The higher chip rate reference configuration uses a chip rate of 7.68Mcps.

4.2 Radio Aspects

Radio aspects of the higher chip rate reference configuration are based on those for 3.84Mcps TDD as defined in [8] and [9]. Significant departures from [8] and [9] required in order to support a higher chip rate are discussed in this subsection.

4.2.1 Transmitter Issues

UE Spectral Mask

The spectrum emission mask of the UE applies to frequencies, which are between 5 MHz and 25MHz from the UE centre carrier frequency. The out of channel emission is specified relative to the RRC filtered mean power of the UE carrier. The power of any UE emission shall not exceed the levels specified in table 1.

Table 1: Spectrum Emission Mask of higher chip rate reference configuration

Δf* in MHz	Minimum requirement	Measurement bandwidth
5.0 – 7.0	$\left\{-38-7.5\cdot\left(\frac{\Delta f}{MHz}-5.0\right)\right\}dBc$	30 kHz **
7.0 - 15	$\left\{-38-0.5\cdot\left(\frac{\Delta f}{MHz}-7.0\right)\right\}dBc$	1 MHz ***
15.0 – 17.0	$\left\{-42-5.0\cdot\left(\frac{\Delta f}{MHz}-15.0\right)\right\}dBc$	1 MHz ***
17.0 – 25.0	-53 dBc	1 MHz ***
*	Δf is the separation between the carrier frequency and the centre of the measuring filter.	
**	The first and last measurement position with a 30 kHz filter is at Δf equals to 5.015 MHz and 6.985 MHz	
***	The first and last measurement position with a 1 MHz filter is at Δf equals to 7.5 MHz and 24.5 MHz. As a general rule, the resolution bandwidth of the measuring equipment should be equal to the measurement bandwidth. To improve measurement accuracy, sensitivity and efficiency, the resolution bandwidth can be different from the measurement bandwidth. When the resolution bandwidth is smaller than the measurement bandwidth, the result should be integrated over the measurement bandwidth in order to obtain the equivalent noise bandwidth of the measurement bandwidth.	
The lower limit shall be –47dBm/7.68 MHz or the minimum requirement presented in this table which ever is the higher.		

Node B Spectral Mask

The Node B spectral mask is derived from the spectral mask in TS25.105 [9] for the 3.84Mcps option by doubling the frequency offset parameters and correcting for the change in power spectral density due to the increased modulation bandwidth. As an example, the Node B spectral mask for the power range ($31 \le P < 39$ dBm) is detailed below.

Emissions shall not exceed the maximum level specified in table 2 for the appropriate BS maximum output power, in the frequency range from $\Delta f = 5.0$ MHz to Δf_{max} from the carrier frequency, where:

- Δf is the separation between the carrier frequency and the nominal -3dB point of the measuring filter closest to the carrier frequency.
- f_offset is the separation between the carrier frequency and the center frequency of the measuring filter.- f_offset_{max} is either 25 MHz or the offset to the UMTS Tx band edge, whichever is the greater.
- Δf_{max} is equal to f_offset_{max} minus half of the bandwidth of the mesurement filter.

Table 2: Node B spectrum emission mask values for the higher chip rate reference configuration, BS maximum output power 31 ≤ P < 39 dBm

Frequency offset of measurement filter –3dB point,Δf	Frequency offset of measurement filter centre frequency, f_offset	Maximum level	Measurement bandwidth
5.0 MHz ≤ Δf < 5.4 MHz	5.015MHz ≤ f_offset < 5.415MHz	P – 56 dB	30 kHz
5.4 MHz ≤ Δf < 7.0 MHz	5.415MHz ≤ f_offset < 7.015MHz	$P-56dB-7.5\cdot\left(\frac{f\_offset}{MHz}-5.415\right)dB$	30 kHz
(see note)	7.015MHz ≤ f_offset < 8.0MHz	P – 68 dB	30 kHz
7.0 MHz ≤ Δf < 15.0 MHz	7.5MHz ≤ f_offset < 15.5MHz	P – 55 dB	1 MHz
15.0 MHz ≤ Δf ≤ Δf_{max}	15.5MHz ≤ f_offset < f_offset_{max}	P - 59 dB	1 MHz

UE ACLR

If the adjacent channel RRC filtered mean power is greater than –50dBm measured with a 3.84Mcps RRC filter then the ACLR shall be higher than the value specified in Table 3.

Table 3: UE ACLR of higher chip rate reference configuration

Power Class	adjacent channel	Chip Rate for RRC Measurement Filter	ACLR limit
2, 3	UE channel ± 7.5 MHz	3.84 MHz	33 dB
2, 3	UE channel ± 12.5 MHz	3.84 MHz	43 dB
2 ,3	UE channel ± 20.0 MHz	7.68 MHz	43 dB

NOTE:

1) The requirement shall still be met in the presence of switching transients.

2) The ACLR requirements reflect what can be achieved with present state of the art technology.

BS ACLR

The ACLR of a single carrier BS or a multi-carrier BS with contiguous carrier frequencies shall be higher than the value specified in Table 4.

Table 4: BS ACLR of higher chip rate reference configuration

BS adjacent channel offset below the first or above the last carrier frequency used	Chip Rate for RRC Measurement Filter	ACLR limit
7.5 MHz	3.84 Mcps	45 dB
12.5 MHz	3.84 Mcps	55 dB
20.0 MHz	7.68 Mcps	55 dB

If a BS provides multiple non-contiguous single carriers or multiple non-contiguous groups of contiguous single carriers, the above requirements shall be applied individually to the single carriers or group of single carriers.

In case the equipment is co-sited to a FDD BS operating on an adjacent channel, the adjacent channel leakage power shall not exceed the limits specified in Table 5.

Table 5: Adjacent channel leakage power of higher chip rate reference configuration in case of co-siting with UTRA FDD on an adjacent channel

BS Class	Offset Frequency for Measurement	Maximum Level	Measurement Bandwidth
Wide Area BS	+/-7.5 MHz	-80 dBm	3,84 MHz
Wide Area BS	+/-12.5 MHz	-80 dBm	3,84 MHz
Wide Area BS	+/-17.5 MHz	-80 dBm	3,84 MHz
Wide Area BS	+/-22.5 MHz	-80 dBm	3,84 MHz

Spurious Emissions

Spurious emissions limits specified in [8] and [9] shall apply at offsets greater than 25MHz from the centre frequency.

4.2.2 Receiver Issues

Adjacent Channel Selectivity

The receiver adjacent channel selectivity is defined to be consistent with the transmitter configuration. Power levels for testing the receiver adjacent channel selectivity are as defined in [8] and [9] with the frequency offsets defined in table 6.

Table 6: Receive ACS test signal frequency offsets of higher chip rate reference configuration

Fuw offset (3.84Mcps Modulated)	7.5	MHz
Fuw offset (7.68Mcps Modulated)	10	MHz

Blocking Characteristics

The minimum frequency offset used in the blocking characteristic specification is 20MHz.

Intermodulation characteristics

Power levels for testing intermodulation characteristics are as defined in [8] and [9] with the frequency offsets and modulation bandwidths defined in table 7.

Table 7: Receive intermodulation test signal frequency offsets of higher chip rate reference configuration

F_{uw1} (CW)	±20	MHz
F_{uw2} (modulated, 7.68Mcps)	±40	MHz

4.3 Layer 1 Aspects

4.3.1 Physical channels and mapping of transport channels onto physical channels

Physical channels

Frame Structure

The higher chip rate reference configuration frame has a duration of 10ms and is subdivided into 15 timeslots (as per 3.84Mcps TDD). Each timeslot is of duration 5120 * T_c and can be allocated to either uplink or downlink.

Spreading for Downlink Physical Channels

Downlink physical channels shall use SF = 32. Multiple parallel physical channels can be used to support higher data rates. These parallel physical channels shall be transmitted using the channelisation codes as defined in section 4.3.3. Operation with a single code with spreading factor 1 is possible for the downlink physical channels.

Spreading for the Uplink Physical Channels

Spreading for uplink physical channels is identical to that of 3.84 Mcps UTRA TDD mode as stated in section 5.2.1.2 of TS 25.221 [5] with the exception that the range of spreading factor that may be used for uplink physical channels shall range from 32 down to 1.

Burst Types

Three burst types are defined : all of them comprise two data fields, a midamble and a guard period, the lengths of which are different for the individual burst types. Thus the number of data symbols in a burst depends upon the spreading factor and burst type as defined in Table 8 below:

Table 8: number of data symbols (N) for burst type 1, 2, and 3

Spreading Factor (SF)	Burst Type 1	Burst Type 2	Burst Type 3
1	3904	4416	3712
2	1952	2208	1856
4	976	1104	928
8	488	552	464
16	244	276	232

32	122	138	116

The support of all three burst types is mandatory for the UE.

Burst Type 1

Burst type 1 can be used for uplink and downlink. The midamble is of length 1024 chips. The maximum number of midambles for burst type 1 shall be 4, 8, or 16. The burst structure of burst type 1 is shown in Figure 1 below:

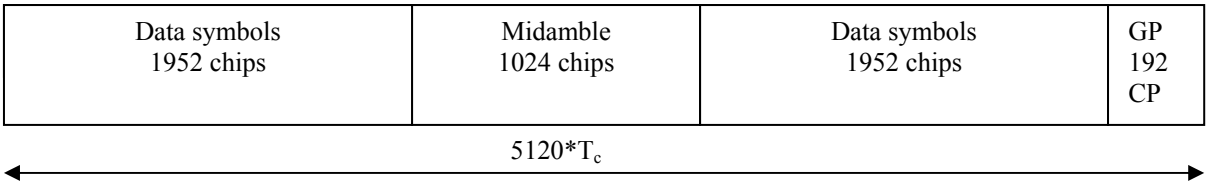

Figure 1: Burst structure of burst type 1. GP denotes the guard period and CP denotes chip periods.

Burst Type 2

Burst type 2 can be used for uplink and downlink. The midamble is of length 512 chips. The maximum number of midambles for burst type 2 shall be 4 or 8. The burst structure of burst type 2 is shown in Figure 2 below:

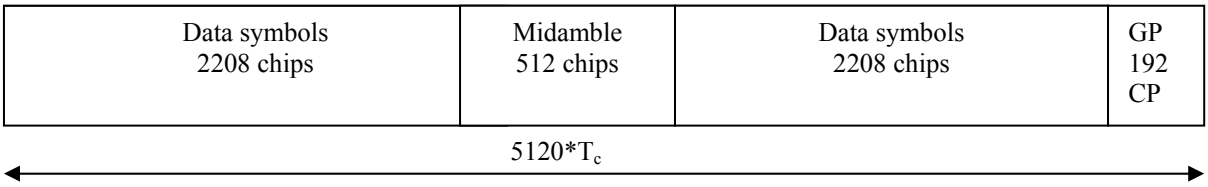

Figure 2: Burst structure of burst type 2. GP denotes the guard period and CP denotes chip periods.

Burst Type 3

Burst type 3 is used in the uplink only. Due to the longer guard period it is suitable for initial access or access to a new cell after handover. The midamble construction is identical to that of burst type 1. The maximum number of midambles for burst type 3 shall be 4, 8, or 16. The second data field is reduced in length compared to the first data field and the structure of burst type 3 is shown in Figure 3 below:

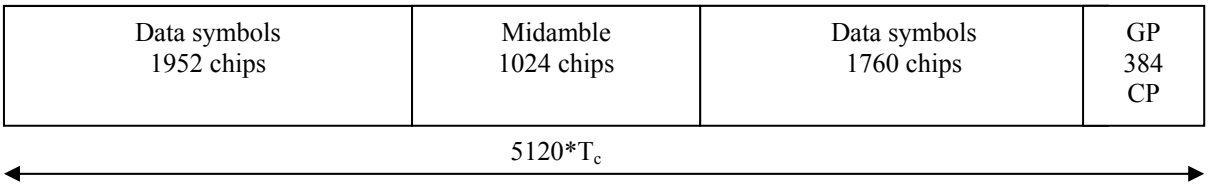

Figure 3: Burst structure of burst type 3. GP denotes the guard period and CP denotes chip periods.

Transmission of TFCI

All burst types 1, 2, and 3 provide the possibility for transmission of TFCI. Transmission of TFCI is identical to that of 3.84 Mcps UTRA TDD mode, see section 5.2.2.4 [5], with the exception that in the uplink the data in the TFCI field are always spread with SF = 32.

Transmission of TPC

All burst types 1, 2, and 3 provide the possibility for transmission of TPC in the uplink. Transmission of TPC is identical to that of 3.84 Mcps UTRA TDD mode, see section 5.2.2.5 [5], with the exception that the data in the TPC field are always spread with SF = 32.

Training sequences for spread bursts

The midamble for burst type 1 or 3 of the reference configuration has a length of Lm=1024, which corresponds to:

K' = 8; W = 114; P = 912.

Depending on the possible delay spread, cells are configured to use K_{Cell} midambles which are generated from the basic midamble codes (which are described below)

- for all k = 1,2,…,K; K = 2K' or
- for k = 1,2,…,K', only, or
- for odd k = 1,3,5,…,≤ K', only.

The basic midamble codes of length 912 chips are formed from the concatenation of successive basic midamble codes of length $P = 456$ (as defined in [5]). I.e. the n^{th} base code is formed from the concatenation of the n^{th} and m^{th} existing base codes of length 456, where $m = (n+1) \bmod 128$. The concatenation is pictured below in Figure 4.

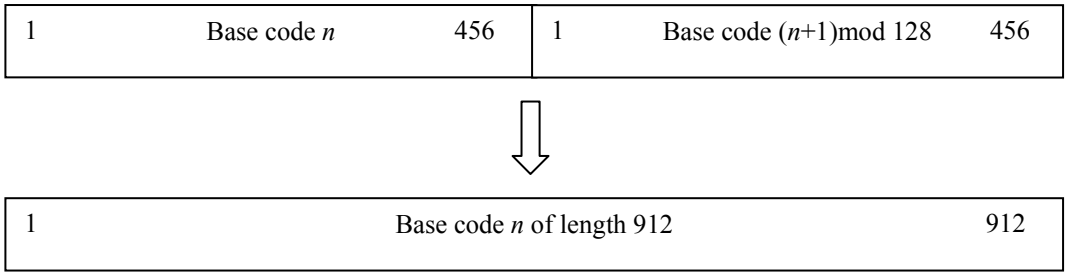

Figure 4: Basic midamble code construction from existing codes of length 456 for burst types 1 and 3.

The basic midamble codes for burst type 2 of the reference configuration are identical to those of burst type 1/3 at 3.84 Mcps as given in Table A-1 of [5]. The maximum number of midambles for burst type 2 shall be 4 or 8 and the midambles are constructed from the basic midamble codes as described in Section 5.2.3 of [5] with the following parameters: Lm = 512; K' = 8; W = 57; P = 456.

Common physical channels

The association between burst type number and physical channels is identical to that of 3.84 Mcps UTRA TDD [5]. All physical channels with the exception of SCH shall be capable of using spreading factor 32. The uplink PRACH uses either spreading factor SF = 32 or SF = 16.

Transmit Diversity for DL Physical Channels

The transmit diversity schemes that may be applied in the reference configuration are identical to those of 3.84Mcps UTRA TDD (sec. 5.4 of [5]).

Beacon characteristics of physical channels

The beacon characteristics of physical channels of the higher chip rate reference configuration shall be identical to those of 3.84Mcps UTRA TDD (sec 5.5 of [5]) with the exception that the beacon channel shall be provided by the physical channel that is allocated to channelisation code $c_{Q=32}^{(k=1)}$.

Midamble Transmit Power

The midamble transmit power of the higher chip rate reference configuration shall be identical to that of 3.84Mcps UTRA TDD (normative part of sec 5.7 of [5]).

Midamble Allocation for Physical Channels

Midamble allocation for physical channels of the higher chip rate reference configuration shall be identical to that of 3.84Mcps UTRA TDD (sec 5.6 of [5]) with the exception that the association between midambles and channelisation codes is as described below :

- Association between Midambles and Channelisation Codes:

The following mapping schemes (defined in Figure 5, Figure 6 and Figure 7) apply for the association between midambles and channelisation codes if no midamble is allocated by higher layers. Secondary channelisation codes are marked with a *. These associations apply both for UL and DL.

-- Association for Burst Type 1/3 and K_{Cell} = 16 Midambles

$\mathbf{m}^{(1)} - \mathbf{c}_1^{(1)}$	$\mathbf{m}^{(1)} - \mathbf{c}_2^{(1)}$	$\mathbf{m}^{(1)} - \mathbf{c}_4^{(1)}$	$\mathbf{m}^{(1)} - \mathbf{c}_8^{(1)}$	$\mathbf{m}^{(1)} - \mathbf{c}_{16}^{(1)}$	$\mathbf{m}^{(1)} - \mathbf{c}_{32}^{(1)}$
					$\mathbf{m}^{(1)} - \mathbf{c}_{32}^{(2)*}$
				$\mathbf{m}^{(9)} - \mathbf{c}_{16}^{(2)}$	$\mathbf{m}^{(9)} - \mathbf{c}_{32}^{(3)}$
					$\mathbf{m}^{(9)} - \mathbf{c}_{32}^{(4)*}$
			$\mathbf{m}^{(2)} - \mathbf{c}_8^{(2)}$	$\mathbf{m}^{(2)} - \mathbf{c}_{16}^{(3)}$	$\mathbf{m}^{(2)} - \mathbf{c}_{32}^{(5)}$
					$\mathbf{m}^{(2)} - \mathbf{c}_{32}^{(6)*}$
				$\mathbf{m}^{(10)} - \mathbf{c}_{16}^{(4)}$	$\mathbf{m}^{(10)} - \mathbf{c}_{32}^{(7)}$
					$\mathbf{m}^{(10)} - \mathbf{c}_{32}^{(8)*}$
		$\mathbf{m}^{(3)} - \mathbf{c}_4^{(2)}$	$\mathbf{m}^{(3)} - \mathbf{c}_8^{(3)}$	$\mathbf{m}^{(3)} - \mathbf{c}_{16}^{(5)}$	$\mathbf{m}^{(3)} - \mathbf{c}_{32}^{(9)}$
					$\mathbf{m}^{(3)} - \mathbf{c}_{32}^{(10)*}$
				$\mathbf{m}^{(11)} - \mathbf{c}_{16}^{(6)}$	$\mathbf{m}^{(11)} - \mathbf{c}_{32}^{(11)}$
					$\mathbf{m}^{(11)} - \mathbf{c}_{32}^{(12)*}$
			$\mathbf{m}^{(6)} - \mathbf{c}_8^{(4)}$	$\mathbf{m}^{(6)} - \mathbf{c}_{16}^{(7)}$	$\mathbf{m}^{(6)} - \mathbf{c}_{32}^{(13)}$
					$\mathbf{m}^{(6)} - \mathbf{c}_{32}^{(14)*}$
				$\mathbf{m}^{(14)} - \mathbf{c}_{16}^{(8)}$	$\mathbf{m}^{(14)} - \mathbf{c}_{32}^{(15)}$
					$\mathbf{m}^{(14)} - \mathbf{c}_{32}^{(16)*}$
	$\mathbf{m}^{(5)} - \mathbf{c}_2^{(2)}$	$\mathbf{m}^{(5)} - \mathbf{c}_4^{(3)}$	$\mathbf{m}^{(5)} - \mathbf{c}_8^{(5)}$	$\mathbf{m}^{(5)} - \mathbf{c}_{16}^{(9)}$	$\mathbf{m}^{(5)} - \mathbf{c}_{32}^{(17)}$
					$\mathbf{m}^{(5)} - \mathbf{c}_{32}^{(18)*}$
				$\mathbf{m}^{(13)} - \mathbf{c}_{16}^{(10)}$	$\mathbf{m}^{(13)} - \mathbf{c}_{32}^{(19)}$
					$\mathbf{m}^{(13)} - \mathbf{c}_{32}^{(20)*}$
			$\mathbf{m}^{(4)} - \mathbf{c}_8^{(6)}$	$\mathbf{m}^{(4)} - \mathbf{c}_{16}^{(11)}$	$\mathbf{m}^{(4)} - \mathbf{c}_{32}^{(21)}$
					$\mathbf{m}^{(4)} - \mathbf{c}_{32}^{(22)*}$
				$\mathbf{m}^{(12)} - \mathbf{c}_{16}^{(12)}$	$\mathbf{m}^{(12)} - \mathbf{c}_{32}^{(23)}$
					$\mathbf{m}^{(12)} - \mathbf{c}_{32}^{(24)*}$
		$\mathbf{m}^{(7)} - \mathbf{c}_4^{(4)}$	$\mathbf{m}^{(7)} - \mathbf{c}_8^{(7)}$	$\mathbf{m}^{(7)} - \mathbf{c}_{16}^{(13)}$	$\mathbf{m}^{(7)} - \mathbf{c}_{32}^{(25)}$
					$\mathbf{m}^{(7)} - \mathbf{c}_{32}^{(26)*}$
				$\mathbf{m}^{(15)} - \mathbf{c}_{16}^{(14)}$	$\mathbf{m}^{(15)} - \mathbf{c}_{32}^{(27)}$
					$\mathbf{m}^{(15)} - \mathbf{c}_{32}^{(28)*}$
			$\mathbf{m}^{(8)} - \mathbf{c}_8^{(8)}$	$\mathbf{m}^{(8)} - \mathbf{c}_{16}^{(15)}$	$\mathbf{m}^{(8)} - \mathbf{c}_{32}^{(29)}$
					$\mathbf{m}^{(8)} - \mathbf{c}_{32}^{(30)*}$
				$\mathbf{m}^{(16)} - \mathbf{c}_{16}^{(16)}$	$\mathbf{m}^{(16)} - \mathbf{c}_{32}^{(31)}$
					$\mathbf{m}^{(16)} - \mathbf{c}_{32}^{(32)*}$

Figure 5 - Association of Midambles to Spreading Codes for Burst Type 1/3 and K_{Cell} = 16

-- Association for Burst Type 1-3 and K_{Cell} = 8 Midambles

$\mathbf{m}^{(1)} - \mathbf{c}_1^{(1)}$	$\mathbf{m}^{(1)} - \mathbf{c}_2^{(1)}$	$\mathbf{m}^{(1)} - \mathbf{c}_4^{(1)}$	$\mathbf{m}^{(1)} - \mathbf{c}_8^{(1)}$	$\mathbf{m}^{(1)} - \mathbf{c}_{16}^{(1)}$	$\mathbf{m}^{(1)} - \mathbf{c}_{32}^{(1)}$
					$\mathbf{m}^{(1)} - \mathbf{c}_{32}^{(2)*}$
				$\mathbf{m}^{(1)} - \mathbf{c}_{16}^{(2)*}$	$\mathbf{m}^{(1)} - \mathbf{c}_{32}^{(3)*}$
					$\mathbf{m}^{(1)} - \mathbf{c}_{32}^{(4)*}$
			$\mathbf{m}^{(2)} - \mathbf{c}_8^{(2)}$	$\mathbf{m}^{(2)} - \mathbf{c}_{16}^{(3)}$	$\mathbf{m}^{(2)} - \mathbf{c}_{32}^{(5)}$
					$\mathbf{m}^{(2)} - \mathbf{c}_{32}^{(6)*}$
				$\mathbf{m}^{(2)} - \mathbf{c}_{16}^{(4)*}$	$\mathbf{m}^{(2)} - \mathbf{c}_{32}^{(7)*}$
					$\mathbf{m}^{(2)} - \mathbf{c}_{32}^{(8)*}$
		$\mathbf{m}^{(3)} - \mathbf{c}_4^{(2)}$	$\mathbf{m}^{(3)} - \mathbf{c}_8^{(3)}$	$\mathbf{m}^{(3)} - \mathbf{c}_{16}^{(5)}$	$\mathbf{m}^{(3)} - \mathbf{c}_{32}^{(9)}$
					$\mathbf{m}^{(3)} - \mathbf{c}_{32}^{(10)*}$
				$\mathbf{m}^{(3)} - \mathbf{c}_{16}^{(6)*}$	$\mathbf{m}^{(3)} - \mathbf{c}_{32}^{(11)*}$
					$\mathbf{m}^{(3)} - \mathbf{c}_{32}^{(12)*}$
			$\mathbf{m}^{(6)} - \mathbf{c}_8^{(4)}$	$\mathbf{m}^{(6)} - \mathbf{c}_{16}^{(7)}$	$\mathbf{m}^{(6)} - \mathbf{c}_{32}^{(13)}$
					$\mathbf{m}^{(6)} - \mathbf{c}_{32}^{(14)*}$
				$\mathbf{m}^{(6)} - \mathbf{c}_{16}^{(8)*}$	$\mathbf{m}^{(6)} - \mathbf{c}_{32}^{(15)*}$
					$\mathbf{m}^{(6)} - \mathbf{c}_{32}^{(16)*}$
	$\mathbf{m}^{(5)} - \mathbf{c}_2^{(2)}$	$\mathbf{m}^{(5)} - \mathbf{c}_4^{(3)}$	$\mathbf{m}^{(5)} - \mathbf{c}_8^{(5)}$	$\mathbf{m}^{(5)} - \mathbf{c}_{16}^{(9)}$	$\mathbf{m}^{(5)} - \mathbf{c}_{32}^{(17)}$
					$\mathbf{m}^{(5)} - \mathbf{c}_{32}^{(18)*}$
				$\mathbf{m}^{(5)} - \mathbf{c}_{16}^{(10)*}$	$\mathbf{m}^{(5)} - \mathbf{c}_{32}^{(19)*}$
					$\mathbf{m}^{(5)} - \mathbf{c}_{32}^{(20)*}$

			$\mathbf{m}^{(4)} - \mathbf{c}_8^{(6)}$	$\mathbf{m}^{(4)} - \mathbf{c}_{16}^{(11)}$	$\mathbf{m}^{(4)} - \mathbf{c}_{32}^{(21)}$
					$\mathbf{m}^{(4)} - \mathbf{c}_{32}^{(22)*}$
				$\mathbf{m}^{(4)} - \mathbf{c}_{16}^{(12)*}$	$\mathbf{m}^{(4)} - \mathbf{c}_{32}^{(23)*}$
					$\mathbf{m}^{(4)} - \mathbf{c}_{32}^{(24)*}$
		$\mathbf{m}^{(7)} - \mathbf{c}_4^{(4)}$	$\mathbf{m}^{(7)} - \mathbf{c}_8^{(7)}$	$\mathbf{m}^{(7)} - \mathbf{c}_{16}^{(13)}$	$\mathbf{m}^{(7)} - \mathbf{c}_{32}^{(25)}$
					$\mathbf{m}^{(7)} - \mathbf{c}_{32}^{(26)*}$
				$\mathbf{m}^{(7)} - \mathbf{c}_{16}^{(14)*}$	$\mathbf{m}^{(7)} - \mathbf{c}_{32}^{(27)*}$
					$\mathbf{m}^{(7)} - \mathbf{c}_{32}^{(28)*}$
			$\mathbf{m}^{(8)} - \mathbf{c}_8^{(8)}$	$\mathbf{m}^{(8)} - \mathbf{c}_{16}^{(15)}$	$\mathbf{m}^{(8)} - \mathbf{c}_{32}^{(29)}$
					$\mathbf{m}^{(8)} - \mathbf{c}_{32}^{(30)*}$
				$\mathbf{m}^{(8)} - \mathbf{c}_{16}^{(16)*}$	$\mathbf{m}^{(8)} - \mathbf{c}_{32}^{(31)*}$
					$\mathbf{m}^{(8)} - \mathbf{c}_{32}^{(32)*}$

Figure 6 - Association of Midambles to Spreading Codes for Burst Type 1-3 and $K_{Cell} = 8$

-- Association for Burst Type 1-3 and $K_{Cell} = 4$ Midambles

$\mathbf{m}^{(1)} - \mathbf{c}_1^{(1)}$	$\mathbf{m}^{(1)} - \mathbf{c}_2^{(1)}$	$\mathbf{m}^{(1)} - \mathbf{c}_4^{(1)}$	$\mathbf{m}^{(1)} - \mathbf{c}_8^{(1)}$	$\mathbf{m}^{(1)} - \mathbf{c}_{16}^{(1)}$	$\mathbf{m}^{(1)} - \mathbf{c}_{32}^{(1)}$
					$\mathbf{m}^{(1)} - \mathbf{c}_{32}^{(2)*}$
				$\mathbf{m}^{(1)} - \mathbf{c}_{16}^{(2)*}$	$\mathbf{m}^{(1)} - \mathbf{c}_{32}^{(3)*}$
					$\mathbf{m}^{(1)} - \mathbf{c}_{32}^{(4)*}$
			$\mathbf{m}^{(1)} - \mathbf{c}_8^{(2)*}$	$\mathbf{m}^{(1)} - \mathbf{c}_{16}^{(3)*}$	$\mathbf{m}^{(1)} - \mathbf{c}_{32}^{(5)*}$
					$\mathbf{m}^{(1)} - \mathbf{c}_{32}^{(6)*}$
				$\mathbf{m}^{(1)} - \mathbf{c}_{16}^{(4)*}$	$\mathbf{m}^{(1)} - \mathbf{c}_{32}^{(7)*}$
					$\mathbf{m}^{(1)} - \mathbf{c}_{32}^{(8)*}$
		$\mathbf{m}^{(3)} - \mathbf{c}_4^{(2)}$	$\mathbf{m}^{(3)} - \mathbf{c}_8^{(3)}$	$\mathbf{m}^{(3)} - \mathbf{c}_{16}^{(5)}$	$\mathbf{m}^{(3)} - \mathbf{c}_{32}^{(9)}$
					$\mathbf{m}^{(3)} - \mathbf{c}_{32}^{(10)*}$
				$\mathbf{m}^{(3)} - \mathbf{c}_{16}^{(6)*}$	$\mathbf{m}^{(3)} - \mathbf{c}_{32}^{(11)*}$
					$\mathbf{m}^{(3)} - \mathbf{c}_{32}^{(12)*}$
			$\mathbf{m}^{(3)} - \mathbf{c}_8^{(4)*}$	$\mathbf{m}^{(3)} - \mathbf{c}_{16}^{(7)*}$	$\mathbf{m}^{(3)} - \mathbf{c}_{32}^{(13)*}$
					$\mathbf{m}^{(3)} - \mathbf{c}_{32}^{(14)*}$
				$\mathbf{m}^{(3)} - \mathbf{c}_{16}^{(8)*}$	$\mathbf{m}^{(3)} - \mathbf{c}_{32}^{(15)*}$
					$\mathbf{m}^{(3)} - \mathbf{c}_{32}^{(16)*}$
	$\mathbf{m}^{(5)} - \mathbf{c}_2^{(2)}$	$\mathbf{m}^{(5)} - \mathbf{c}_4^{(3)}$	$\mathbf{m}^{(5)} - \mathbf{c}_8^{(5)}$	$\mathbf{m}^{(5)} - \mathbf{c}_{16}^{(9)}$	$\mathbf{m}^{(5)} - \mathbf{c}_{32}^{(17)}$
					$\mathbf{m}^{(5)} - \mathbf{c}_{32}^{(18)*}$
				$\mathbf{m}^{(5)} - \mathbf{c}_{16}^{(10)*}$	$\mathbf{m}^{(5)} - \mathbf{c}_{32}^{(19)*}$
					$\mathbf{m}^{(5)} - \mathbf{c}_{32}^{(20)*}$
			$\mathbf{m}^{(5)} - \mathbf{c}_8^{(6)*}$	$\mathbf{m}^{(5)} - \mathbf{c}_{16}^{(11)*}$	$\mathbf{m}^{(5)} - \mathbf{c}_{32}^{(21)*}$
					$\mathbf{m}^{(5)} - \mathbf{c}_{32}^{(22)*}$
				$\mathbf{m}^{(5)} - \mathbf{c}_{16}^{(12)*}$	$\mathbf{m}^{(5)} - \mathbf{c}_{32}^{(23)*}$
					$\mathbf{m}^{(5)} - \mathbf{c}_{32}^{(24)*}$
		$\mathbf{m}^{(7)} - \mathbf{c}_4^{(4)}$	$\mathbf{m}^{(7)} - \mathbf{c}_8^{(7)}$	$\mathbf{m}^{(7)} - \mathbf{c}_{16}^{(13)}$	$\mathbf{m}^{(7)} - \mathbf{c}_{32}^{(25)}$
					$\mathbf{m}^{(7)} - \mathbf{c}_{32}^{(26)*}$
				$\mathbf{m}^{(7)} - \mathbf{c}_{16}^{(14)*}$	$\mathbf{m}^{(7)} - \mathbf{c}_{32}^{(27)*}$
					$\mathbf{m}^{(7)} - \mathbf{c}_{32}^{(28)*}$
			$\mathbf{m}^{(7)} - \mathbf{c}_8^{(8)*}$	$\mathbf{m}^{(7)} - \mathbf{c}_{16}^{(15)*}$	$\mathbf{m}^{(7)} - \mathbf{c}_{32}^{(29)*}$
					$\mathbf{m}^{(7)} - \mathbf{c}_{32}^{(30)*}$
				$\mathbf{m}^{(7)} - \mathbf{c}_{16}^{(16)*}$	$\mathbf{m}^{(7)} - \mathbf{c}_{32}^{(31)*}$
					$\mathbf{m}^{(7)} - \mathbf{c}_{32}^{(32)*}$

Figure 7 - Association of Midambles to Spreading Codes for Burst Type 1-3 and $K_{Cell} = 4$

Mapping of transport channels to physical channels

The mapping of transport channels to physical channels is identical to that of 3.84Mcps TDD of section 7 of [5] with the exception that a maximum of (M=8) HS-SCCH may be associated with an HS-DSCH for one UE.

4.3.2 Multiplexing and channel coding

The higher chip rate reference configuration shall apply the 3.84Mcps TDD method of multiplexing and channel coding as defined in 25.222 [3] with the following exceptions :

The channelisation code-set information field of the HS-SCCH shall be 10 bits ($x_{ccs,1},\ldots x_{ccs,10}$) (cf section 4.6 of 25.222 [3]). $x_{ccs,1},\ldots x_{ccs,5}$ define the start code of the allocation, $x_{ccs,6},\ldots x_{ccs,10}$ define the stop code of the allocation. If the signaled start code of the allocation is 32 and the signaled stop code is 1, a spreading factor SF=1 shall be used for the HS-PDSCH resources.

Note that the transport block size information for HS-SCCH for the higher chip rate reference configuration shall be coded on 9 bits as per 3.84Mcps TDD. It may be assumed that a mapping of transport block size information to actual transport block size is available that does not significantly impact performance.

4.3.3 Spreading and modulation

The higher chip rate reference configuration shall apply the 3.84Mcps TDD method of spreading and modulation as defined in TS 25.223 [4] with the following exceptions:

General

The basic modulation parameters of the 7.68 Mcps UTRA TDD reference system are given in Table 9 :

Table 9 - Basic modulation parameters of reference configuration

Chip rate	7.68 Mcps
Data modulation	QPSK / 16 QAM (HS-PDSCH only)
Spreading characteristics	Orthogonal Q chips / symbol, Where $Q = 2^p$, $0 <= p <= 5$

Data Modulation

The data modulation is identical to that of 3.84 Mcps UTRA TDD mode (cf section 5 of 25.223 [4]). The number of symbols per data field is adapted to the burst formats defined in section 4.3.1.

Spreading Modulation

The spreading modulation is identical to that of 3.84 Mcps UTRA TDD mode (cf section 7 of 25.223 [4]) with the exception that the real valued channelisation codes are of length $Q_k \in \{1,2,4,8,16,32\}$. The channelisation codes are Orthogonal Variable Spreading Factor (OVSF) codes and are generated as described for 3.84 Mcps UTRA TDD mode.

Associated with each channelisation code is a multiplier taking values from the set $\{e^{j\pi/2\cdot p_k}\}$, where p_k is a permutation of the integer set $\{0,\ldots,Q_k\text{-}1\}$ and Q_k is the spreading factor. The values of the multiplier for $Q_k = \{1,2,4,8,16\}$ are identical to those of 3.84 Mcps UTRA TDD mode. For $Q_k = 32$ the multiplier values are given in Table 10:

Table 10 - multiplier values for $Q_k = 32$

K	1	2	3	4	5	6	7	8	9	10	11	12	13	14	15	16
$W_{Q=32}^{(k)}$	-i	-1	-1	1	-1	-i	i	1	-1	1	1	-i	i	-1	i	-i

K	17	18	19	20	21	22	23	24	25	26	27	28	29	30	31	32

$W_{Q=32}^{(k)}$	-i	-i	1	i	-1	-i	-i	-i	-1	-1	i	-1	-i	1	-1	-1

The scrambling codes for the 7.68 Mcps UTRA TDD reference system shall be of length 32 chips and are formed by concatenation of the existing length 16 chip scrambling codes described in Annex A of TS 25.223 [4]. The concatenation of existing scrambling codes *m* and *n* is shown in Figure 8 where $m, n \in \{0,\ldots,127\}$ and $m \neq n$:

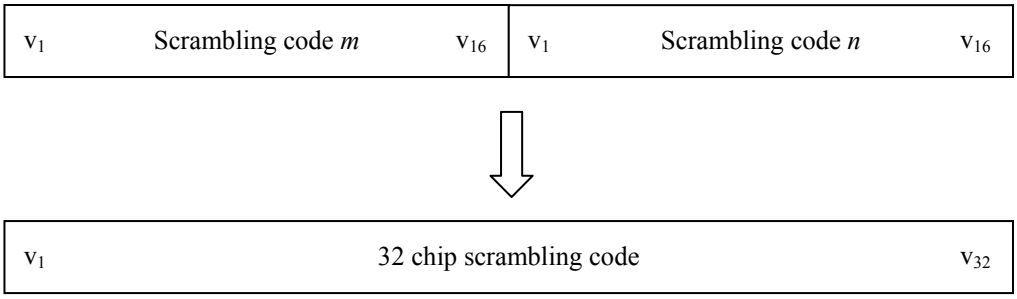

Figure 8: Concatenation of length 16 chip scrambling codes.

The mapping scheme for Cell Parameters and constituent scrambling codes for the 7.68 Mcps UTRA TDD reference system is shown in Table 11. The cycling of cell parameters with system frame numbering is identical to that of the 3.84 Mcps UTRA TDD mode as described in Section 8.3 (Table 7) of TS 25.233 [4].

Table 11: Mapping scheme for Cell Parameters and TS 25.223 constituent scrambling codes.

Cell Parameter	TS 25.223 scrambling code *m*	TS 25.223 scrambling code *n*
0	0	2
1	1	3
2	2	4
3	3	5
	. . . .	
124	124	126
125	125	127
126	126	0
127	127	1

When different physical channels are combined in the uplink the weight factors γ_i of Table 12 are applied depending on the spreading factor SF of the corresponding DPCH.

Table 12 - weight factors for reference configuration

SF of $DPCH_i$	γ_i
32	$\sqrt{2}/8$
16	$1/4$
8	$\sqrt{2}/4$

4	$1/2$
2	$\sqrt{2}/2$
1	1

Synchronisation codes

Code Generation

The synchronisation codes shall be constructed in the same manner as defined in sub-clause 8.1 of [4]. For the 7.68Mcps reference configuration repetition encoding shall be applied to both the primary and secondary synchronization codes. In this instance each element of the code is repeated twice.

Using the notation of sub-clause 8.1 of [4], the primary synchronization code is defined as

$$C_p = \langle y(0), y(0), y(1), y(1), \ldots, y(255), y(255) \rangle$$

Similarly, the ith secondary SCH code word, $C_{,i}$, i = 0, 1, 3, 4, 5, 6, 8, 10, 12, 13, 14, 15 is defined as

$$C_i = (1+j) \times \langle h_m(0) \times z(0), h_m(0) \times z(0), h_m(1) \times z(1), h_m(1) \times z(1), \ldots, h_m(255) \times z(255), h_m(255) \times z(255) \rangle$$

where $m = (16 \times i)$ and the leftmost chip in the sequence corresponds to the chip transmitted first in time. The length of the synchronization codes in the SCH is 512.

Code Allocation

Code allocation is identical to sub-clause 8.2 of [4] with the following exceptions to 8.2.1 and 8.2.2:

Code Allocation for Case 1

There are 32 code groups 0,1,..,31, define $u = (u_0, u_1, u_2, u_3, u_4)$ as the binary representation of the code group number. The radio frame is denoted by

$$f = \begin{cases} 0 & \text{Frame1} \\ 1 & \text{Frame2} \end{cases}$$

and denote C_r as a Boolean variable, where

$$C_r = \begin{cases} 0 & 3.84\text{Mcps} \\ 1 & 7.68\text{Mcps} \end{cases}$$

Define the following generator matrix

$$G^{(1)} = \begin{bmatrix} 0 & 0 & 0 & 0 & 1 & 0 \\ 0 & 0 & 0 & 0 & 0 & 1 \\ 0 & 0 & 0 & 1 & 0 & 0 \\ 0 & 1 & 0 & 0 & 0 & 0 \\ 1 & 0 & 1 & 0 & 0 & 0 \end{bmatrix}$$

with rows $g_0^{(1)}, g_1^{(1)}, g_2^{(1)}, g_3^{(1)}, g_4^{(1)}$, and the binary codeword a as

$$a = (dG^{(1)} + z) \bmod 2$$

where $a = (a_0, \ldots, a_5)$, $d = (C_r, f, u_0, u_1, u_2)$ and $z = u_3(u_2 + 1) \bmod 2 \times g_4^{(1)}$. Map the elements of the codeword a pairwise to the set of integers $(0,1,2,3)$ using the expression

$$s_k = 2a_{2k+1} + a_{2k} \quad ; \; k = 0,1,2$$

The sequence $s=(s_0,s_1,s_2)$ has an associated complex sequence $b=\left(j^{s_0},j^{s_1},j^{s_2}\right)$. The code construction is defined by the component wise product:

$$C_s = bC$$

The code set permutation is given in Table 13 below. When $C_r = 0$, the codeword produced by the generator matrix matches the sequences defined in sub-clause 8.2.1 of [4].

Table 13- code set permutations for case 1

(u_4,u_3,u_2)	Code Group	Code Set Permutation, C
000	0→3	$c_1c_3c_5$
001	4→7	$c_1c_3c_5$
010	8→11	$c_1c_5c_3$
011	12→15	$c_3c_5c_1$
100	16→19	$c_{10}c_{13}c_{14}$
101	20→23	$c_{10}c_{13}c_{14}$
110	24→27	$c_{10}c_{14}c_{13}$
111	28→31	$c_{13}c_{14}c_{10}$

Code Allocation for Case 2

There are 32 code groups 0,1,..,31, define $u=(u_0,u_1,u_2,u_3,u_4)$ as the binary representation of the code group number, where u_0 is the LSB. The radio frame is denoted by

$$f=\begin{cases}0 & \text{Frame1}\\ 1 & \text{Frame2}\end{cases}$$

Denote C_r as a Boolean variable, where

$$C_r=\begin{cases}0 & 3.84\text{Mcps}\\ 1 & 7.68\text{Mcps}\end{cases}$$

and

$$TS=\begin{cases}0 & \text{slot } k\\ 1 & \text{slot } k+8\end{cases}$$

Define the following generator matrix

$$G^{(2)}=\begin{bmatrix}0&0&0&0&1&0\\0&0&0&0&0&1\\0&1&0&1&0&0\\0&0&0&1&0&0\\1&0&1&0&0&0\end{bmatrix}$$

with rows labelled $g_0^{(2)},g_1^{(2)},g_2^{(2)},g_3^{(2)},g_4^{(2)}$ and the binary codeword a as

$$a=\left(dG^{(2)}+z\right)\bmod 2$$

where $a=(a_0,\ldots,a_5)$, $d=(C_r,TS,f,u_0,u_1)$, and $z=u_2(u_1+1)\bmod 2\times g_4^{(2)}$. Map the elements of the codeword a pairwise to the set of integers $(0,1,2,3)$ using the expression

$$s_k = 2a_{2k+1}+a_{2k}\ ;\ k=0,1,2$$

The sequence $s=(s_0,s_1,s_2)$ has an associated complex sequence $b=\left(j^{s_0},j^{s_1},j^{s_2}\right)$. The code construction is defined by the component wise product:

$$C_s = bC$$

The code set permutation is defined in Table 14 below. When $C_r = 0$ the codeword produced by the generator matrix matches the sequences defined in sub-clause 8.2.2 of [4].

Table 14 - code set permutations for case 2

(u_4, u_3, u_2, u_1)	Code Group	Code Set Permutation, C
0000	0→1	$c_1 c_3 c_5$
0001	2→3	$c_1 c_3 c_5$
0010	4→5	$c_1 c_5 c_3$
0011	6→7	$c_3 c_5 c_1$
0100	8→9	$c_{10} c_{13} c_{14}$
0101	10→11	$c_{10} c_{13} c_{14}$
0110	12→13	$c_{10} c_{14} c_{13}$
0111	14→15	$c_{13} c_{14} c_{10}$
1000	16→17	$c_0 c_6 c_{12}$
1001	18→19	$c_0 c_6 c_{12}$
1010	20→21	$c_0 c_{12} c_6$
1011	22→23	$c_6 c_{12} c_0$
1100	24→25	$c_4 c_8 c_{15}$
1101	26→27	$c_4 c_8 c_{15}$
1110	28→29	$c_4 c_{15} c_8$
1111	30→31	$c_8 c_{15} c_4$

4.3.4 Physical Layer Procedures

The higher chip rate reference configuration shall apply the 3.84Mcps TDD physical layer procedures as defined in 25.224 [6] with the following exceptions:

Timing Advance

The required timing advance shall be represented as a 6-bit number (0-63) 'UL Timing Advance' TA_{ul} , being the multiplier of $4 \times (C_r + 1)$ chips which is nearest to the required timing advance, where

$$C_r = \begin{cases} 0 & 3.84\text{Mcps} \\ 1 & 7.68\text{Mcps} \end{cases}$$

On receipt of TA_{ul} the UE shall adjust the timing of its transmissions accordingly in steps of $4 \times (C_r + 1)$ chips.

Cell Search Procedure

A higher chip rate enabled UE can be reconfigured to operate at 3.84Mcps and 7.68Mcps.

Step 2: Cell Chip Rate, Code Group Identification and Slot synchronization

During the second step of the cell search procedure, the UE shall use the SCH's secondary synchronization codes to simultaneously identify both cell chip rate and 1 out of 32 code groups for the cell found in the first step. Since this information is solely contained in the modulation sequence, the same method of sequence identification employed at

3.84Mcps can be reused at 7.68Mcps. Before proceeding to the third step of the cell search procedure, there shall be a reconfiguration of the UE transmitter and receiver to reflect the signaled cell chip rate.

4.3.5 Physical Layer Measurements

The physical layer measurements defined for the reference configuration are identical to those defined in [7] for 3.84Mcps TDD with the following exceptions :

SFN-SFN Observed time difference

The SFN-SFN observed time difference is defined identically to [7] where for 7.68Mcps :

SFN-SFN observed time difference = $OFF \times 76800 + T_m$ *in chips for* 7.68*Mcps TDD* where:

T_m is in the range $[0,1,...,76799$ *chips for* 7.68 *Mcps TDD*$]$

SFN-CFN observed time difference

T_m is in the range $[0,1,...,76799$ *chips for* 7.68 *Mcps TDD*$]$

4.3.6 UE Capabilities

The reference configuration shall assume that UEs are not restricted in terms of their UE capabilities. The reference configuration shall assume that a form of multi-user detector used at 3.84Mcps is modified to operate at the higher chip rate.

4.4 Protocol aspects

The reference configuration assumes that there are no protocol changes from 3.84Mcps TDD. It is assumed that higher layer signalling is extended to cover the higher chip rate.

5 Analysis

[Editor's note : This section will provide results on the performance and complexity of the reference higher chip rate configuration described in section 4].

5.1 Reference Channel Models

The simulations in this section are based on the channel models defined in subclause A.2.

5.2 Link Level Results

5.2.1 Release 99/4 type bearers

Link level results for 3.84Mcps and 7.68Mcps release 99/4 type bearers are provided in the figures of this subclause according to table 15.

Table 15 - List of Link Level Results Figures

figure	Link	mean instantaneous	Bearer	channel	chip rate

9	Downlink	mean	12.2kbps	AWGN	3.84, 7.68
10	Downlink	mean	12.2kbps	PA3	3.84, 7.68
11	Downlink	mean	12.2kbps	PB3	3.84, 7.68
12	Downlink	mean	12.2kbps	VA30	3.84, 7.68
13	Downlink	mean	12.2kbps	VA120	3.84, 7.68
14	Downlink	Instantaneous	12.2kbps	AWGN	3.84, 7.68
15	Downlink	instantaneous	12.2kbps	PA3	3.84, 7.68
16	Downlink	instantaneous	12.2kbps	PB3	3.84, 7.68
17	Downlink	instantaneous	12.2kbps	VA30	3.84, 7.68
18	Downlink	instantaneous	12.2kbps	VA120	3.84, 7.68
19	Downlink	mean	384kbps	AWGN	3.84, 7.68
20	Downlink	mean	384kbps	PA3	3.84, 7.68
21	Downlink	mean	384kbps	PB3	3.84, 7.68
22	Downlink	mean	384kbps	VA30	3.84, 7.68
23	Downlink	mean	384kbps	VA120	3.84, 7.68
24	Downlink	Instantaneous	384kbps	AWGN	3.84, 7.68
25	Downlink	instantaneous	384kbps	PA3	3.84, 7.68
26	Downlink	instantaneous	384kbps	PB3	3.84, 7.68
27	Downlink	instantaneous	384kbps	VA30	3.84, 7.68
28	Downlink	instantaneous	384kbps	VA120	3.84, 7.68
29	Uplink	mean	12.2kbps	AWGN	3.84, 7.68
30	Uplink	mean	12.2kbps	PA3	3.84, 7.68
31	Uplink	mean	12.2kbps	PB3	3.84, 7.68
32	Uplink	mean	12.2kbps	VA30	3.84, 7.68
33	Uplink	mean	12.2kbps	VA120	3.84, 7.68
34	Uplink	instantaneous	12.2kbps	AWGN	3.84, 7.68
35	Uplink	instantaneous	12.2kbps	PA3	3.84, 7.68
36	Uplink	instantaneous	12.2kbps	PB3	3.84, 7.68
37	Uplink	instantaneous	12.2kbps	VA30	3.84, 7.68
38	Uplink	instantaneous	12.2kbps	VA120	3.84, 7.68
39	Uplink	mean	384kbps	AWGN	3.84, 7.68
40	Uplink	mean	384kbps	PA3	3.84, 7.68
41	Uplink	mean	384kbps	PB3	3.84, 7.68
42	Uplink	mean	384kbps	VA30	3.84, 7.68
43	Uplink	mean	384kbps	VA120	3.84, 7.68
44	Uplink	instantaneous	384kbps	AWGN	3.84, 7.68
45	Uplink	instantaneous	384kbps	PA3	3.84, 7.68
46	Uplink	instantaneous	384kbps	PB3	3.84, 7.68
47	Uplink	instantaneous	384kbps	VA30	3.84, 7.68
48	Uplink	instantaneous	384kbps	VA120	3.84, 7.68

5.2.1.1 Downlink 12.2kbps

Simulation Notes:

- Results for DTCH DCH and TFCI are shown
- Closed inner loop power control is in operation with a step size of 1dB. The power control target is adjusted in order to maintain the transmitted power ratios described in Annex A.6.
- Due to the action of power control the input to the channel may be correlated with the channel for the user of interest, but not for other users. As a result the mean received $DPCH\_\hat{E}_c/\hat{I}_{or}$ is always less than or equal to the mean transmitted $DPCH\_E_c/I_{or}$. For cases in which power control is unable to track the channel envelope the transmitted and received ratios are the same. For cases in which power control is able to track the channel envelope the received ratio will be lower than the transmitted ratio. To ease interpretation of the results (plotted against mean $\hat{I}_{or}/I_{oc}$), the received $DPCH\_\hat{E}_c/\hat{I}_{or}$ ratio is stated at the bottom of the figure for each channel type.
- In the case of the instantaneous results, the BLER of the DTCH DCH is plotted against the instantaneous received $DPCH\_\hat{E}_c/I_{oc}$ as due to the interaction between power control of each of the users and the fading channel the received power $\hat{I}_{or}$ comprises non-correlated fluctuations in the wanted and the intracell interfering users.
- Code rate:
  - (244+16) / 764 = 0.34
- Processing gain:
  - 3.84Mcps (0.809*2*(2560-96)) / 122 = 15.14 dB
  - 7.68Mcps 2*(0.809*2*(2560-96)) / 122 = 18.15 dB

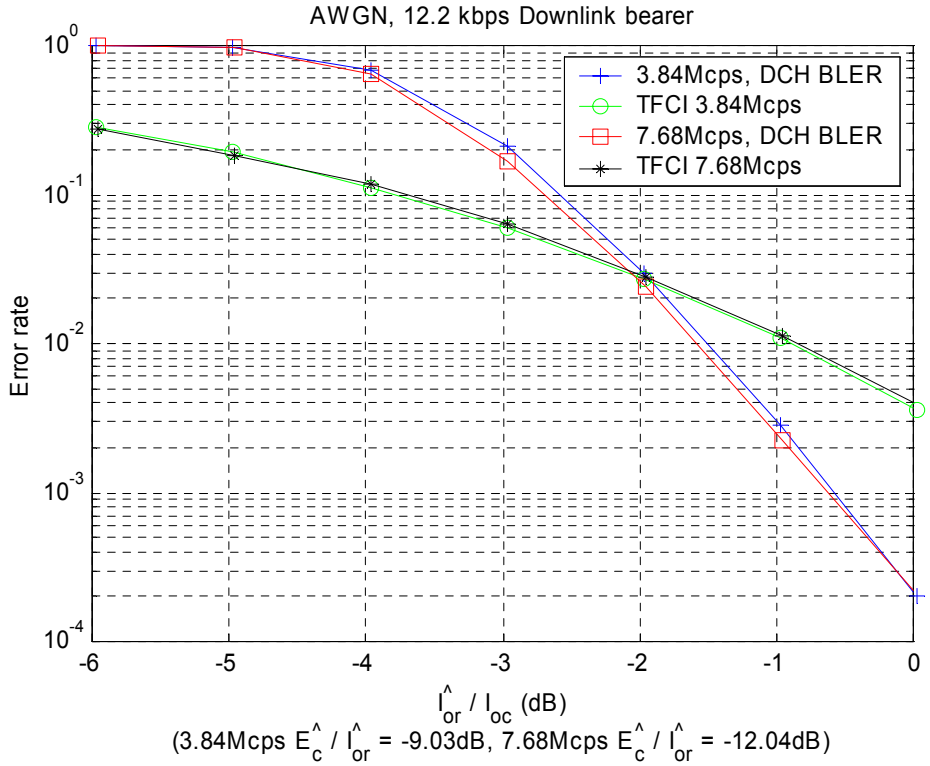

Figure 9 - Link Level Results for 12.2kbps Bearer, Downlink, AWGN, (mean $\hat{I}_{or}/I_{oc}$)

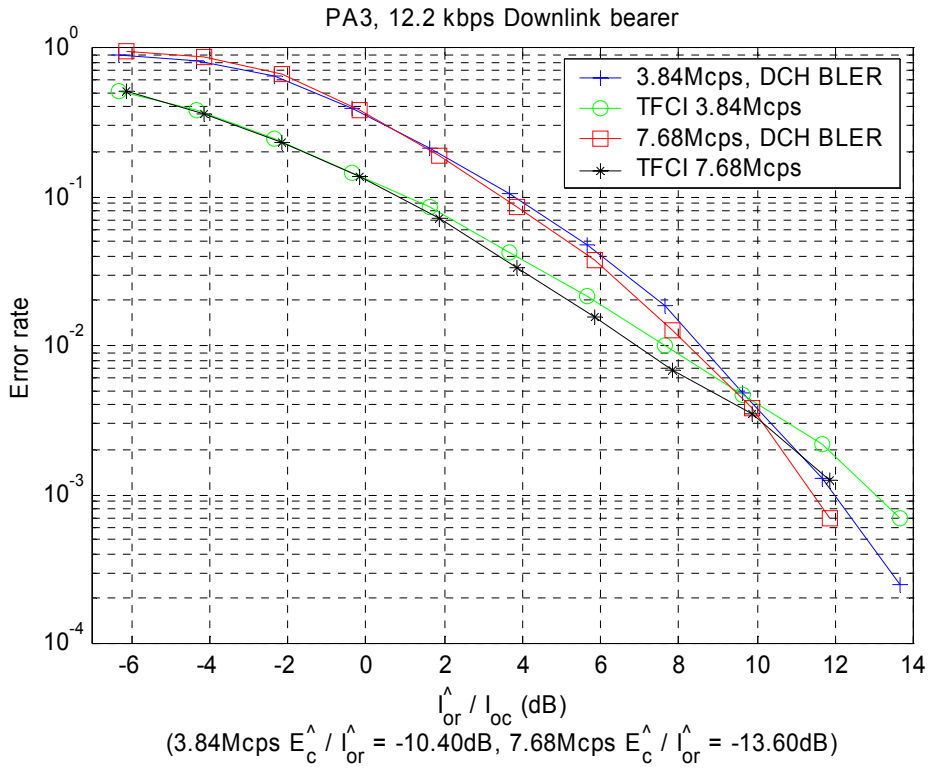

Figure 10 – Link Level Results for 12.2kbps Bearer, Downlink, PA3, (mean $\hat{I}_{or}/I_{oc}$)

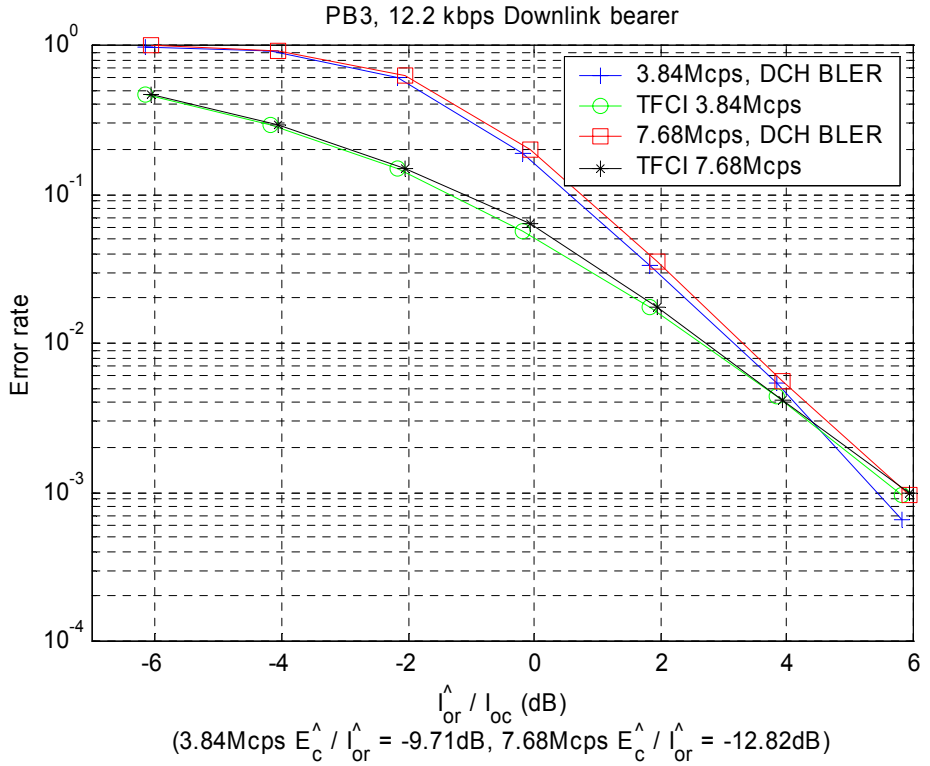

Figure 11 – Link Level Results for 12.2kbps Bearer, Downlink, PB3, (mean $\hat{I}_{or}/I_{oc}$)

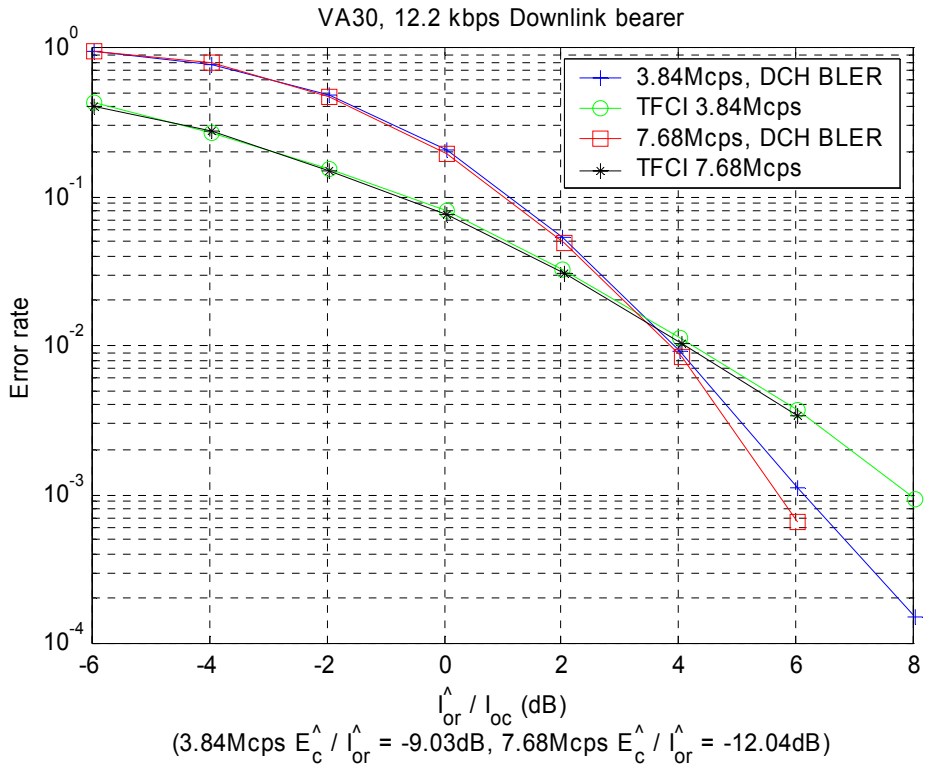

Figure 12 – Link Level Results for 12.2kbps Bearer, Downlink, VA30, (mean $\hat{I}_{or}/I_{oc}$)

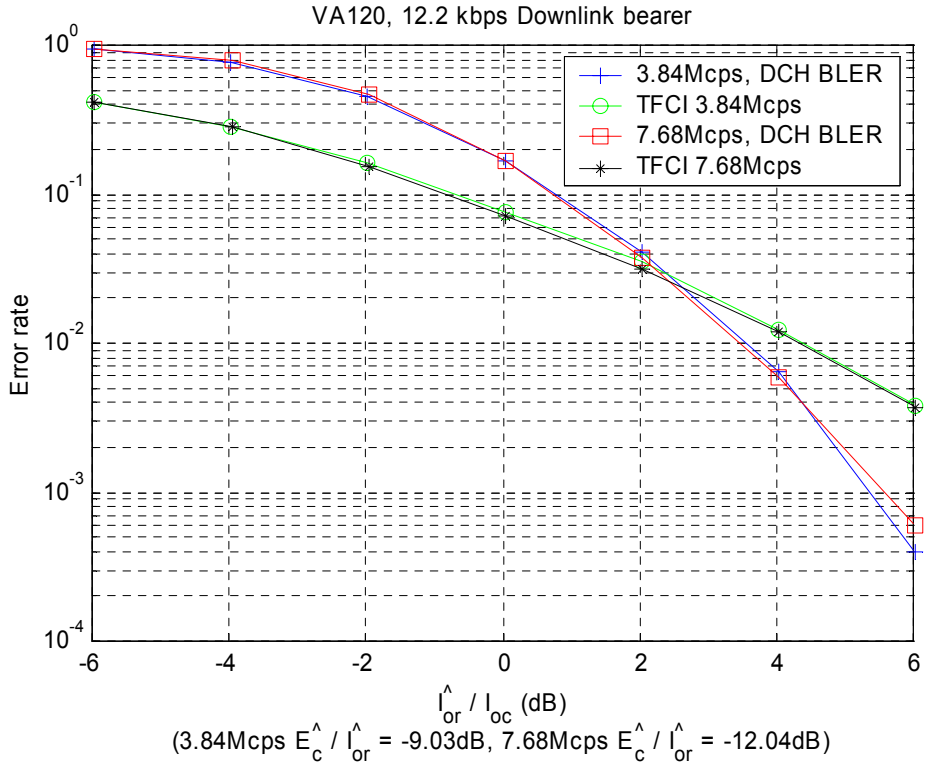

Figure 13 – Link Level Results for 12.2kbps Bearer, Downlink, VA120, (mean $\hat{I}_{or}/I_{oc}$)

A summary of performance with respect to mean $\hat{I}_{or}/I_{oc}$ (figures 9 to 13) including calculated E_b / N_0 for the 12.2kbps bearer is provided in Table 16:

Table 16 – Link Level Performance Summary, Downlink 12.2kps Bearer

Chip rate (Mcps)	Channel	BLER (%)	$\hat{I}_{or}/I_{oc}$ (dB)	$\hat{E}_c/\hat{I}_{or}$ (dB)	E_b/N_0 (dB)
3.84	AWGN	10%	-2.59	-9.03	3.52
3.84	AWGN	1%	-1.51	-9.03	4.60
3.84	PA3	10%	3.77	-10.40	8.51
3.84	PA3	1%	8.58	-10.40	13.32
3.84	PB3	10%	0.56	-9.71	5.99
3.84	PB3	1%	3.16	-9.71	8.59
3.84	VA30	10%	1.08	-9.03	7.19
3.84	VA30	1%	3.94	-9.03	10.05
3.84	VA120	10%	0.76	-9.03	6.87
3.84	VA120	1%	3.55	-9.03	9.66
7.68	AWGN	10%	-2.69	-12.04	3.42
7.68	AWGN	1%	-1.59	-12.04	4.52
7.68	PA3	10%	3.44	-13.60	7.99
7.68	PA3	1%	8.26	-13.60	12.81
7.68	PB3	10%	0.74	-12.82	6.07
7.68	PB3	1%	3.31	-12.82	8.64
7.68	VA30	10%	1.00	-12.04	7.11
7.68	VA30	1%	3.85	-12.04	9.96
7.68	VA120	10%	0.74	-12.04	6.85
7.68	VA120	1%	3.47	-12.04	9.58

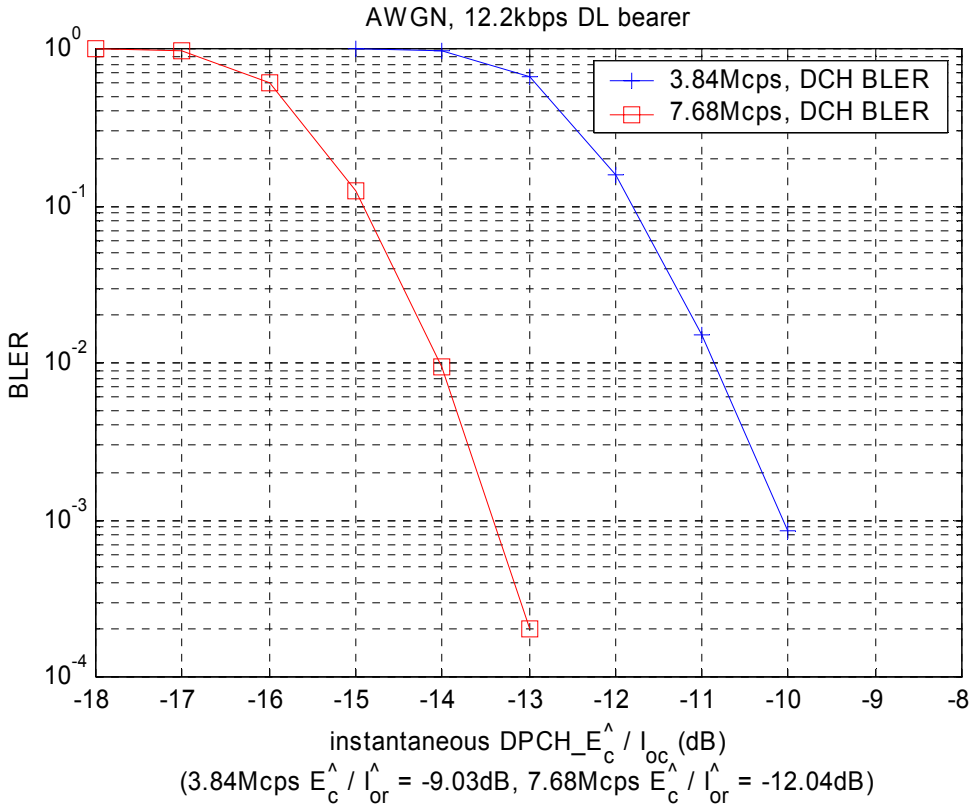

Figure 14 – Link Level Results for 12.2kbps Bearer, Downlink, AWGN, (instantaneous $DPCH\_\hat{E}_c / I_{oc}$)

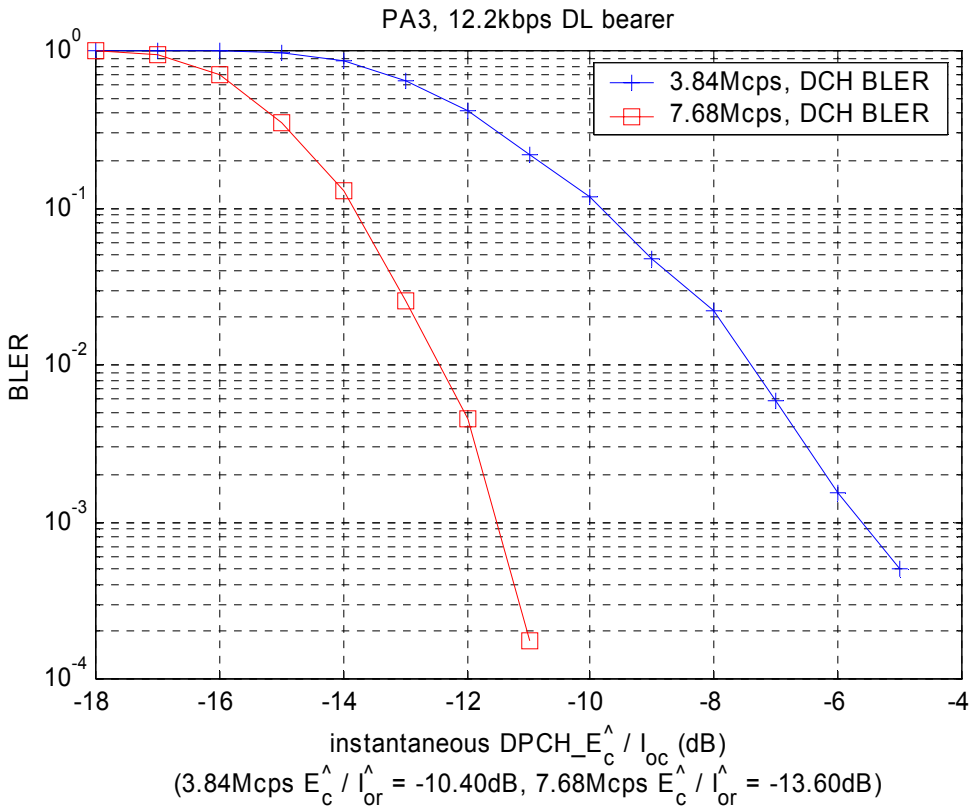

Figure 15 – Link Level Results for 12.2kbps Bearer, Downlink, PA3, (instantaneous $DPCH\_\hat{E}_c / I_{oc}$)

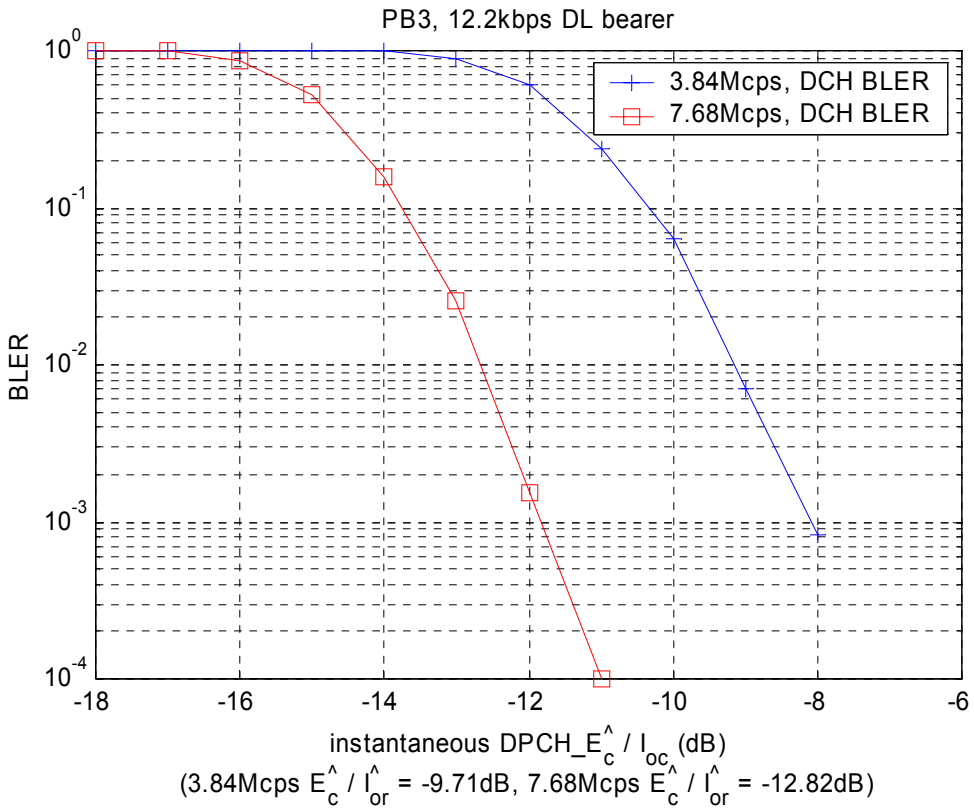

Figure 16 – Link Level Results for 12.2kbps Bearer, Downlink, PB3, (instantaneous $DPCH\_\hat{E}_c / I_{oc}$)

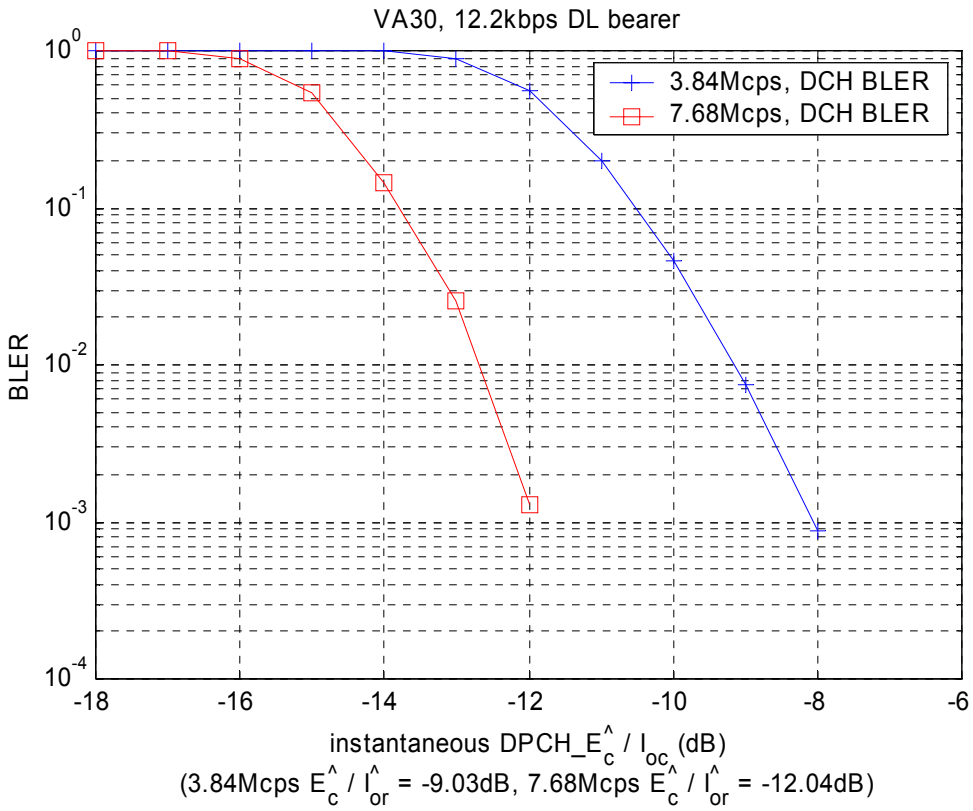

Figure 17 – Link Level Results for 12.2kbps Bearer, Downlink, VA30, (instantaneous $DPCH\_\hat{E}_c / I_{oc}$)

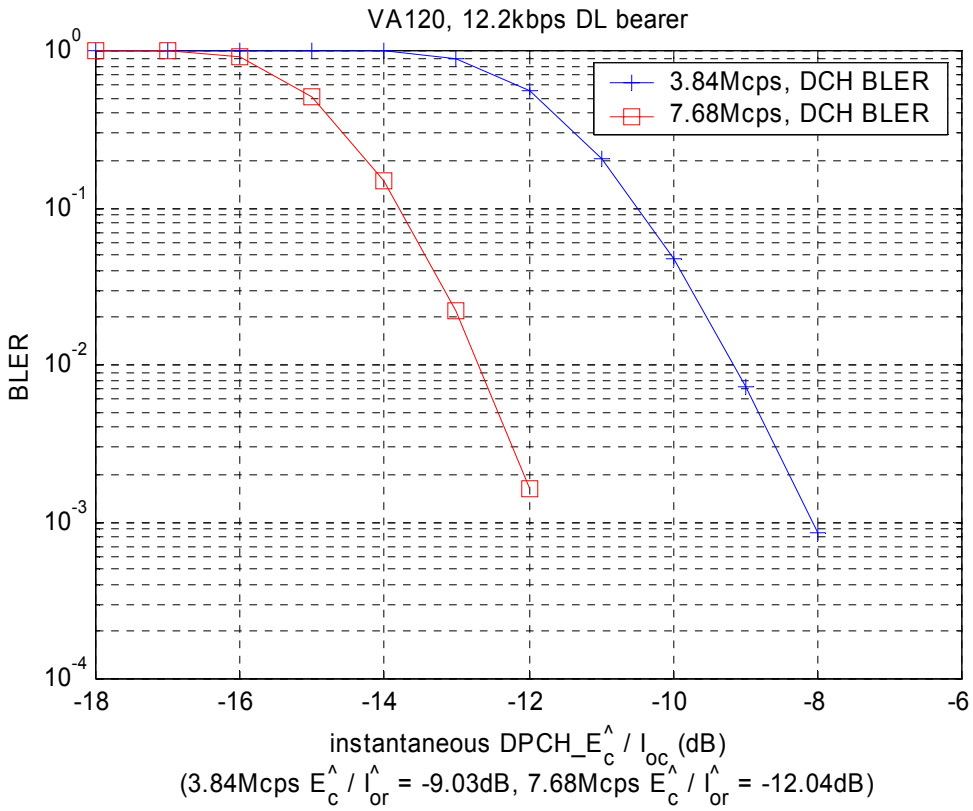

Figure 18 – Link Level Results for 12.2kbps Bearer, Downlink, VA120, (instantaneous $DPCH\_\hat{E}_c/I_{oc}$)

5.2.1.2 Downlink 384kbps

Simulation Notes:

- Results for DTCH DCH and TFCI are shown
- Closed inner loop power control is in operation with a step size of 1dB. The power control target is adjusted in order to maintain the transmitted power ratios described in Annex A.6.
- Due to the action of power control the input to the channel may be correlated with the channel for the user of interest, but not for other users. As a result the mean received $DPCH\_\hat{E}_c/\hat{I}_{or}$ is always less than or equal to the mean transmitted $DPCH\_E_c/I_{or}$. For cases in which power control is unable to track the channel envelope the transmitted and received ratios are the same. For cases in which power control is able to track the channel envelope the received ratio will be lower than the transmitted ratio. To ease interpretation of the results (plotted against mean $\hat{I}_{or}/I_{oc}$), the received $DPCH\_\hat{E}_c/\hat{I}_{or}$ ratio is stated at the bottom of the figure for each channel type.
- In the case of the instantaneous results, the BLER of the DTCH DCH is plotted against the instantaneous received $DPCH\_\hat{E}_c/I_{oc}$ as due to the interaction between power control of each of the users and the fading channel the received power $\hat{I}_{or}$ comprises non-correlated fluctuations in the wanted and the intracell interfering users.
- Code rate:
  - (3840+16) / 6557 = 0.59

- Processing gain:
  - 3.84Mcps (0.9923*24*(2560-96)) / 3840 = 11.84 dB
  - 7.68Mcps 2*(0.9923*24*(2560-96)) / 3840 = 14.85 dB

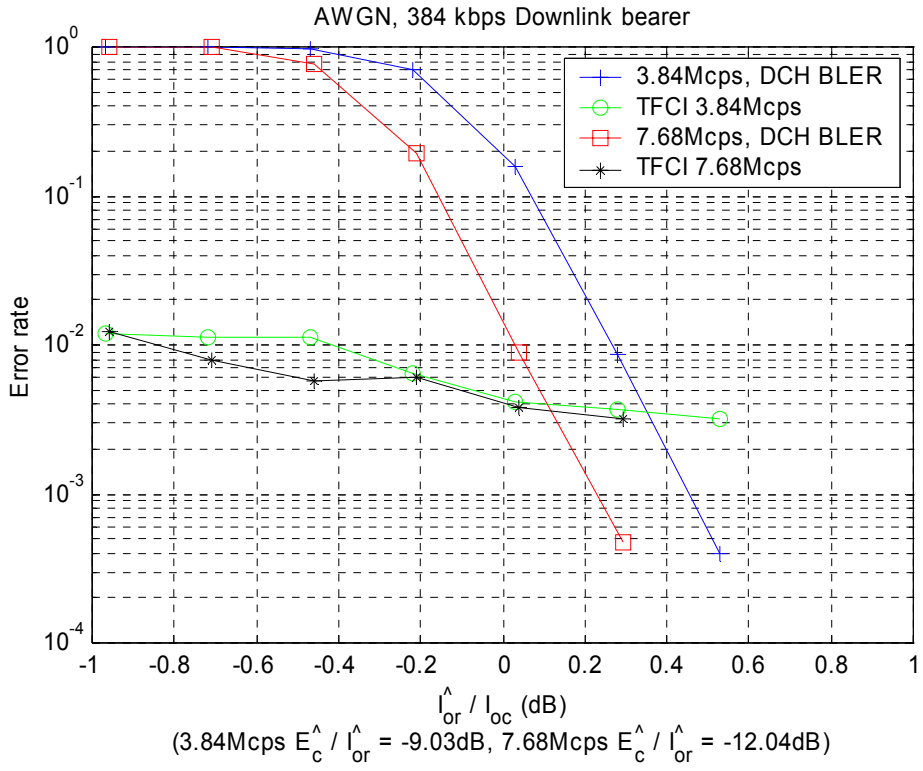

Figure 19 - Link Level Results for 384kbps Bearer, Downlink, AWGN, (mean $\hat{I}_{or}/I_{oc}$)

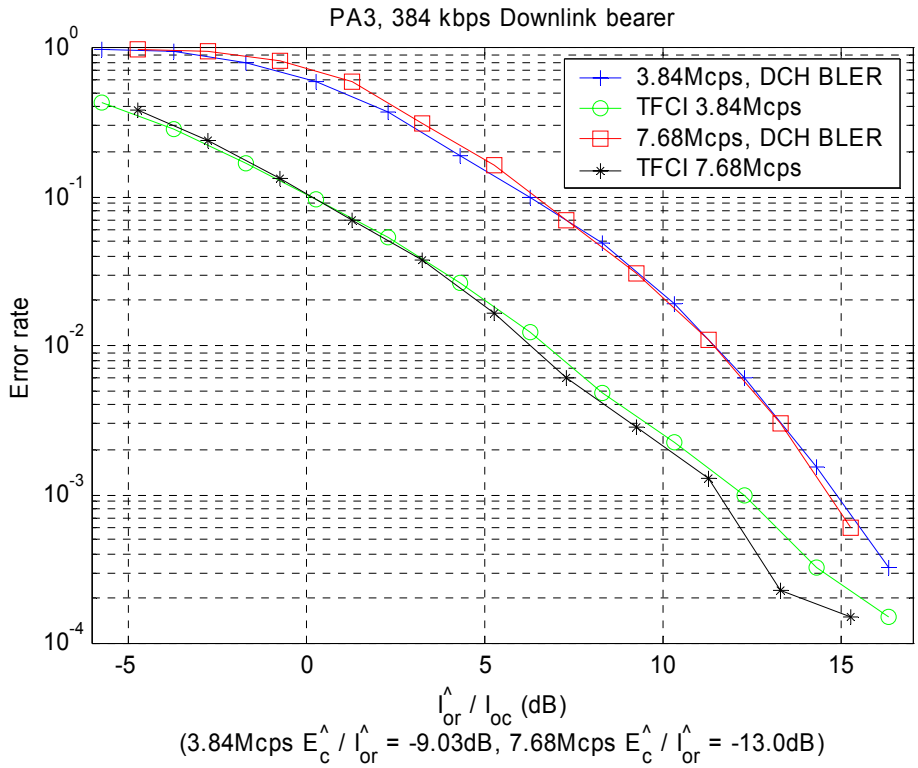

Figure 20 - Link Level Results for 384kbps Bearer, Downlink, PA3, (mean $\hat{I}_{or}/I_{oc}$)

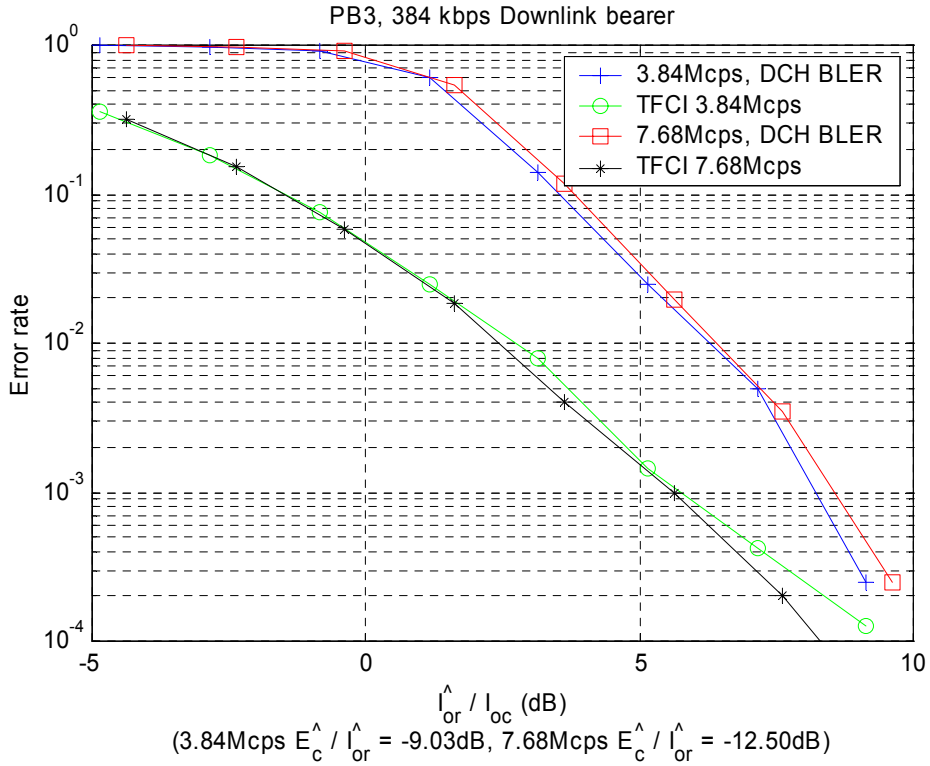

Figure 21- Link Level Results for 384kbps Bearer, Downlink, PB3, (mean $\hat{I}_{or}/I_{oc}$)

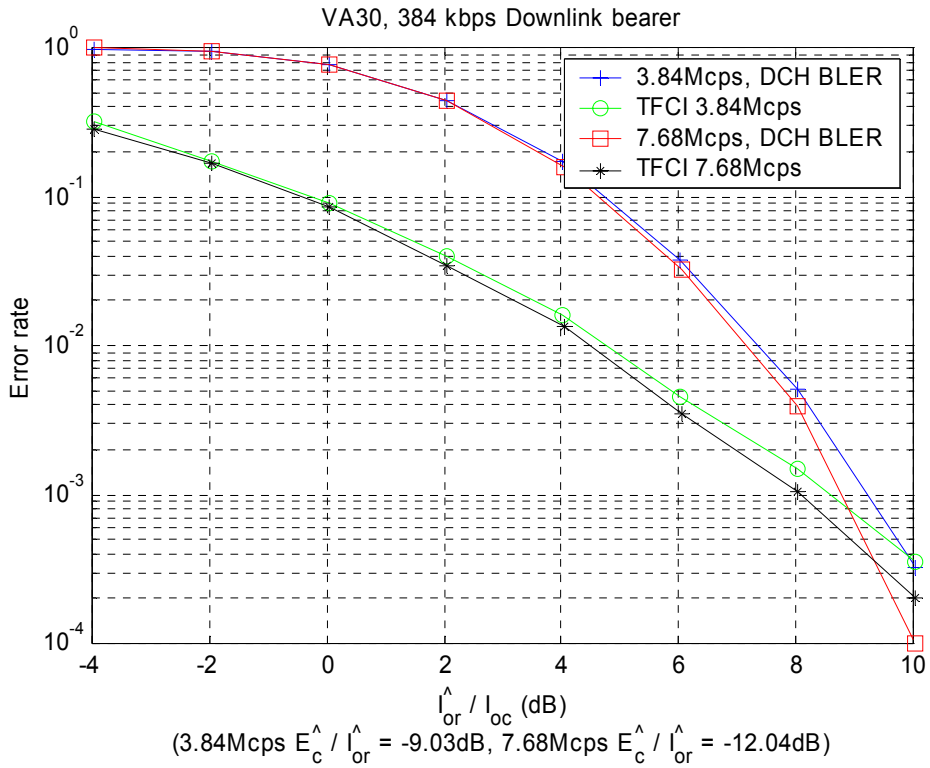

Figure 22 - Link Level Results for 384kbps Bearer, Downlink, VA30, (mean $\hat{I}_{or}/I_{oc}$)

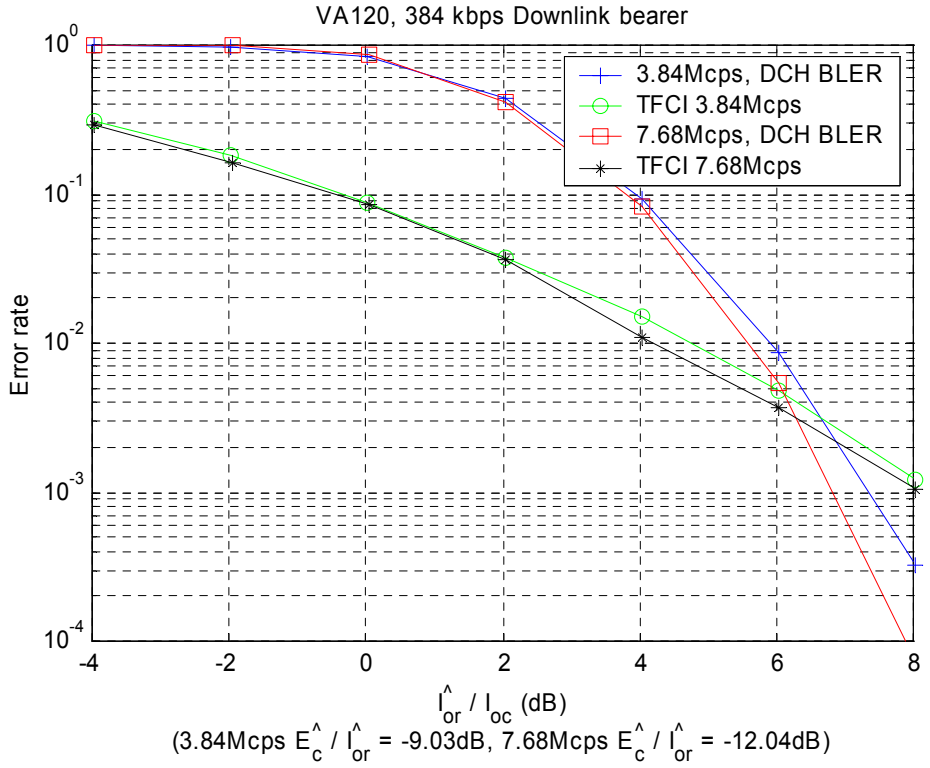

Figure 23 - Link Level Results for 384kbps Bearer, Downlink, VA120, (mean $\hat{I}_{or}/I_{oc}$)

A summary of performance with respect to mean $\hat{I}_{or}/I_{oc}$ (figures 19 to 23) including calculated E_b / N_0 for the 384kbps bearer is provided in Table 17:

Table 17 - Link Level Performance Summary, Downlink 384kps Bearer

Chip rate (Mcps)	Channel	BLER (%)	$\hat{I}_{or}/I_{oc}$ (dB)	$\hat{E}_c/\hat{I}_{or}$ (dB)	E_b/N_0 (dB)
3.84	AWGN	10%	0.07	-9.03	2.88
3.84	AWGN	1%	0.27	-9.03	3.08
3.84	PA3	10%	6.26	-9.03	9.07
3.84	PA3	1%	11.42	-9.03	14.23
3.84	PB3	10%	3.55	-9.03	6.36
3.84	PB3	1%	6.28	-9.03	9.09
3.84	VA30	10%	4.74	-9.03	7.55
3.84	VA30	1%	7.34	-9.03	10.15
3.84	VA120	10%	3.95	-9.03	6.76
3.84	VA120	1%	5.91	-9.03	8.72
7.68	AWGN	10%	-0.15	-12.04	2.66
7.68	AWGN	1%	0.03	-12.04	2.84
7.68	PA3	10%	6.41	-13.00	8.26
7.68	PA3	1%	11.41	-13.00	13.26
7.68	PB3	10%	3.79	-12.50	6.14
7.68	PB3	1%	6.40	-12.50	8.75
7.68	VA30	10%	4.61	-12.04	7.42
7.68	VA30	1%	7.15	-12.04	9.96
7.68	VA120	10%	3.79	-12.04	6.60
7.68	VA120	1%	5.59	-12.04	8.40

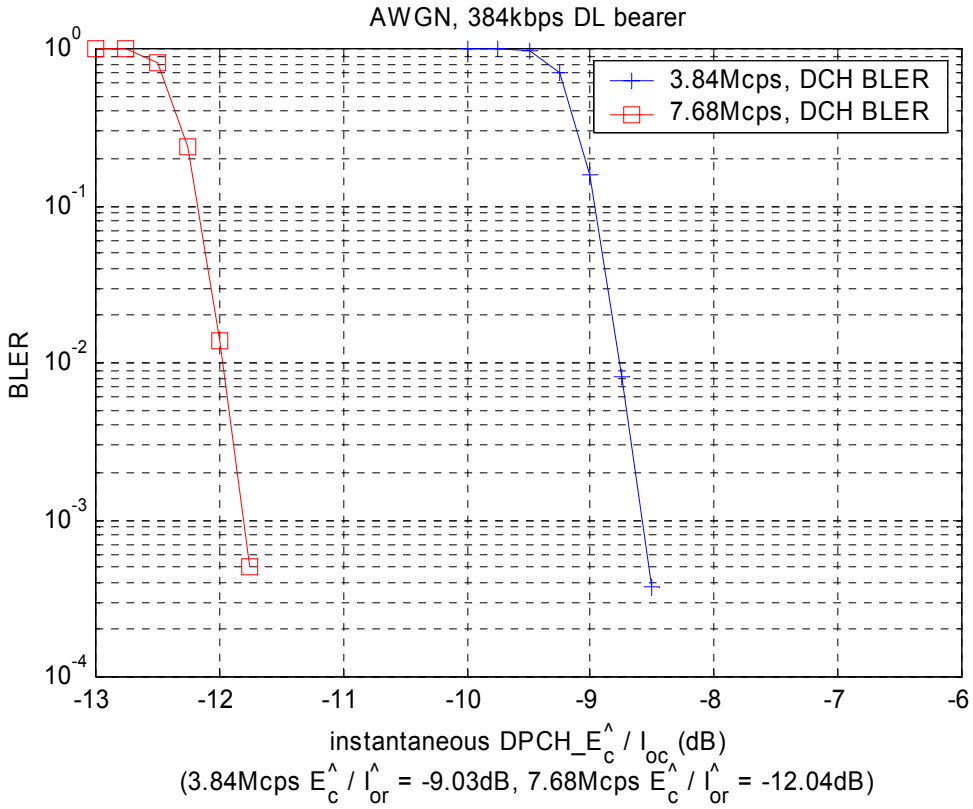

Figure 24 – Link Level Results for 384kbps Bearer, Downlink, AWGN, (instantaneous $DPCH\_\hat{E}_c / I_{oc}$)

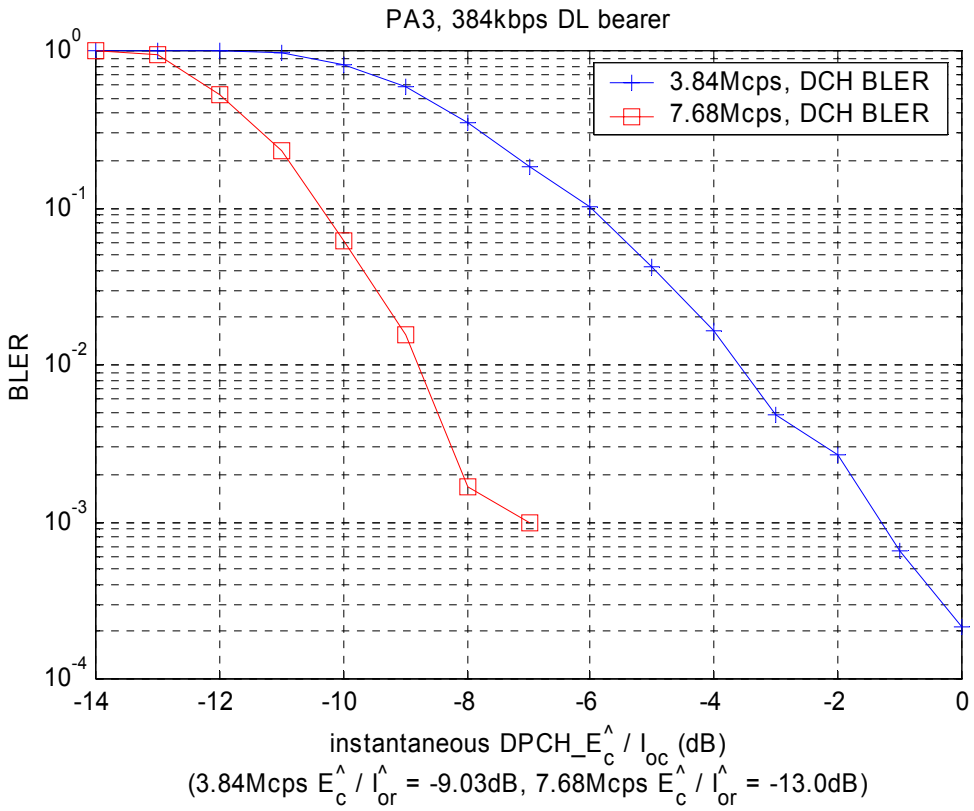

Figure 25 – Link Level Results for 384kbps Bearer, Downlink, PA3, (instantaneous $DPCH\_\hat{E}_c / I_{oc}$)

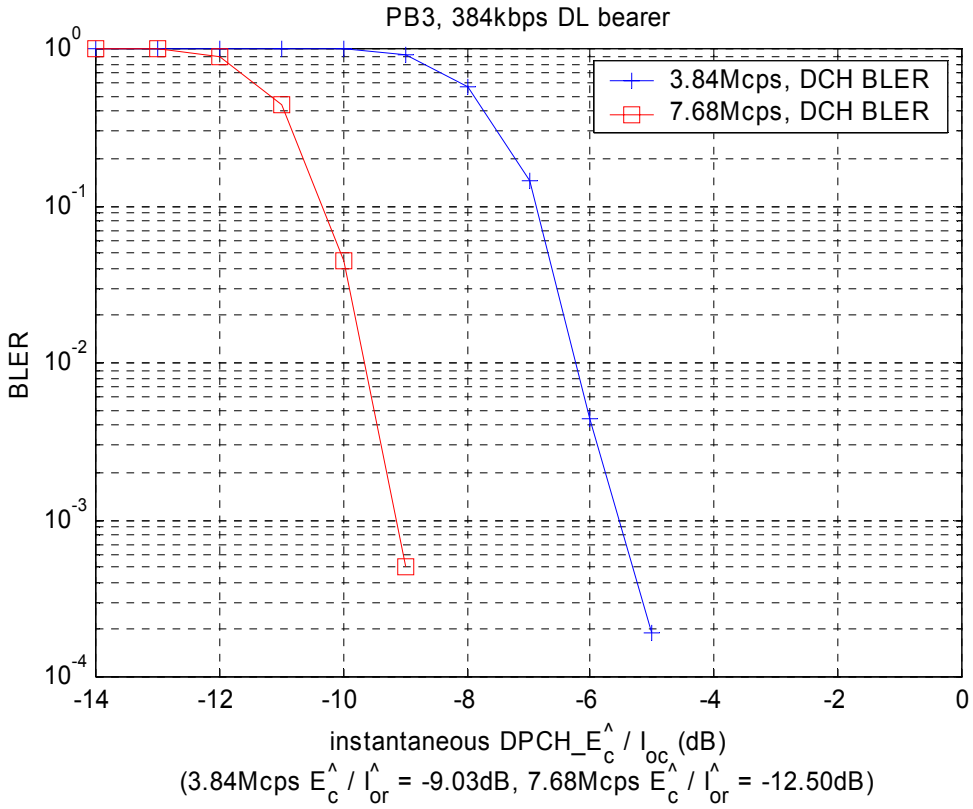

Figure 26 – Link Level Results for 384kbps Bearer, Downlink, PB3, (instantaneous $DPCH\_\hat{E}_c / I_{oc}$)

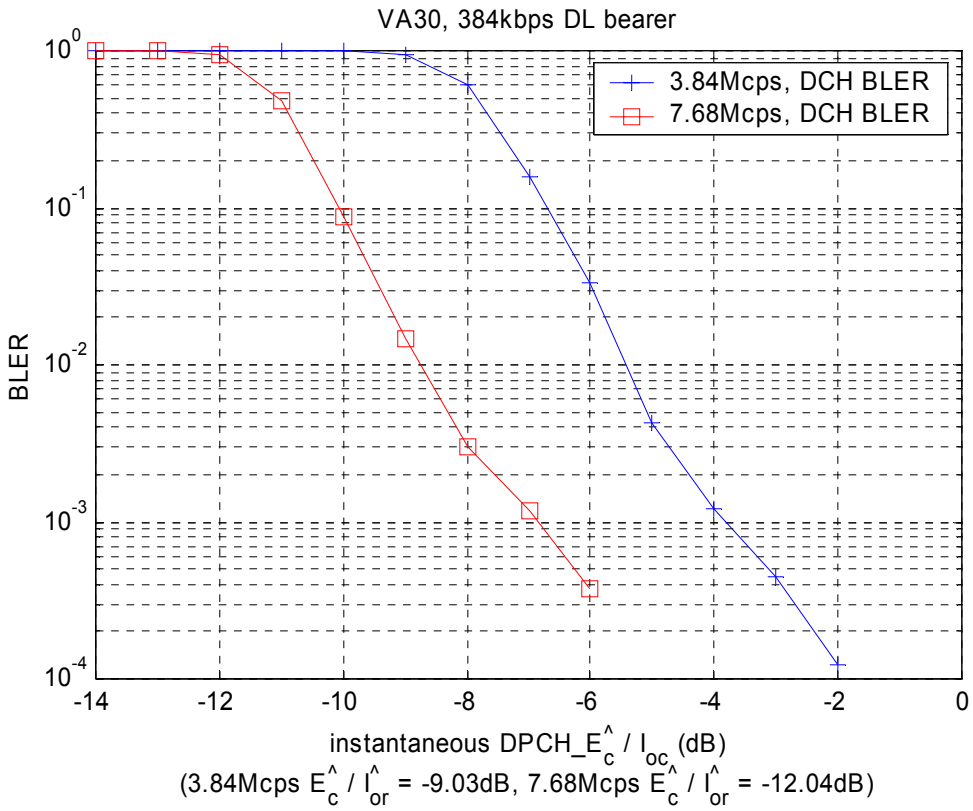

Figure 27 – Link Level Results for 384kbps Bearer, Downlink, VA30, (instantaneous $DPCH\_\hat{E}_c / I_{oc}$)

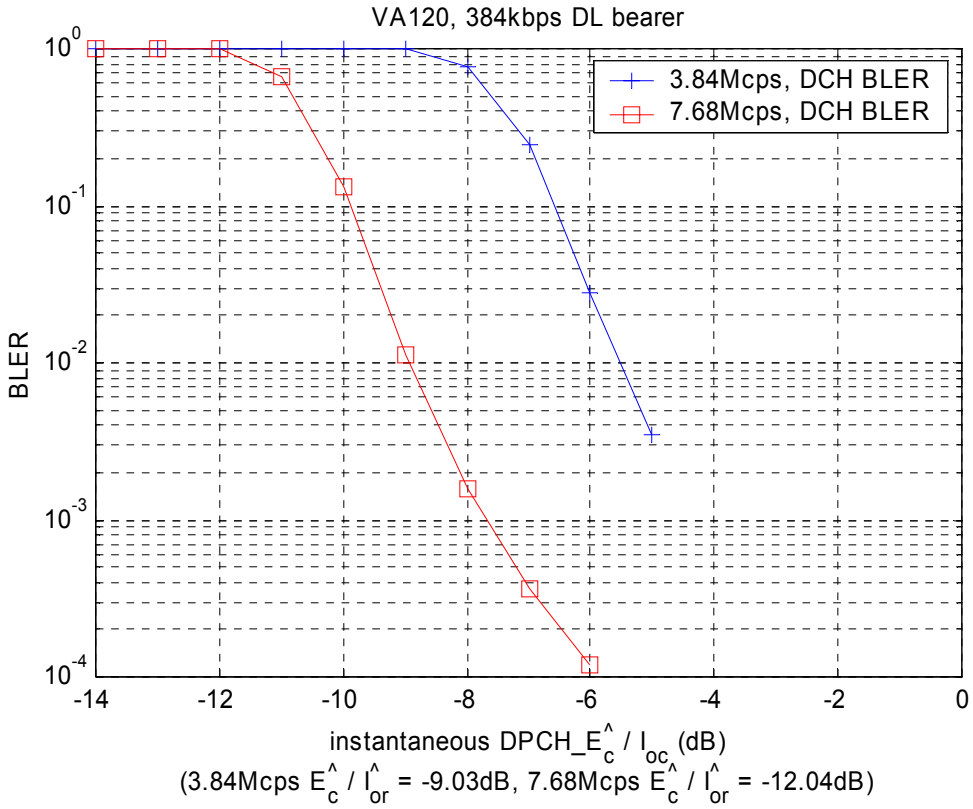

Figure 28 – Link Level Results for 384kbps Bearer, Downlink, VA120, (instantaneous $DPCH\_\hat{E}_c / I_{oc}$)

5.2.1.3 Uplink 12.2kbps

Simulation notes

- Results for DTCH DCH, TFCI and TPC are shown.
- Open inner loop power control is in operation for *all* UEs, with the UEs measuring the power of the beacon transmission on the principal antenna and the uplink transmission commencing 4 timeslots later.
- 50% of the code space is occupied at both chip rates comprising the user of interest and the intracell interfers.
- At 3.84Mcps the bearer of interest occupies 1 code at SF = 8 per timeslot and 1 timeslot per frame. The intracell interference occupies 6 codes at SF = 16 per timeslot.
- At 7.68Mcps the bearer of interest occupies 1 code at SF = 16 per timeslot and 1 timeslot per frame. The intracell interference is 7 users each with 2 codes of SF = 32 per timeslot.
- Code rate:
  - (244+16) / 724 = 0.36
- Processing gain:
  - 3.84Mcps (0.801*(2560-96)) / 122 = 12.09dB.
  - 7.68Mcps 2*(0.801*(2560-96)) / 122 = 15.10dB

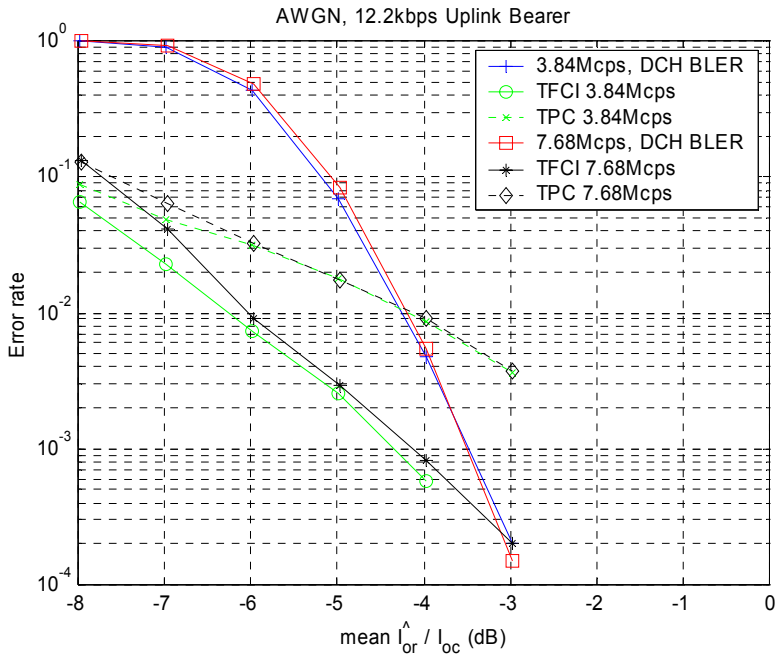

Figure 29 - Link Level Results for 12.2kbps Bearer, Uplink, AWGN, (mean $\hat{I}_{or}/I_{oc}$)

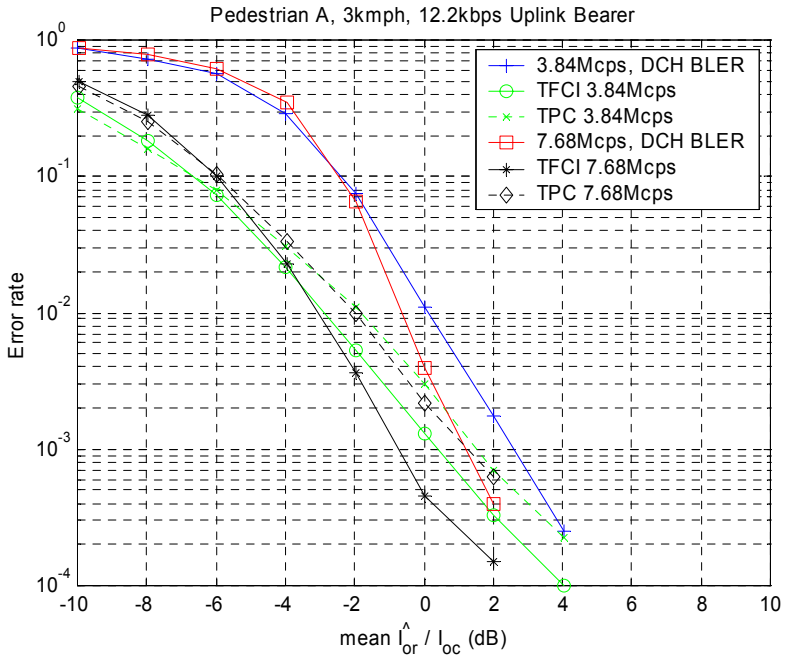

Figure 30 - Link Level Results for 12.2kbps Bearer, Uplink, PA3, (mean $\hat{I}_{or}/I_{oc}$)

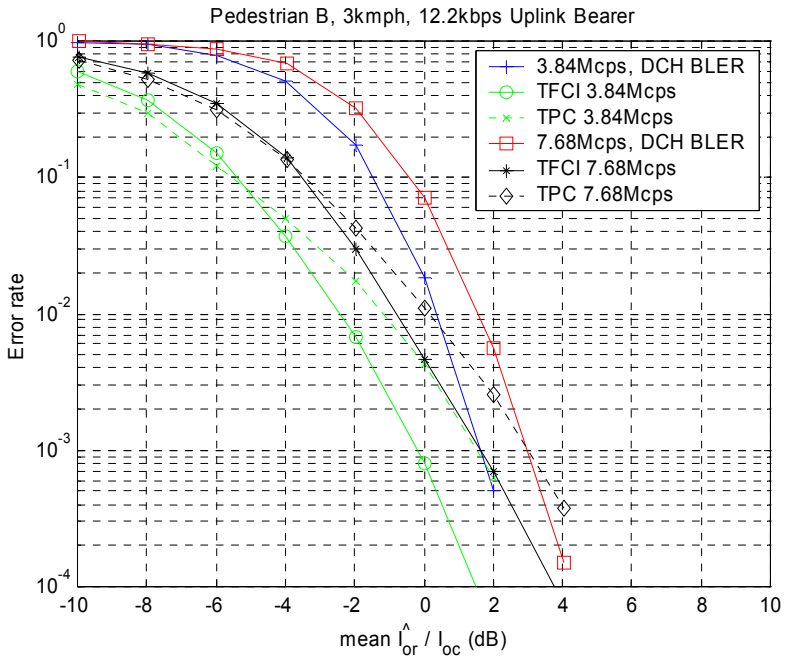

Figure 31- Link Level Results for 12.2kbps Bearer, Uplink, PB3, (mean $\hat{I}_{or}/I_{oc}$)

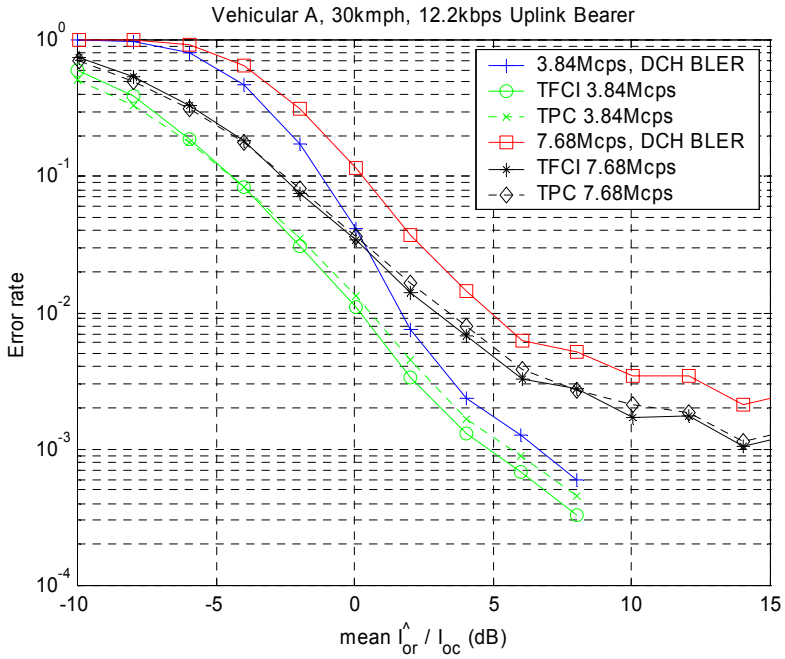

Figure 32 - Link Level Results for 12.2kbps Bearer, Uplink, VA30, (mean $\hat{I}_{or}/I_{oc}$)

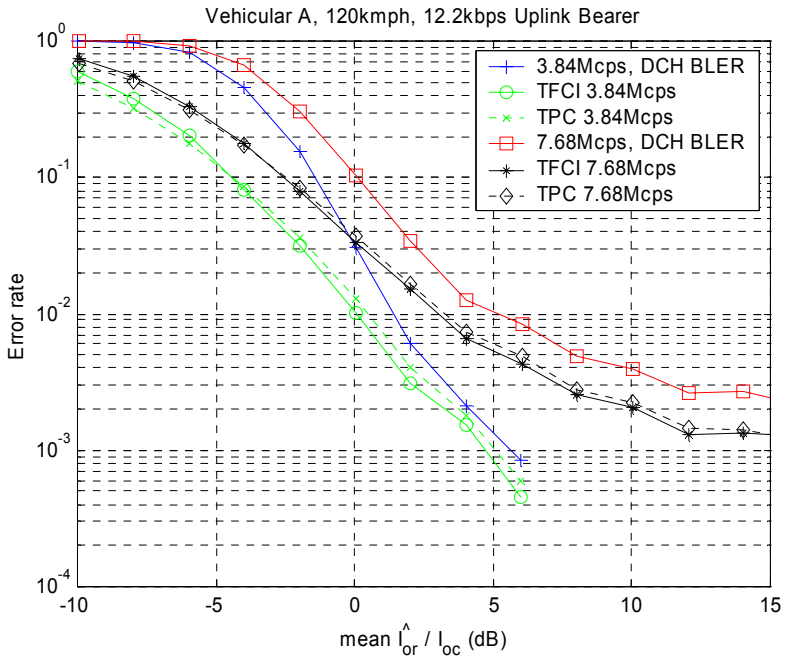

Figure 33 - Link Level Results for 12.2kbps Bearer, Uplink, VA120, (mean $\hat{I}_{or}/I_{oc}$)

A summary of performance with respect to mean $\hat{I}_{or}/I_{oc}$ (figures 29 to 33) including calculated E_b / N_0 for the 12.2kbps bearer is provided in Table 18:

Table 18 – Link Level Performance Summary, Uplink 12.2kbps bearer

Chip rate (Mcps)	Channel	DCH BLER (%)	P.G. (dB)	$\hat{I}_{or}/I_{oc}$ (dB)	# Rx antenna (dB)	$\hat{E}_c/\hat{I}_{or}$ (dB)	E_b/N_0 (dB)	~ TPC error rate
3.84	AWGN	10%	12.09	-5.18	3.01	-6.02	3.90	-
3.84	AWGN	1%	12.09	-4.26	3.01	-6.02	4.82	0.010
3.84	PA3	10%	12.09	-2.42	3.01	-6.02	6.66	-
3.84	PA3	1%	12.09	0.13	3.01	-6.02	9.21	0.003
3.84	PB3	10%	12.09	-1.50	3.01	-6.02	7.58	-
3.84	PB3	1%	12.09	0.36	3.01	-6.02	9.44	0.003
3.84	VA30	10%	12.09	-1.23	3.01	-6.02	7.85	-
3.84	VA30	1%	12.09	1.68	3.01	-6.02	10.76	0.005
3.84	VA120	10%	12.09	-1.44	3.01	-6.02	7.64	-
3.84	VA120	1%	12.09	1.40	3.01	-6.02	10.48	0.006
7.68	AWGN	10%	15.10	-5.07	3.01	-9.03	4.01	-
7.68	AWGN	1%	15.10	-4.19	3.01	-9.03	4.89	0.010
7.68	PA3	10%	15.10	-2.47	3.01	-9.03	6.61	-
7.68	PA3	1%	15.10	-0.63	3.01	-9.03	8.45	0.003
7.68	PB3	10%	15.10	-0.42	3.01	-9.03	8.66	-
7.68	PB3	1%	15.10	1.58	3.01	-9.03	10.66	0.003
7.68	VA30	10%	15.10	0.28	3.01	-9.03	9.33	-
7.68	VA30	1%	15.10	4.92	3.01	-9.03	14.00	0.006
7.68	VA120	10%	15.10	0.11	3.01	-9.03	9.19	-
7.68	VA120	1%	15.10	5.15	3.01	-9.03	14.23	0.006

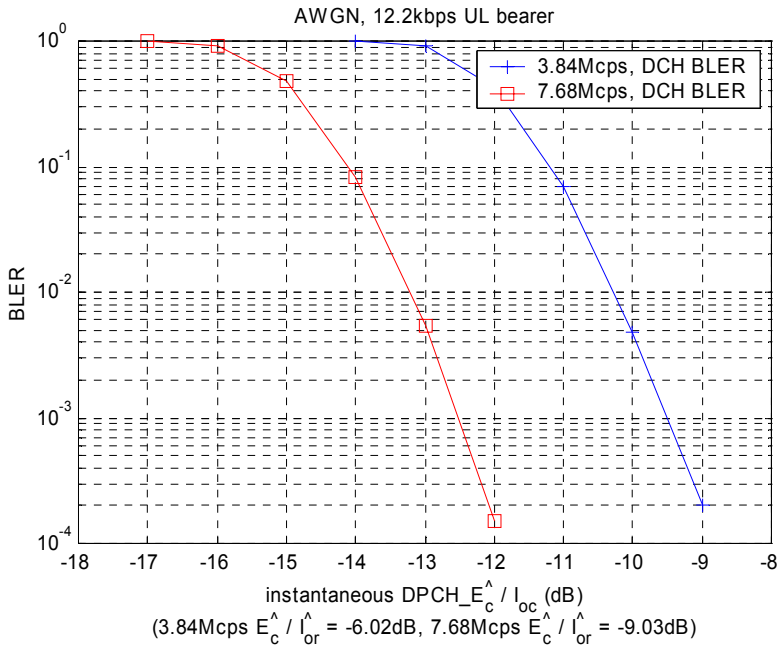

Figure 34 – Link Level Results for 12.2kbps Bearer, Uplink, AWGN, (instantaneous $DPCH\_\hat{E}_c / I_{oc}$)

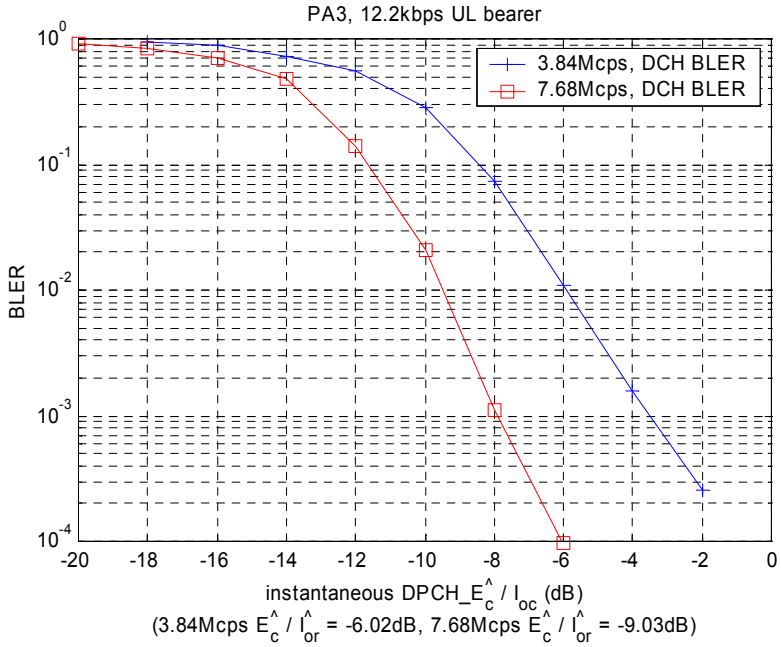

Figure 35 – Link Level Results for 12.2kbps Bearer, Uplink, PA3, (instantaneous $DPCH\_\hat{E}_c / I_{oc}$)

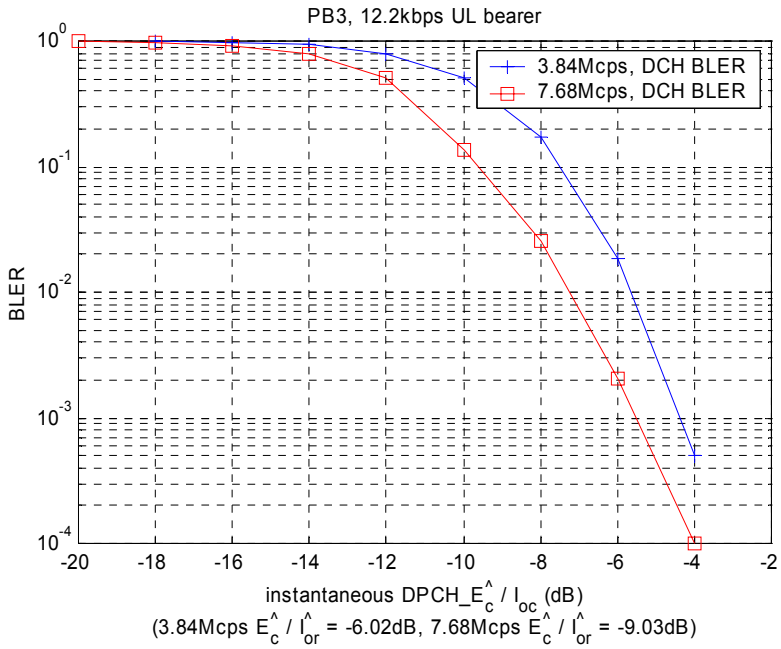

Figure 36 – Link Level Results for 12.2kbps Bearer, Uplink, PB3, (instantaneous $DPCH\_\hat{E}_c / I_{oc}$)

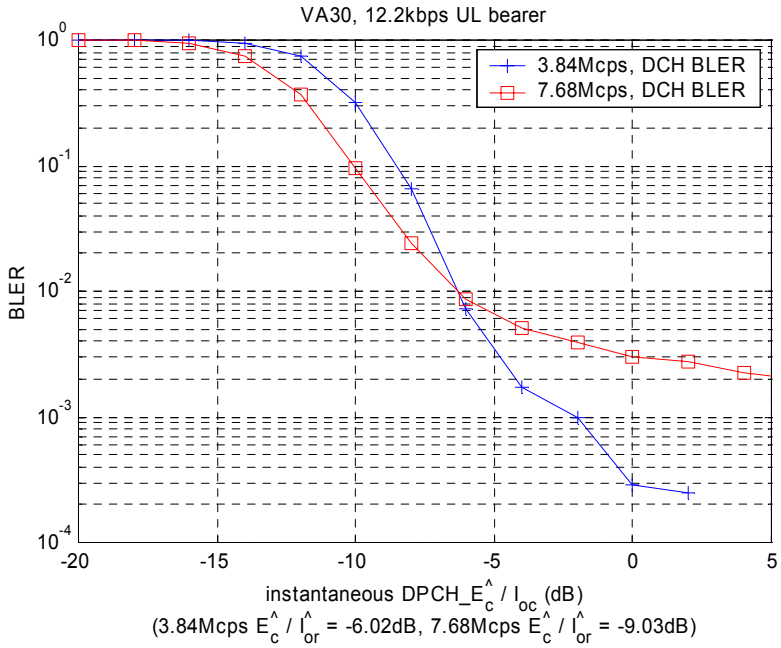

Figure 37 – Link Level Results for 12.2kbps Bearer, Uplink, VA30, (instantaneous $DPCH\_\hat{E}_c / I_{oc}$)

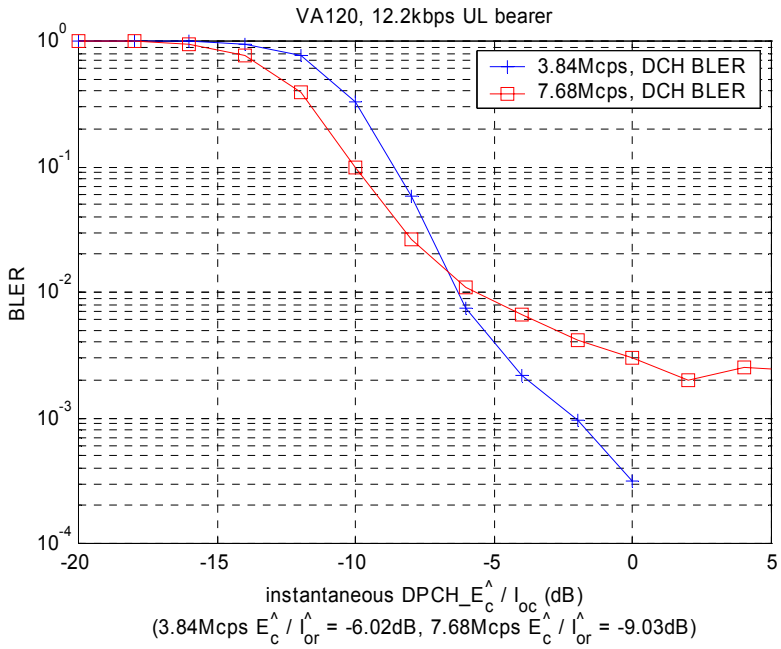

Figure 38 – Link Level Results for 12.2kbps Bearer, Uplink, VA120, (instantaneous $DPCH\_\hat{E}_c / I_{oc}$)

5.2.1.4 Uplink 384kbps

Simulation notes

- Results for DTCH DCH, TFCI and TPC are shown.
- Open inner loop power control is in operation for *all* UEs, with the UEs measuring the power of the beacon transmission on the principal antenna and the uplink transmission commencing 4 timeslots later.
- 50% of the code space is occupied at both chip rates comprising the user of interest and the intracell interfers.
- At 3.84Mcps the bearer of interest occupies 1 code at SF = 2 per timeslot and 3 timeslots per frame. There is no intracell interference.
- At 7.68Mcps the bearer of interest occupies 1 code at SF = 4 per timeslot and 3 timeslots per frame. The intracell interference is 4 users each with 2 codes of SF = 32 per timeslot.
- Code rate:
  - (3840+16) / 6429 = 0.60
- Processing gain:
  - 3.84Mcps (0.9921*3*(2560-96)) / 3840 = 2.81dB.
  - 7.68Mcps 2*(0.9921*3*(2560-96)) / 3840 = 5.82dB

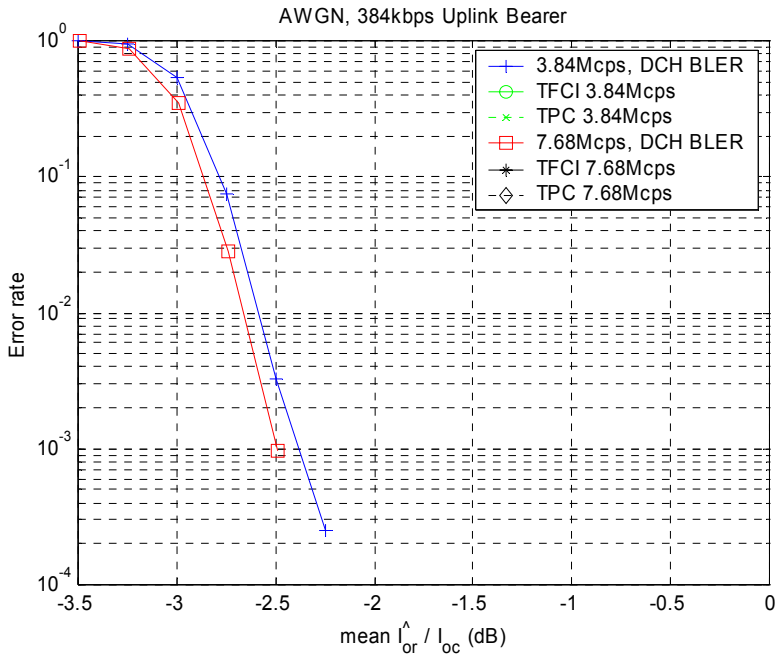

Figure 39 - Link Level Results for 384kbps Bearer, Uplink, AWGN, (mean $\hat{I}_{or}/I_{oc}$)

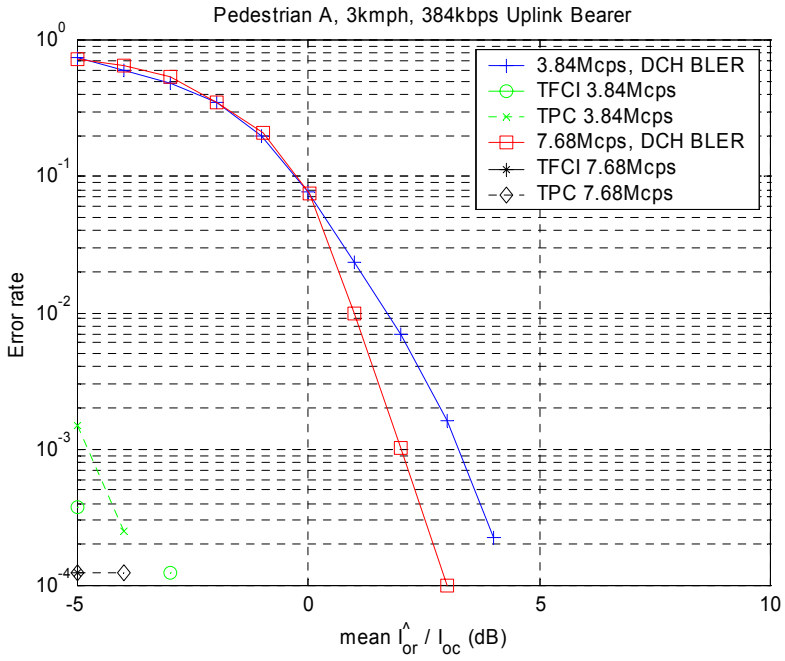

Figure 40 - Link Level Results for 384kbps Bearer, Uplink, PA3, (mean $\hat{I}_{or}/I_{oc}$)

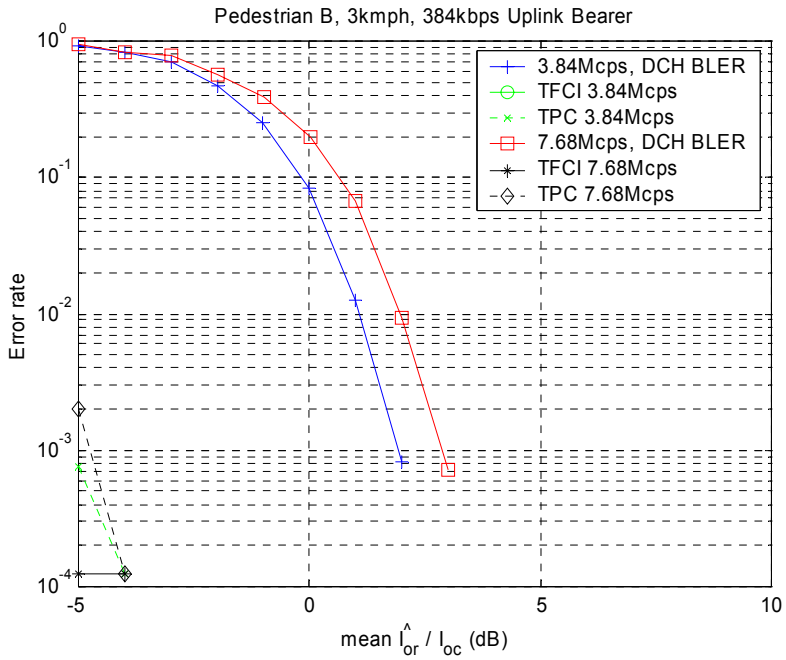

Figure 41- Link Level Results for 384kbps Bearer, Uplink, PB3, (mean $\hat{I}_{or}/I_{oc}$)

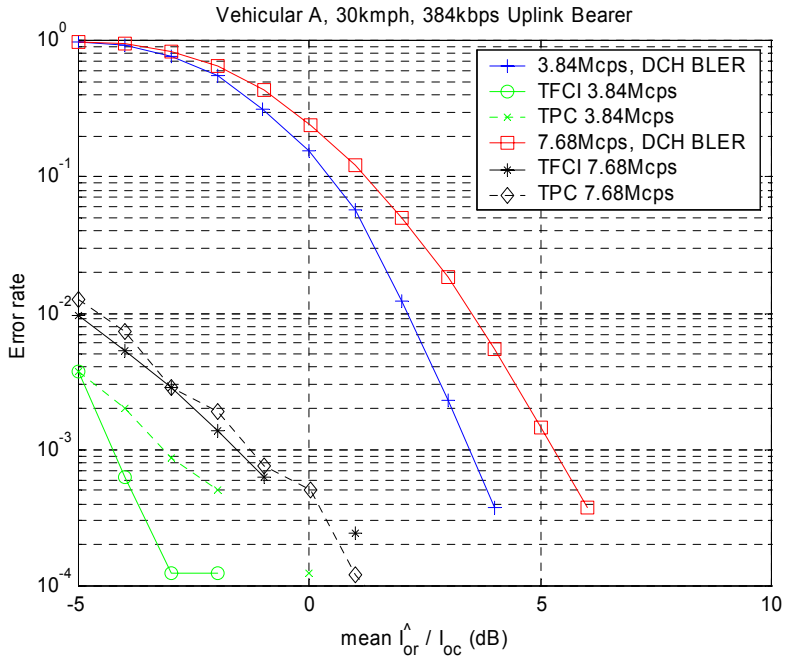

Figure 42 - Link Level Results for 384kbps Bearer, Uplink, VA30, (mean $\hat{I}_{or}/I_{oc}$)

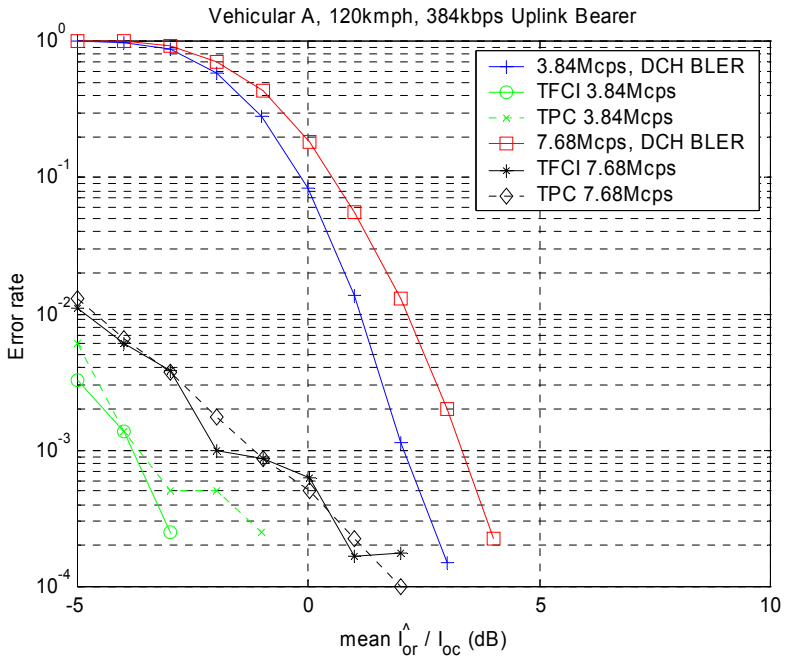

Figure 43 - Link Level Results for 384kbps Bearer, Uplink, VA120, (mean $\hat{I}_{or}/I_{oc}$)

A summary of performance with respect to mean $\hat{I}_{or}/I_{oc}$ (figures 39 to 43) including calculated E_b / N_0 for the 384kbps bearer is provided in Table 19:

Table 19 – Link Level Performance Summary, Uplink 384kbps bearer

Chip rate (Mcps)	Channel	DCH BLER (%)	P.G. (dB)	$\hat{I}_{or}/I_{oc}$ (dB)	# Rx antenna (dB)	$\hat{E}_c/\hat{I}_{or}$ (dB)	E_b/N_0 (dB)	~ TPC error rate
3.84	AWGN	10%	2.81	-2.79	3.01	0	3.03	-
3.84	AWGN	1%	2.81	-2.59	3.01	0	3.23	< 0.0001
3.84	PA3	10%	2.81	-0.28	3.01	0	5.54	-
3.84	PA3	1%	2.81	1.70	3.01	0	7.52	< 0.0001
3.84	PB3	10%	2.81	-0.17	3.01	0	5.65	-
3.84	PB3	1%	2.81	1.09	3.01	0	6.91	< 0.0001
3.84	VA30	10%	2.81	0.44	3.01	0	6.26	-
3.84	VA30	1%	2.81	2.13	3.01	0	7.95	< 0.0001
3.84	VA120	10%	2.81	-0.16	3.01	0	5.66	-
3.84	VA120	1%	2.81	1.12	3.01	0	6.94	< 0.0001
7.68	AWGN	10%	5.82	-2.87	3.01	-3.01	2.95	-
7.68	AWGN	1%	5.82	-2.66	3.01	-3.01	3.16	< 0.0001
7.68	PA3	10%	5.82	-0.27	3.01	-3.01	5.55	-
7.68	PA3	1%	5.82	1.01	3.01	-3.01	6.83	< 0.0001
7.68	PB3	10%	5.82	0.64	3.01	-3.01	6.46	-
7.68	PB3	1%	5.82	1.97	3.01	-3.01	7.79	< 0.0001
7.68	VA30	10%	5.82	1.22	3.01	-3.01	7.04	-
7.68	VA30	1%	5.82	3.51	3.01	-3.01	9.33	< 0.0001
7.68	VA120	10%	5.82	0.52	3.01	-3.01	6.34	-
7.68	VA120	1%	5.82	2.15	3.01	-3.01	7.97	< 0.0001

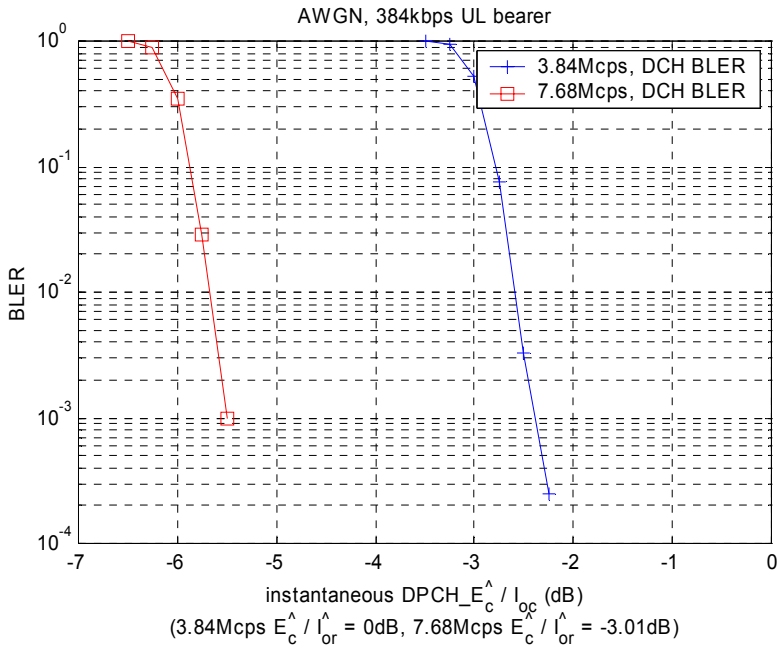

Figure 44 – Link Level Results for 384kbps Bearer, Uplink, AWGN, (instantaneous $DPCH\_\hat{E}_c / I_{oc}$)

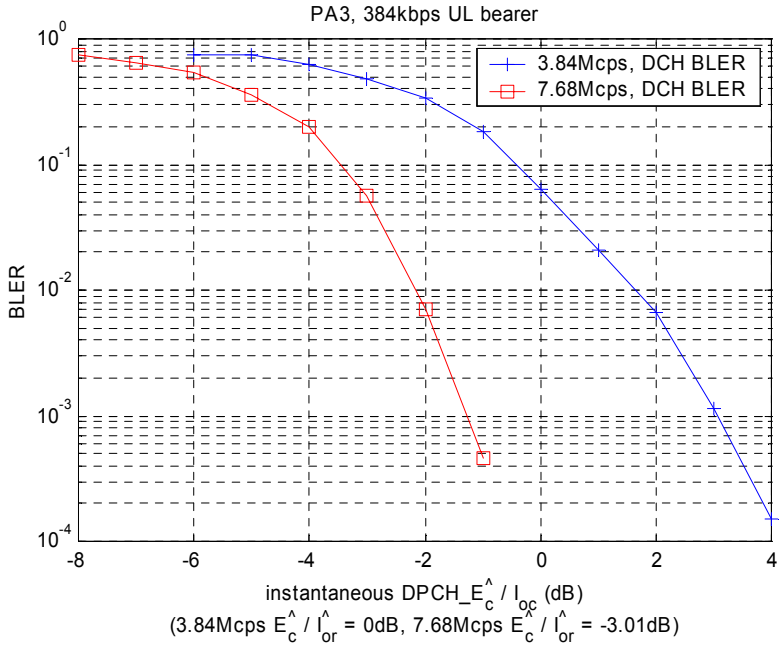

Figure 45 – Link Level Results for 384kbps Bearer, Uplink, PA3, (instantaneous $DPCH\_\hat{E}_c / I_{oc}$)

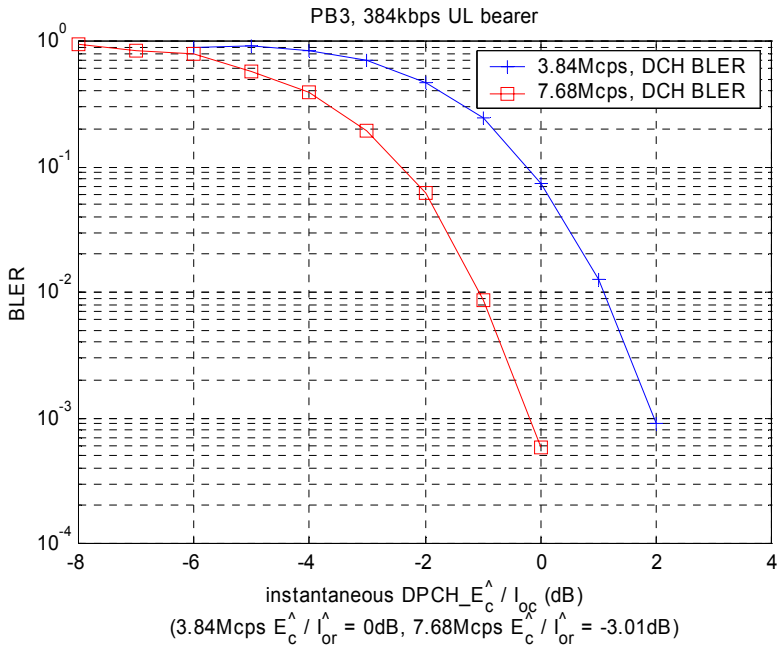

Figure 46 – Link Level Results for 384kbps Bearer, Uplink, PB3, (instantaneous $DPCH\_\hat{E}_c / I_{oc}$)

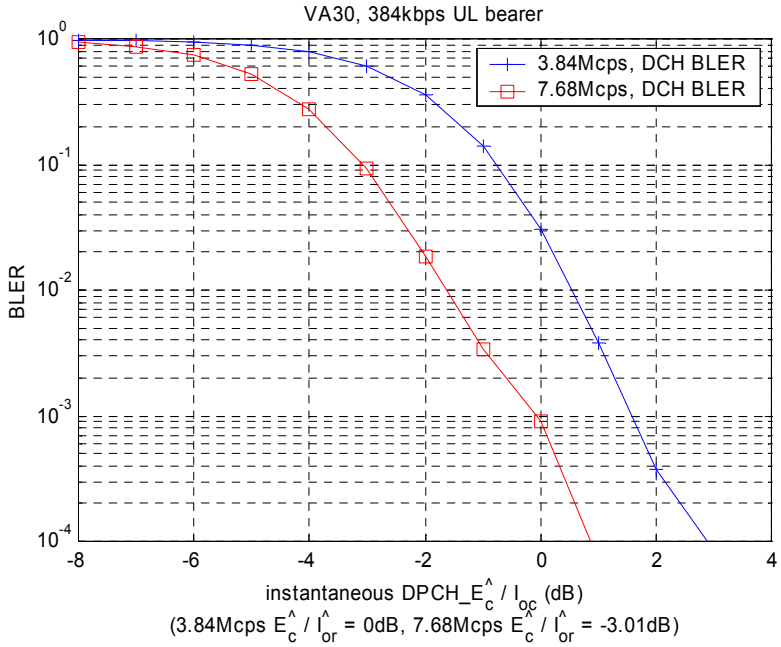

Figure 47 – Link Level Results for 384kbps Bearer, Uplink, VA30, (instantaneous $DPCH\_\hat{E}_c / I_{oc}$)

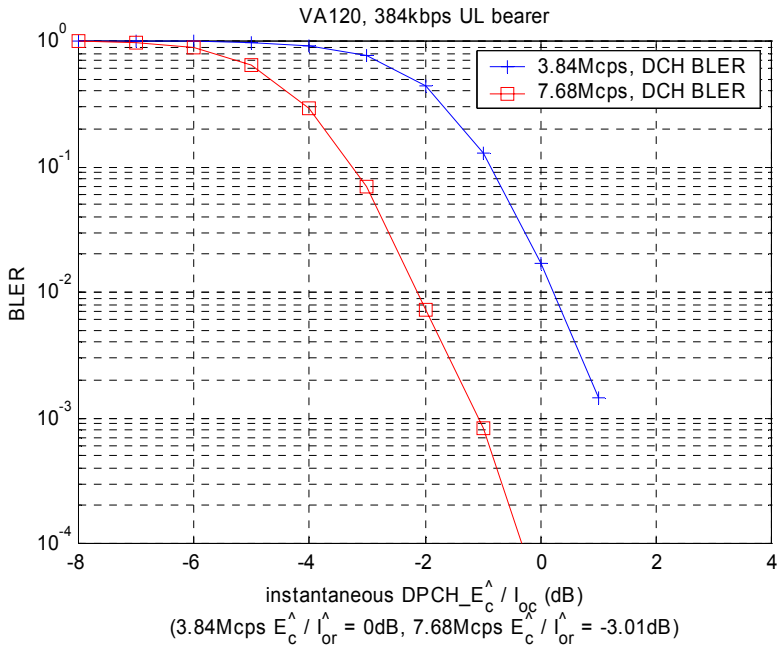

Figure 48 – Link Level Results for 384kbps Bearer, Uplink, VA120, (instantaneous $DPCH\_\hat{E}_c / I_{oc}$)

5.2.2 Release 5 type (HSDPA) bearers

Link level results for 3.84Mcps and 7.68Mcps release 5 type HSDPA bearers are provided in the figures of this subclause according to table 20. Note that the "ID" in these figures refers to the fixed reference channel ID of Table A.1. At both the 3.84Mcps and 7.68Mcps chip rates, burst type 2 is used, the code utilization is 75% and the HSDPA bearer occupies 4 codes per timeslot.

Table 20 - List of Link Level Results Figures

figure	channel	mean / instantaneous	chip rate
49	AWGN	mean / instantaneous	3.84, 7.68
50	PA3	mean	3.84, 7.68
51	PB3	mean	3.84, 7.68
52	VA30	mean	3.84, 7.68
53	VA120	mean	3.84, 7.68
54	PA3	instantaneous	3.84, 7.68
55	PB3	instantaneous	3.84, 7.68
56	VA30	instantaneous	3.84, 7.68
57	VA120	instantaneous	3.84, 7.68

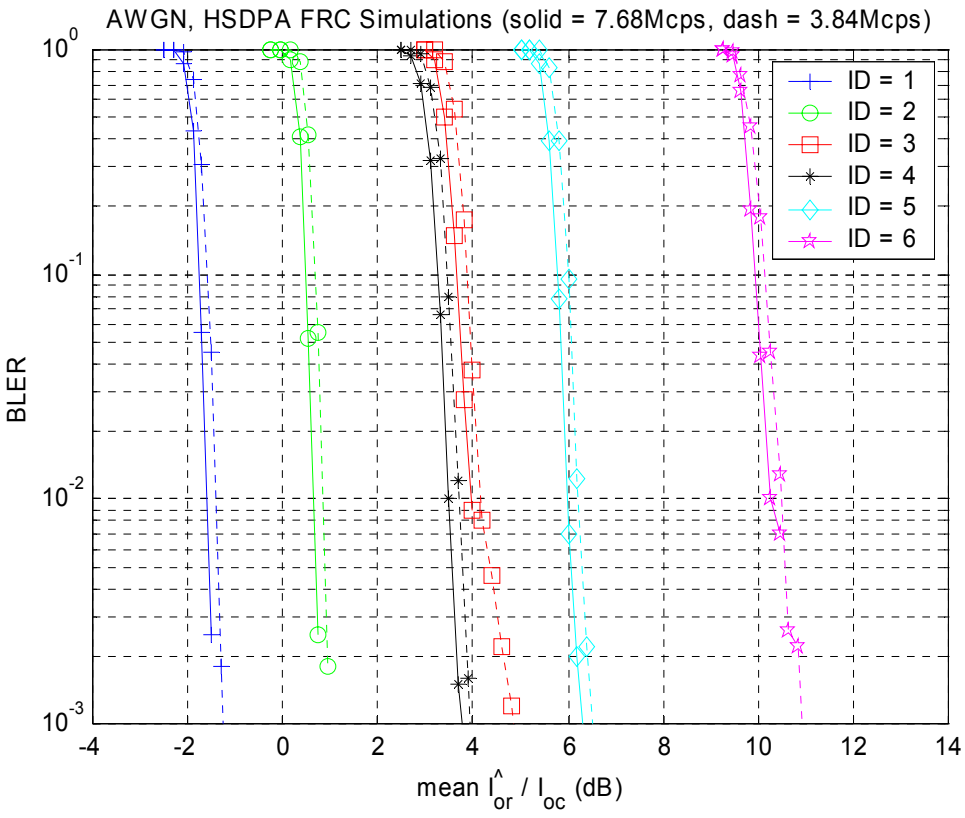

Figure 49 - Link level results for 3.84Mcps and 7.68Mcps HSDPA fixed reference channel simulations in AWGN (mean = instantaneous $\hat{I}_{or}/I_{oc}$)

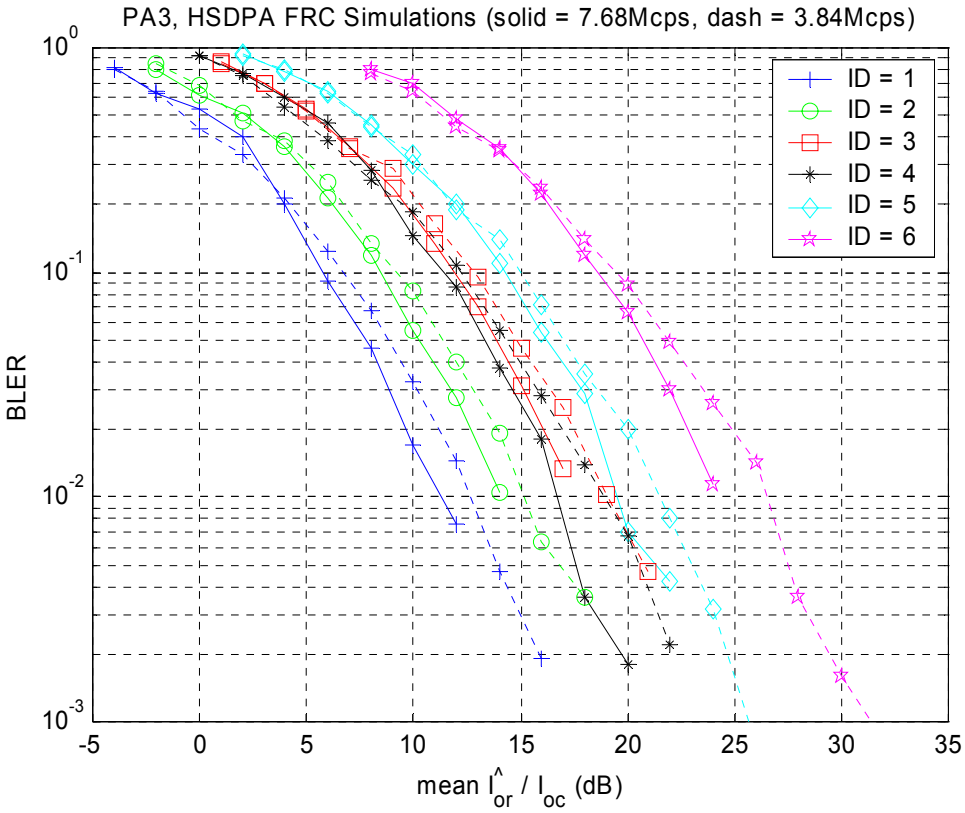

Figure 50 - Link level results for 3.84Mcps and 7.68Mcps HSDPA fixed reference channel simulations in PA3 (mean $\hat{I}_{or}/I_{oc}$)

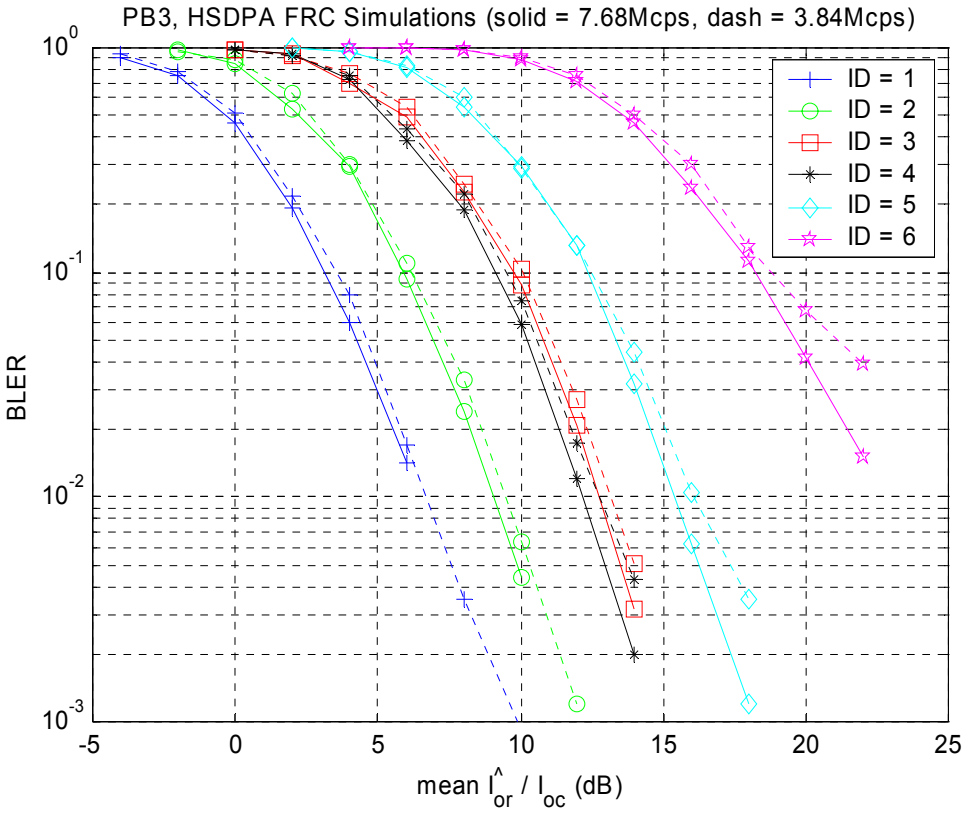

Figure 51 - Link level results for 3.84Mcps and 7.68Mcps HSDPA fixed reference channel simulations in PB3 (mean $\hat{I}_{or}/I_{oc}$)

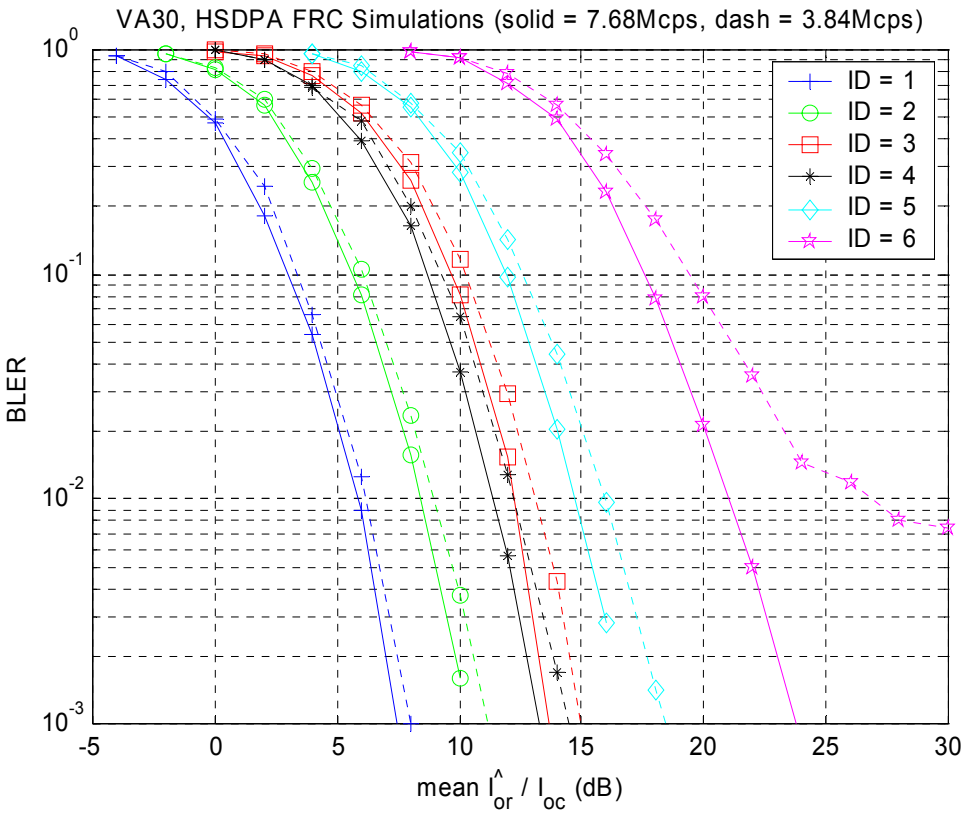

Figure 52 - Link level results for 3.84Mcps and 7.68Mcps HSDPA fixed reference channel simulations in VA30 (mean $\hat{I}_{or}/I_{oc}$)

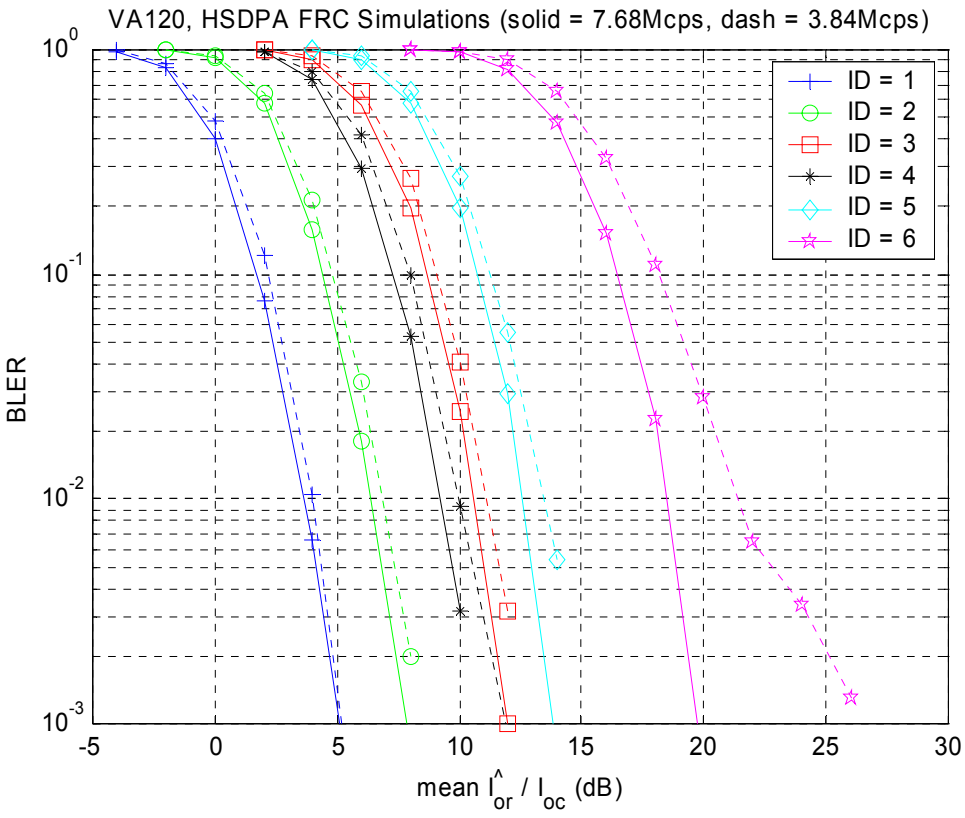

Figure 53 - Link level results for 3.84Mcps and 7.68Mcps HSDPA fixed reference channel simulations in VA120 (mean $\hat{I}_{or}/I_{oc}$)

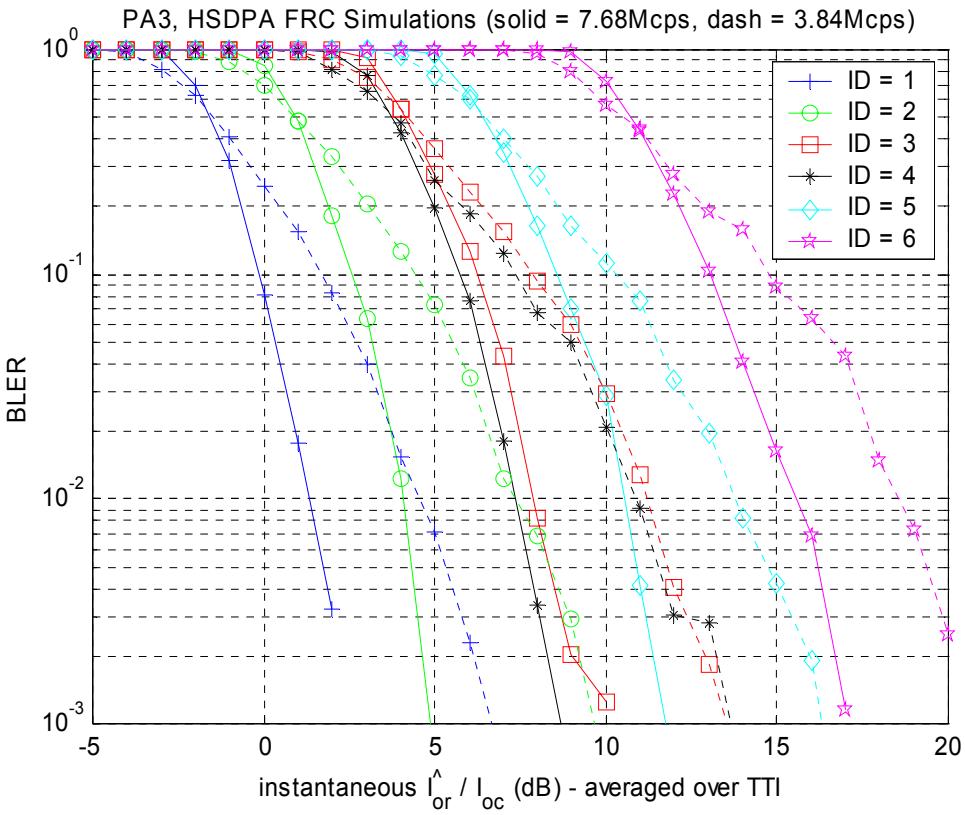

Figure 54 - Link level results for 3.84Mcps and 7.68Mcps HSDPA fixed reference channel simulations in PA3 (instantaneous $\hat{I}_{or}/I_{oc}$)

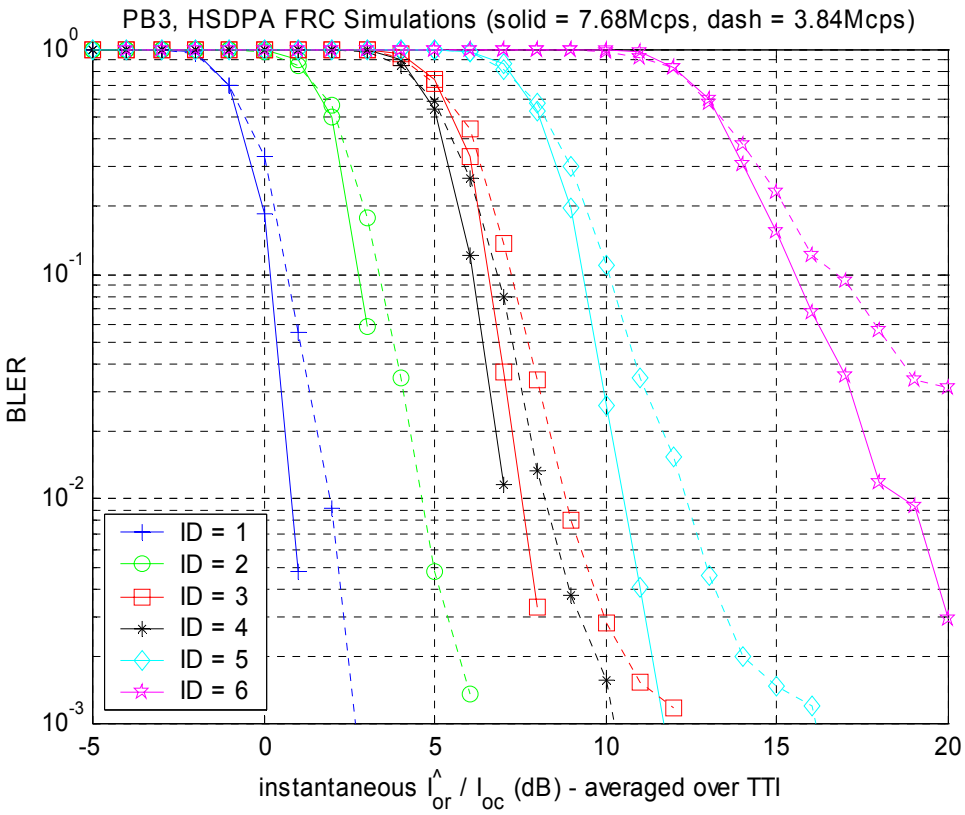

Figure 55 - Link level results for 3.84Mcps and 7.68Mcps HSDPA fixed reference channel simulations in PB3 (instantaneous $\hat{I}_{or}/I_{oc}$)

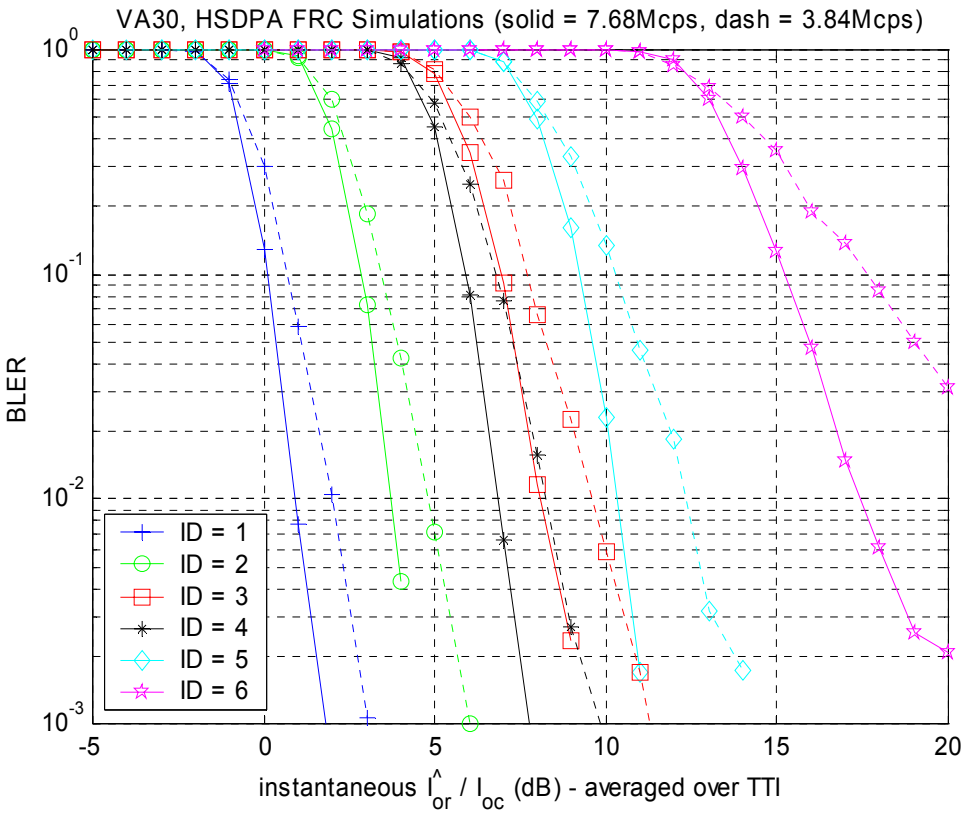

Figure 56 - Link level results for 3.84Mcps and 7.68Mcps HSDPA fixed reference channel simulations in VA30 (instantaneous $\hat{I}_{or}/I_{oc}$)

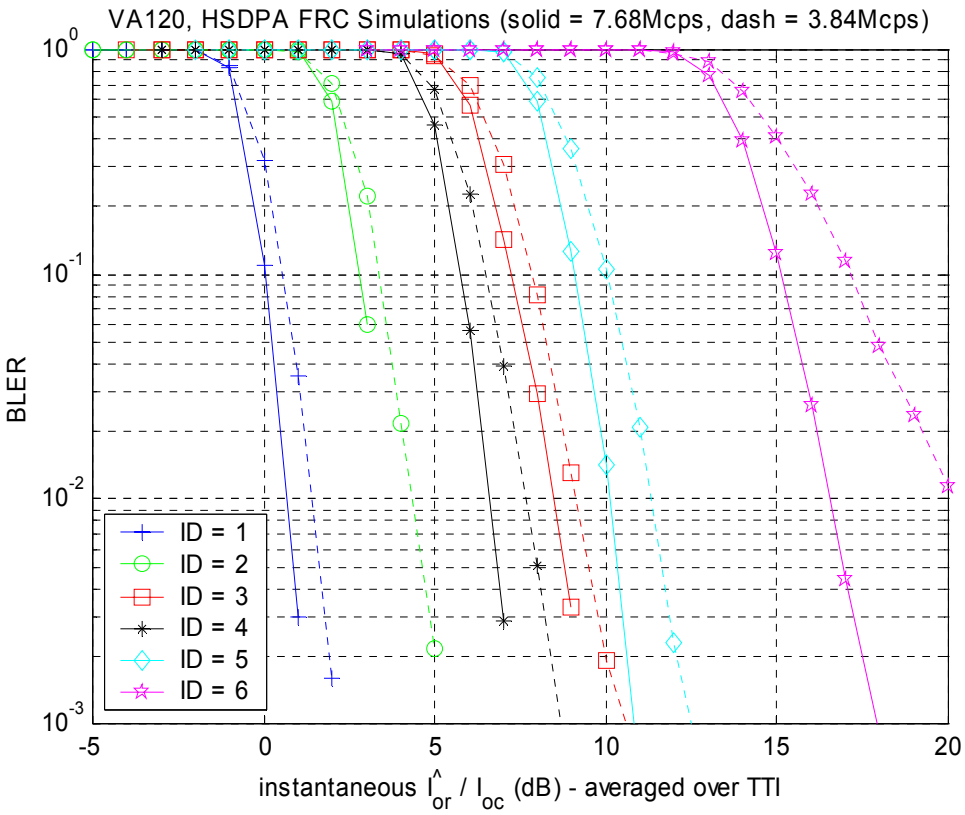

Figure 57 - Link level results for 3.84Mcps and 7.68Mcps HSDPA fixed reference channel simulations in VA120 (instantaneous $\hat{I}_{or}/I_{oc}$)

5.3 System Level Results

5.3.1 Release 99 / 4 type bearers

5.3.1.1 Simulation Assumptions

The simulation results presented in section 5.3.1 were performed using dynamic system simulations employing DCA, CAC and Release 99 uplink and downlink power control algorithms. The simulation assumptions of Annex B are applied to these simulations.

These simulations log the number of dropped calls, blocked calls, completed calls and satisfied users for a range of offered loads (expressed in Erlangs). A satisfied user is considered to be a user whose call is successfully completed (not blocked, not dropped) at an acceptable call quality (block error rate exceeds 10% for less than 5% of the call). The results of the 7.68Mcps TDD system are compared to those of two independent 3.84Mcps TDD systems (thus the "x-axis" of the graphs is "offered Erlangs per 10MHz").

5.3.1.2 Simulation Results

Simulation results are presented for a 12,2kbps bearer in channels AWGN, PA3, PB3, VA30 and VA120 in Figures 58, 59, 60, 61 and 62.

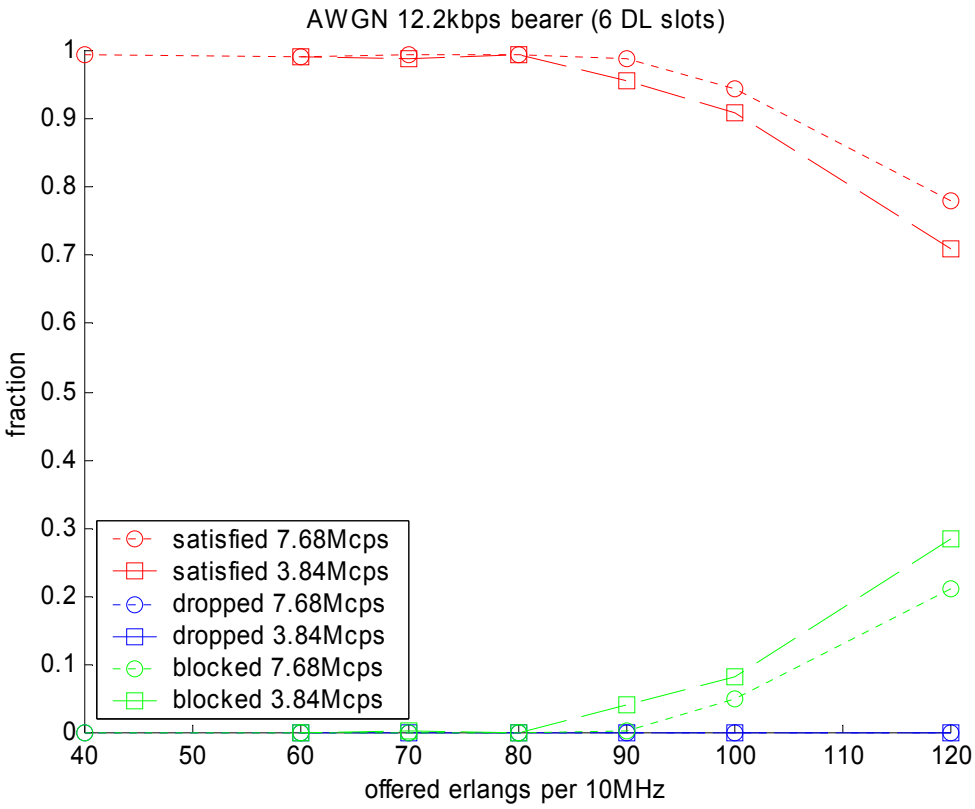

Figure 58 - System Level Results - 12.2kbps DCH bearer, AWGN

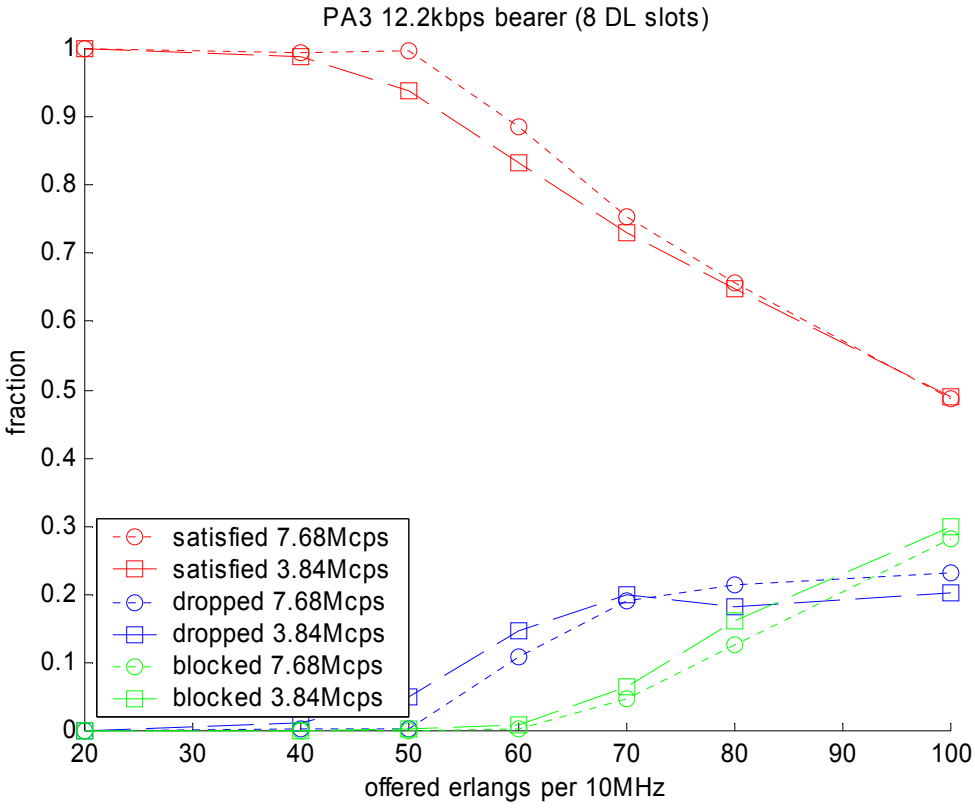

Figure 59 - System Level Results - 12.2kbps DCH bearer, PA3

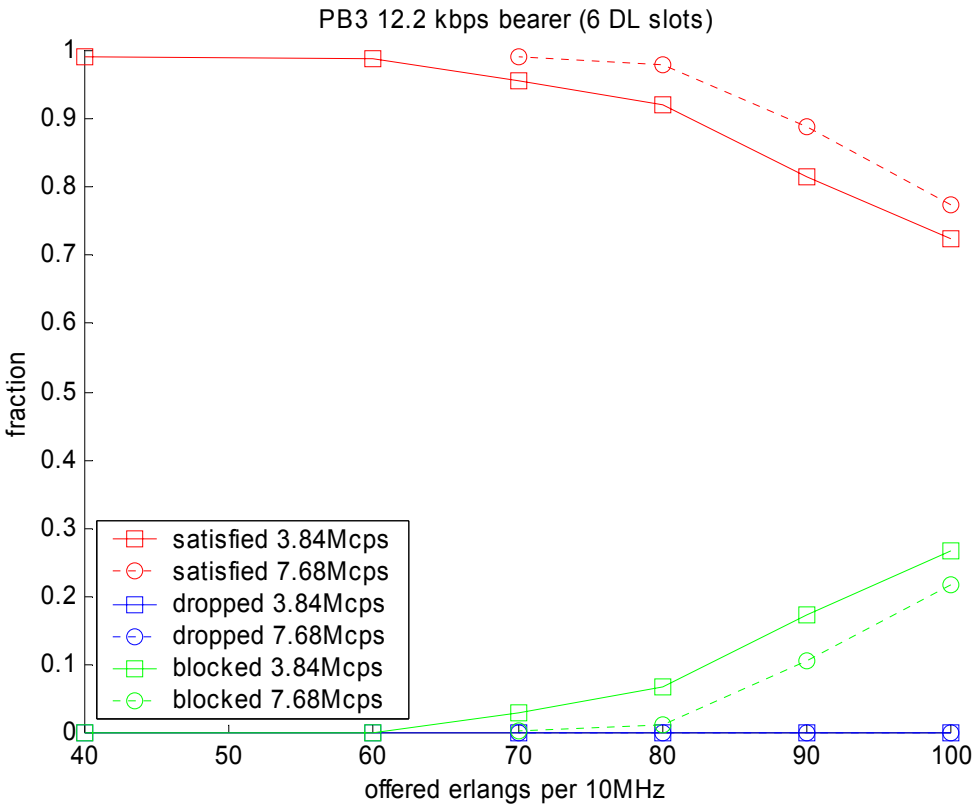

Figure 60 - System Level Results - 12.2kbps DCH bearer, PB3

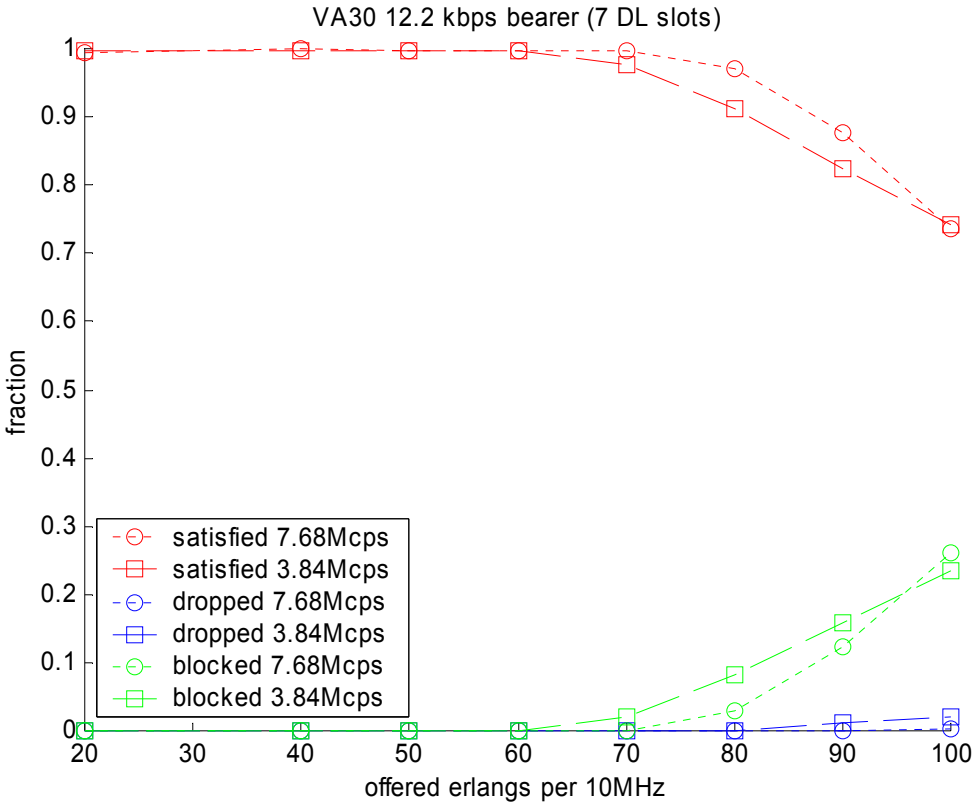

Figure 61 - System Level Results - 12.2kbps DCH bearer, VA30

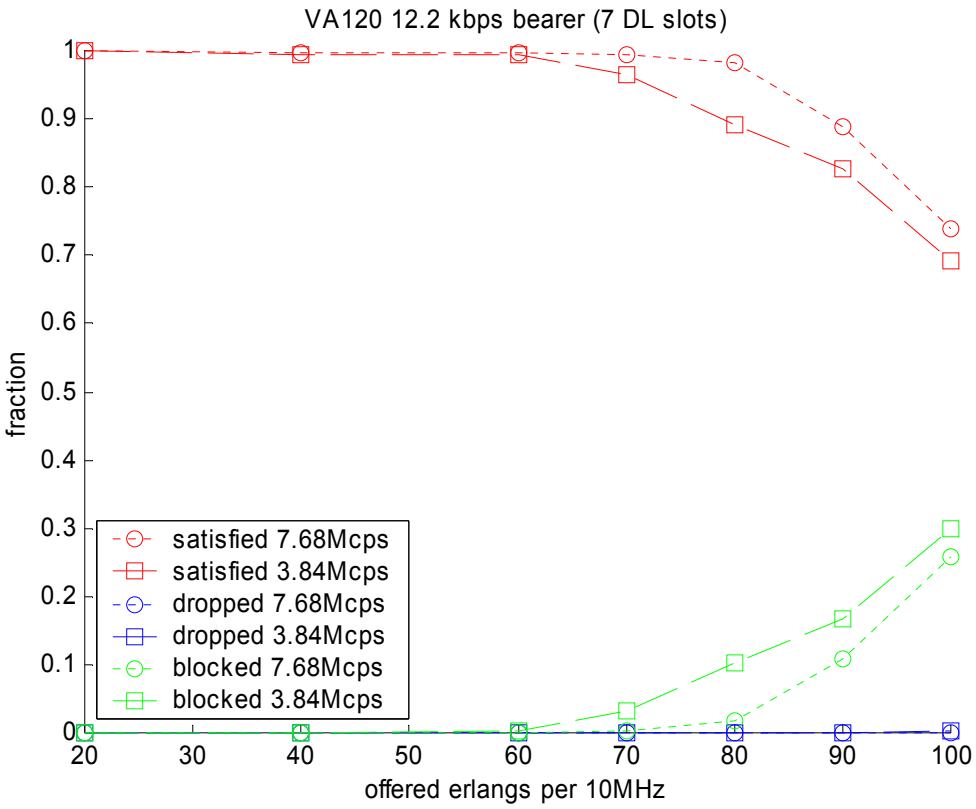

Figure 62 - System Level Results - 12.2kbps DCH bearer, VA120

System capacities in terms of supported numbers of Erlangs at percentages of satisfied users of 95% and 90% are shown in Table 21 for 3.84Mcps and 7.68Mcps systems for the channel models studied.

Table 21 - System Capacity (Erlangs) for 12.2kbps bearer

channel	Offered Erlangs for 90% satisfied users		Offered Erlangs for 95% satisfied users		Capacity gain at 7.68Mcps
	3.84Mcps	7.68Mcps	3.84Mcps	7.68Mcps	
AWGN	101	105	91	99	4-9%
PA3	54	59	48	54	9-12%
PB3	82	89	72	83	9-15%
VA30	81	87	74	82	7-11%
VA120	78	88	72	83	13-15%

In the AWGN channel, the system is code limited and here system level gains are due mainly to trunking efficiency gains. In channels VA30 and VA120, the system is code limited in the uplink due to the use of an asymmetric timeslot split (a 6/6 DL/UL timeslot split causes the system to be power limited in the downlink and inferior performance is obtained with this symmetric timeslot split). As the available code resource is less in these channels (the uplink code resource supports a maximum of 40 concurrent circuits), the trunking efficiency gains of 7.68Mcps over 3.84Mcps are greater. In channels PA3 and PB3, the system is power limited (in the downlink). In these channels, the system level gains are due to a combination of both trunking efficiency gains and link level gains (downlink link level gains are evident in figures 15 to 18 of section 5.2.1.1).

When the system is operated such that 95% of users are satisfied, the capacity gain of a 7.68Mcps TDD system over two 3.84Mcps TDD systems is of the order of 10-15% in terms of the number of supported calls.

5.3.2 Release 5 type (HSDPA) bearers

5.3.2.1 Simulation Parameters

The simulation parameters detailed in Annex B and the link level results of section 5.2.2 are used for the simulation results detailed in this section.

The parameter termed the "code based over the air throughput" is also measured (this is labeled COTA in the figures of this section). This is defined as the total number of bits passing the CRC check per sector / (simulation time * resource utilization).

5.3.2.2 Schedulers

Simulation results are detailed for both Both max C/I and Round robin schedulers.

Scheduler decisions are performed on the basis of CQI reports from the UE.

The Node B is able to track fast fading on pedestrian speed channels and it thus schedules and selects transport formats on the basis of the instantaneous CQI reported from the UE. The CQI report that is used for scheduling on these channels is derated by a derating parameter (this derating parameter reduces the CQI value as a function of time such that the scheduler schedules UEs with old CQI report in a conservative fashion). The CQI value used for scheduling and transport format selection in pedestrian channels is thus :

$$CQI_{sched} = CQI_{t_0} + \varepsilon \cdot (t - t_0)$$

where ε is the derating parameter (in units of dB / TTI) and t_0 is the time of the CQI report from the UE. A derating parameter of $\varepsilon = -0.25\text{dB / TTI}$ is applied for the simulation results presented within this document.

The Node B maintains data on each UE. For the purposes of scheduling, the Node B stores the times at which each UE was last scheduled and the latest CQI report from each UE. At every TTI, the Node B calculates the modulation and coding that could be applied for each UE.

At each TTI, the Node B prioritises UEs for scheduling by performing two "sort" operations on the data that it holds for each UE. In the first sort operation, the UE separates UEs that have a pending retransmission from those that have pending data for initial transmissions. UEs with pending retransmissions are scheduled in preference to those UEs with pending data for initial transmissions. In the second sort operation :

- The Round robin scheduler sorts UEs in terms of increasing time since last allocation.
- The max C/I scheduler sorts UEs in terms of increasing possible modulation and coding rate (note that in the case where all the UEs are in the same channel, this is equivalent to sorting in increasing CQI).

At the conclusion of the "sort" operations, the Node B has an ordered list of UEs to schedule. At the head of the list are UEs to schedule with retransmissions, at the tail of the list are UEs to schedule with initial transmissions.

The scheduler works down the sorted list and allocates the maximum resource it can to each UE in turn. The resource and amount of data that are allocated to each UE are thus a function of :

1. amount of pending data for each UE
2. UE turbo capability
3. UE soft buffer capability

Thus for UEs that are experiencing poor channel quality conditions, the scheduler will tend to schedule an amount of physical resource that fills the UE soft buffer capability and an amount of pending data that is less than the UE turbo capability (this can lead to the whole physical resource of one TTI being assigned to a single UE). For UEs that are experiencing favourable channel conditions, the scheduler will tend to schedule an amount of data equal to the UE turbo capability, and an amount of physical resource that is less than the UE soft buffer capability (this can lead to many UEs being scheduled in the same TTI).

A UE is only scheduled with HS-DSCH resource if the scheduler is able to schedule that UE with HS-SCCH resource : if all of the HS-SCCH within the HS-SCCH set of a UE have previously been allocated to other UEs, the UE in question is not scheduled at all in the current cycle.

In both the max C/I and Round robin cases, the scheduler elicits CQI information from the UE by scheduling transmissions to a small UE HARQ memory partition that is not used for the transfer of higher layer data. This functionality implements a "CQI request" within the framework of the Release 5 specifications. The Node B generates CQI reports from the UE by performing the following operations :

- The Node B explicitly partitions the UE HARQ memory into 2 large partitions (for the purposes of transmission of MAC-hs PDUs) and 1 small partition (for the purpose of generating CQI reports).
- the Node B sets aside a small amount of HS-DSCH resource for the purpose of generating CQI reports (8 codes at 3.84Mcps / 16 codes at 7.68Mcps)
- at each TTI, the Node B schedules data on HS-DSCH to UEs according to the main scheduling algorithm
- after "main scheduling", there will be a set of HS-SCCH that have not been used for scheduling of HS-DSCH resource, these HS-SCCH are used for generating CQI reports
- the scheduler schedules UEs that have pending data to transmit and have not already been allocated HS-DSCH resource with one of the previously unused HS-SCCH and one of the HS-DSCH physical channels that was previously set aside by the Node B. These UEs are scheduled with these HS-SCCH / HS-DSCH pairs in a round-robin fashion in order to effectively request CQI reports from the UEs.
- the CQI request HS-SCCH is coded according to Release 5 specifications with the following attributes :
    - the HS-SCCH signals transmission to the small HARQ partition
    - the HS-SCCH aborts previous transmissions to the small HARQ partition
    - the HS-SCCH indicates the transport block size applied to the associated HS-DSCH and the physical resource applied to HS-DSCH (i.e. it indicates the HS-PDSCH that is transmitted in association with the HS-SCCH). The information signalled on HS-SCCH ensures that MAC-hs PDUs within the associated HS-DSCH are not transferred to higher layers within the UE. One example way of ensuring that MAC-hs PDUs are not transmitted to upper layers within the UE is to indicate that HS-DSCH is encoded with a coding rate of greater than unity.
- the Node B transmits the associated HS-DSCH to the UE according to the details signalled to the UE on the HS-SCCH. The HS-DSCH need not contain higher layer data (it may consist of solely a MAC-hs header and padding)
- the UE receives the HS-DSCH in its small memory partition and generates a CQI report (the UE will always generate a CQI report when it receives HS-DSCH according to Release 5 specifications). The measurement for the CQI report may be based on the HS-DSCH resource that was recently transmitted to the UE (according to Release 5 specifications). The UE will never send MAC-hs PDUs to higher layers as a consequence of receiving an HS-DSCH in the small memory partition due to steps previously taken by the Node B (e.g. ensuring a code rate of greater than unity on HS-DSCH).

The Node B receives CQI reports on HS-SICHs from UEs that are either scheduled with user data on HS-DSCH or "CQI requests" on HS-DSCH and schedules according to both these types of CQI report. Note that a Node B that implements the "CQI request" function has a greater amount of channel quality information that it can use in order to schedule UEs.

5.3.2.3 HTTP Traffic Model Results

In the HTTP simulations, for each simulation run, the system is simulated for 300 seconds after a warm up period of 100 seconds (i.e. 30000 TTIs are simulated per simulation run). Multiple simulation runs (>20) are performed to achieve statistical significance. UEs are randomly dropped onto the 19 cell layout for each simulation run.

5.3.2.3.1 AWGN

Results are presented for a max C/I scheduler and a Round robin scheduler.

Figure 63 to Figure 66 present results using a max C/I scheduler in an AWGN channel.

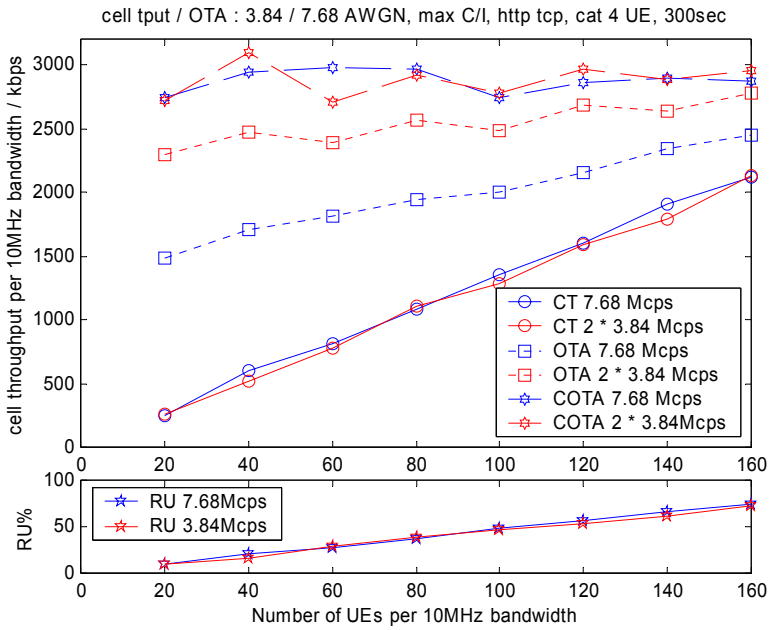

Figure 63 - AWGN : cell throughput / over the air throughput / resource utilisation HTTP, max C/I scheduler

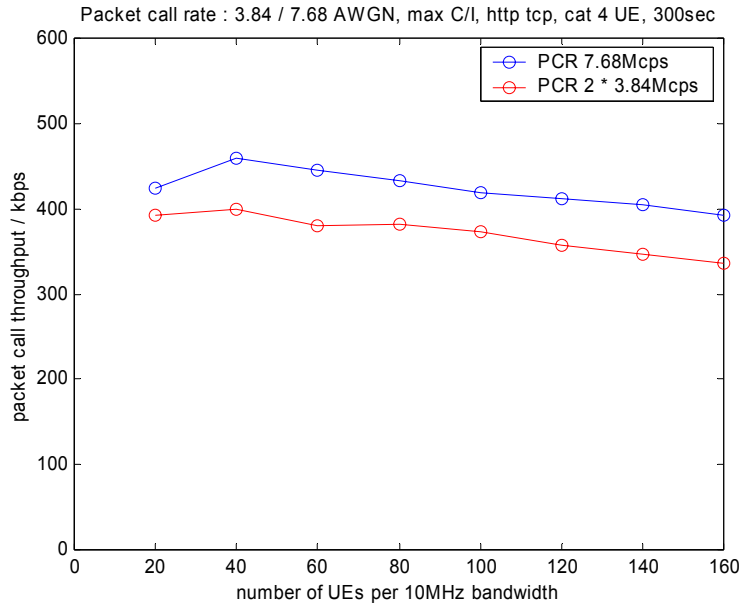

Figure 64 - AWGN : mean packet call rate HTTP, max C/I scheduler

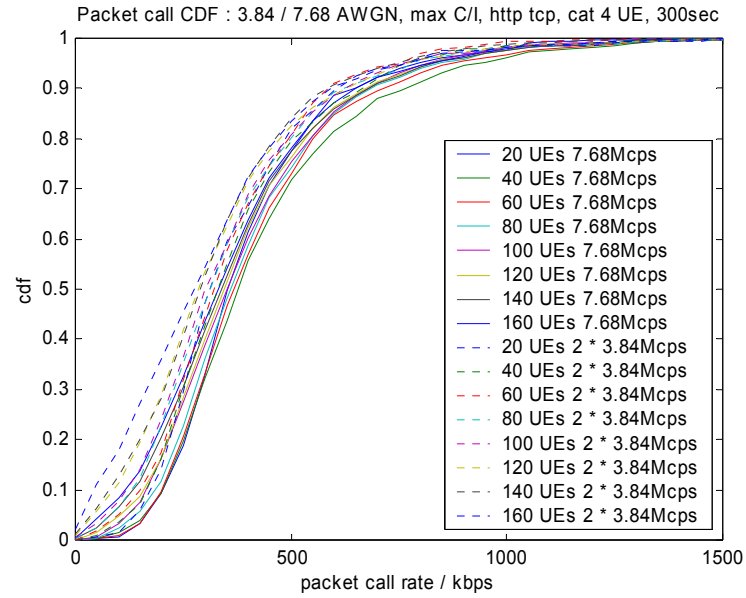

Figure 65 - AWGN : packet call rate CDFs HTTP, max C/I scheduler

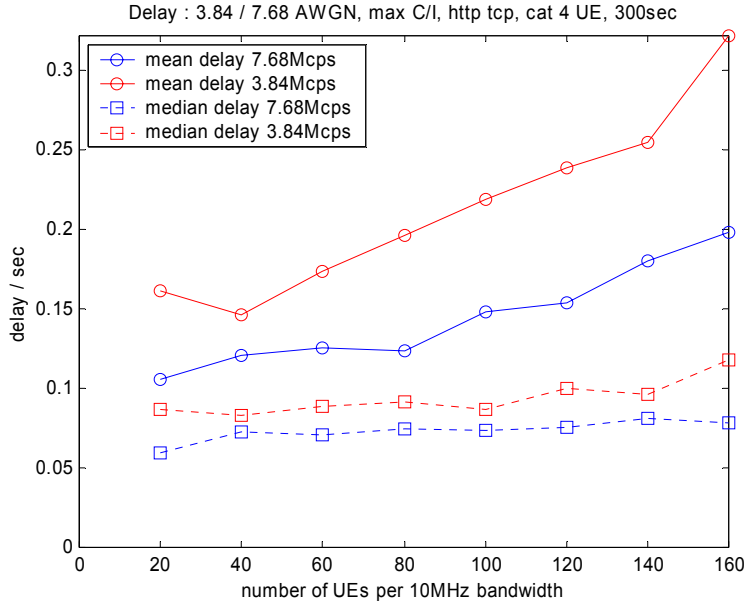

Figure 66 - AWGN : mean and median packet delays HTTP, max C/I scheduler

The MAC-hs failure rate in the AWGN channel with a max C/I scheduler was significantly less than 10^{-4} for both the 3.84Mcps and 7.68Mcps chip rates.

The AWGN results with the max C/I scheduler are summarized in Table 22 (7.68Mcps) and Table 23 (3.84Mcps).

Table 22 - Summary of 7.68Mcps AWGN results for HTTP with max C/I scheduler

#users per sector	average centre cell throughput / kbps			resource utilization %	delay (sec)		packet call rate CDF
	cell t/put	OTA	pkt call rate		mean	median	<32k/64k/128k/384k/1M
20	244	1488	424	9	0.11	0.06	0 / 0 / 2 / 58 / 97
40	601	1707	459	20	0.12	0.07	0 / 1 / 3 / 52 / 96
80	1083	1942	432	37	0.12	0.07	0 / 1 / 4 / 55 / 98
120	1600	2158	412	56	0.15	0.08	1 / 2 / 7 / 59 / 98
160	2118	2443	393	74	0.20	0.08	3 / 5 / 11 / 61 / 98

Table 23 - Summary of 3.84Mcps AWGN results for HTTP with max C/I scheduler

2 x #users per sector	average centre cell throughput / kbps			resource utilization %	delay (sec)		packet call rate CDF
	2 x cell t/put	2 x OTA	pkt call rate		mean	median	<32k/64k/128k/384k/1M
20	258	2290	392	9	0.16	0.09	0 / 1 / 4 / 64 / 99
40	522	2465	399	17	0.15	0.08	1 / 2 / 6 / 62 / 99
80	1106	2570	381	38	0.20	0.09	2 / 4 / 10 / 65 / 98
120	1594	2679	357	54	0.24	0.10	4 / 7 / 16 / 69 / 98
160	2125	2774	336	72	0.32	0.12	8 / 13 / 23 / 70 / 98

Figure 67 to Figure 70 present results using a Round Robin scheduler in AWGN.

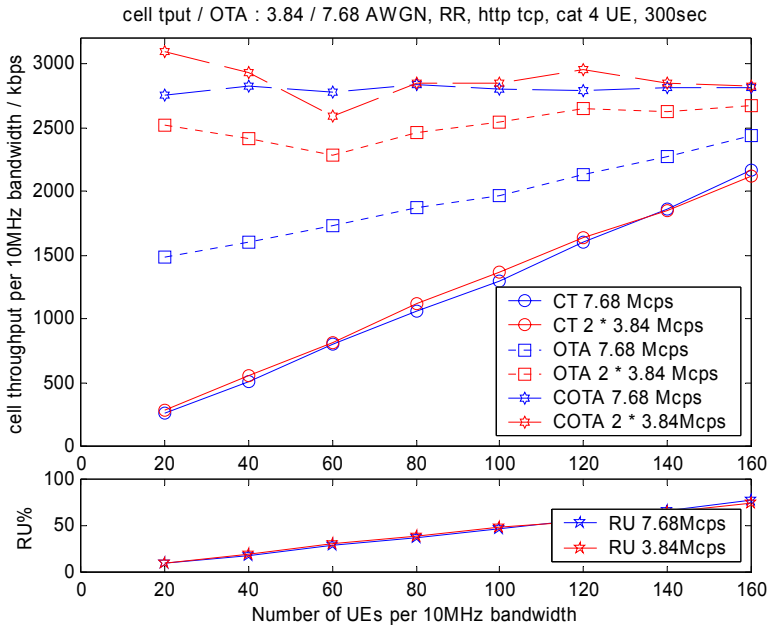

Figure 67 - AWGN : cell throughput / over the air throughput / resource utilisation HTTP, Round robin scheduler

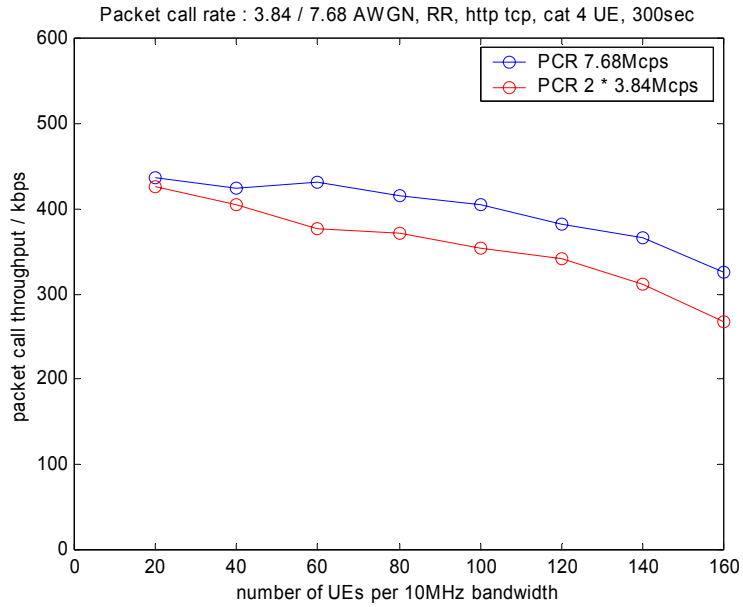

Figure 68 - AWGN : mean packet call rate HTTP, Round robin scheduler

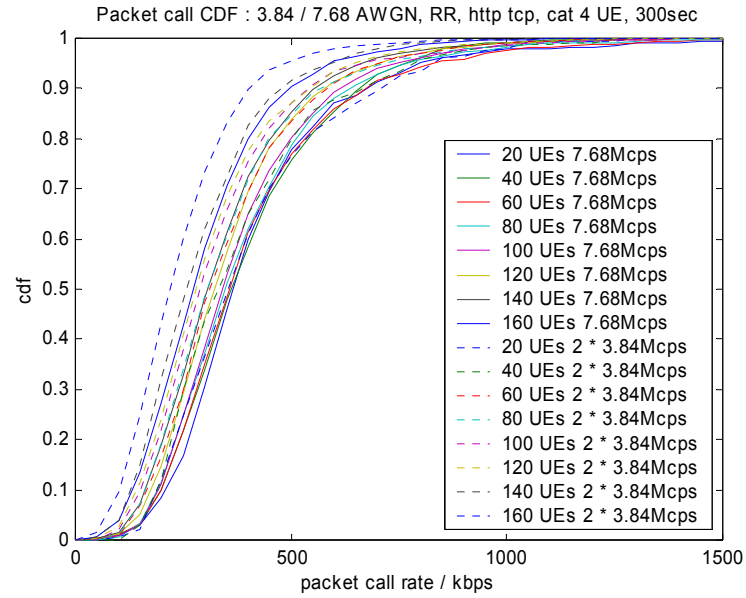

Figure 69 - AWGN : packet call rate CDFs HTTP, Round robin scheduler

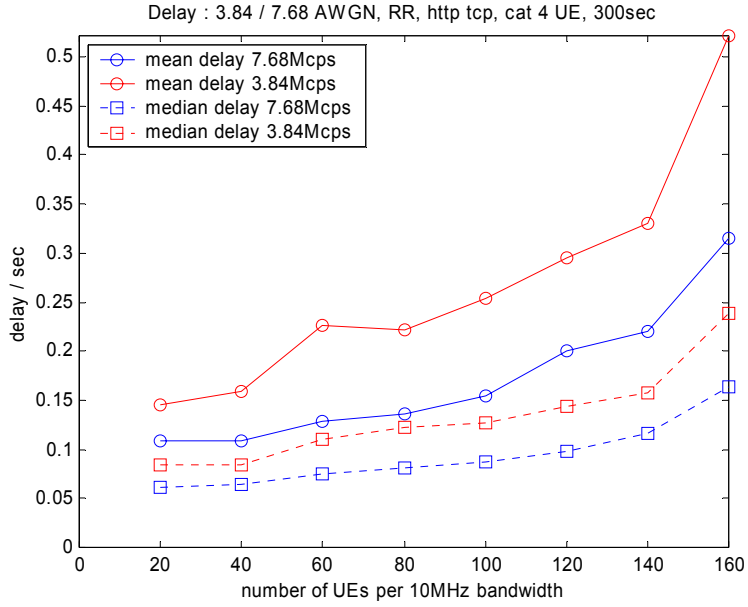

Figure 70 - AWGN : mean and median packet delays HTTP, Round robin scheduler

The MAC-hs failure rate in the AWGN channel with a Round robin scheduler was significantly less than 10^{-4} for both the 3.84Mcps and 7.68Mcps chip rates.

The AWGN results with the Round robin scheduler are summarized in Table 24 (7.68Mcps) and Table 25 (3.84Mcps).

Table 24 - Summary of 7.68Mcps AWGN results for HTTP with Round robin scheduler

#users per sector	average centre cell throughput / kbps			resource utilization %	delay (sec)		packet call rate CDF
	cell t/put	OTA	pkt call rate		mean	median	<32k/64k/128k/384k/1M
20	257	1481	436	9	0.11	0.06	0 / 0 / 2 / 55 / 98
40	508	1604	424	18	0.11	0.06	0 / 0 / 2 / 55 / 99
80	1059	1867	415	37	0.14	0.08	0 / 0 / 2 / 59 / 98
120	1596	2125	382	57	0.20	0.10	0 / 0 / 3 / 66 / 99
160	2164	2437	325	77	0.31	0.16	0 / 1 / 9 / 77 / 100

Table 25 - Summary of 3.84Mcps AWGN results for HTTP with Round robin scheduler

2 x #users per sector	average centre cell throughput / kbps			resource utilization %	delay (sec)		packet call rate CDF
	2 x cell t/put	2 x OTA	pkt call rate		mean	median	<32k/64k/128k/384k/1M
20	281	2517	425	9	0.15	0.08	0 / 0 / 1 / 57 / 98
40	553	2408	405	19	0.16	0.08	0 / 0 / 2 / 61 / 98
80	1112	2458	371	39	0.22	0.12	0 / 0 / 5 / 68 / 98
120	1640	2651	341	56	0.29	0.14	0 / 1 / 8 / 75 / 99
160	2115	2669	268	75	0.52	0.24	1 / 4 / 18 / 88 / 100

5.3.2.3.2 Pedestrian A 3kmph

Results are presented for a max C/I scheduler and a Round robin scheduler.

Figure 71 to Figure 75 present results using a max C/I scheduler in channel PA3.

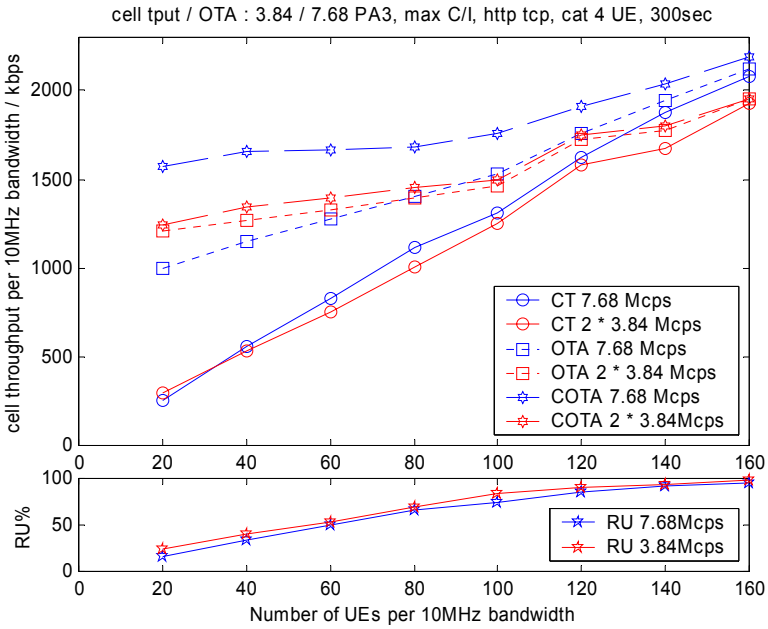

Figure 71 - PA3 : cell throughput / over the air throughput / resource utilisation HTTP, max C/I scheduler

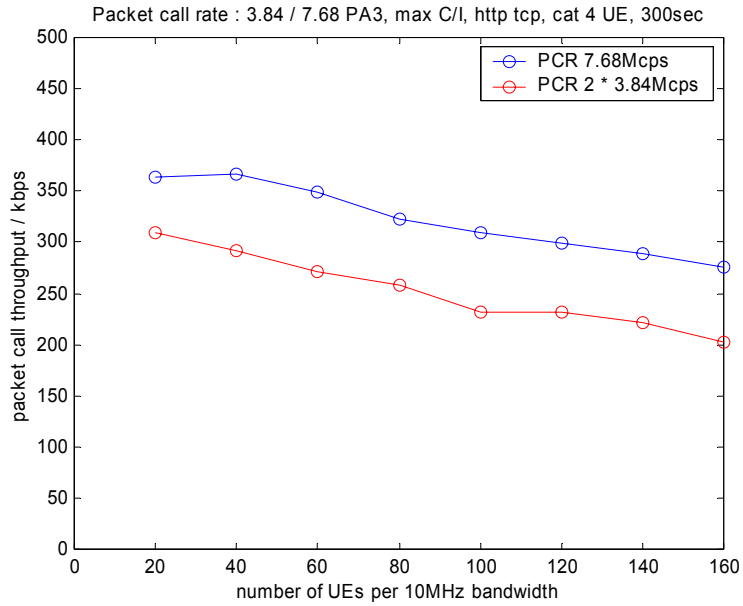

Figure 72 - PA3 : mean packet call rate HTTP, max C/I scheduler

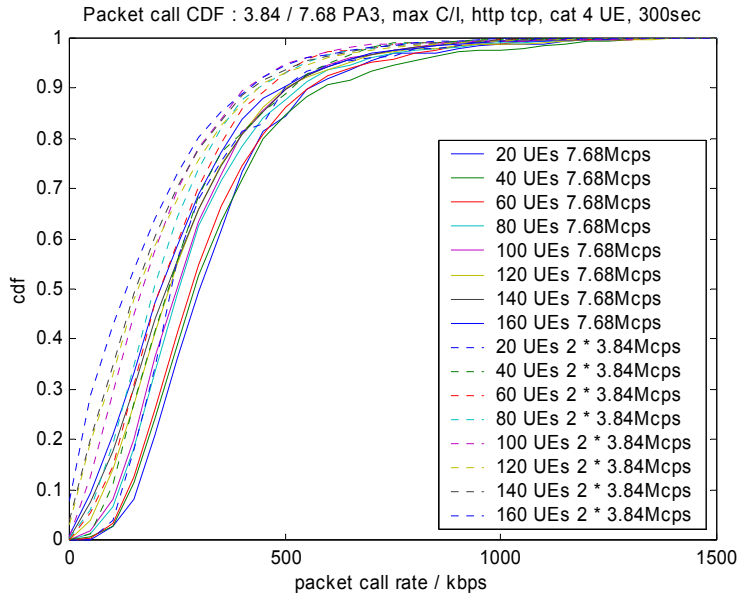

Figure 73 - PA3 : packet call rate CDFs HTTP, max C/I scheduler

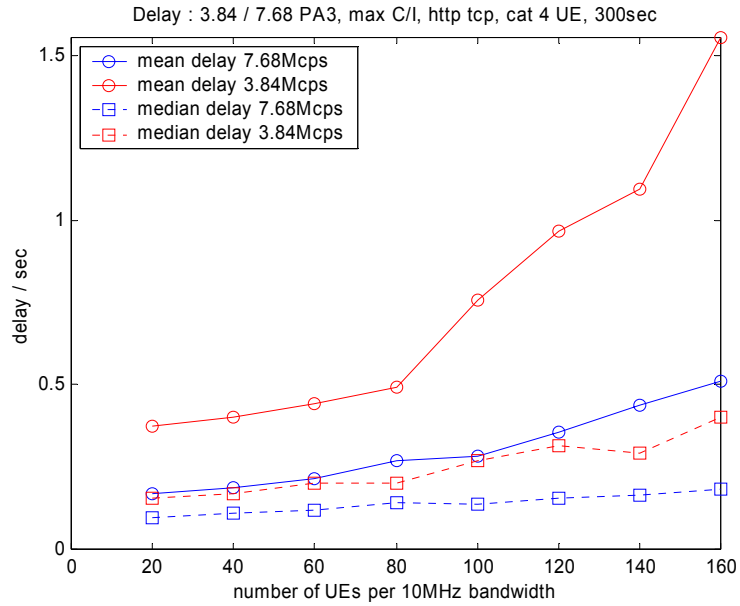

Figure 74 - PA3 : mean and median packet delays HTTP, max C/I scheduler

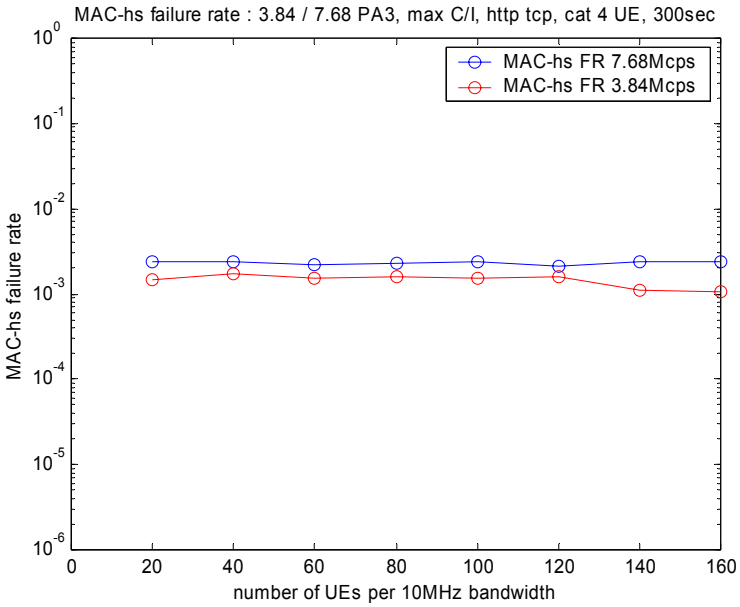

Figure 75 - PA3 : MAC-hs failure rate HTTP, max C/I scheduler

The PA3 results with the max C/I scheduler are summarized in Table 26 (7.68Mcps) and Table 27 (3.84Mcps).

Table 26 - Summary of 7.68Mcps PA3 results for HTTP with max C/I scheduler

#users per sector	average centre cell throughput / kbps			resource utilization %	delay (sec)		packet call rate CDF
	cell t/put	OTA	pkt call rate		mean	median	<32k/64k/128k/384k/1M
20	252	998	364	16	0.17	0.10	0 / 1 / 6 / 70 / 99
40	558	1150	366	34	0.19	0.11	0 / 1 / 7 / 69 / 98
80	1118	1408	323	66	0.27	0.14	1 / 3 / 13 / 76 / 99
120	1622	1756	299	85	0.36	0.15	2 / 7 / 21 / 79 / 99
160	2080	2125	276	95	0.51	0.18	6 / 13 / 28 / 82 / 99

Table 27 - Summary of 3.84Mcps PA3 results for HTTP with max C/I scheduler

2 x #users per sector	average centre cell throughput / kbps			resource utilization %	delay (sec)		packet call rate CDF
	2 x cell t/put	2 x OTA	pkt call rate		mean	median	<32k/64k/128k/384k/1M
20	294	1207	309	24	0.37	0.16	0 / 1 / 12 / 80 / 100
40	533	1271	291	40	0.40	0.17	1 / 4 / 20 / 80 / 100
80	1004	1399	259	69	0.49	0.20	4 / 10 / 28 / 86 / 100
120	1577	1722	231	90	0.96	0.31	13 / 23 / 41 / 86 / 100
160	1926	1950	203	98	1.55	0.40	21 / 33 / 49 / 88 / 100

Figure 76 to Figure 80 present results using a Round Robin scheduler in PA3.

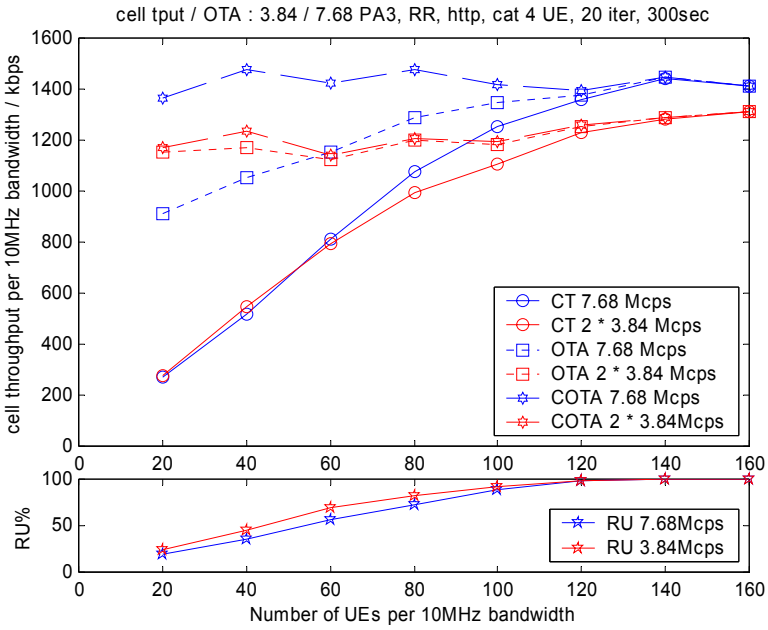

Figure 76 - PA3 : cell throughput / over the air throughput / resource utilisation HTTP, Round robin scheduler

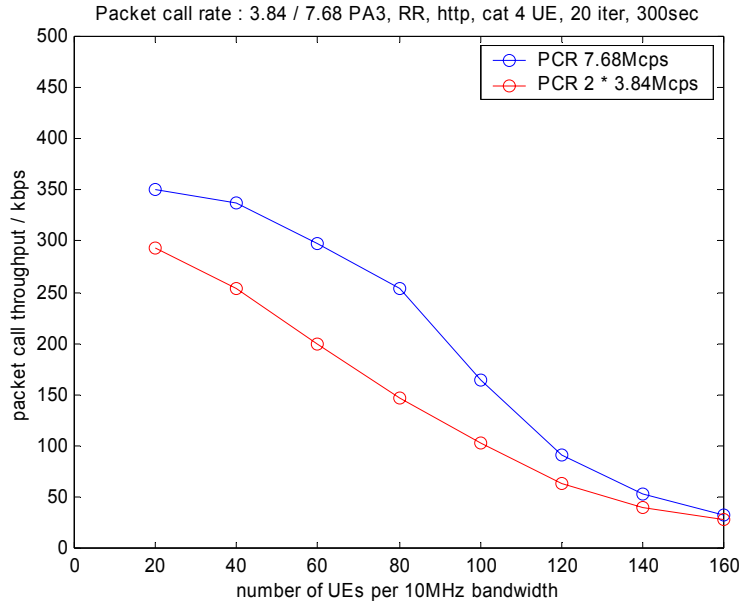

Figure 77 - PA3 : mean packet call rate HTTP, Round robin scheduler

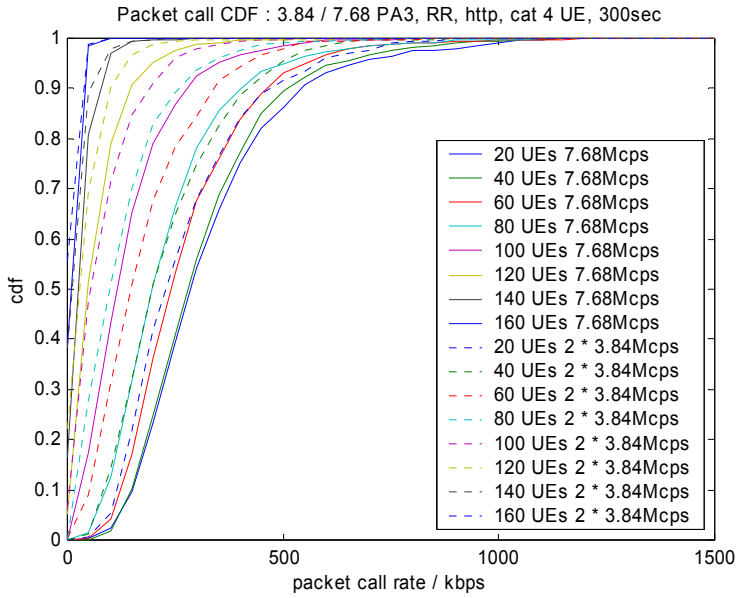

Figure 78 - PA3 : packet call rate CDFs HTTP, Round robin scheduler

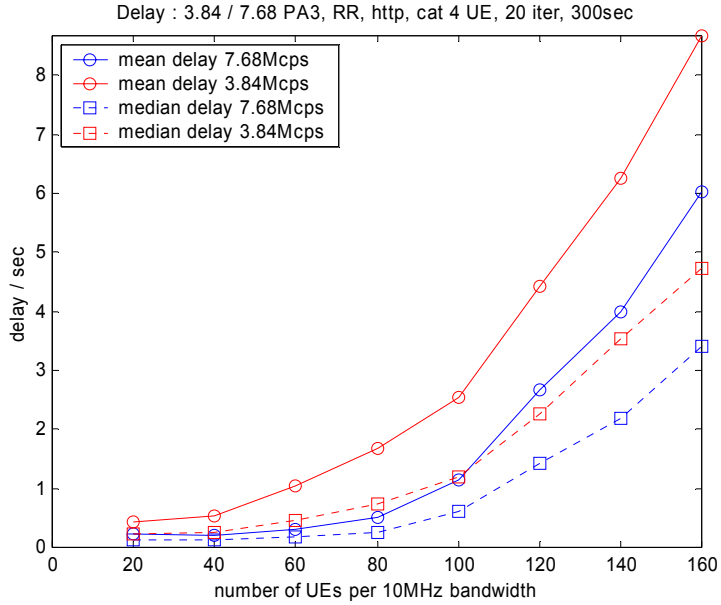

Figure 79 - PA3 : mean and median packet delays HTTP, Round robin scheduler

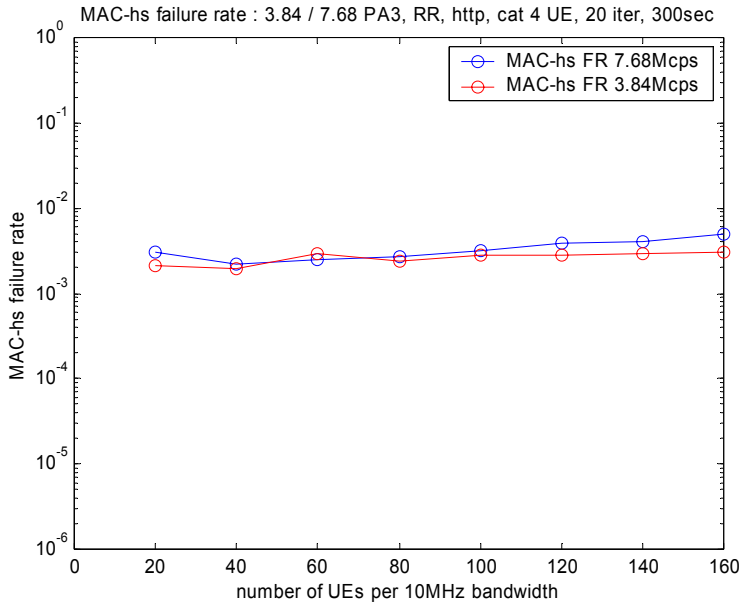

Figure 80 - PA3 : MAC-hs failure rate HTTP, Round robin scheduler

The PA3 results with the Round robin scheduler are summarized in Table 28 (7.68Mcps) and Table 29 (3.84Mcps).

Table 28 - Summary of 7.68Mcps PA3 results for HTTP with Round robin scheduler

#users per sector	average centre cell throughput / kbps			resource utilization %	delay (sec)		packet call rate CDF
	cell t/put	OTA	pkt call rate		mean	median	<32k/64k/128k/384k/1M
20	273	914	350	20	0.22	0.12	0 / 1 / 6 / 72 / 99
40	516	1050	337	35	0.20	0.12	0 / 1 / 6 / 75 / 99
80	1074	1286	253	73	0.51	0.25	1 / 5 / 23 / 89 / 100
120	1358	1375	91	98	2.68	1.43	35 / 59 / 85 / 100 / 100
160	1413	1413	33	100	6.83	3.40	77 / 99 / 100 / 100 / 100

Table 29 - Summary of 3.84Mcps PA3 results for HTTP with Round robin scheduler

2 x #users per sector	average centre cell throughput / kbps			resource utilization %	delay (sec)		packet call rate CDF
	2 x cell t/put	2 x OTA	pkt call rate		mean	median	<32k/64k/128k/384k/1M
20	276	1155	293	24	0.42	0.23	0 / 2 / 15 / 82 / 100
40	550	1173	254	45	0.52	0.25	1 / 5 / 24 / 87 / 100
80	994	1200	147	83	1.69	0.75	18 / 34 / 62 / 97 / 100
120	1232	1254	63	98	4.43	2.27	53 / 75 / 94 / 100 / 100
160	1314	1314	27	100	8.67	4.74	83 / 99 / 100 / 100 / 100

5.3.2.3.3 Pedestrian B 3kmph

Results are presented for a max C/I scheduler and a Round robin scheduler.

Figure 81 to Figure 85 present results using a max C/I scheduler in channel PB3.

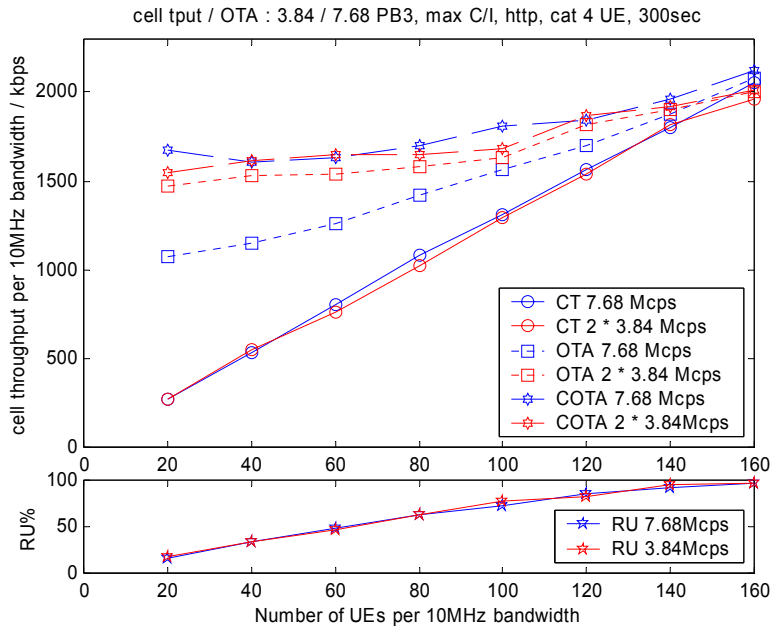

Figure 81 - PB3 : cell throughput / over the air throughput / resource utilisation HTTP, max C/I scheduler

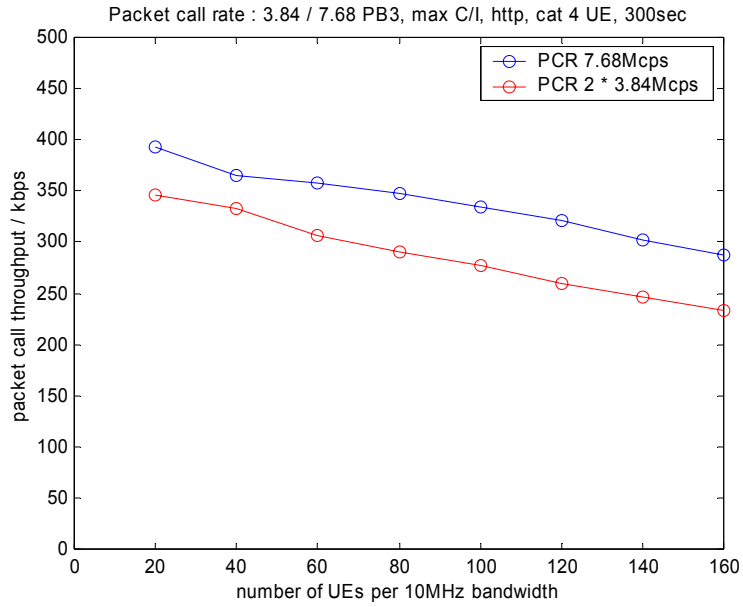

Figure 82 - PB3 : mean packet call rate HTTP, max C/I scheduler

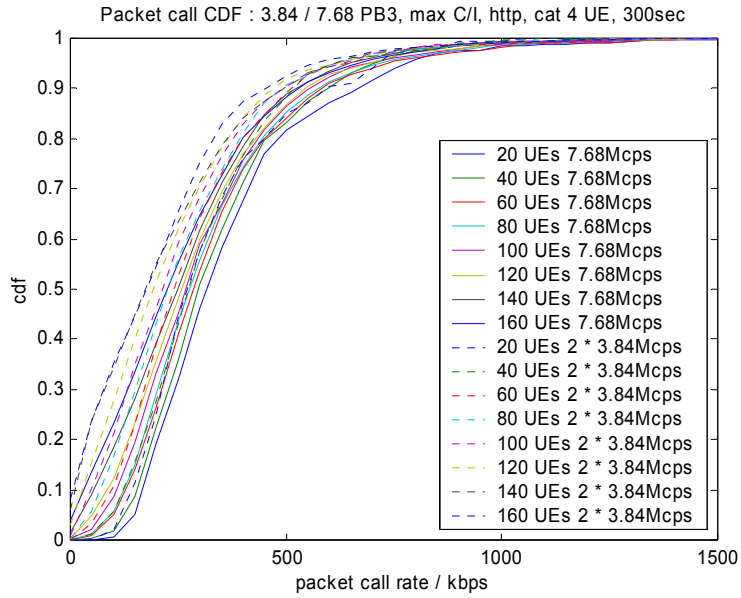

Figure 83 - PB3 : packet call rate CDFs HTTP, max C/I scheduler

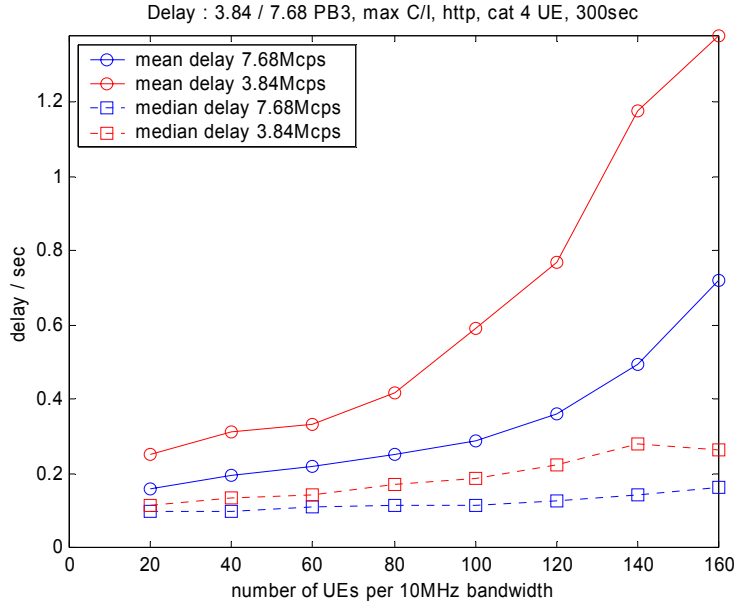

Figure 84 - PB3 : mean and median packet delays HTTP, max C/I scheduler

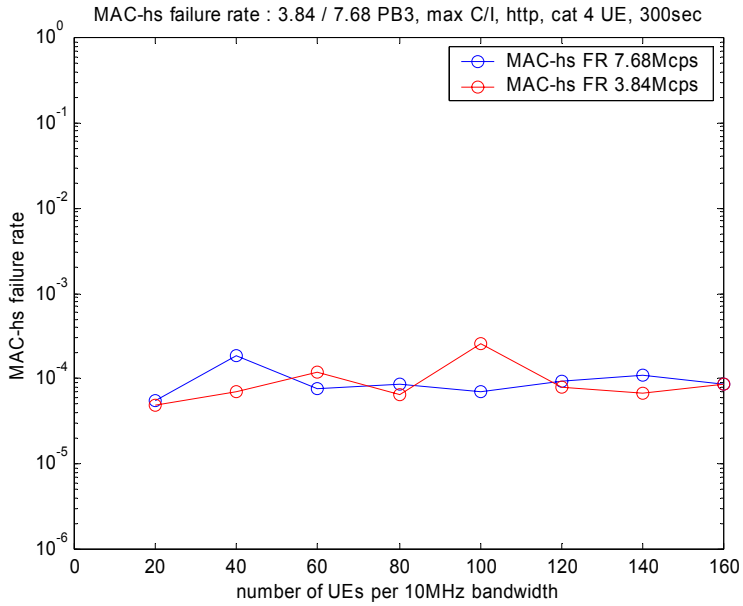

Figure 85 - PB3 : MAC-hs failure rate HTTP, max C/I scheduler

The PB3 results with the max C/I scheduler are summarized in Table 30 (7.68Mcps) and Table 31 (3.84Mcps).

Table 30 - Summary of 7.68Mcps PB3 results for HTTP with max C/I scheduler

#users per sector	average centre cell throughput / kbps			resource utilization %	delay (sec)		packet call rate CDF
	cell t/put	OTA	pkt call rate		mean	median	<32k/64k/128k/384k/1M
20	270	1074	392	16	0.16	0.10	0 / 0 / 3 / 65 / 98
40	533	1152	365	33	0.20	0.10	0 / 1 / 6 / 68 / 99
80	1079	1417	348	64	0.25	0.11	1 / 2 / 11 / 72 / 99
120	1566	1698	322	85	0.36	0.12	3 / 7 / 18 / 75 / 99
160	2054	2082	288	97	0.72	0.16	10 / 16 / 29 / 78 / 99

Table 31 - Summary of 3.84Mcps PB3 results for HTTP with max C/I scheduler

2 x #users per sector	average centre cell throughput / kbps			resource utilization %	delay (sec)		packet call rate CDF
	2 x cell t/put	2 x OTA	pkt call rate		mean	median	<32k/64k/128k/384k/1M
20	272	1474	346	18	0.25	0.11	0 / 1 / 7 / 74 / 100
40	551	1531	333	34	0.31	0.13	1 / 3 / 11 / 74 / 100
80	1024	1578	291	62	0.42	0.17	4 / 9 / 24 / 79 / 99
120	1543	1817	260	83	0.77	0.22	11 / 19 / 35 / 82 / 99
160	1965	2005	234	97	1.38	0.26	18 / 27 / 41 / 86 / 99

Figure 86 to Figure 90 present results using a Round Robin scheduler in PB3.

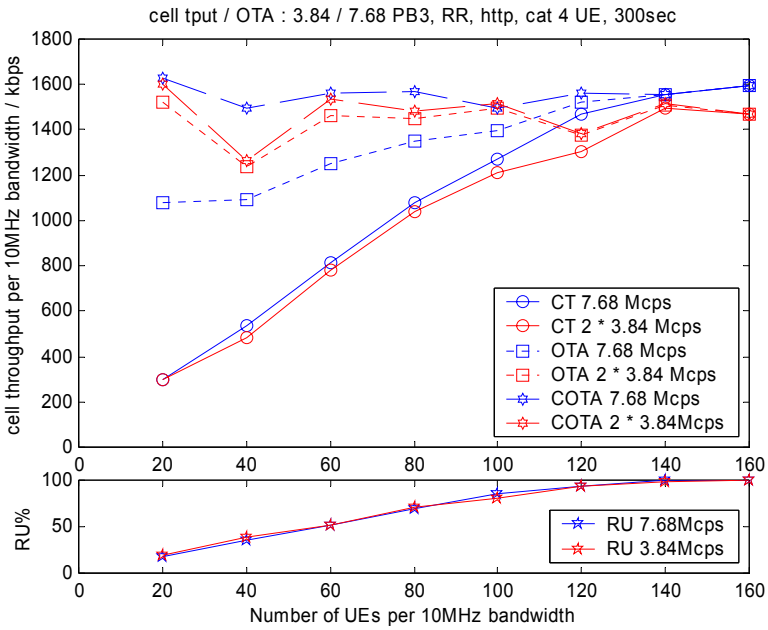

Figure 86 - PB3 : cell throughput / over the air throughput / resource utilisation HTTP, Round robin scheduler

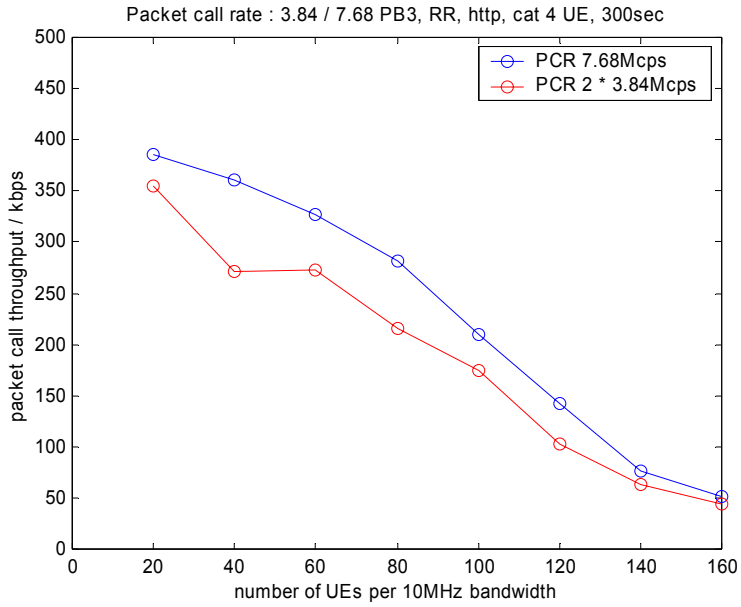

Figure 87 - PB3 : mean packet call rate HTTP, Round robin scheduler

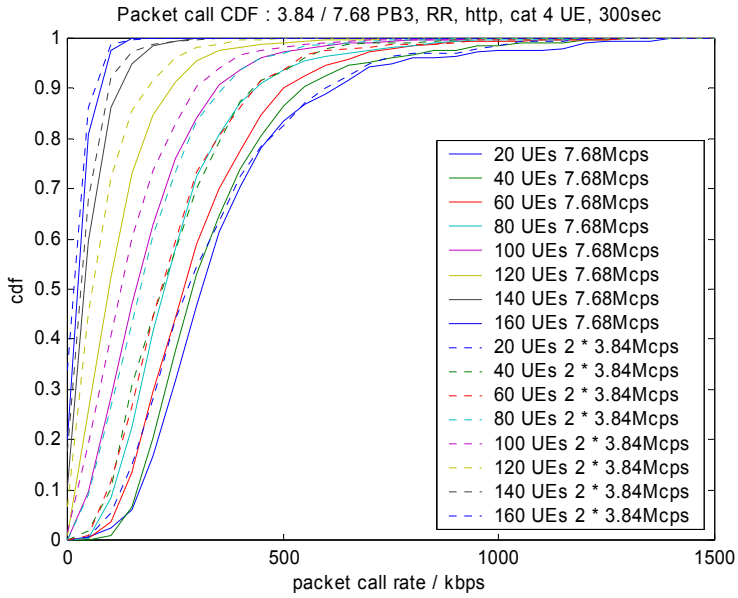

Figure 88 - PB3 : packet call rate CDFs HTTP, Round robin scheduler

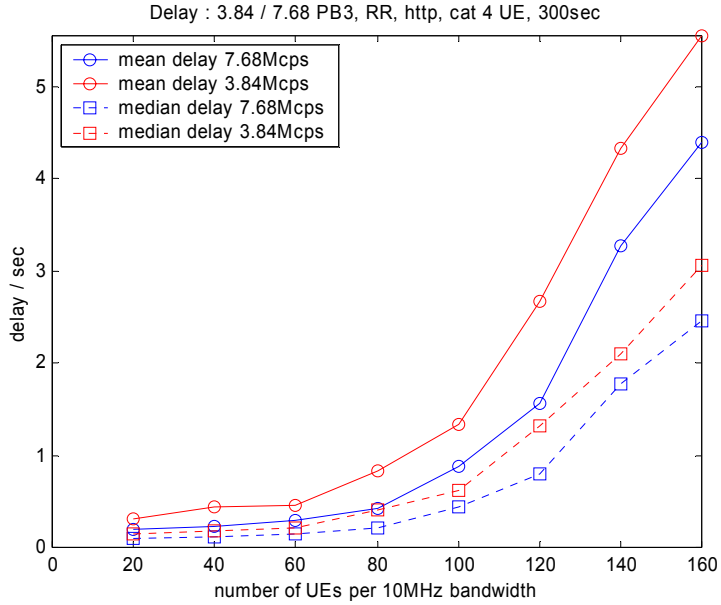

Figure 89 - PB3 : mean and median packet delays HTTP, Round robin scheduler

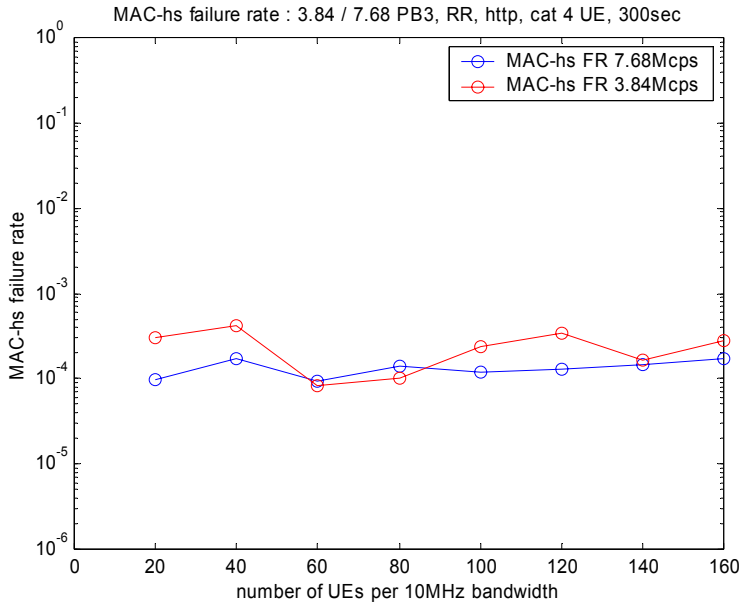

Figure 90 - PB3 : MAC-hs failure rate HTTP, Round robin scheduler

The PB3 results with the Round robin scheduler are summarized in Table 32 (7.68Mcps) and Table 33 (3.84Mcps).

Table 32 - Summary of 7.68Mcps PB3 results for HTTP with Round robin scheduler

#users per sector	average centre cell throughput / kbps			resource utilization %	delay (sec)		packet call rate CDF
	cell t/put	OTA	pkt call rate		mean	median	<32k/64k/128k/384k/1M
20	295	1078	386	18	0.19	0.10	0 / 1 / 4 / 67 / 98
40	535	1090	360	36	0.22	0.12	0 / 0 / 4 / 71 / 99
80	1077	1353	282	69	0.42	0.20	0 / 3 / 16 / 85 / 100
120	1471	1521	142	94	1.56	0.79	17 / 33 / 64 / 98 / 100
160	1596	1596	51	100	4.39	2.45	59 / 85 / 99 / 100 / 100

Table 33 - Summary of 3.84Mcps PB3 results for HTTP with Round robin scheduler

2 x #users per sector	average centre cell throughput / kbps			resource utilization %	delay (sec)		packet call rate CDF
	2 x cell t/put	2 x OTA	pkt call rate		mean	median	<32k/64k/128k/384k/1M
20	297	1523	355	19	0.30	0.15	0 / 2 / 11 / 70 / 99
40	486	1235	271	38	0.44	0.17	1 / 4 / 22 / 85 / 100
80	1041	1446	216	70	0.84	0.41	6 / 14 / 36 / 92 / 100
120	1306	1377	103	94	2.68	1.32	31 / 53 / 80 / 99 / 100
160	1468	1469	44	100	5.55	3.06	67 / 90 / 99 / 100 / 100

5.3.2.3.4 Vehicular A 30kmph

Results are presented for a max C/I scheduler and a Round robin scheduler.

Figure 91 to Figure 95 present results using a max C/I scheduler in channel VA30.

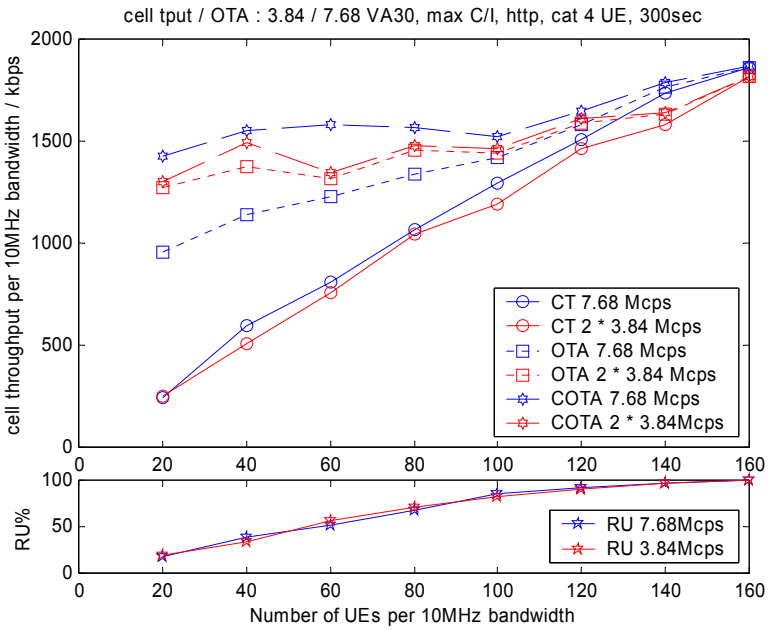

Figure 91 - VA30 : cell throughput / over the air throughput / resource utilisation HTTP, max C/I scheduler

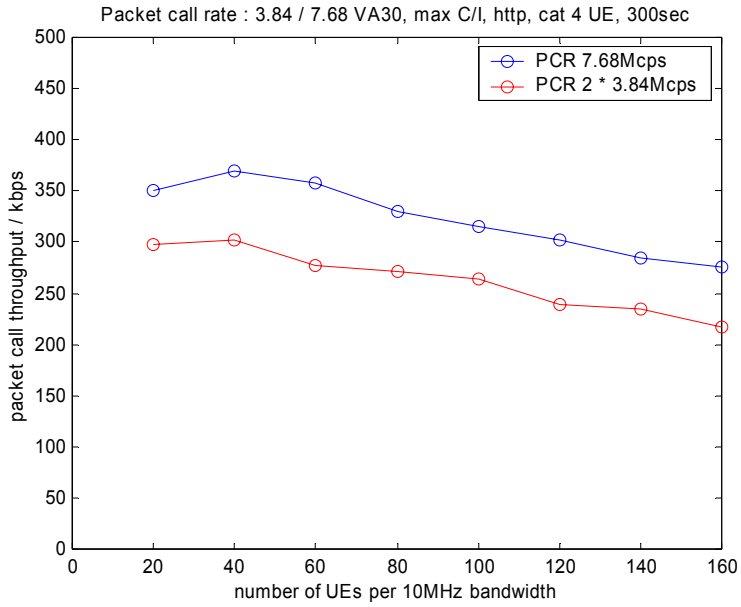

Figure 92 - VA30 : mean packet call rate HTTP, max C/I scheduler

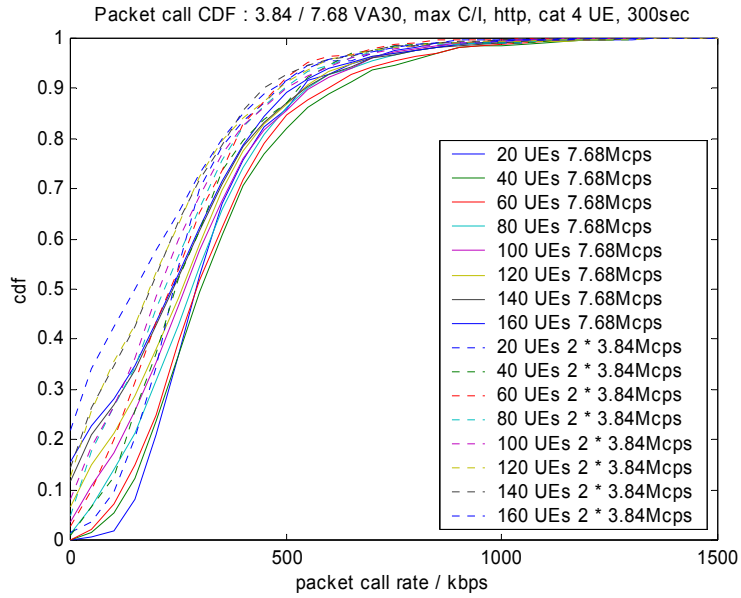

Figure 93 - VA30 : packet call rate CDFs HTTP, max C/I scheduler

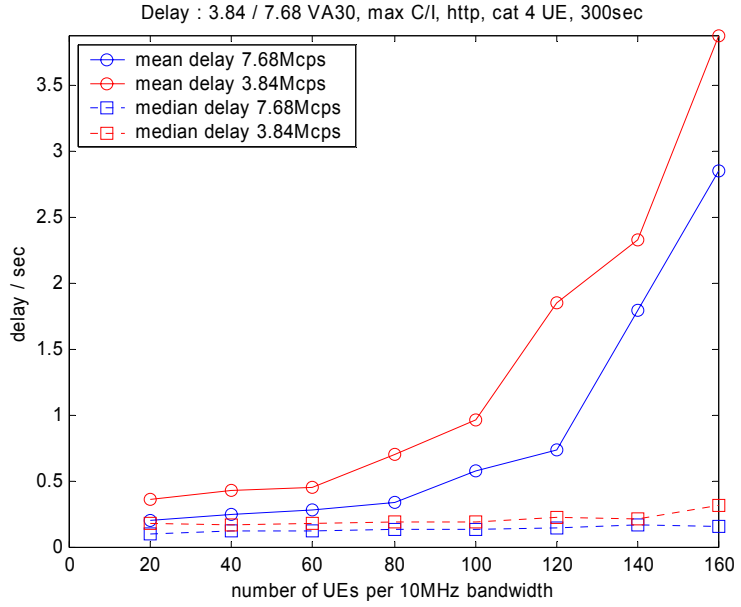

Figure 94 - VA30 : mean and median packet delays HTTP, max C/I scheduler

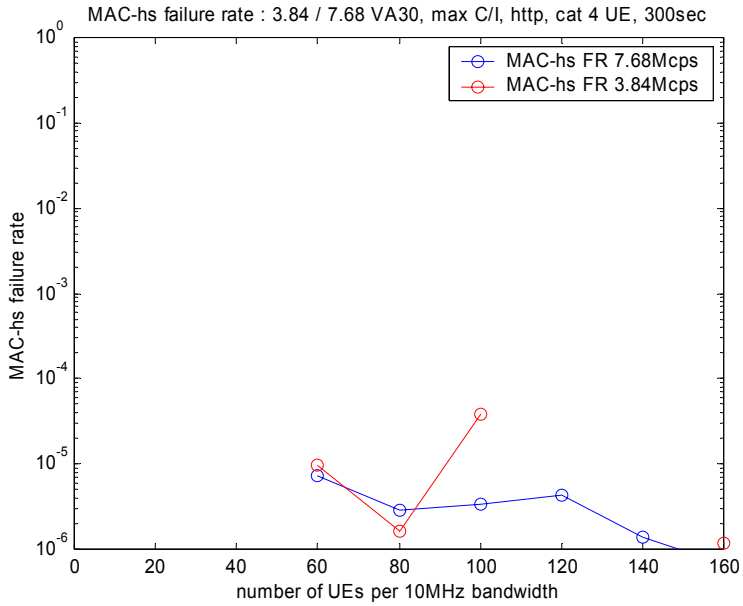

Figure 95 - VA30 : MAC-hs failure rate HTTP, max C/I scheduler

The VA30 results with the max C/I scheduler are summarized in Table 34 (7.68Mcps) and Table 35 (3.84Mcps).

Table 34 - Summary of 7.68Mcps VA30 results for HTTP with max C/I scheduler

#users per sector	average centre cell throughput / kbps			resource utilization %	delay (sec)		packet call rate CDF
	cell t/put	OTA	pkt call rate		mean	median	<32k/64k/128k/384k/1M
20	242	954	350	17	0.20	0.10	0 / 1 / 5 / 73 / 100
40	592	1139	370	38	0.25	0.13	1 / 3 / 9 / 67 / 99
80	1066	1336	330	68	0.34	0.14	5 / 9 / 18 / 72 / 99
120	1511	1580	302	92	0.74	0.15	12 / 17 / 25 / 75 / 99
160	1863	1864	275	100	2.86	0.16	20 / 24 / 32 / 77 / 99

Table 35 - Summary of 3.84Mcps VA30 results for HTTP with max C/I scheduler

2 x #users per sector	average centre cell throughput / kbps			resource utilization %	delay (sec)		packet call rate CDF
	2 x cell t/put	2 x OTA	pkt call rate		mean	median	<32k/64k/128k/384k/1M
20	253	1271	297	20	0.36	0.18	3 / 5 / 16 / 82 / 99
40	510	1375	302	34	0.44	0.17	5 / 8 / 20 / 78 / 99
80	1044	1455	271	71	0.70	0.19	13 / 20 / 31 / 80 / 99
120	1461	1588	240	91	1.85	0.23	21 / 28 / 40 / 83 / 99
160	1815	1817	217	100	3.88	0.32	30 / 36 / 47 / 83 / 100

Figure 96 to Figure 100 present results using a Round Robin scheduler in channel VA30.

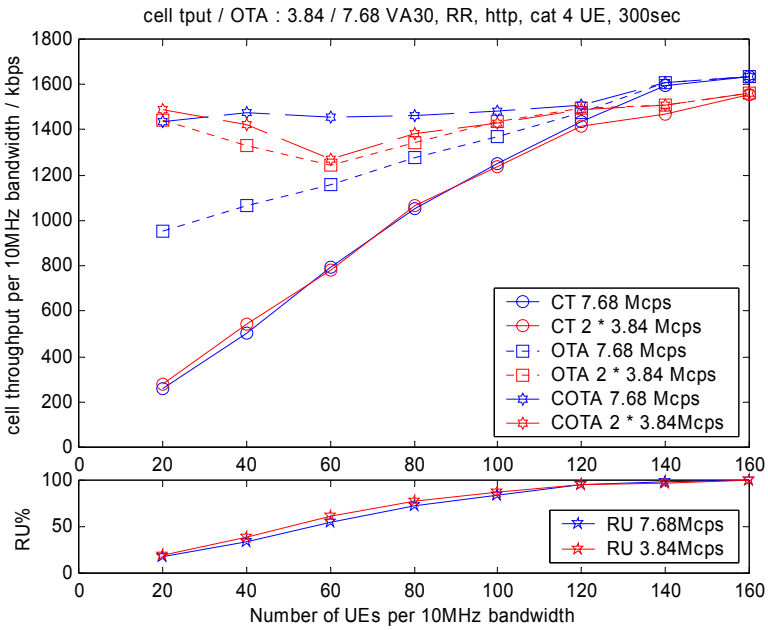

Figure 96 - VA30 : cell throughput / over the air throughput / resource utilisation HTTP, Round robin scheduler

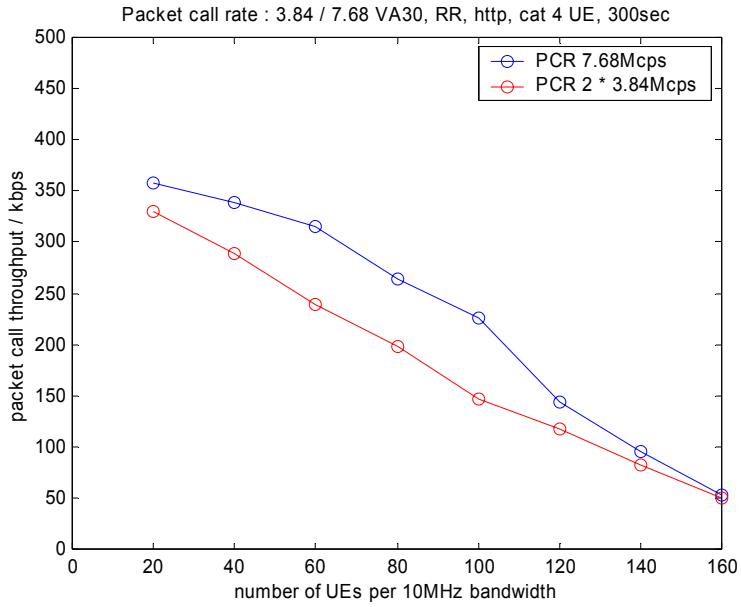

Figure 97 - VA30 : mean packet call rate HTTP, Round robin scheduler

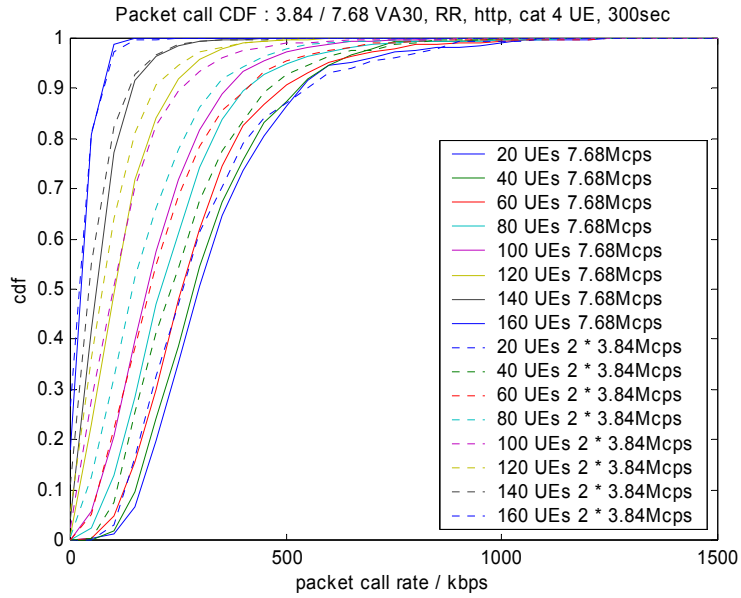

Figure 98 - VA30 : packet call rate CDFs HTTP, Round robin scheduler

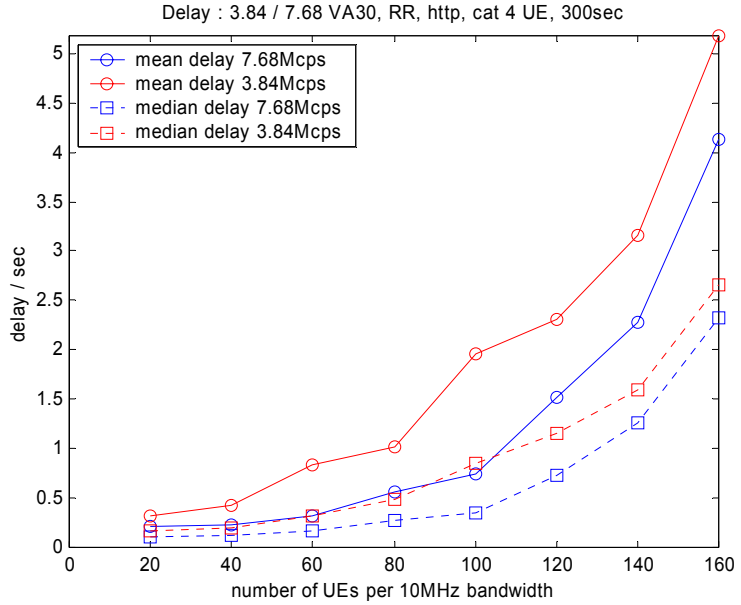

Figure 99 - VA30 : and median packet delays HTTP, Round robin scheduler

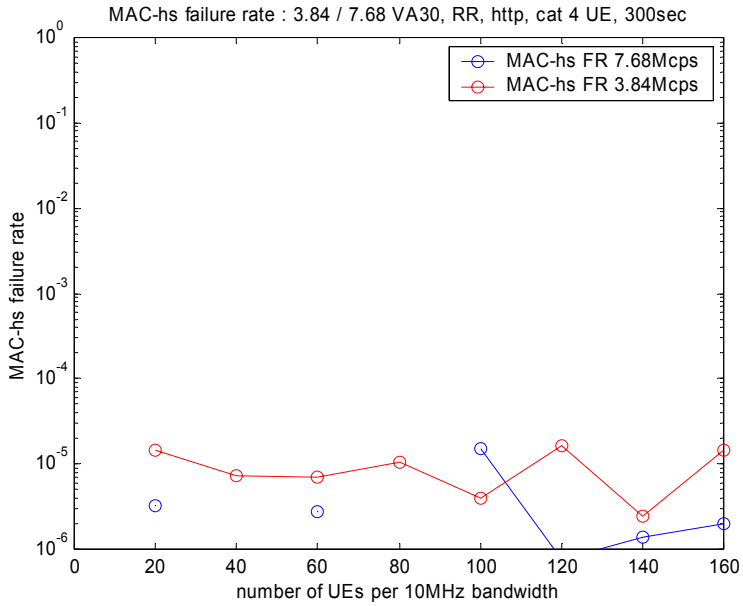

Figure 100 - VA30 : MAC-hs failure rate HTTP, Round robin scheduler

The VA30 results with the Round robin scheduler are summarized in Table 36 (7.68Mcps) and Table 37 (3.84Mcps).

Table 36 - Summary of 7.68Mcps VA30 results for HTTP with Round robin scheduler

#users per sector	average centre cell throughput / kbps			resource utilization %	delay (sec)		packet call rate CDF
	cell t/put	OTA	pkt call rate		mean	median	<32k/64k/128k/384k/1M
20	255	955	358	18	0.21	0.10	0 / 1 / 4 / 71 / 99
40	504	1065	339	34	0.23	0.12	0 / 1 / 6 / 73 / 100
80	1053	1276	263	72	0.56	0.28	2 / 5 / 22 / 88 / 100
120	1434	1475	143	95	1.52	0.73	15 / 30 / 62 / 99 / 100
160	1637	1638	52	100	4.13	2.33	58 / 86 / 99 / 100 / 100

Table 37 - Summary of 3.84Mcps VA30 results for HTTP with Round robin scheduler

2 x #users per sector	average centre cell throughput / kbps			resource utilization %	delay (sec)		packet call rate CDF
	2 x cell t/put	2 x OTA	pkt call rate		mean	median	<32k/64k/128k/384k/1M
20	280	1444	330	19	0.32	0.17	0 / 1 / 11 / 76 / 100
40	542	1331	288	38	0.43	0.19	0 / 2 / 18 / 82 / 100
80	1064	1344	198	77	1.02	0.49	8 / 18 / 44 / 94 / 100
120	1413	1497	117	95	2.30	1.15	25 / 44 / 74 / 99 / 100
160	1558	1562	50	100	5.18	2.65	62 / 86 / 99 / 100 / 100

5.3.2.3.5 Vehicular A 120kmph

Results are presented for a max C/I scheduler and a Round robin scheduler.

Figure 101 to Figure 104 present results using a max C/I scheduler in channel VA120.

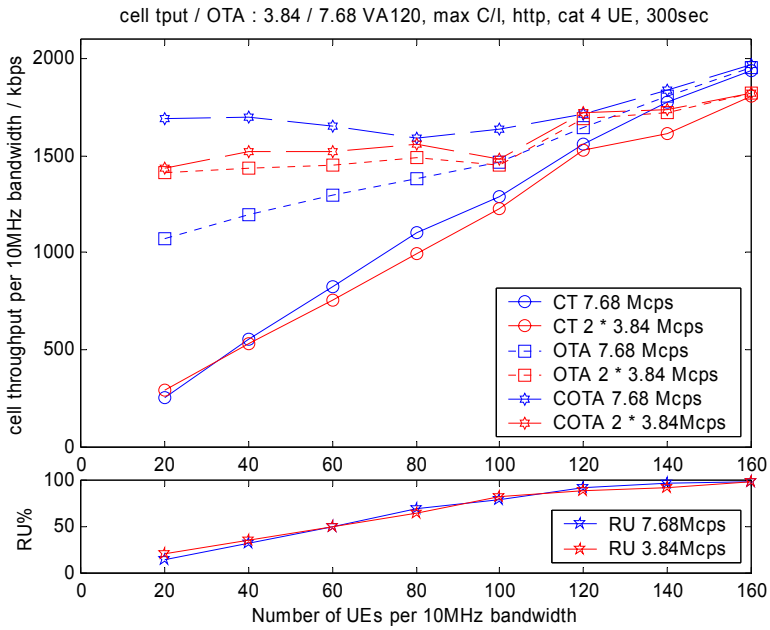

Figure 101 - VA120 : cell throughput / over the air throughput / resource utilisation HTTP, max C/I scheduler

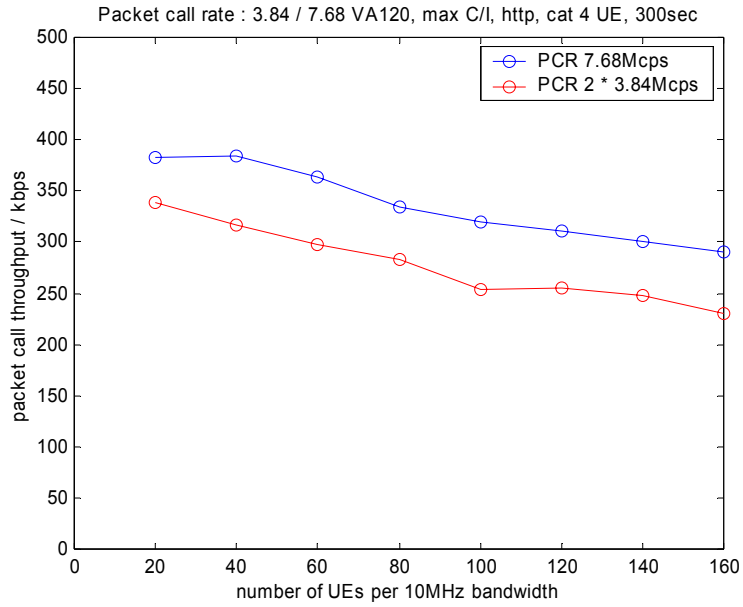

Figure 102 - VA120 : mean packet call rate HTTP, max C/I scheduler

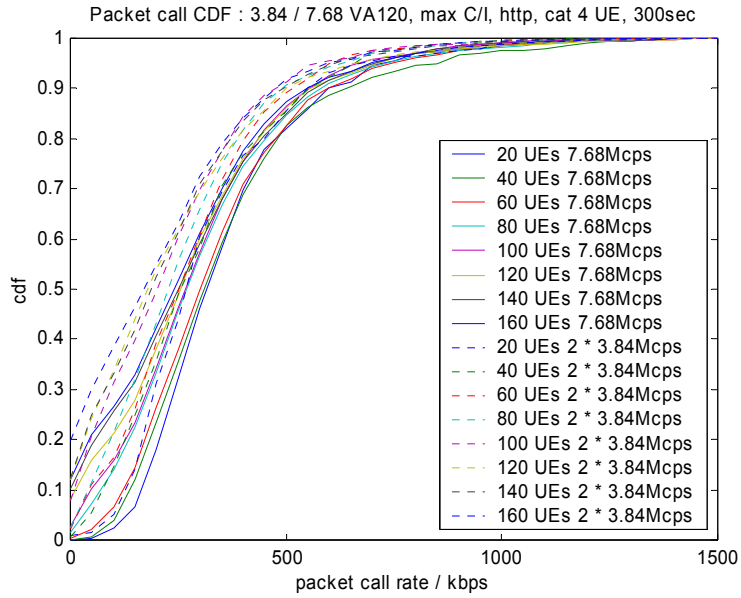

Figure 103 - VA120 : packet call rate CDFs HTTP, max C/I scheduler

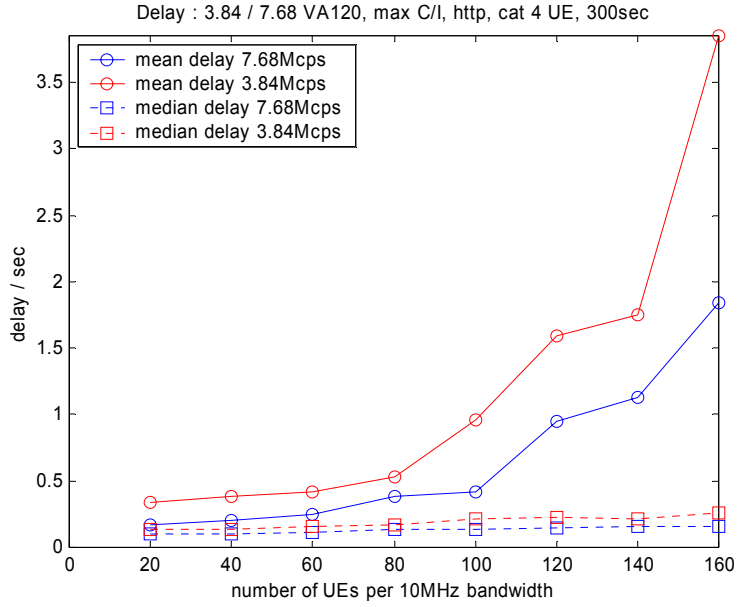

Figure 104 - VA120 : mean and median packet delays HTTP, max C/I scheduler

The MAC-hs failure rate in channel VA120 with a max C/I scheduler was significantly less than 10^{-4} for both the 3.84Mcps and 7.68Mcps chip rates.

The VA120 results with the max C/I scheduler are summarized in Table 38 (7.68Mcps) and Table 39 (3.84Mcps).

Table 38 - Summary of 7.68Mcps VA120 results for HTTP with max C/I scheduler

#users per sector	average centre cell throughput / kbps			resource utilization %	delay (sec)		packet call rate CDF
	cell t/put	OTA	pkt call rate		mean	median	<32k/64k/128k/384k/1M
20	252	1070	382	15	0.17	0.10	0 / 1 / 5 / 66 / 98
40	559	1200	384	33	0.20	0.10	0 / 2 / 8 / 66 / 98
80	1107	1378	334	70	0.39	0.14	5 / 9 / 19 / 72 / 98
120	1563	1645	310	91	0.95	0.14	13 / 17 / 25 / 74 / 99
160	1936	1951	291	98	1.84	0.15	18 / 23 / 30 / 75 / 99

Table 39 - Summary of 3.84Mcps VA120 results for HTTP with max C/I scheduler

2 x #users per sector	average centre cell throughput / kbps			resource utilization %	delay (sec)		packet call rate CDF
	2 x cell t/put	2 x OTA	pkt call rate		mean	median	<32k/64k/128k/384k/1M
20	295	1410	338	21	0.34	0.14	1 / 2 / 10 / 74 / 99
40	531	1434	317	35	0.38	0.13	4 / 8 / 20 / 75 / 100
80	998	1492	283	64	0.54	0.17	8 / 14 / 27 / 80 / 99
120	1527	1694	255	89	1.59	0.23	20 / 27 / 40 / 80 / 99
160	1803	1819	230	99	3.85	0.26	26 / 32 / 43 / 82 / 99

Figure 105 to Figure 108 present results using a Round Robin scheduler in channel VA120.

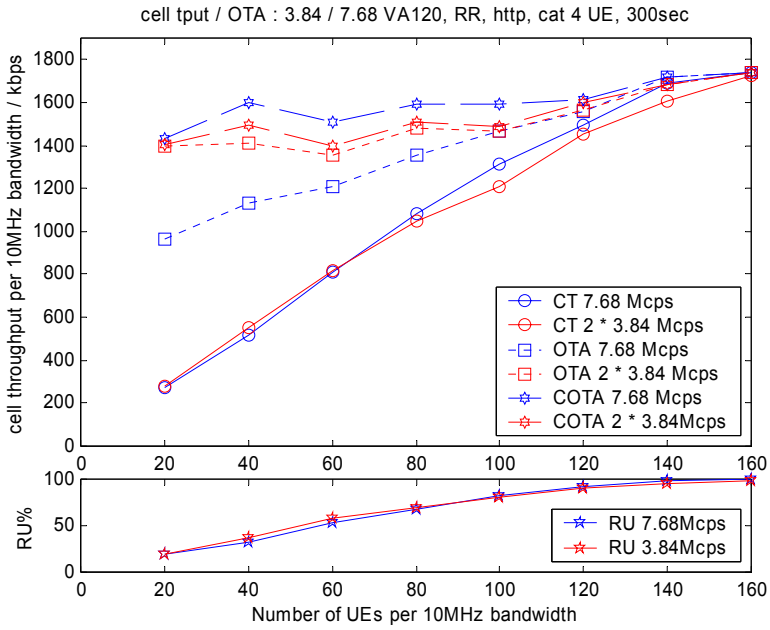

Figure 105 - VA120 : cell throughput / over the air throughput / resource utilisation HTTP, Round robin scheduler

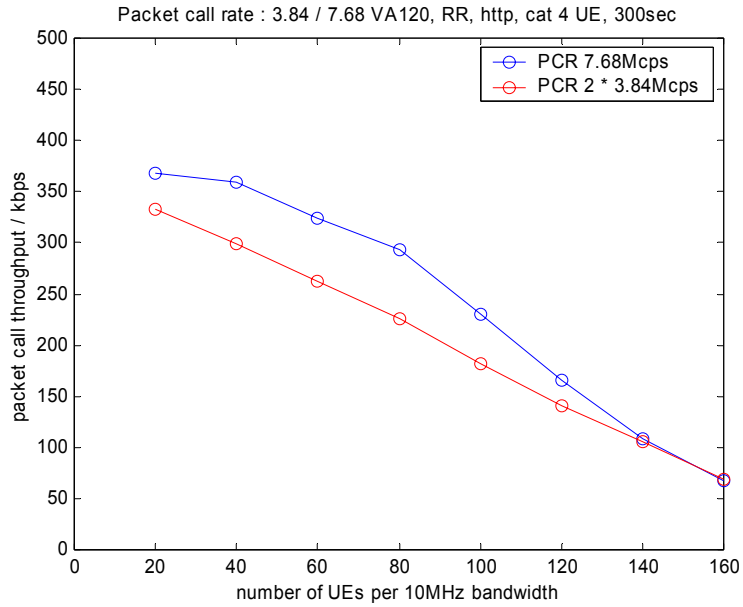

Figure 106 - VA120 : mean packet call rate HTTP, Round robin scheduler

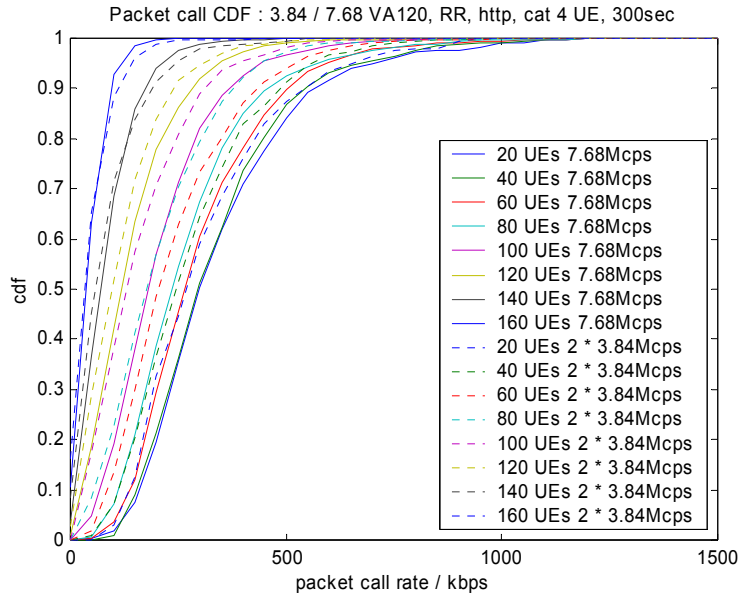

Figure 107 - VA120 : packet call rate CDFs HTTP, Round robin scheduler

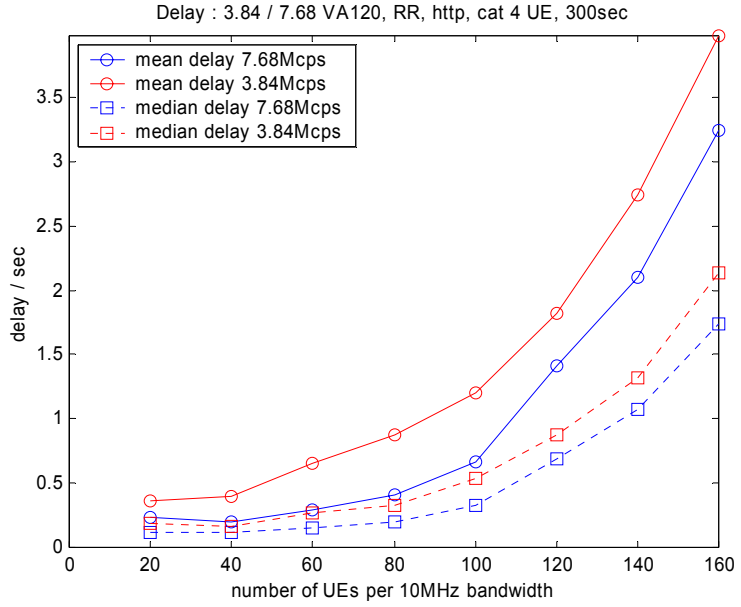

Figure 108 - VA120 : mean and median packet delays HTTP, Round robin scheduler

The MAC-hs failure rate in the VA120 channel with a Round robin scheduler was significantly less than 10^{-4} for both the 3.84Mcps and 7.68Mcps chip rates.

The VA120 results with the Round robin scheduler are summarized in Table 40 (7.68Mcps) and Table 41 (3.84Mcps).

Table 40 - Summary of 7.68Mcps VA120 results for HTTP with Round robin scheduler

#users per sector	average centre cell throughput / kbps			resource utilization %	delay (sec)		packet call rate CDF
	cell t/put	OTA	pkt call rate		mean	median	<32k/64k/128k/384k/1M
20	273	966	369	19	0.23	0.11	0 / 1 / 5 / 68 / 99
40	516	1129	359	32	0.20	0.11	0 / 0 / 5 / 70 / 99
80	1084	1356	294	68	0.41	0.19	0 / 2 / 15 / 83 / 100
120	1494	1560	165	93	1.41	0.69	12 / 25 / 54 / 97 / 100
160	1737	1738	67	100	3.24	1.74	44 / 72 / 96 / 100 / 100

Table 41 - Summary of 3.84Mcps VA120 results for HTTP with Round robin scheduler

2 x #users per sector	average centre cell throughput / kbps			resource utilization %	delay (sec)		packet call rate CDF
	2 x cell t/put	2 x OTA	pkt call rate		mean	median	<32k/64k/128k/384k/1M
20	278	1396	332	20	0.36	0.19	0 / 1 / 8 / 74 / 100
40	552	1409	299	37	0.40	0.16	1 / 3 / 15 / 80 / 100
80	1046	1482	226	69	0.87	0.33	5 / 12 / 33 / 91 / 100
120	1450	1567	140	91	1.82	0.88	19 / 35 / 63 / 98 / 100
160	1722	1737	69	99	3.98	2.14	48 / 72 / 93 / 100 / 100

5.3.2.3.6 Mixed Channel Model

Mixed channel model results with the HTTP traffic model are obtained with UEs being randomly assigned a channel with the probabilities specified in Table B.5.

Results are presented for a max C/I scheduler and a Round robin scheduler.

Figure 109 to Figure 113 present results using a max C/I scheduler with the mixed channel model.

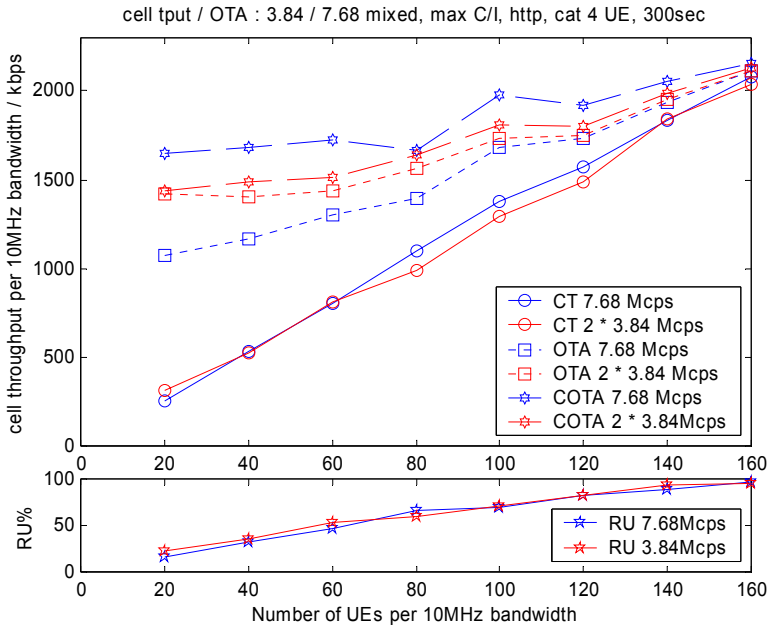

Figure 109 - mixed channel model : cell throughput / over the air throughput / resource utilisation HTTP, max C/I scheduler

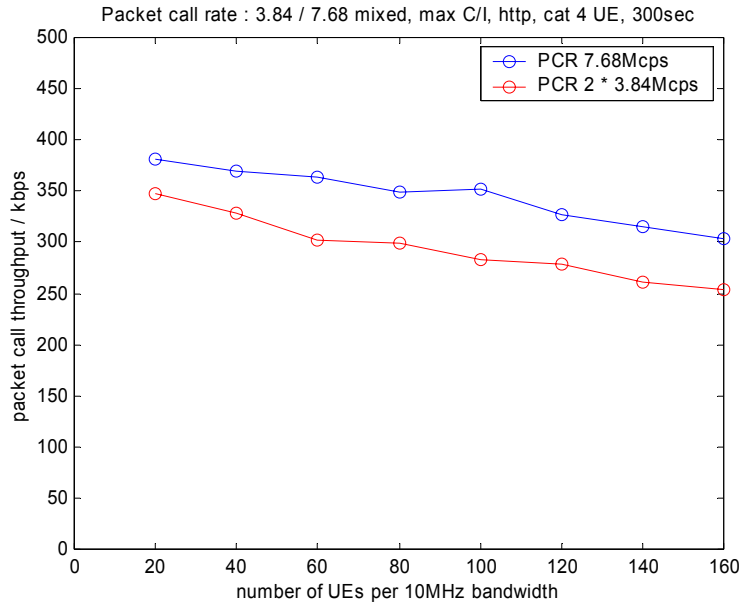

Figure 110 - mixed channel model : mean packet call rate HTTP, max C/I scheduler

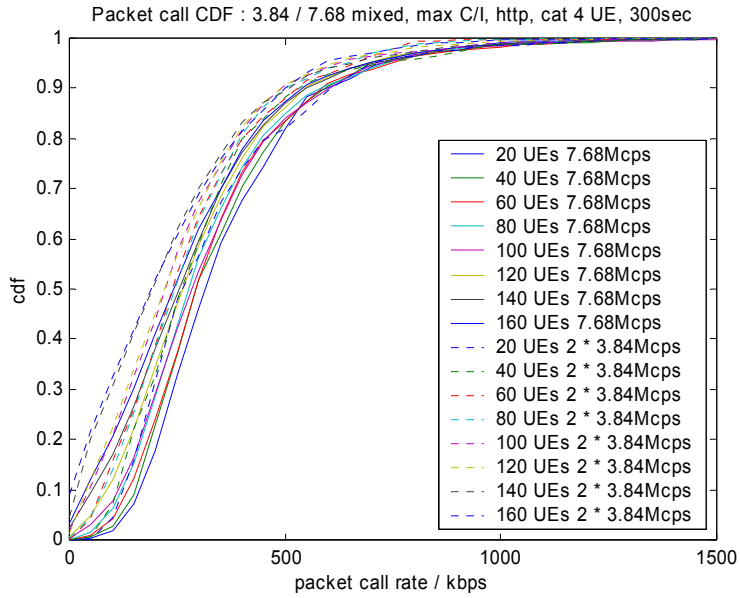

Figure 111 – mixed channel model : packet call rate CDFs HTTP, max C/I scheduler

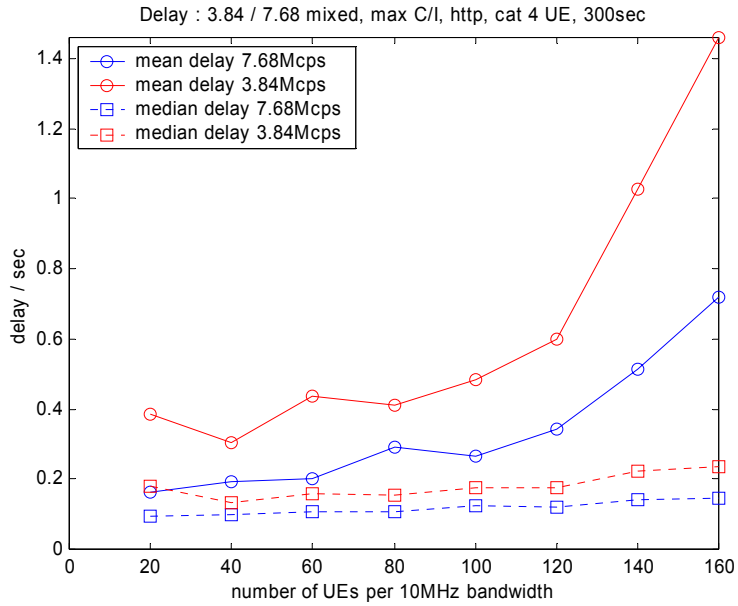

Figure 112 - mixed channel model : mean and median packet delays HTTP, max C/I scheduler

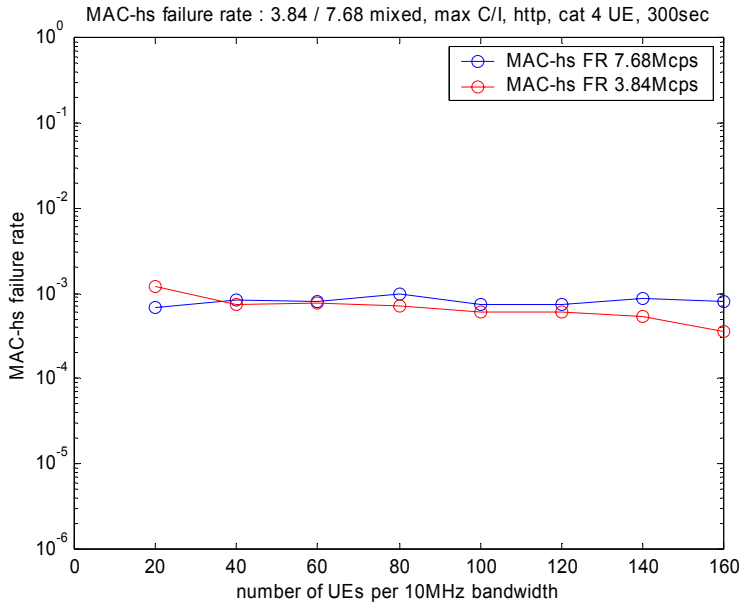

Figure 113 - mixed channel model : MAC-hs failure rate HTTP, max C/I scheduler

The mixed channel model results with the max C/I scheduler are summarized in Table 42 (7.68Mcps) and Table 43 (3.84Mcps).

Table 42 - Summary of 7.68Mcps mixed channel model results for HTTP with max C/I scheduler

#users per sector	average centre cell throughput / kbps			resource utilization %	delay (sec)		packet call rate CDF
	cell t/put	OTA	pkt call rate		mean	median	<32k/64k/128k/384k/1M
20	253	1071	382	15	0.16	0.10	0 / 1 / 5 / 65 / 99
40	530	1168	369	31	0.19	0.10	0 / 1 / 6 / 67 / 98
80	1096	1398	349	66	0.29	0.11	1 / 3 / 11 / 72 / 99
120	1570	1736	327	82	0.34	0.12	3 / 7 / 18 / 74 / 99
160	2079	2112	304	96	0.72	0.14	9 / 14 / 26 / 75 / 99

Table 43 - Summary of 3.84Mcps mixed channel model results for HTTP with max C/I scheduler

2 x #users per sector	average centre cell throughput / kbps			resource utilization %	delay (sec)		packet call rate CDF
	2 x cell t/put	2 x OTA	pkt call rate		mean	median	<32k/64k/128k/384k/1M
20	316	1421	348	22	0.39	0.18	0 / 1 / 11 / 72 / 99
40	528	1402	328	35	0.30	0.13	0 / 2 / 16 / 77 / 99
80	989	1565	300	60	0.41	0.15	3 / 7 / 20 / 78 / 100
120	1490	1750	278	83	0.60	0.17	8 / 15 / 29 / 80 / 99
160	2035	2115	254	95	1.46	0.24	17 / 25 / 38 / 80 / 100

Figure 114 to Figure 118 present results using a Round robin scheduler with the mixed channel model.

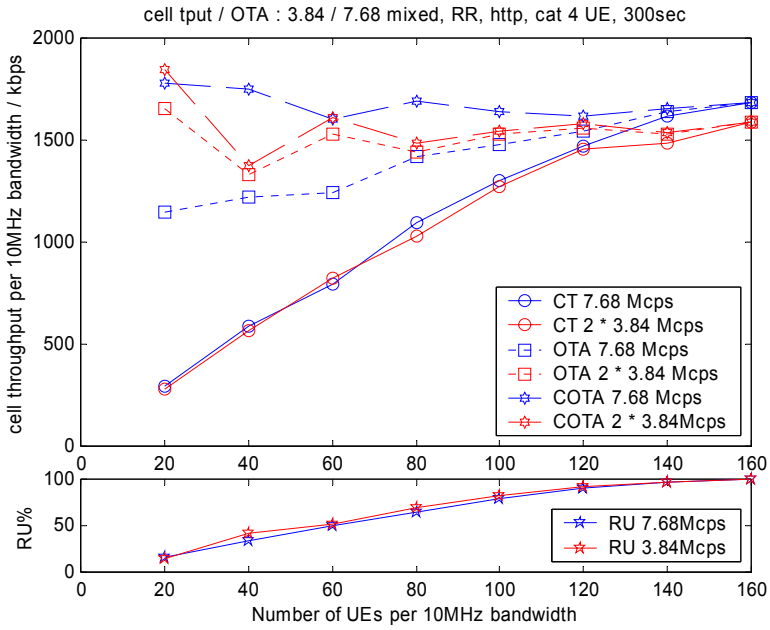

Figure 114 - mixed channel model : cell throughput / over the air throughput / resource utilisation HTTP, Round robin scheduler

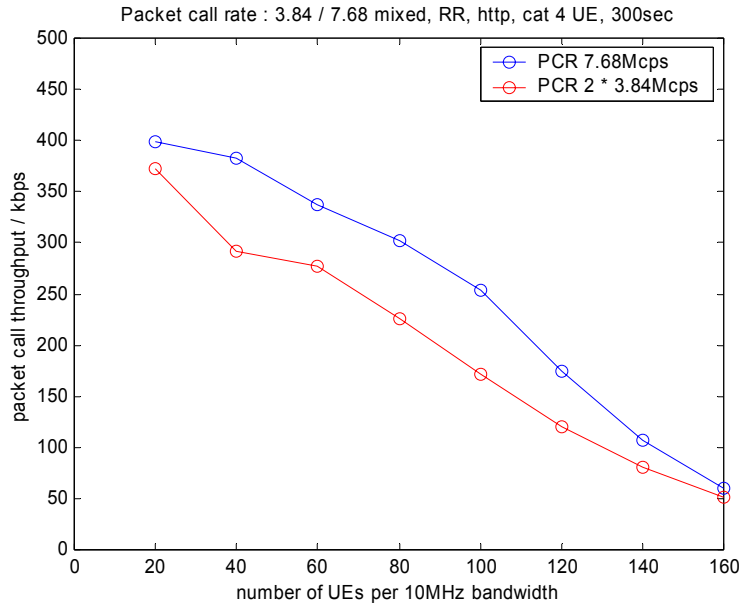

Figure 115 - mixed channel model : mean packet call rate HTTP, Round robin scheduler

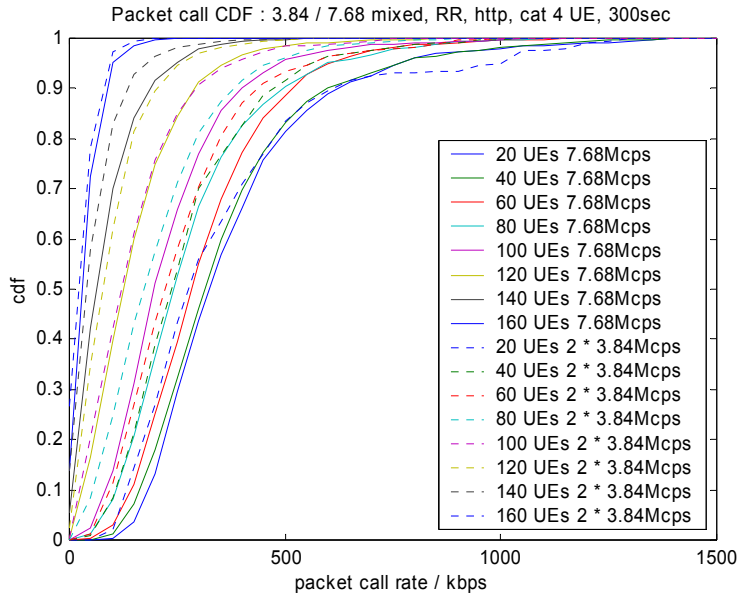

Figure 116 – mixed channel model : packet call rate CDFs HTTP, Round robin scheduler

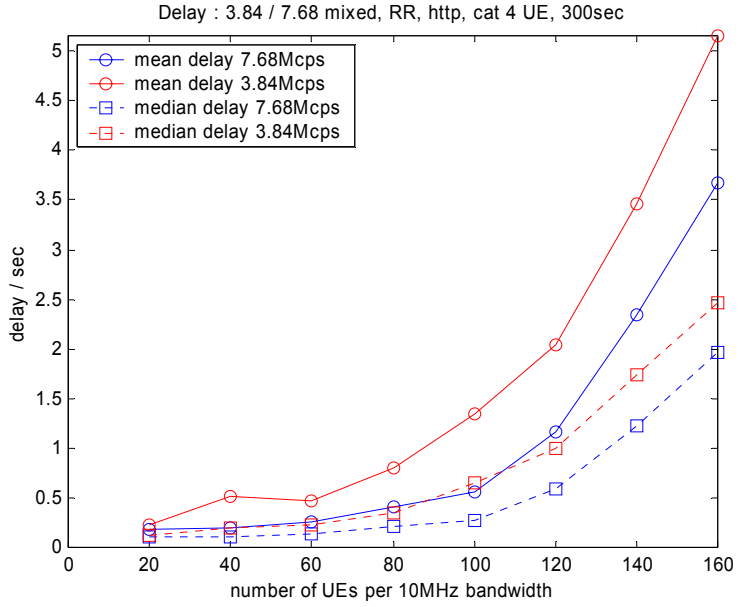

Figure 117 - mixed channel model : mean and median packet delays HTTP, Round robin scheduler

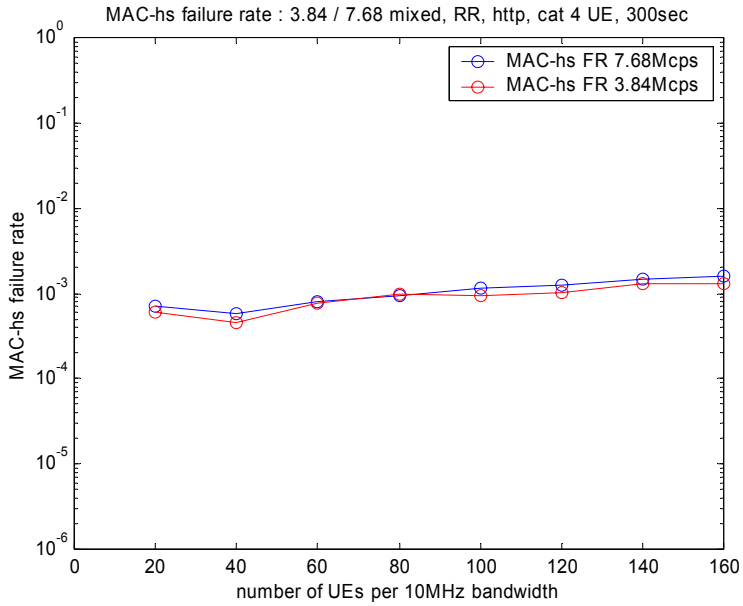

Figure 118 - mixed channel model : MAC-hs failure rate HTTP, Round robin scheduler

The mixed channel model results with the Round robin scheduler are summarized in Table 44 (7.68Mcps) and Table 45 (3.84Mcps).

Table 44 - Summary of 7.68Mcps mixed channel model results for HTTP with Round robin scheduler

#users per sector	average centre cell throughput / kbps			resource utilization %	delay (sec)		packet call rate CDF
	cell t/put	OTA	pkt call rate		mean	median	<32k/64k/128k/384k/1M
20	298	1145	399	17	0.18	0.10	0 / 0 / 2 / 63 / 98
40	589	1223	383	34	0.20	0.11	0 / 0 / 4 / 67 / 98
80	1093	1421	302	65	0.41	0.20	1 / 3 / 15 / 81 / 100
120	1473	1547	174	91	1.16	0.59	11 / 23 / 51 / 96 / 100
160	1681	1683	60	100	3.68	1.97	51 / 79 / 97 / 100 / 100

Table 45 - Summary of 3.84Mcps mixed channel model results for HTTP with Round robin scheduler

2 x #users per sector	average centre cell throughput / kbps			resource utilization %	delay (sec)		packet call rate CDF
	2 x cell t/put	2 x OTA	pkt call rate		mean	median	<32k/64k/128k/384k/1M
20	279	1653	373	15	0.23	0.12	0 / 1 / 9 / 69 / 95
40	566	1331	293	41	0.51	0.20	0 / 3 / 16 / 81 / 100
80	1032	1440	225	70	0.81	0.35	5 / 13 / 35 / 90 / 100
120	1459	1561	120	92	2.04	0.99	23 / 42 / 73 / 99 / 100
160	1591	1591	51	100	5.15	2.46	60 / 84 / 99 / 100 / 100

5.3.2.4 FTP Traffic Model Results

In the FTP simulations, for each simulation run, the system is simulated for 700 seconds after a warm up period of 200 seconds (i.e. 70000 TTIs are simulated per simulation run). Multiple simulation runs (>20) are performed to achieve statistical significance. UEs are randomly dropped onto the 19 cell layout for each simulation run.

5.3.2.4.1 AWGN

Results are presented for a max C/I scheduler and a Round robin scheduler.

Figure 119 to Figure 122 present results using a max C/I scheduler in an AWGN channel.

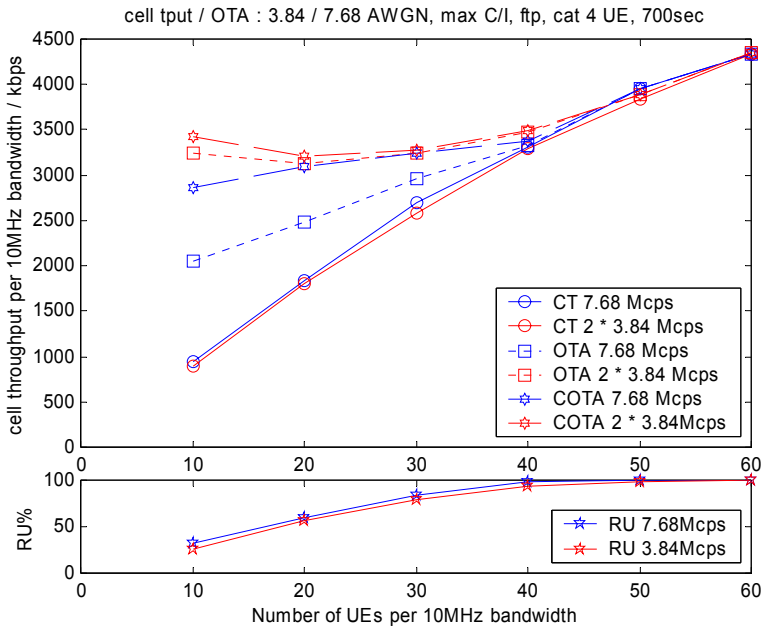

Figure 119 - AWGN : cell throughput / over the air throughput / resource utilisation FTP, max C/I scheduler

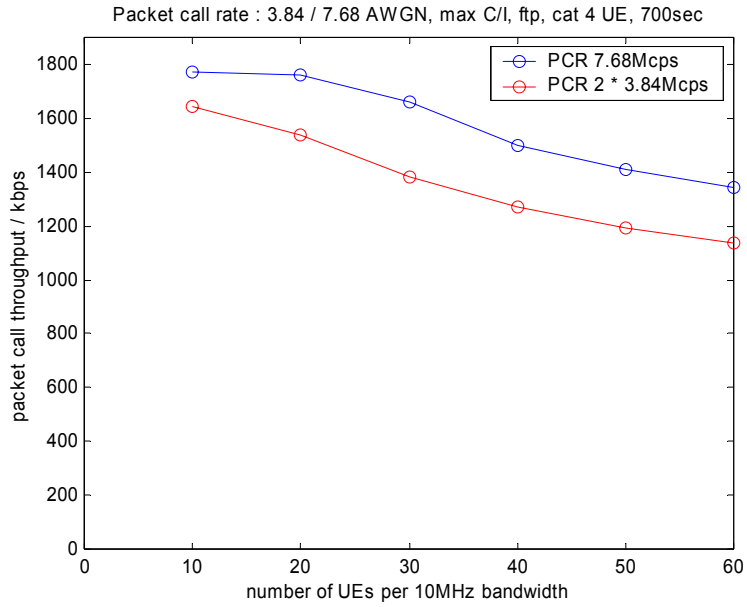

Figure 120 - AWGN : mean packet call rate FTP, max C/I scheduler

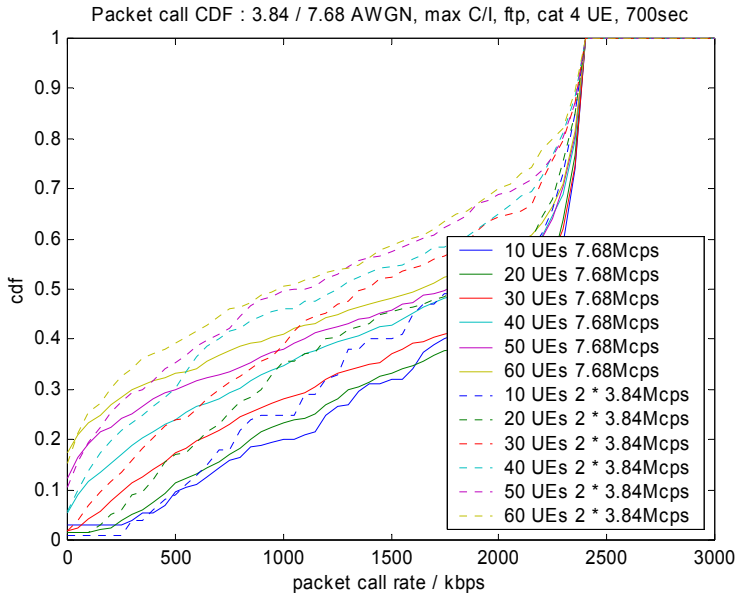

Figure 121 - AWGN : packet call rate CDFs FTP, max C/I scheduler

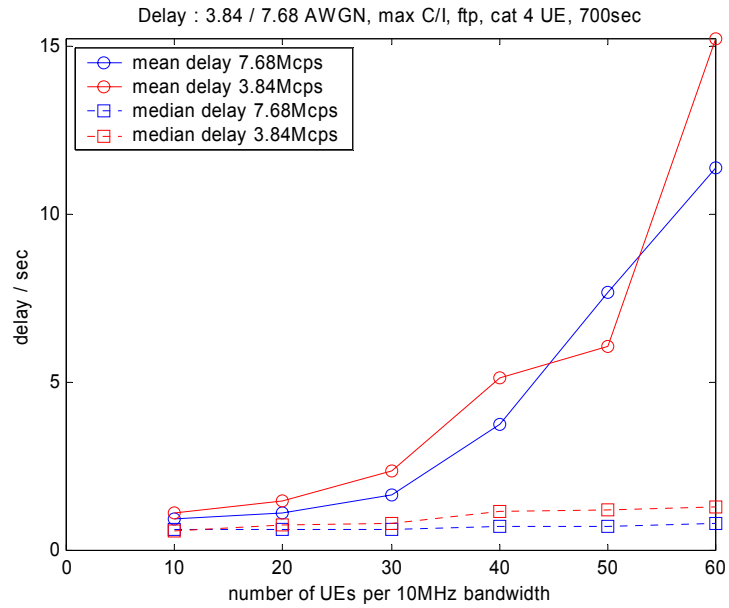

Figure 122 - AWGN : mean and median packet delays FTP, max C/I scheduler

The MAC-hs failure rate in the AWGN channel with a max C/I scheduler was significantly less than 10^{-4} for both the 3.84Mcps and 7.68Mcps chip rates.

The AWGN results with the max C/I scheduler are summarized in Table 46 (7.68Mcps) and Table 47 (3.84Mcps).

Table 46 - Summary of 7.68Mcps AWGN results for FTP with max C/I scheduler

#users per sector	average centre cell throughput / kbps			resource utilization %	delay (sec)		packet call rate CDF
	cell t/put	OTA	pkt call rate		mean	median	<32k/64k/128k/384k/1M
10	946	2046	1771	33	0.95	0.62	3 / 3 / 3 / 5 / 20
20	1834	2484	1762	59	1.11	0.61	2 / 2 / 2 / 7 / 23
30	2704	2966	1663	83	1.67	0.62	2 / 3 / 5 / 14 / 28
40	3303	3334	1497	98	3.75	0.72	8 / 10 / 13 / 21 / 35
50	3947	3947	1410	100	7.68	0.72	15 / 17 / 20 / 28 / 38
60	4328	4328	1341	100	11.41	0.81	20 / 22 / 24 / 31 / 41

Table 47 - Summary of 3.84Mcps AWGN results for FTP with max C/I scheduler

2 x #users per sector	average centre cell throughput / kbps			resource utilization %	delay (sec)		packet call rate CDF
	2 x cell t/put	2 x OTA	pkt call rate		mean	median	<32k/64k/128k/384k/1M
10	889	3241	1644	26	1.10	0.59	1 / 1 / 1 / 5 / 25
20	1803	3122	1538	56	1.47	0.77	2 / 2 / 2 / 11 / 36
30	2574	3239	1382	79	2.38	0.81	3 / 5 / 8 / 20 / 39
40	3286	3481	1270	94	5.13	1.16	8 / 11 / 16 / 26 / 46
50	3837	3888	1192	99	6.08	1.20	14 / 17 / 21 / 31 / 50
60	4333	4333	1136	100	15.23	1.29	19 / 22 / 26 / 37 / 50

Figure 123 to Figure 126 present results using a Round robin scheduler in an AWGN channel.

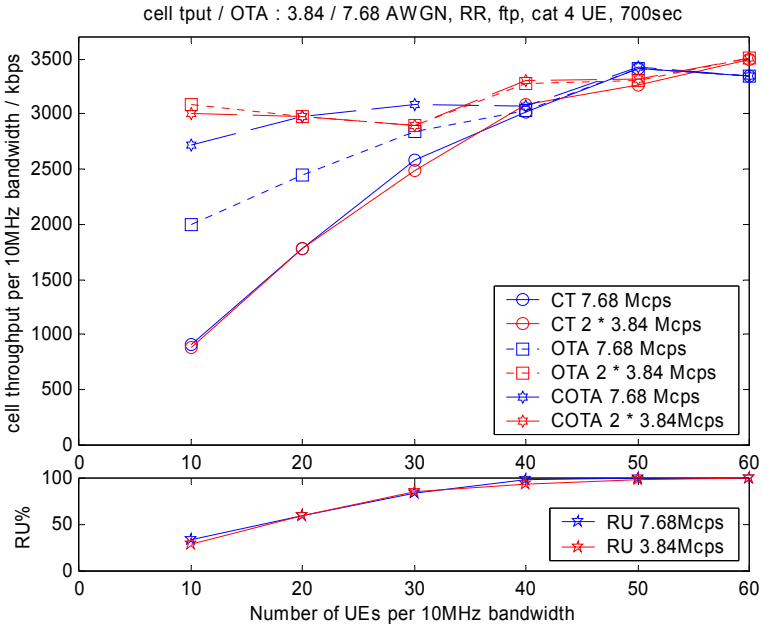

Figure 123 - AWGN : cell throughput / over the air throughput / resource utilisation FTP, Round robin scheduler

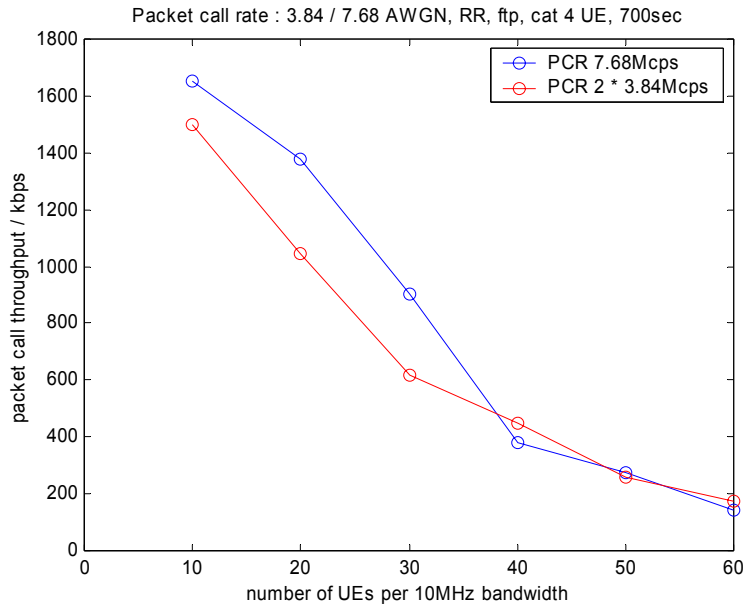

Figure 124 - AWGN : mean packet call rate FTP, Round robin scheduler

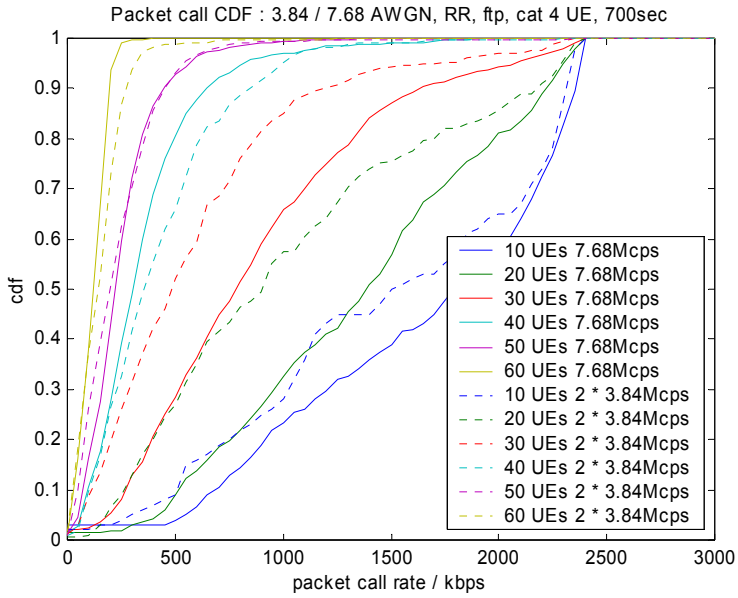

Figure 125 - AWGN : packet call rate CDFs FTP, Round robin scheduler

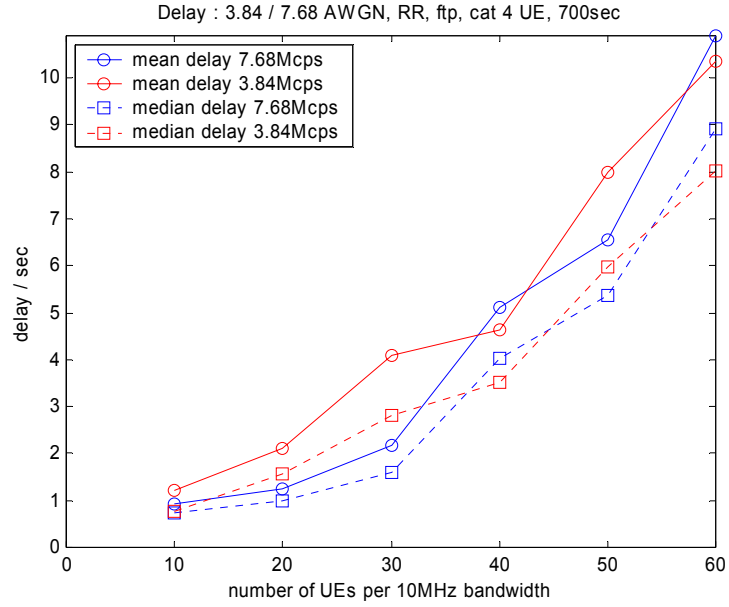

Figure 126 - AWGN : mean and median packet delays FTP, Round robin scheduler

The MAC-hs failure rate in the AWGN channel with a Round robin scheduler was significantly less than 10^{-4} for both the 3.84Mcps and 7.68Mcps chip rates.

The AWGN results with the Round robin scheduler are summarized in Table 48 (7.68Mcps) and Table 49 (3.84Mcps).

Table 48 - Summary of 7.68Mcps AWGN results for FTP with Round robin scheduler

#users per sector	average centre cell throughput / kbps			resource utilization %	delay (sec)		packet call rate CDF
	cell t/put	OTA	pkt call rate		mean	median	<32k/64k/128k/384k/1M
10	908	2003	1653	33	0.92	0.73	3 / 3 / 3 / 3 / 24
20	1775	2446	1379	60	1.23	0.99	2 / 2 / 2 / 4 / 33
30	2584	2842	901	84	2.17	1.61	2 / 2 / 3 / 19 / 66
40	3015	3040	380	98	5.12	4.03	2 / 5 / 15 / 66 / 97
50	3413	3418	275	99	6.54	5.38	3 / 8 / 22 / 85 / 100
60	3344	3344	142	100	10.90	8.93	11 / 22 / 54 / 100 / 100

Table 49 - Summary of 3.84Mcps AWGN results for FTP with Round robin scheduler

2 x #users per sector	average centre cell throughput / kbps			resource utilization %	delay (sec)		packet call rate CDF
	2 x cell t/put	2 x OTA	pkt call rate		mean	median	<32k/64k/128k/384k/1M
10	883	3087	1498	29	1.23	0.78	2 / 2 / 3 / 7 / 28
20	1776	2981	1047	60	2.12	1.57	1 / 1 / 2 / 19 / 58
30	2491	2891	617	86	4.09	2.80	2 / 4 / 11 / 41 / 85
40	3087	3277	448	94	4.65	3.50	1 / 4 / 14 / 53 / 95
50	3268	3308	259	98	8.00	5.98	7 / 14 / 34 / 83 / 99
60	3492	3503	174	100	10.34	8.02	12 / 23 / 46 / 98 / 100

5.3.2.4.2 Pedestrian A 3kmph

Results are presented for a max C/I scheduler and a Round robin scheduler.

Figure 127 to Figure 131 present results using a max C/I scheduler in channel PA3.

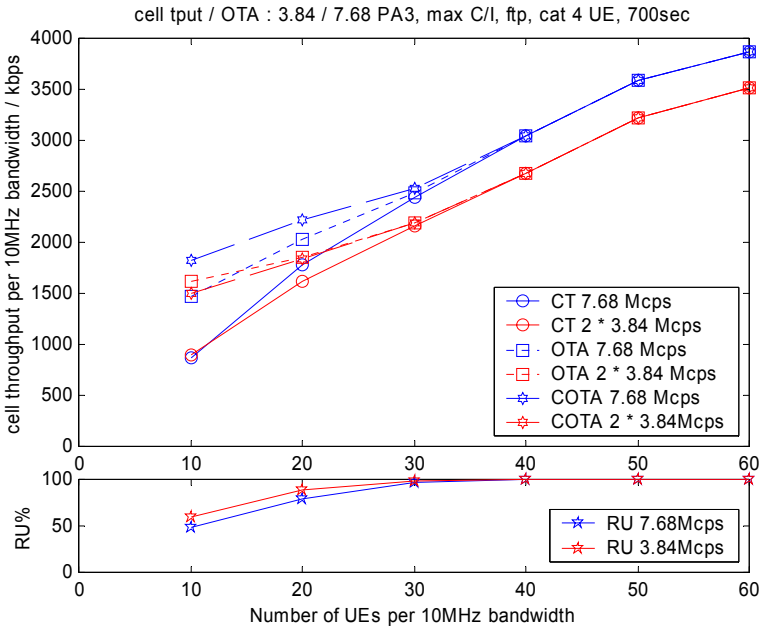

Figure 127 - PA3 : cell throughput / over the air throughput / resource utilisation FTP, max C/I scheduler

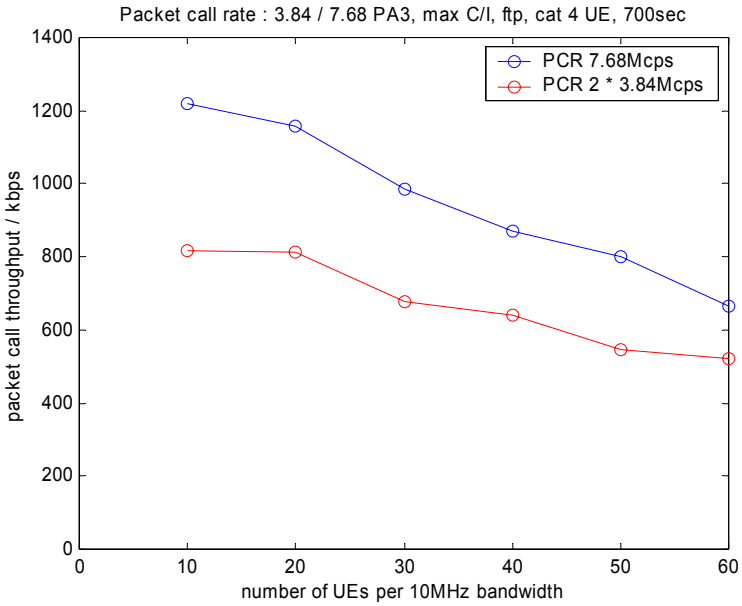

Figure 128 - PA3 : mean packet call rate FTP, max C/I scheduler

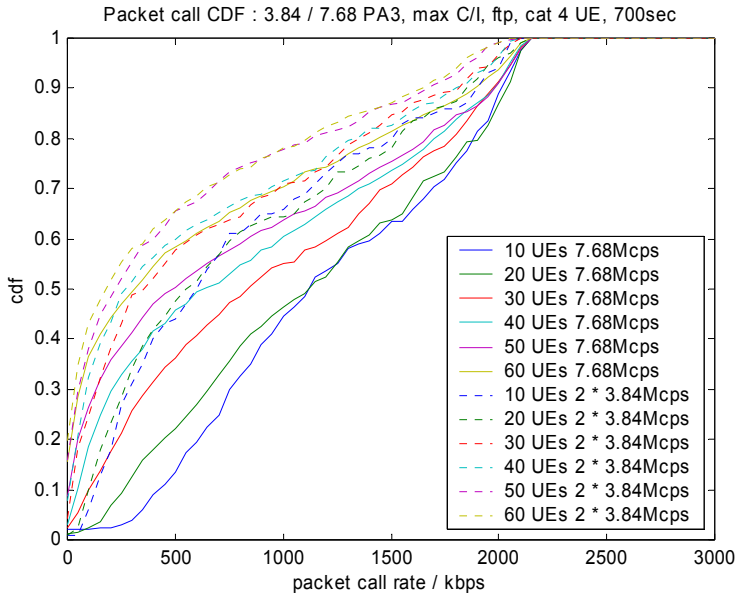

Figure 129 - PA3 : packet call rate CDFs FTP, max C/I scheduler

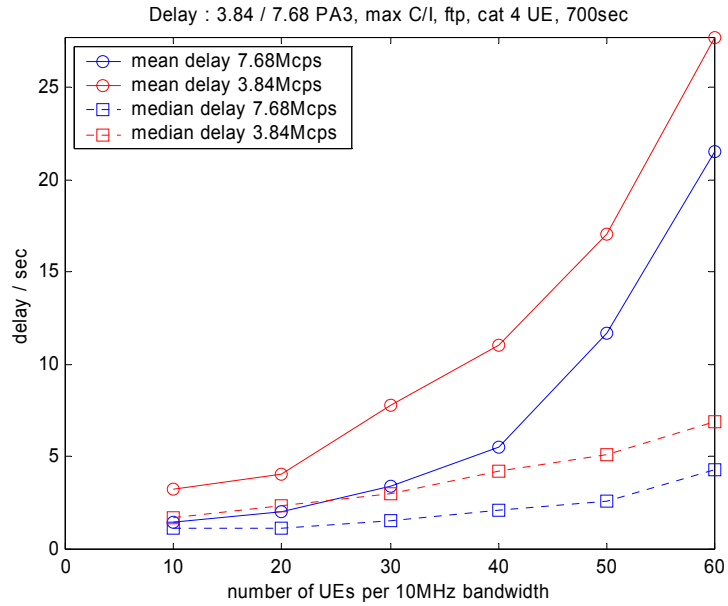

Figure 130 - PA3 : mean and median packet delays FTP, max C/I scheduler

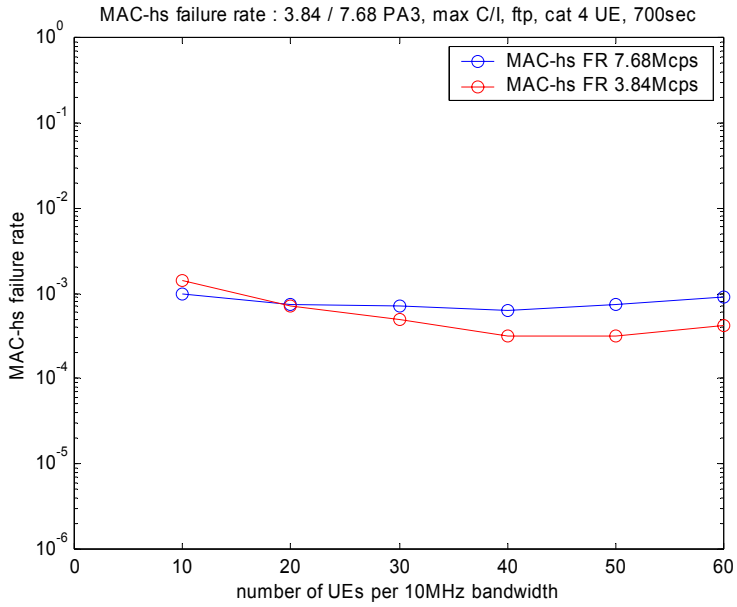

Figure 131 - PA3 : MAC-hs failure rate FTP, max C/I scheduler

The PA3 results with the max C/I scheduler are summarized in Table 50 (7.68Mcps) and Table 51 (3.84Mcps).

Table 50 - Summary of 7.68Mcps PA3 results for FTP with max C/I scheduler

#users per sector	average centre cell throughput / kbps			resource utilization %	delay (sec)		packet call rate CDF
	cell t/put	OTA	pkt call rate		mean	median	<32k/64k/128k/384k/1M
10	872	1469	1221	48	1.47	1.13	2 / 2 / 2 / 8 / 45
20	1773	2027	1157	80	2.01	1.16	1 / 2 / 3 / 17 / 47
30	2439	2483	984	97	3.42	1.50	4 / 7 / 12 / 30 / 55
40	3045	3046	871	100	5.55	2.14	8 / 12 / 22 / 40 / 60
50	3581	3581	801	100	11.65	2.60	16 / 22 / 29 / 46 / 64
60	3874	3874	665	100	21.50	4.34	24 / 31 / 39 / 54 / 70

Table 51 - Summary of 3.84Mcps PA3 results for FTP with max C/I scheduler

2 x #users per sector	average centre cell throughput / kbps			resource utilization %	delay (sec)		packet call rate CDF
	2 x cell t/put	2 x OTA	pkt call rate		mean	median	<32k/64k/128k/384k/1M
10	901	1618	817	60	3.28	1.70	1 / 2 / 10 / 38 / 66
20	1619	1846	811	88	4.07	2.33	2 / 5 / 14 / 41 / 65
30	2155	2188	675	99	7.78	3.02	13 / 20 / 29 / 51 / 71
40	2676	2682	641	100	11.06	4.18	16 / 24 / 36 / 56 / 71
50	3222	3222	546	100	17.07	5.12	25 / 32 / 42 / 60 / 78
60	3509	3509	522	100	27.67	6.86	29 / 37 / 46 / 61 / 78

Figure 132 to Figure 136 present results using a Round robin scheduler in channel PA3.

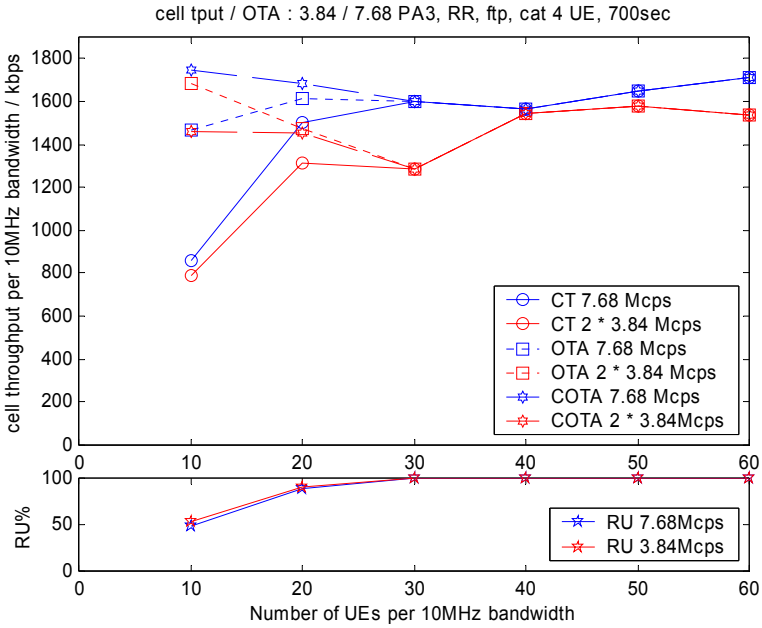

Figure 132 – PA3 : cell throughput / over the air throughput / resource utilisation FTP, Round robin scheduler

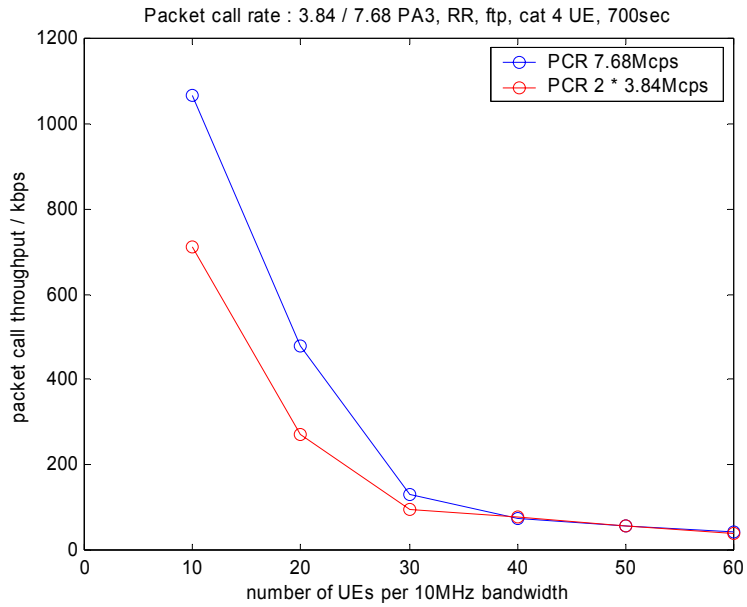

Figure 133 – PA3 : mean packet call rate FTP, Round robin scheduler

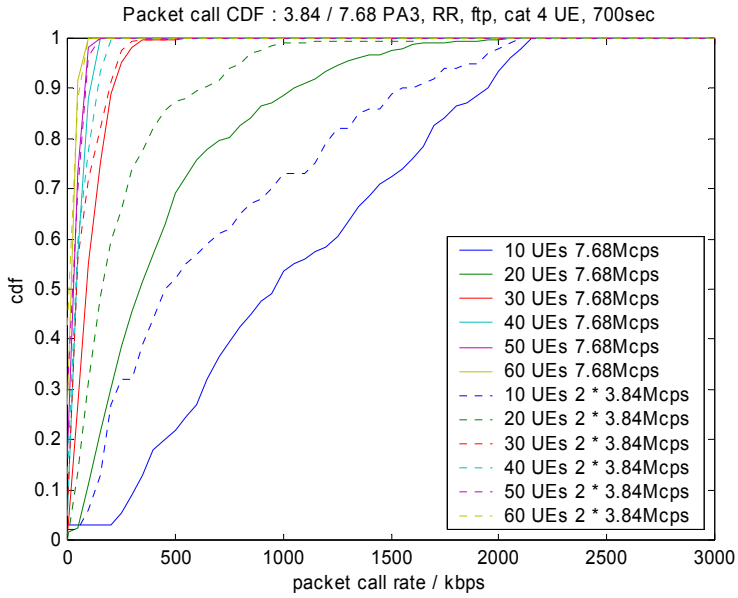

Figure 134 – PA3 : packet call rate CDFs FTP, Round robin scheduler

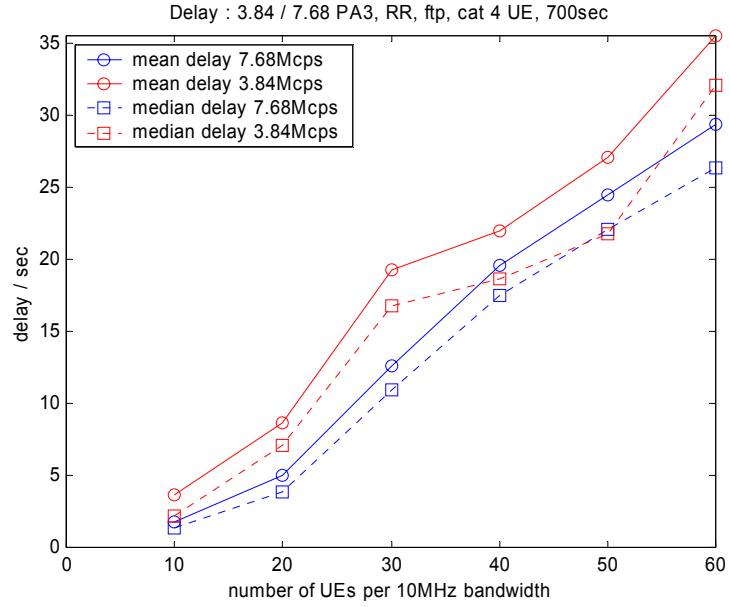

Figure 135 – PA3 : mean and median packet delays FTP, Round robin scheduler

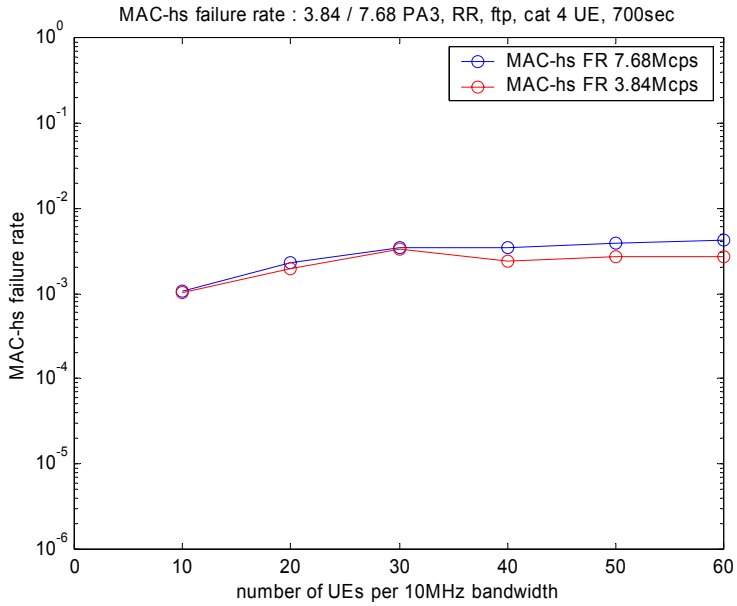

Figure 136 - PA3 : MAC-hs failure rate FTP, Round robin scheduler

The PA3 results with the Round robin scheduler are summarized in Table 52 (7.68Mcps) and Table 53 (3.84Mcps).

Table 52 - Summary of 7.68Mcps PA3 results for FTP with Round robin scheduler

#users per sector	average centre cell throughput / kbps			resource utilization %	delay (sec)		packet call rate CDF
	cell t/put	OTA	pkt call rate		mean	median	<32k/64k/128k/384k/1M
10	857	1470	1067	49	1.74	1.40	3 / 3 / 3 / 16 / 54
20	1499	1617	479	89	4.97	3.85	2 / 5 / 17 / 55 / 88
30	1598	1598	130	100	12.61	10.95	18 / 35 / 66 / 100 / 100
40	1567	1567	73	100	19.56	17.44	38 / 66 / 95 / 100 / 100
50	1645	1645	55	100	24.43	22.06	53 / 80 / 99 / 100 / 100
60	1713	1713	43	100	29.36	26.28	68 / 94 / 100 / 100 / 100

Table 53 - Summary of 3.84Mcps PA3 results for FTP with Round robin scheduler

2 x #users per sector	average centre cell throughput / kbps			resource utilization %	delay (sec)		packet call rate CDF
	2 x cell t/put	2 x OTA	pkt call rate		mean	median	<32k/64k/128k/384k/1M
10	787	1682	712	54	3.63	2.14	2 / 3 / 10 / 42 / 73
20	1316	1472	270	91	8.61	7.06	9 / 19 / 41 / 81 / 99
30	1284	1287	98	100	19.23	16.77	38 / 60 / 78 / 100 / 100
40	1541	1541	76	100	21.92	18.67	43 / 65 / 86 / 100 / 100
50	1579	1579	55	100	27.07	21.72	55 / 77 / 98 / 100 / 100
60	1539	1539	38	100	35.47	32.01	72 / 91 / 100 / 100 / 100

5.3.2.4.3 Pedestrian B 3kmph

Results are presented for a max C/I scheduler and a Round robin scheduler.

Figure 137 to Figure 141 present results using a max C/I scheduler in channel PB3.

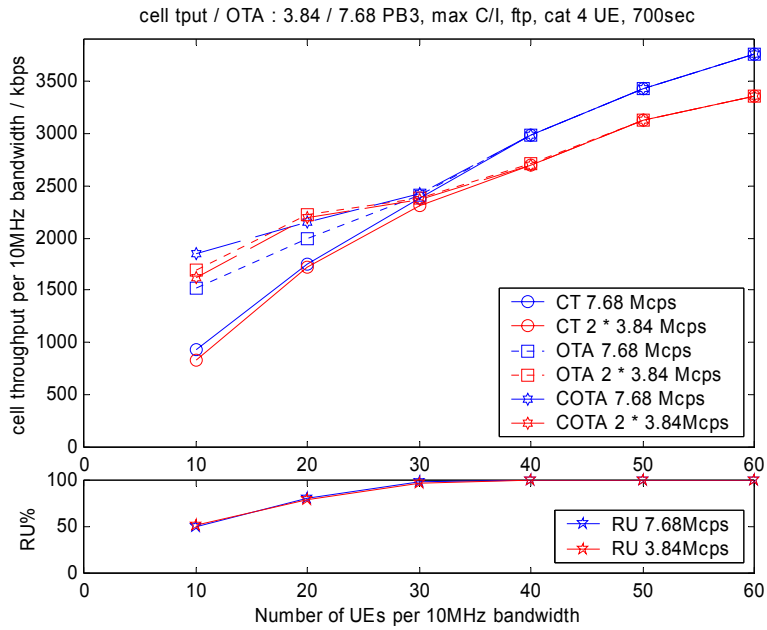

Figure 137 - PB3 : cell throughput / over the air throughput / resource utilisation FTP, max C/I scheduler

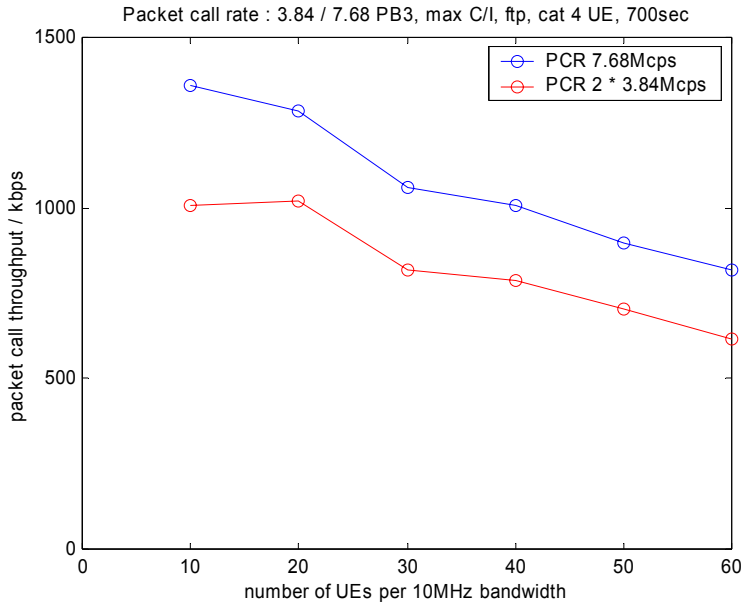

Figure 138 - PB3 : mean packet call rate FTP, max C/I scheduler

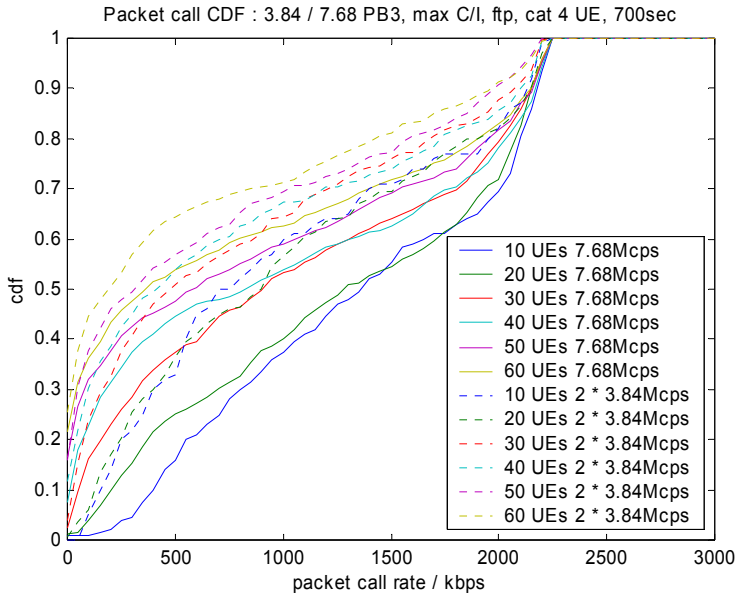

Figure 139 - PB3 : packet call rate CDFs FTP, max C/I scheduler

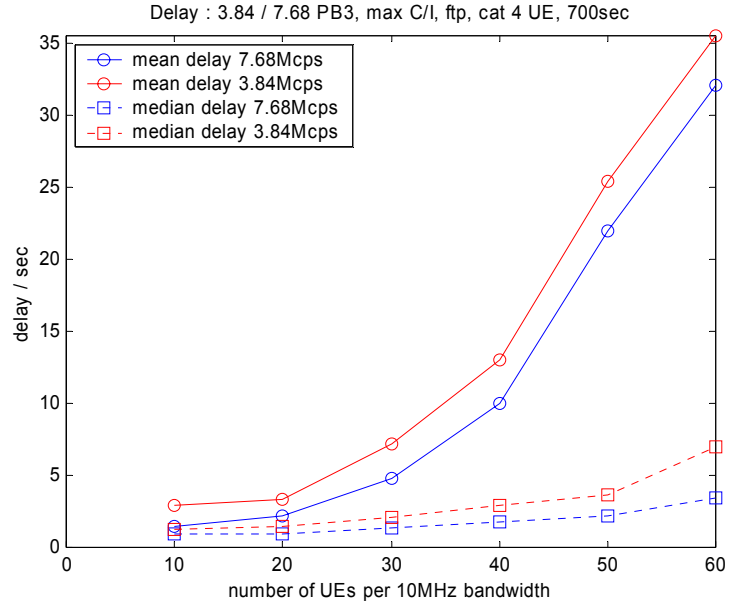

Figure 140 - PB3 : mean and median packet delays FTP, max C/I scheduler

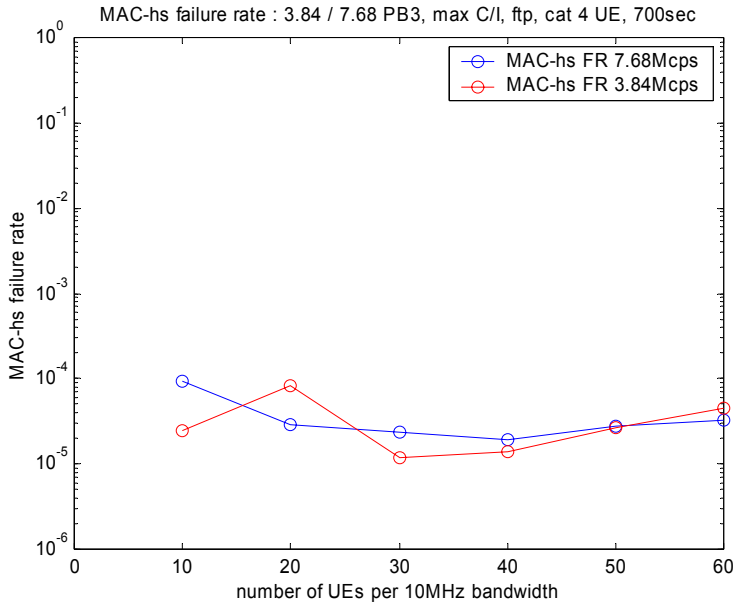

Figure 141 - PB3 : MAC-hs failure rate FTP, max C/I scheduler

The PB3 results with the max C/I scheduler are summarized in Table 54 (7.68Mcps) and Table 55 (3.84Mcps).

Table 54 - Summary of 7.68Mcps PB3 results for FTP with max C/I scheduler

#users per sector	average centre cell throughput / kbps			resource utilization %	delay (sec)		packet call rate CDF
	cell t/put	OTA	pkt call rate		mean	median	<32k/64k/128k/384k/1M
10	927	1519	1361	50	1.45	0.96	1 / 1 / 1 / 9 / 38
20	1745	1991	1282	81	2.14	0.95	1 / 2 / 6 / 21 / 40
30	2384	2406	1059	98	4.79	1.36	7 / 11 / 18 / 33 / 53
40	2982	2982	1008	100	10.00	1.81	14 / 19 / 26 / 40 / 54
50	3428	3428	899	100	21.95	2.20	23 / 28 / 34 / 45 / 59
60	3763	3763	816	100	32.02	3.43	28 / 33 / 38 / 51 / 63

Table 55 - Summary of 3.84Mcps PB3 results for FTP with max C/I scheduler

2 x #users per sector	average centre cell throughput / kbps			resource utilization %	delay (sec)		packet call rate CDF
	2 x cell t/put	2 x OTA	pkt call rate		mean	median	<32k/64k/128k/384k/1M
10	832	1691	1008	51	2.92	1.23	0 / 1 / 8 / 28 / 60
20	1727	2226	1019	79	3.37	1.51	2 / 4 / 10 / 29 / 57
30	2309	2375	818	97	7.21	2.07	11 / 18 / 27 / 46 / 64
40	2696	2704	788	100	13.00	2.90	18 / 24 / 33 / 49 / 67
50	3119	3119	705	100	25.36	3.69	25 / 32 / 40 / 53 / 70
60	3359	3359	618	100	35.50	6.96	33 / 40 / 47 / 61 / 71

Figure 142 to Figure 146 present results using a Round robin scheduler in channel PB3.

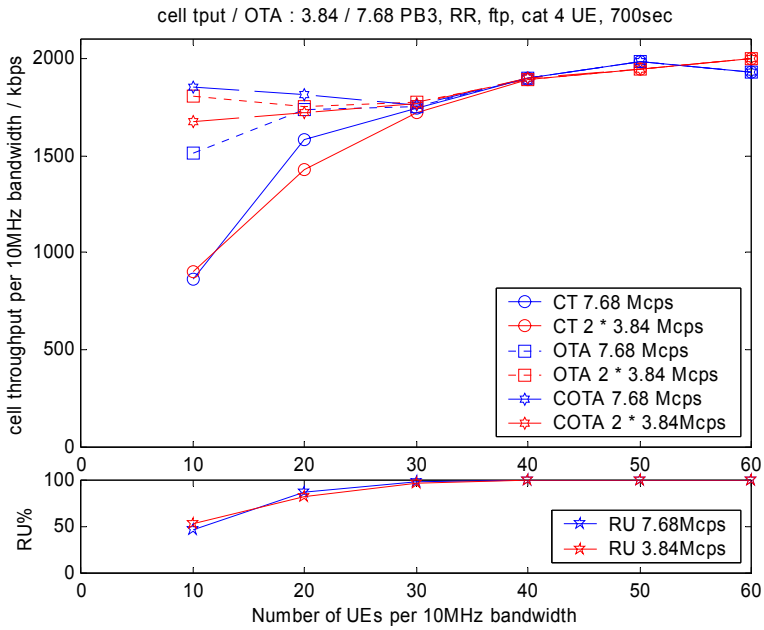

Figure 142 - PB3 : cell throughput / over the air throughput / resource utilisation FTP, Round robin scheduler

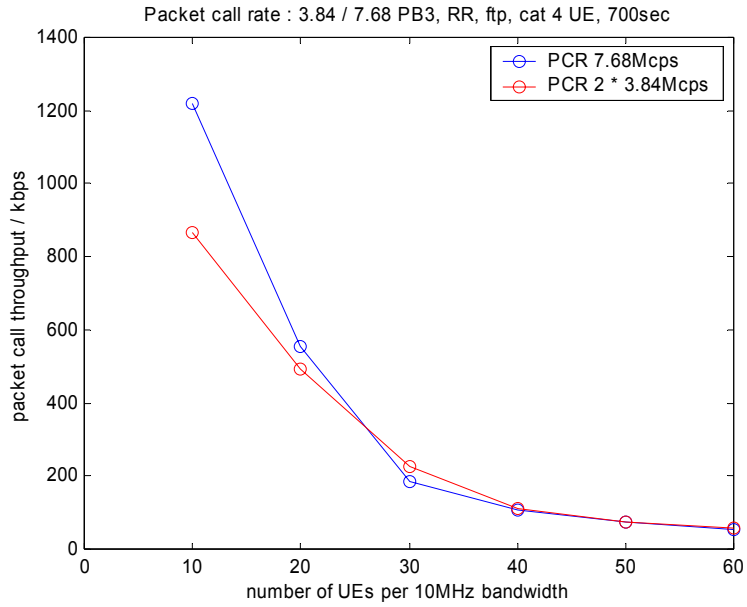

Figure 143 - PB3 : mean packet call rate FTP, Round robin scheduler

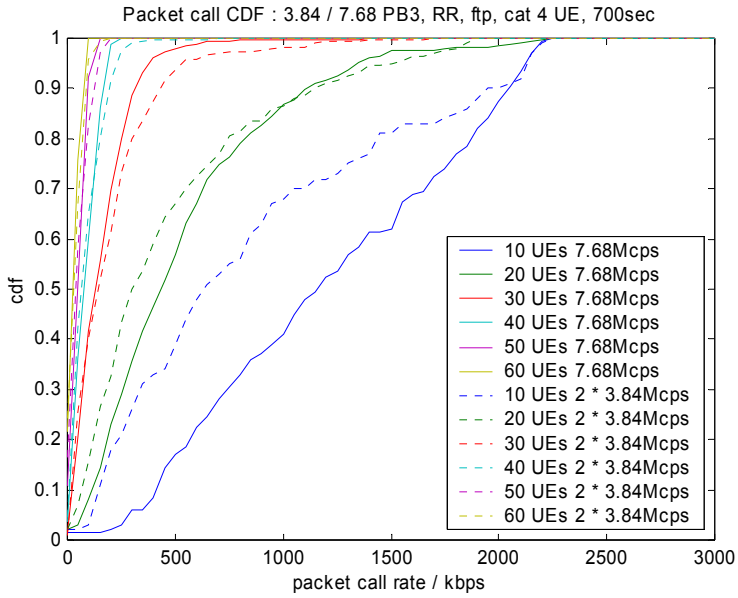

Figure 144 - PB3 : packet call rate CDFs FTP, Round robin scheduler

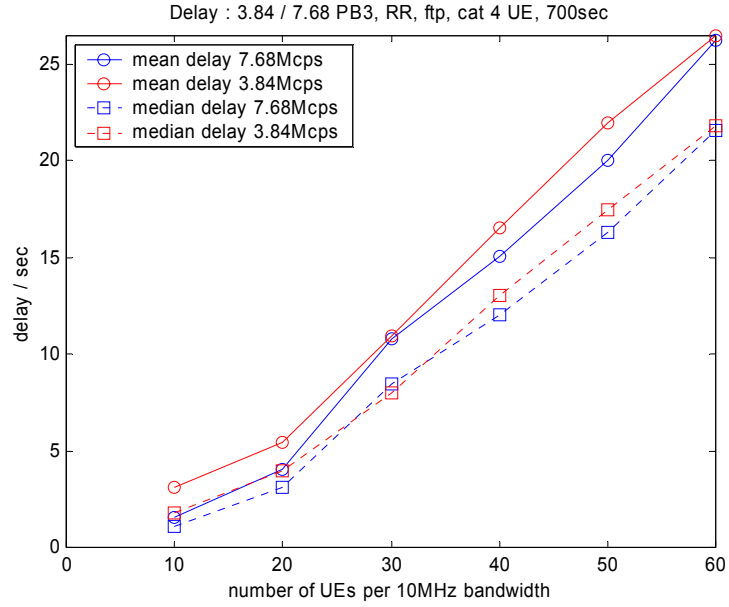

Figure 145 - PB3 : mean and median packet delays FTP, Round robin scheduler

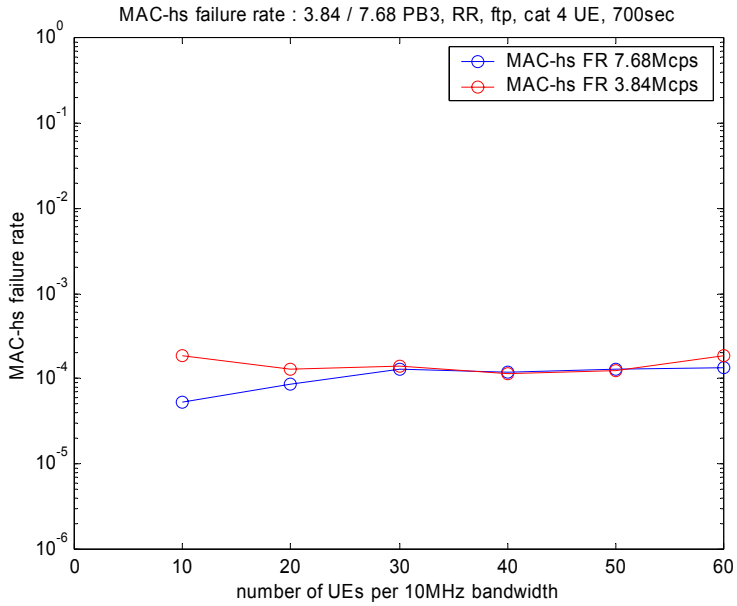

Figure 146 - PB3 : MAC-hs failure rate FTP, Round robin scheduler

The PB3 results with the Round robin scheduler are summarized in Table 56 (7.68Mcps) and Table 57 (3.84Mcps).

Table 56 - Summary of 7.68Mcps PB3 results for FTP with max C/I scheduler

#users per sector	average centre cell throughput / kbps			resource utilization %	delay (sec)		packet call rate CDF
	cell t/put	OTA	pkt call rate		mean	median	<32k/64k/128k/384k/1M
10	865	1510	1218	47	1.52	1.10	2 / 2 / 2 / 8 / 41
20	1581	1736	556	87	4.06	3.09	3 / 4 / 12 / 45 / 87
30	1743	1753	183	99	10.78	8.49	14 / 26 / 49 / 95 / 100
40	1900	1900	106	100	15.05	12.05	25 / 43 / 75 / 100 / 100
50	1987	1987	73	100	20.03	16.27	36 / 62 / 97 / 100 / 100
60	1933	1933	51	100	26.24	21.58	56 / 82 / 100 / 100 / 100

Table 57 - Summary of 3.84Mcps PB3 results for FTP with max C/I scheduler

2 x #users per sector	average centre cell throughput / kbps			resource utilization %	delay (sec)		packet call rate CDF
	2 x cell t/put	2 x OTA	pkt call rate		mean	median	<32k/64k/128k/384k/1M
10	903	1807	867	54	3.11	1.78	2 / 2 / 7 / 32 / 68
20	1426	1754	494	83	5.40	3.98	5 / 9 / 22 / 57 / 87
30	1723	1777	224	97	10.94	7.99	17 / 29 / 47 / 86 / 98
40	1894	1895	109	100	16.49	13.01	29 / 49 / 74 / 100 / 100
50	1948	1948	74	100	21.94	17.44	43 / 65 / 91 / 100 / 100
60	2000	2000	58	100	26.46	21.81	51 / 75 / 98 / 100 / 100

5.3.2.4.4 Vehicular A 30kmph

Results are presented for a max C/I scheduler and a Round robin scheduler.

Figure 147 to Figure 151 present results using a max C/I scheduler in channel VA30.

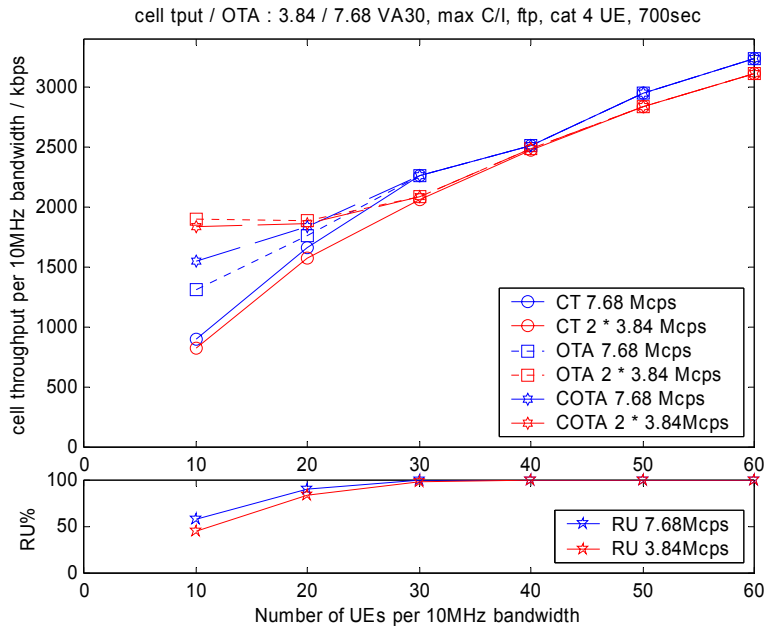

Figure 147 - VA30 : cell throughput / over the air throughput / resource utilisation FTP, max C/I scheduler

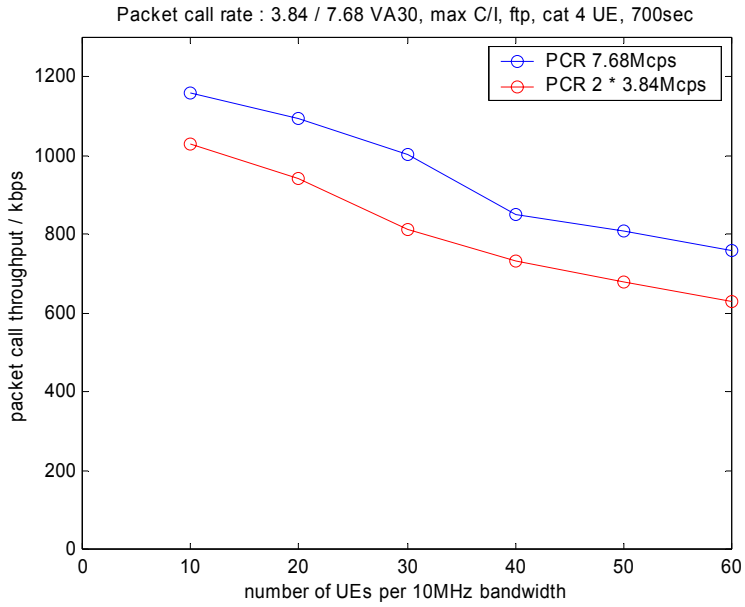

Figure 148 - VA30 : mean packet call rate FTP, max C/I scheduler

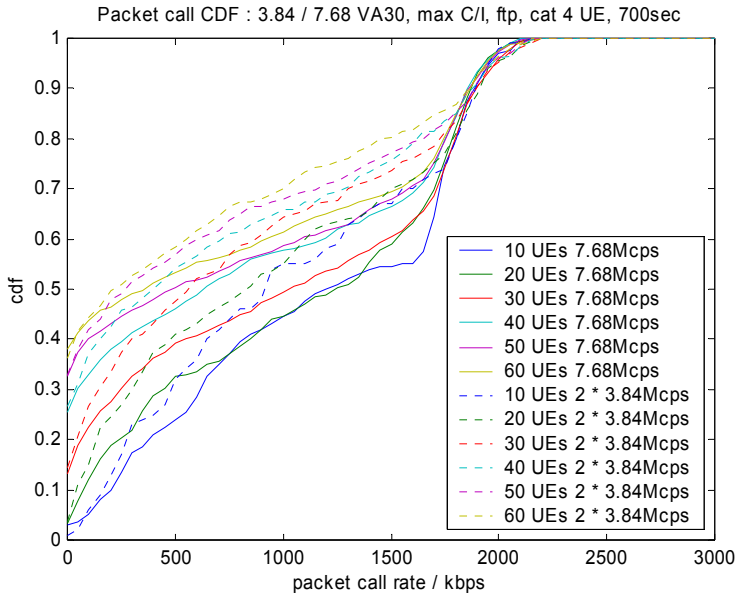

Figure 149 - VA30 : packet call rate CDFs FTP, max C/I scheduler

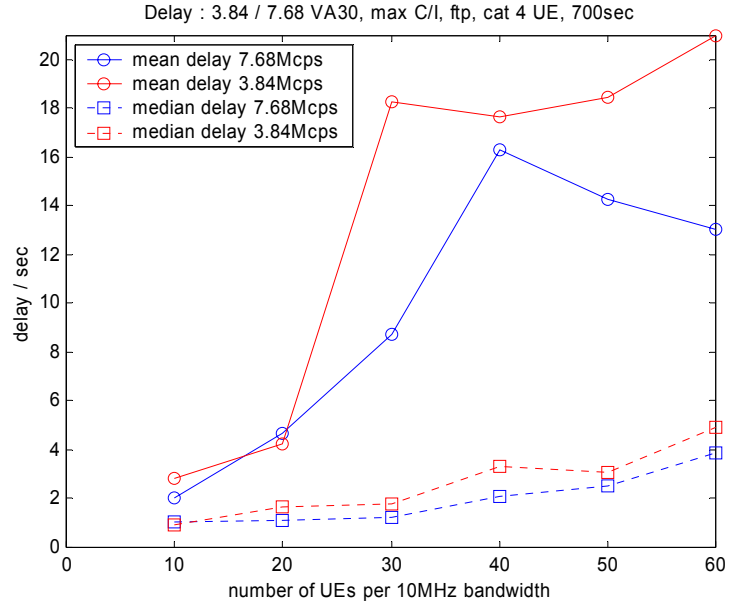

Figure 150 - VA30 : mean and median packet delays FTP, max C/I scheduler

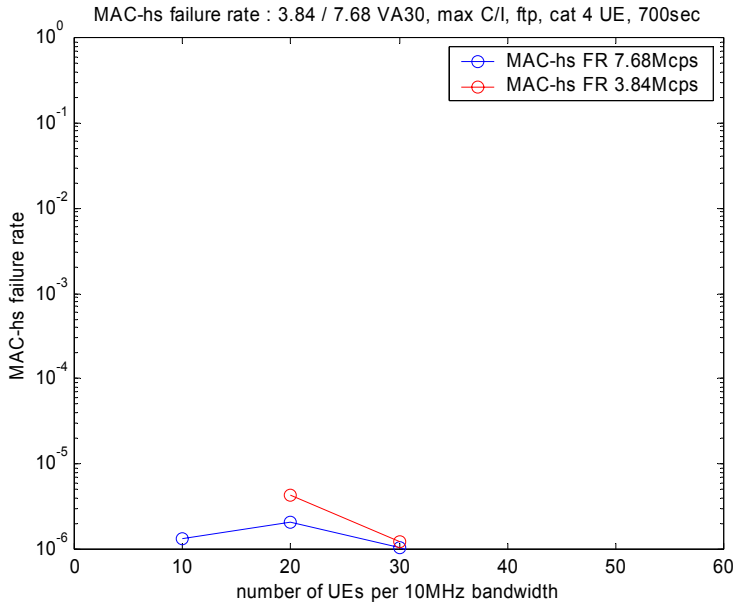

Figure 151 - VA30 : MAC-hs failure rate FTP, max C/I scheduler

The VA30 results with the max C/I scheduler are summarized in Table 58 (7.68Mcps) and Table 59 (3.84Mcps).

Table 58 - Summary of 7.68Mcps VA30 results for FTP with max C/I scheduler

#users per sector	average centre cell throughput / kbps			resource utilization %	delay (sec)		packet call rate CDF
	cell t/put	OTA	pkt call rate		mean	median	<32k/64k/128k/384k/1M
10	905	1308	1157	58	2.05	1.05	3 / 4 / 7 / 20 / 45
20	1668	1760	1095	91	4.70	1.13	6 / 9 / 14 / 28 / 45
30	2259	2260	1004	100	8.73	1.23	17 / 20 / 24 / 35 / 49
40	2514	2514	850	100	16.28	2.09	29 / 31 / 35 / 43 / 58
50	2954	2954	808	100	14.28	2.52	36 / 38 / 41 / 48 / 59
60	3232	3232	758	100	13.05	3.85	40 / 42 / 45 / 51 / 62

Table 59 - Summary of 3.84Mcps VA30 results for FTP with max C/I scheduler

2 x #users per sector	average centre cell throughput / kbps			resource utilization %	delay (sec)		packet call rate CDF
	2 x cell t/put	2 x OTA	pkt call rate		mean	median	<32k/64k/128k/384k/1M
10	827	1902	1029	45	2.81	0.92	2 / 3 / 8 / 25 / 55
20	1577	1885	943	84	4.24	1.67	8 / 12 / 19 / 36 / 55
30	2056	2084	813	99	18.28	1.77	18 / 22 / 29 / 42 / 64
40	2470	2487	731	99	17.67	3.34	30 / 33 / 39 / 49 / 66
50	2838	2838	680	100	18.46	3.10	36 / 39 / 43 / 54 / 68
60	3118	3118	630	100	20.98	4.91	40 / 42 / 46 / 55 / 70

Figure 152 to Figure 156 present results using a Round robin scheduler in channel VA30.

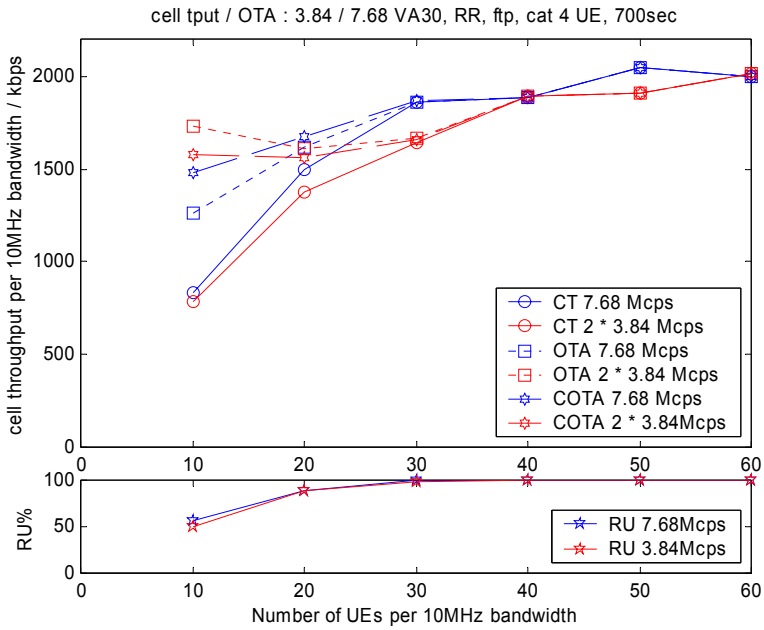

Figure 152 – VA30 : cell throughput / over the air throughput / resource utilisation FTP, Round robin scheduler

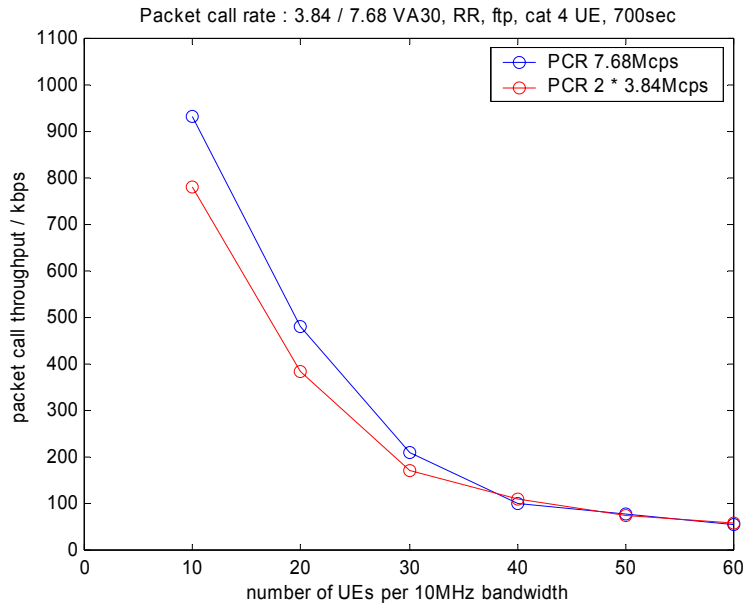

Figure 153 – VA30 : mean packet call rate FTP, Round robin scheduler

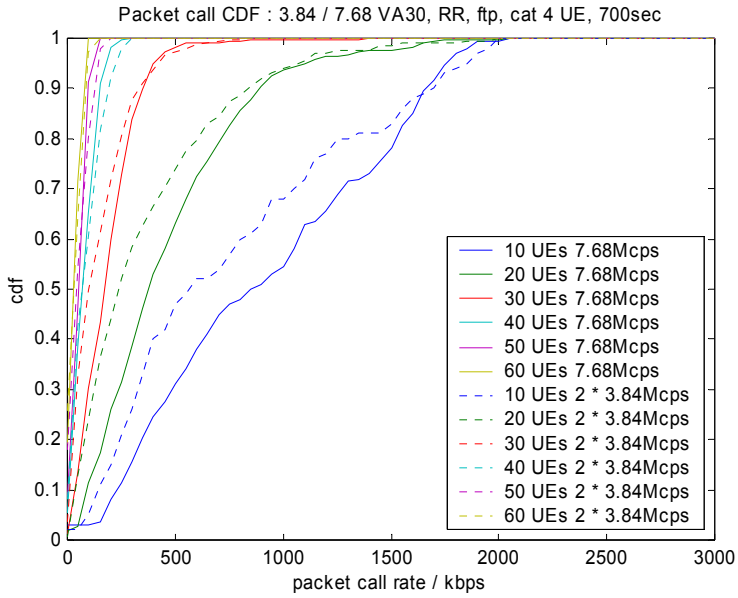

Figure 154 – VA30 : packet call rate CDFs FTP, Round robin scheduler

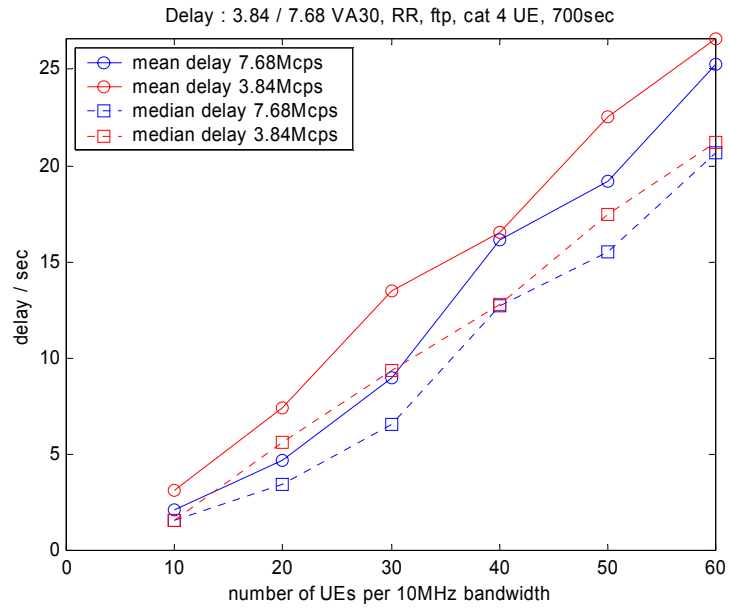

Figure 155 – VA30 : mean and median packet delays FTP, Round robin scheduler

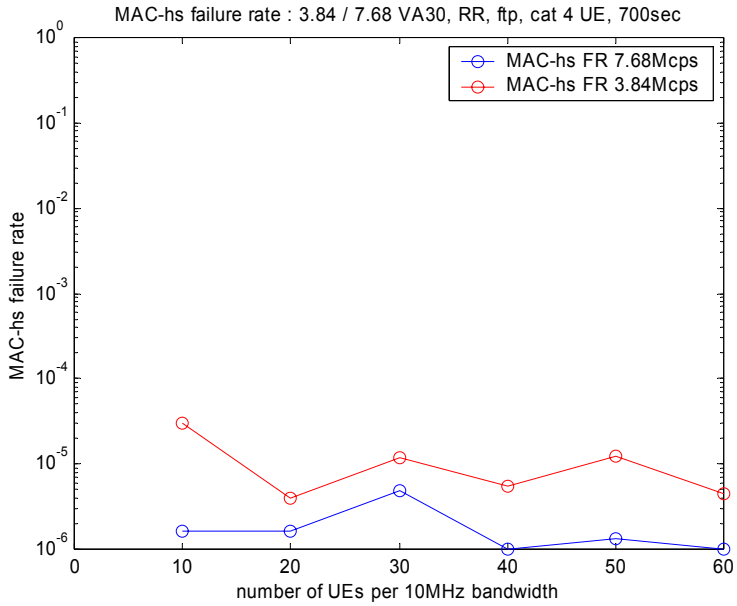

Figure 156 - VA30 : MAC-hs failure rate FTP, Round robin scheduler

The VA30 results with the Round robin scheduler are summarized in Table 60 (7.68Mcps) and Table 61 (3.84Mcps).

Table 60 - Summary of 7.68Mcps VA30 results for FTP with Round robin scheduler

#users per sector	average centre cell throughput / kbps			resource utilization %	delay (sec)		packet call rate CDF
	cell t/put	OTA	pkt call rate		mean	median	<32k/64k/128k/384k/1M
10	835	1264	931	57	2.13	1.55	3 / 3 / 3 / 23 / 55
20	1495	1614	481	89	4.65	3.44	2 / 5 / 15 / 51 / 94
30	1861	1862	211	100	8.96	6.56	9 / 18 / 38 / 93 / 100
40	1887	1887	101	100	16.11	12.67	27 / 46 / 80 / 100 / 100
50	2043	2043	77	100	19.16	15.49	33 / 59 / 96 / 100 / 100
60	2001	2001	54	100	25.29	20.68	53 / 79 / 100 / 100 / 100

Table 61 - Summary of 3.84Mcps VA30 results for FTP with Round robin scheduler

2 x #users per sector	average centre cell throughput / kbps			resource utilization %	delay (sec)		packet call rate CDF
	2 x cell t/put	2 x OTA	pkt call rate		mean	median	<32k/64k/128k/384k/1M
10	787	1734	782	50	3.09	1.58	2 / 3 / 8 / 38 / 68
20	1377	1606	383	88	7.40	5.62	9 / 16 / 31 / 65 / 94
30	1641	1668	170	99	13.46	9.32	22 / 37 / 56 / 93 / 100
40	1893	1893	109	100	16.53	12.81	30 / 48 / 72 / 100 / 100
50	1908	1908	75	100	22.57	17.48	41 / 61 / 90 / 100 / 100
60	2016	2016	58	100	26.60	21.21	51 / 74 / 99 / 100 / 100

5.3.2.4.5 Vehicular A 120kmph

Results are presented for a max C/I scheduler and a Round robin scheduler.

Figure 157 to Figure 160 present results using a max C/I scheduler in channel VA120.

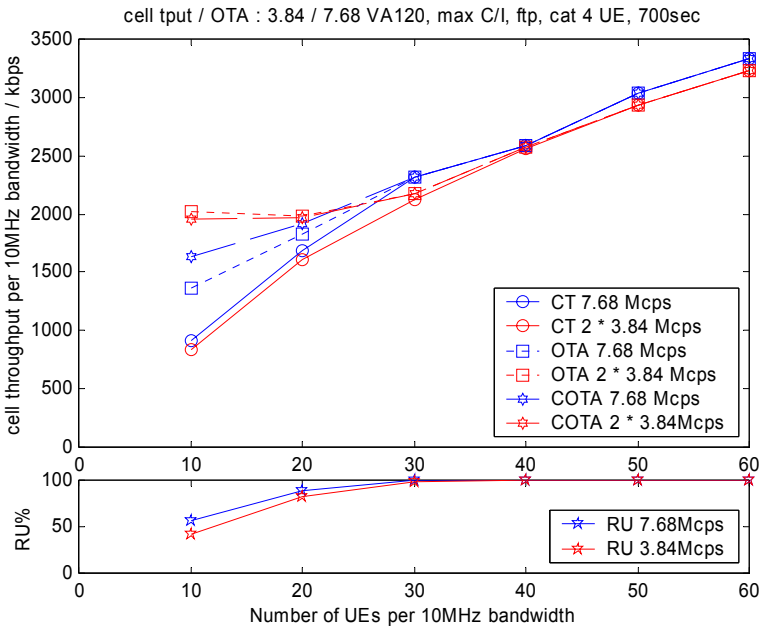

Figure 157 - VA120 : cell throughput / over the air throughput / resource utilisation FTP, max C/I scheduler

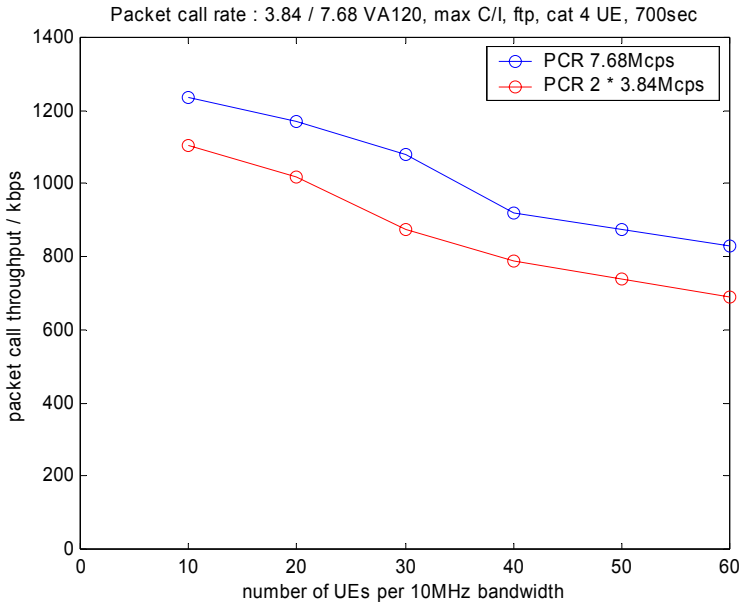

Figure 158 - VA120 : mean packet call rate FTP, max C/I scheduler

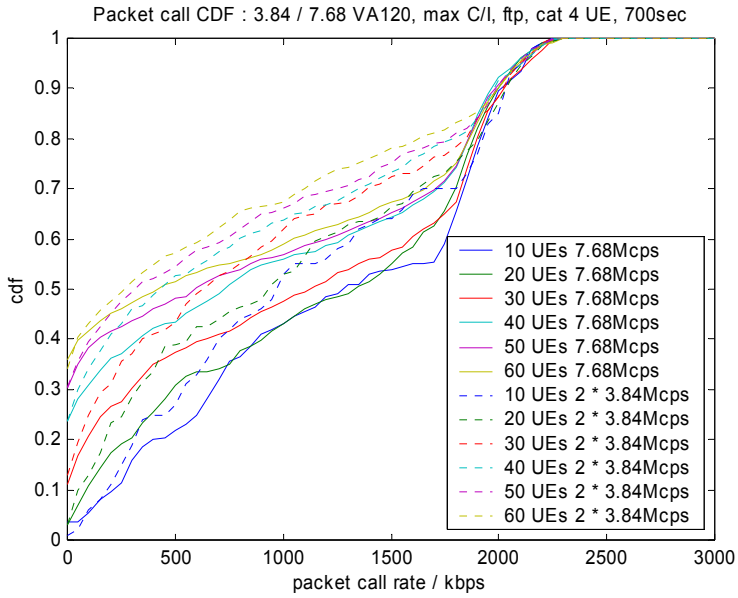

Figure 159 - VA120 : packet call rate CDFs FTP, max C/I scheduler

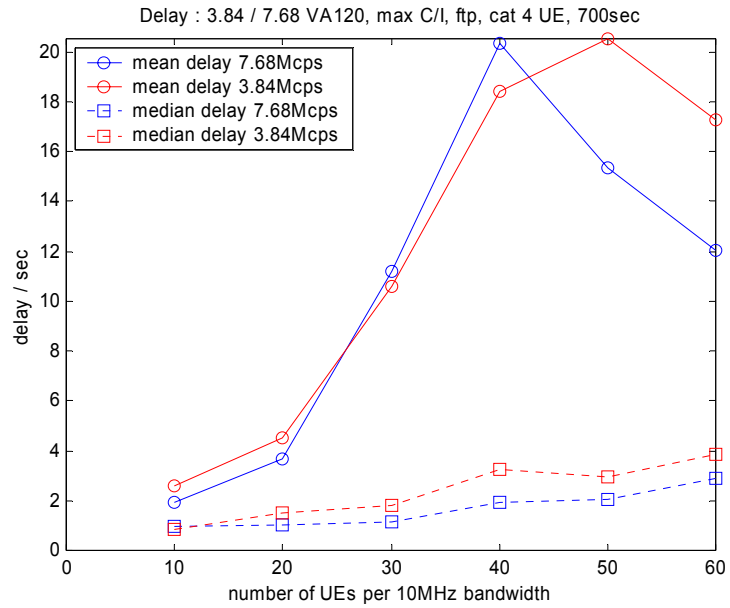

Figure 160 - VA120 : mean and median packet delays FTP, max C/I scheduler

The VA120 results with the max C/I scheduler are summarized in Table 62 (7.68Mcps) and Table 63 (3.84Mcps).

Table 62 - Summary of 7.68Mcps VA120 results for FTP with max C/I scheduler

#users per sector	average centre cell throughput / kbps			resource utilization %	delay (sec)		packet call rate CDF
	cell t/put	OTA	pkt call rate		mean	median	<32k/64k/128k/384k/1M
10	912	1365	1235	56	1.94	0.98	4 / 4 / 7 / 20 / 43
20	1691	1822	1170	88	3.65	1.05	5 / 8 / 13 / 25 / 43
30	2314	2317	1079	100	11.21	1.12	15 / 18 / 23 / 34 / 48
40	2583	2583	922	100	20.36	1.90	26 / 29 / 32 / 42 / 56
50	3042	3042	875	100	15.36	2.06	33 / 36 / 39 / 46 / 57
60	3331	3331	829	100	12.03	2.86	38 / 40 / 43 / 49 / 59

Table 63 - Summary of 3.84Mcps VA120 results for FTP with max C/I scheduler

2 x #users per sector	average centre cell throughput / kbps			resource utilization %	delay (sec)		packet call rate CDF
	2 x cell t/put	2 x OTA	pkt call rate		mean	median	<32k/64k/128k/384k/1M
10	836	2017	1105	43	2.58	0.87	2 / 3 / 7 / 25 / 53
20	1611	1988	1016	82	4.51	1.52	7 / 11 / 16 / 33 / 53
30	2124	2174	875	98	10.57	1.81	17 / 21 / 27 / 41 / 62
40	2556	2577	789	99	18.44	3.25	28 / 31 / 36 / 48 / 64
50	2940	2940	738	100	20.53	2.96	34 / 37 / 41 / 52 / 66
60	3225	3225	689	100	17.28	3.87	38 / 41 / 44 / 54 / 68

Figure 161 to Figure 164 present results using a Round robin scheduler in channel VA120.

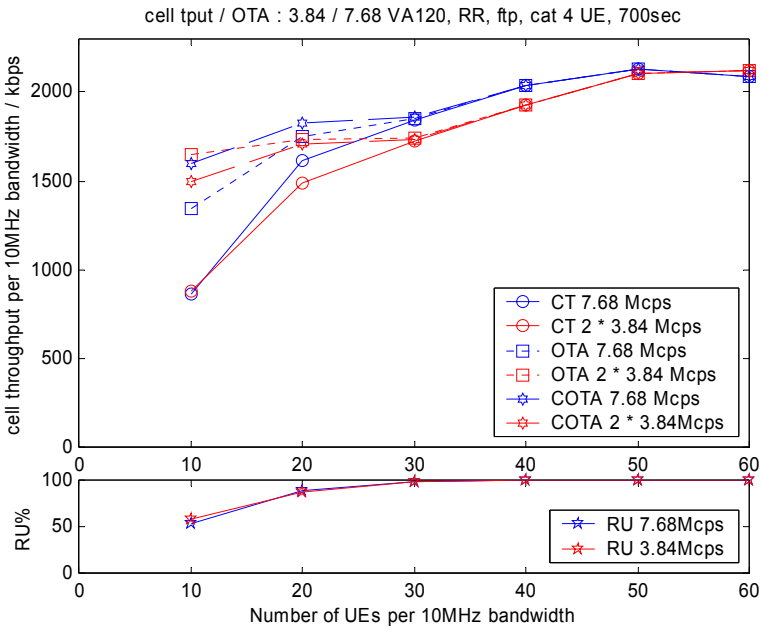

Figure 161 – VA120 : cell throughput / over the air throughput / resource utilisation FTP, Round robin scheduler

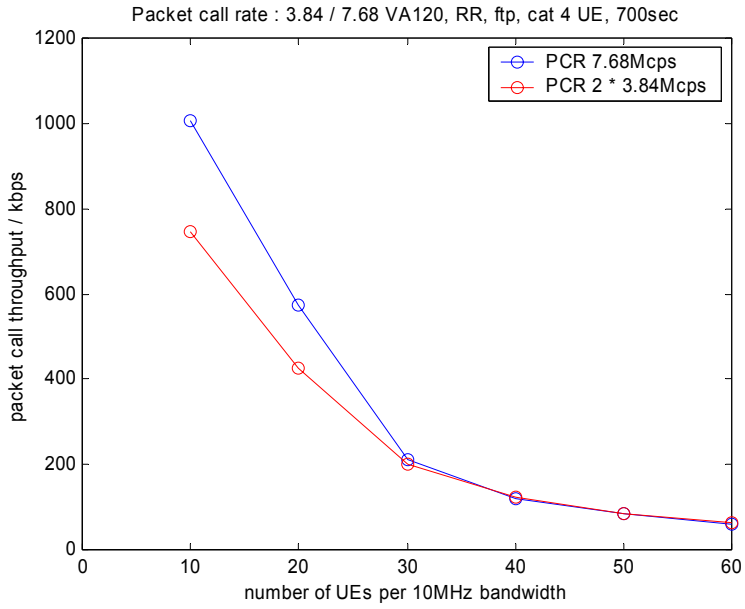

Figure 162 – VA120 : mean packet call rate FTP, Round robin scheduler

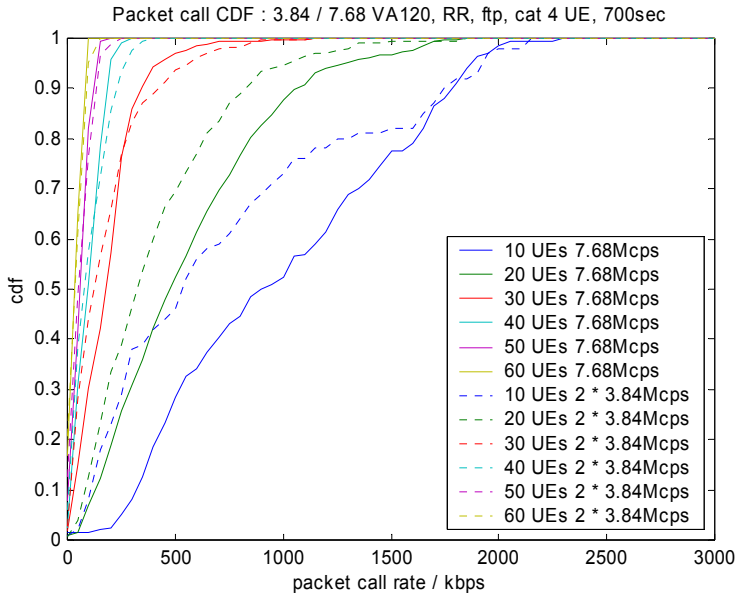

Figure 163 – VA120 : packet call rate CDFs FTP, Round robin scheduler

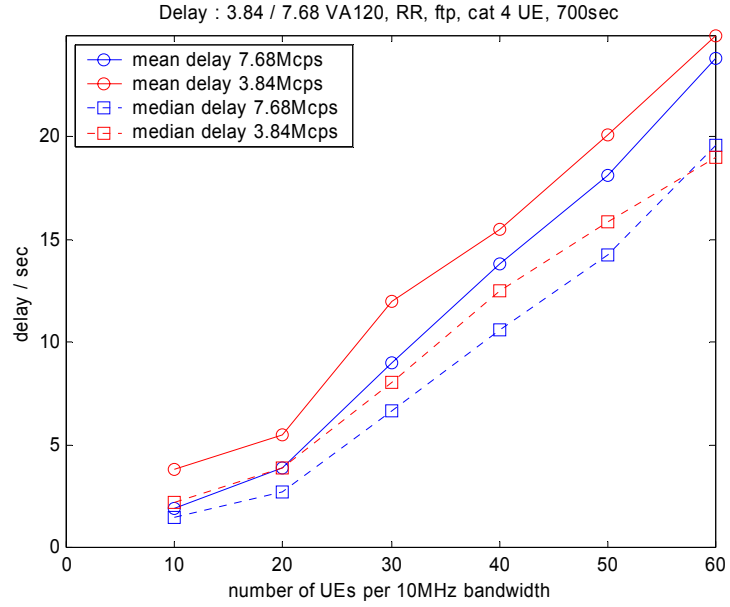

Figure 164 – VA120 : mean and median packet delays FTP, Round robin scheduler

The VA120 results with the Round robin scheduler are summarized in Table 64 (7.68Mcps) and Table 65 (3.84Mcps).

Table 64 - Summary of 7.68Mcps VA120 results for FTP with Round robin scheduler

#users per sector	average centre cell throughput / kbps			resource utilization %	delay (sec)		packet call rate CDF
	cell t/put	OTA	pkt call rate		mean	median	<32k/64k/128k/384k/1M
10	859	1346	1006	54	1.93	1.49	2 / 2 / 2 / 17 / 53
20	1616	1748	575	89	3.87	2.74	1 / 3 / 10 / 40 / 88
30	1842	1853	211	99	8.97	6.65	10 / 19 / 37 / 93 / 100
40	2038	2038	121	100	13.82	10.60	20 / 36 / 66 / 100 / 100
50	2133	2133	84	100	18.15	14.26	29 / 53 / 92 / 100 / 100
60	2085	2085	59	100	23.83	19.60	48 / 75 / 100 / 100 / 100

Table 65 - Summary of 3.84Mcps VA120 results for FTP with Round robin scheduler

2 x #users per sector	average centre cell throughput / kbps			resource utilization %	delay (sec)		packet call rate CDF
	2 x cell t/put	2 x OTA	pkt call rate		mean	median	<32k/64k/128k/384k/1M
10	881	1653	747	59	3.79	2.16	2 / 4 / 14 / 41 / 73
20	1484	1734	425	87	5.49	3.85	3 / 6 / 19 / 58 / 95
30	1721	1740	200	99	12.01	8.06	19 / 32 / 51 / 88 / 100
40	1930	1930	124	100	15.51	12.49	27 / 44 / 66 / 100 / 100
50	2108	2108	83	100	20.09	15.84	36 / 57 / 88 / 100 / 100
60	2124	2124	63	100	24.93	18.99	47 / 71 / 98 / 100 / 100

5.3.2.4.6 Mixed channel model

Mixed channel model results with the FTP traffic model are obtained with UEs being randomly assigned a channel with the probabilities specified in Table B.5.

Results are presented for a max C/I scheduler and a Round robin scheduler.

Figure 165 to Figure 169 present results using a max C/I scheduler with the mixed channel model.

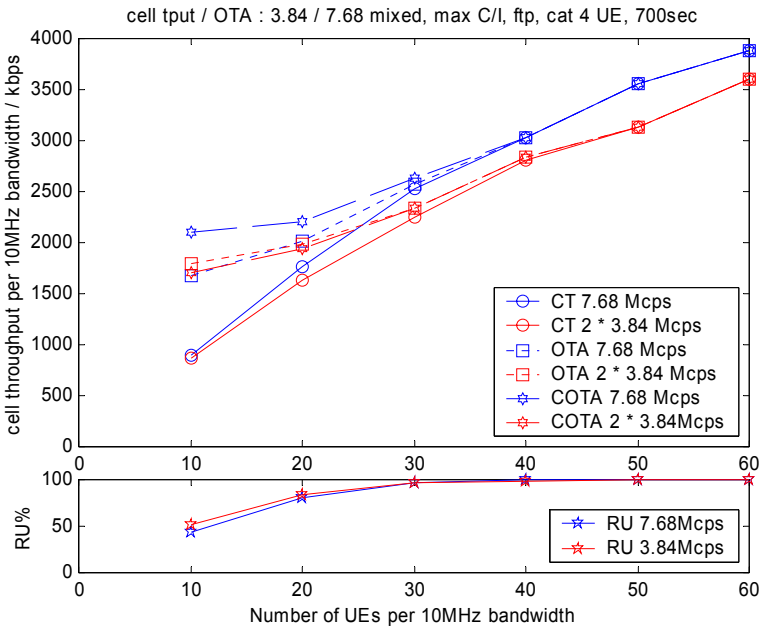

Figure 165 - mixed channel model : cell throughput / over the air throughput / resource utilisation FTP, max C/I scheduler

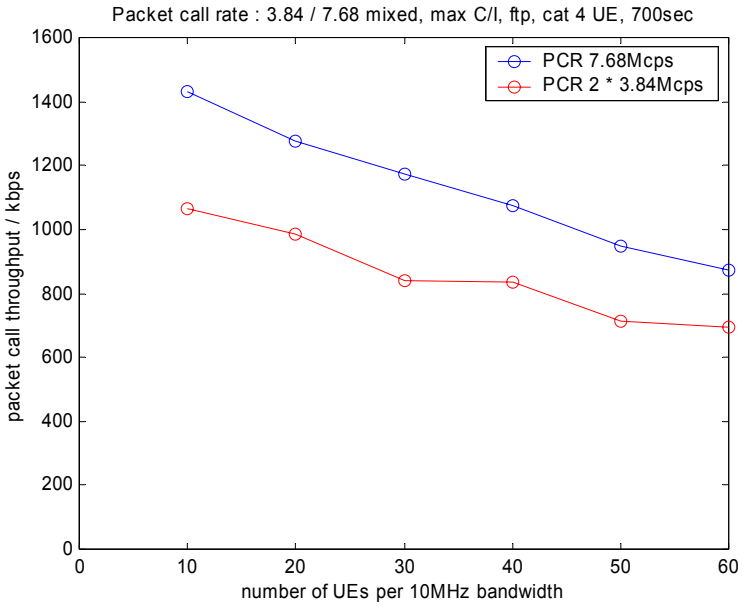

Figure 166 - mixed channel model : mean packet call rate FTP, max C/I scheduler

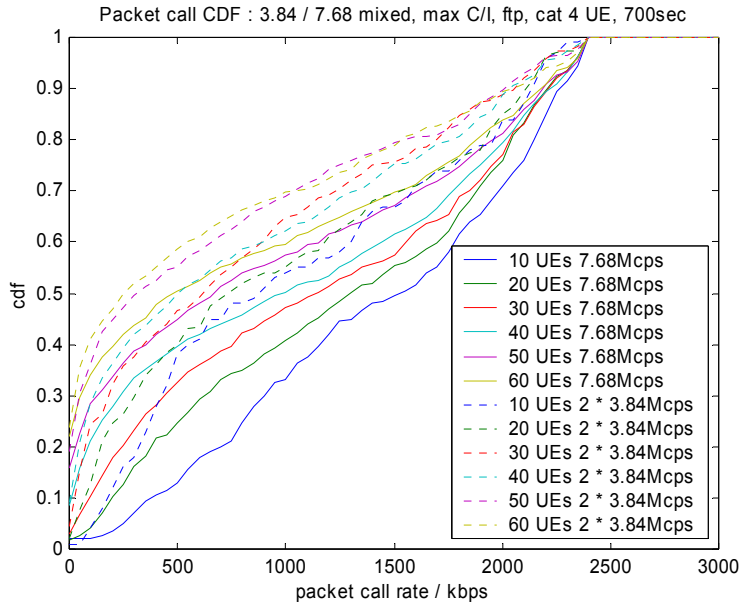

Figure 167 – mixed channel model : packet call rate CDFs FTP, max C/I scheduler

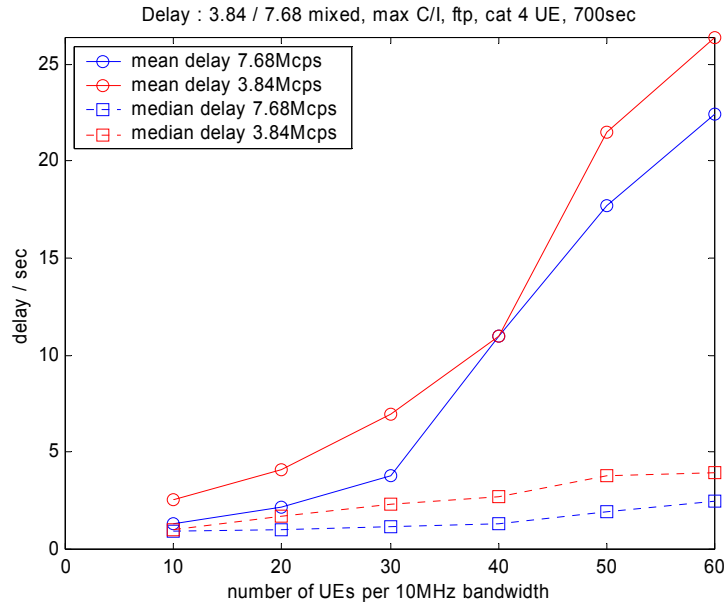

Figure 168 - mixed channel model : mean and median packet delays FTP, max C/I scheduler

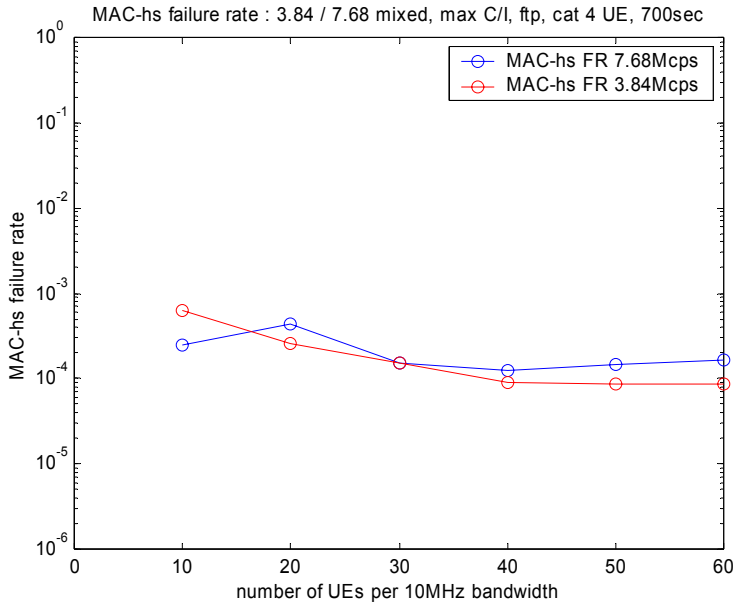

Figure 169 - mixed channel model : MAC-hs failure rate FTP, max C/I scheduler

The mixed channel model results with the max C/I scheduler are summarized in Table 66 (7.68Mcps) and Table 67 (3.84Mcps).

Table 66 - Summary of 7.68Mcps mixed channel model results for FTP with max C/I scheduler

#users per sector	average centre cell throughput / kbps			resource utilization %	delay (sec)		packet call rate CDF
	cell t/put	OTA	pkt call rate		mean	median	<32k/64k/128k/384k/1M
10	903	1670	1432	43	1.34	0.89	2 / 2 / 2 / 10 / 33
20	1765	2015	1277	80	2.18	0.99	2 / 3 / 6 / 21 / 41
30	2536	2579	1173	96	3.82	1.18	5 / 8 / 13 / 28 / 47
40	3035	3035	1073	100	10.94	1.31	13 / 17 / 23 / 36 / 50
50	3558	3558	948	100	17.71	1.94	20 / 24 / 30 / 41 / 57
60	3887	3887	871	100	22.44	2.50	27 / 31 / 36 / 47 / 60

Table 67 - Summary of 3.84Mcps mixed channel model results for FTP with max C/I scheduler

2 x #users per sector	average centre cell throughput / kbps			resource utilization %	delay (sec)		packet call rate CDF
	2 x cell t/put	2 x OTA	pkt call rate		mean	median	<32k/64k/128k/384k/1M
10	871	1793	1066	51	2.57	1.00	1 / 2 / 6 / 26 / 54
20	1626	1991	987	84	4.08	1.72	6 / 9 / 17 / 35 / 55
30	2257	2341	841	96	6.97	2.28	11 / 18 / 25 / 42 / 65
40	2811	2843	835	99	10.97	2.68	17 / 23 / 31 / 45 / 62
50	3135	3135	714	100	21.48	3.75	26 / 32 / 40 / 52 / 69
60	3605	3605	695	100	26.35	3.97	31 / 37 / 43 / 55 / 70

Figure 170 to Figure 174 present results using a Round robin scheduler with the mixed channel model.

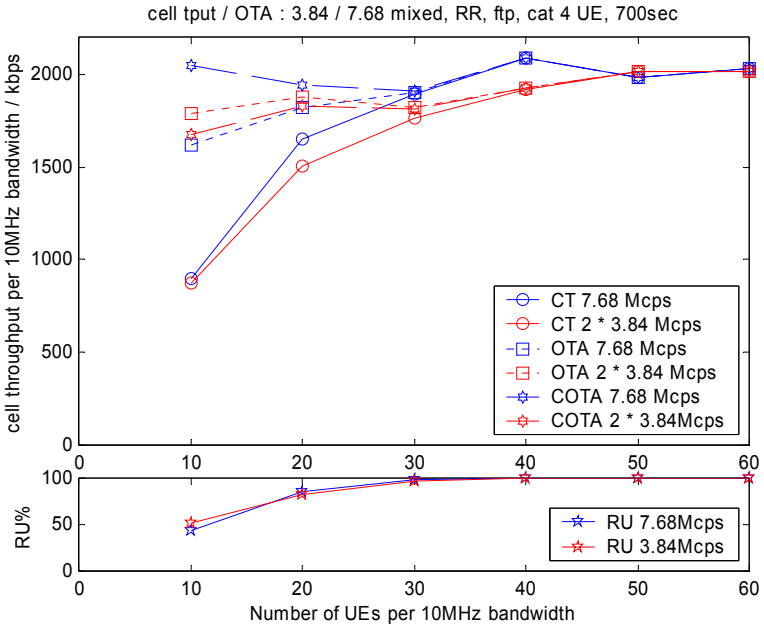

Figure 170 - mixed channel model : cell throughput / over the air throughput / resource utilisation FTP, Round robin scheduler

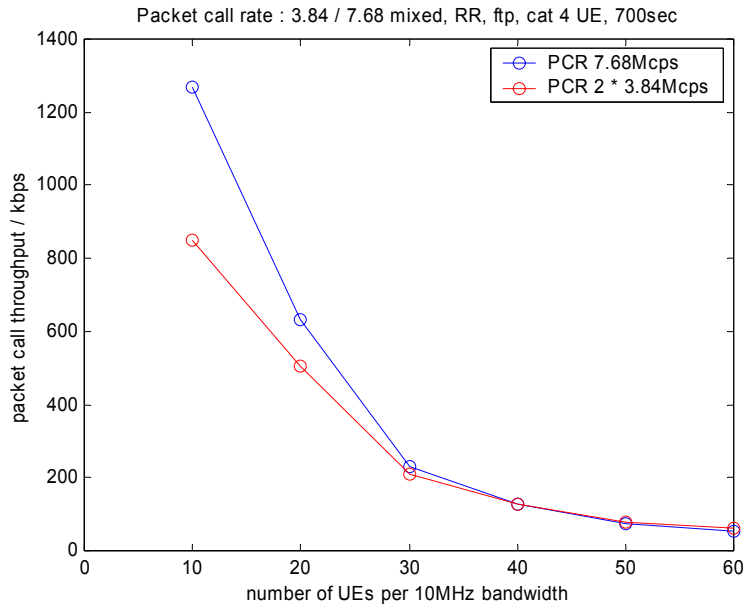

Figure 171 - mixed channel model : mean packet call rate FTP, Round robin scheduler

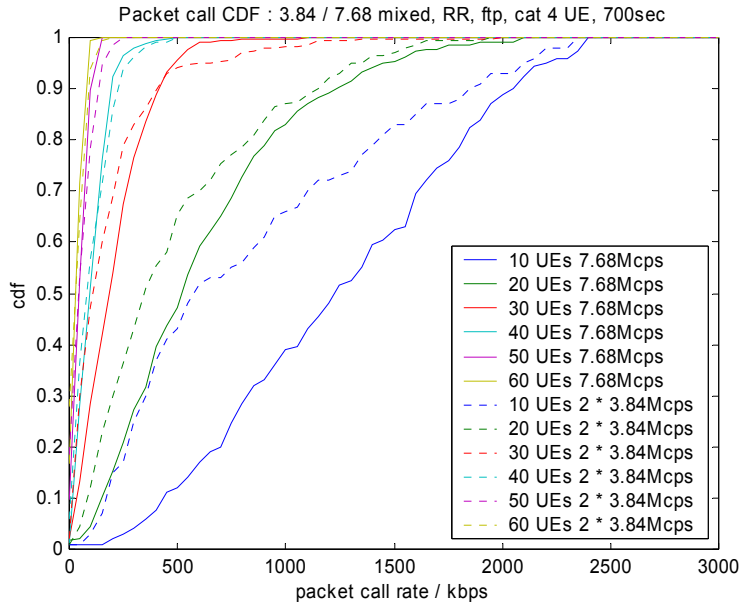

Figure 172 – mixed channel model : packet call rate CDFs FTP, Round robin scheduler

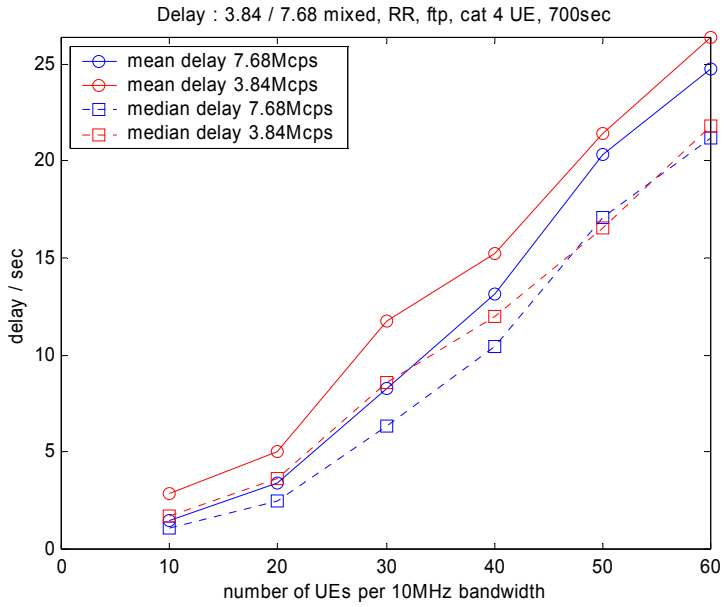

Figure 173 - mixed channel model : mean and median packet delays FTP, Round robin scheduler

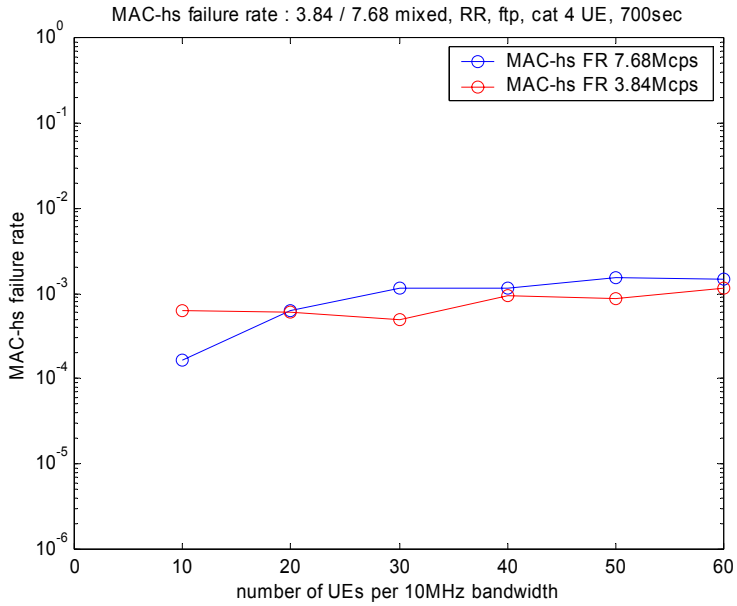

Figure 174 - mixed channel model : MAC-hs failure rate FTP, Round robin scheduler

The MAC-hs failure rate is higher than the desired rate of 10^{-4}. This rate is dominated by those UEs in channel PA3 and can be reduced by increasing the maximum number of MAC-hs retransmissions as described in [4].

The mixed channel model results with the Round robin scheduler are summarized in Table 68 (7.68Mcps) and Table 69 (3.84Mcps).

Table 68 - Summary of 7.68Mcps mixed channel model results for FTP with Round robin scheduler

#users per sector	average centre cell throughput / kbps			resource utilization %	delay (sec)		packet call rate CDF
	cell t/put	OTA	pkt call rate		mean	median	<32k/64k/128k/384k/1M
10	896	1615	1267	44	1.43	1.07	1 / 1 / 1 / 7 / 39
20	1650	1822	632	85	3.39	2.47	2 / 3 / 8 / 37 / 83
30	1891	1902	231	99	8.27	6.37	9 / 18 / 36 / 87 / 100
40	2088	2088	128	100	13.15	10.42	18 / 35 / 65 / 99 / 100
50	1982	1982	73	100	20.29	17.07	37 / 63 / 96 / 100 / 100
60	2034	2034	55	100	24.71	21.16	52 / 79 / 100 / 100 / 100

Table 69 - Summary of 3.84Mcps mixed channel model results for FTP with Round robin scheduler

2 x #users per sector	average centre cell throughput / kbps			resource utilization %	delay (sec)		packet call rate CDF
	2 x cell t/put	2 x OTA	pkt call rate		mean	median	<32k/64k/128k/384k/1M
10	877	1787	850	52	2.88	1.71	1 / 2 / 5 / 35 / 66
20	1504	1877	507	82	5.04	3.65	3 / 7 / 18 / 54 / 87
30	1766	1823	208	97	11.74	8.59	20 / 35 / 54 / 89 / 98
40	1918	1921	128	100	15.21	12.02	25 / 42 / 65 / 99 / 100
50	2016	2016	79	100	21.42	16.53	41 / 60 / 87 / 100 / 100
60	2016	2016	60	100	26.36	21.82	51 / 73 / 97 / 100 / 100

5.3.2.5 Analysis of System Level Simulation Results

5.3.2.5.1 Higher Packet Call Rates at 7.68Mcps

The packet call rate at the reference configuration chip rate of 7.68Mcps is higher than that for 3.84Mcps in all the studied channel types. At 80 users per sector for 7.68Mcps and 80 users per two sectors for 3.84Mcps, the packet call rates observed with the HTTP / TCP traffic model and max C/I scheduler are given in Table 70. A similar comparison is made in Table 71 for the case of the FTP / TCP traffic model with 30 UEs per sector for 7.68Mcps and 30 UEs per two sectors for 3.84Mcps.

Table 70 - Packet call rate gains for 7.68Mcps wrt 3.84Mcps for the HTTP traffic model (80 UEs)

channel	7.68Mcps packet call rate / kbps	3.84Mcps packet call rate / kbps	packet call rate increase (%)
AWGN	432	381	13
PA3	323	259	25
PB3	348	291	20
VA30	330	271	22
VA120	334	283	18
mixed	349	300	16

Table 71 - Packet call rate gains for 7.68Mcps wrt 3.84Mcps for the FTP traffic model (30 UEs)

channel	7.68Mcps packet call rate / kbps	3.84Mcps packet call rate / kbps	packet call rate increase (%)
AWGN	1663	1382	20
PA3	984	675	46
PB3	1059	818	30
VA30	1004	813	23
VA120	1079	875	23
mixed	1173	841	40

There are three effects that lead to an increase in packet call rate at 7.68Mcps compared to 3.84Mcps :

- At 7.68Mcps, a UE is more likely to be scheduled resource when it has data to transmit than at 3.84Mcps (there is a greater "blocking probability" at the lower chip rate). This blocking probability naturally decreases the packet call rate (the packet call takes a longer time to complete when there are times at which the UE has data to transmit, but it is not scheduled to do so). A secondary effect of the increased blocking probability is that the rate of CQI reports from the UE decreases as the blocking probability increases (i.e. as the time between scheduling instants increases). This latter effect will reduce the packet call rate when the Node B attempts to track the fast fading profile of a channel.

- The scheduler is able to allocate more physical resource to a category 4 7.68Mcps UE with QPSK than it can to a 3.84Mcps UE, due to the fundamental extra physical resource available at the higher chip rate (see below).

- Link level performance gains at 7.68Mcps (as seen most noticeably in channels PA3, VA30 and VA120) allow the scheduler to use a higher modulation and coding scheme at the higher chip rate.

Figure 175 shows the packet call rates and scheduler blocking probabilities for both the 7.68Mcps chip rate and the 3.84Mcps chip rate in the AWGN channel (this channel is not time-varying therefore effects related to CQI age are not exhibited in these results). The increased blocking probability witnessed at 3.84Mcps increases the time taken for a 3.84Mcps system to complete a packet call.

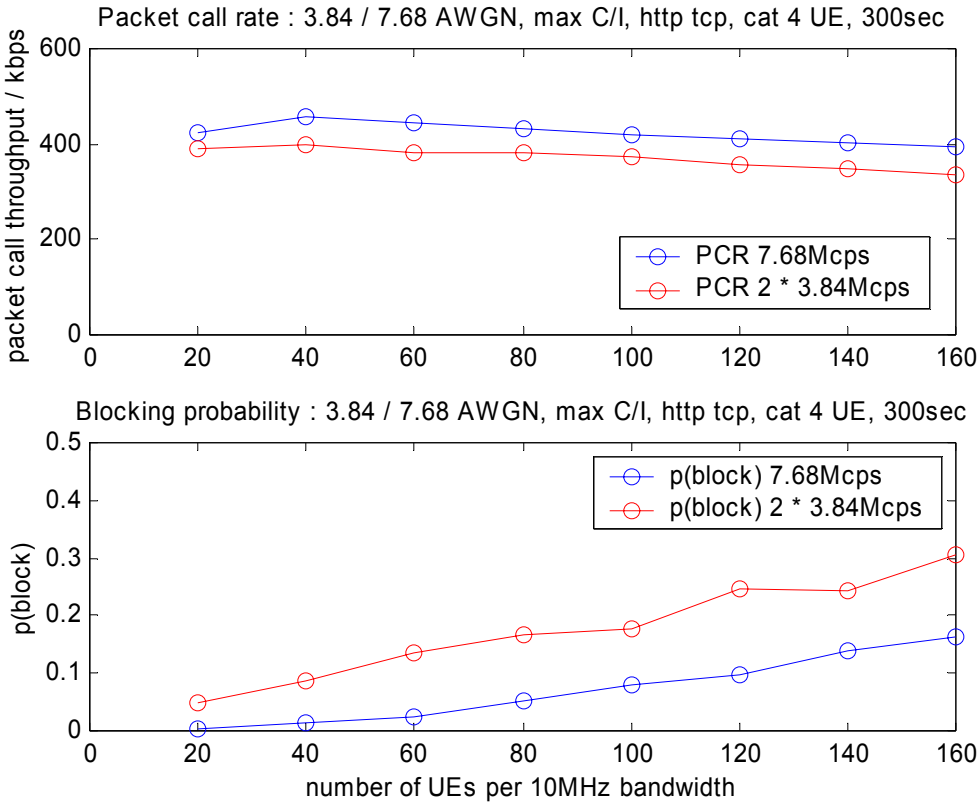

Figure 175 - Packet call rate and blocking probability for the AWGN channel with a max C/I scheduler

The effect of the scheduler being able to allocate more physical resource at 7.68Mcps compared to 3.84Mcps is illustrated by the following example. A category 4 UE has a turbo capability of 24000 bits per TTI and a soft buffer capability of 105984 soft channel bits. The maximum number of soft channel bits that an 8 slot 16 code HSDPA TTI can support is 35328 bits at QPSK for 3.84Mcps and 70656 bits at 7.68Mcps. A UE that has a low C/I has to be scheduled with a low code rate (for example rate 1/3). The number of transport channel bits that can be transmitted for a 3.84Mcps UE at rate 1/3 QPSK is thus approximately min(35328,105984/2) / 3 = 11776 bits at 3.84Mcps and min(70656, 105984/2) / 3 = 17664 bits at 7.68Mcps. In this manner, for low QPSK code rates, the 7.68Mcps UE is able to transmit more data bits per TTI than a 3.84Mcps UE, thus the packet call rate for the higher chip rate UE is increased.

Note that the effect described in the above paragraph does not occur for 16QAM where the number of soft channel bits that the HSDPA TTI supports is greater than the soft buffer capability of the UE (per HARQ process) at both chip rates. The effect also does not occur for high QPSK code rates when the UE is turbo capability limited rather than soft buffer capability limited.

Note that a category 2 UE has a soft buffer capability of 52992 soft channel bits and the scheduler is thus restricted by the soft buffer UE capability for both chip rates [min(35328,52992/2) = 26496 soft channel bits at 3.84Mcps and min(70656,52992/2) = 26496 soft channel bits at 7.68Mcps].

Figure 176 shows the packet call rates for 3.84Mcps and 7.68Mcps in AWGN for category 2 UEs. With these low capability UEs, the scheduler is unable to allocate more resource to 7.68Mcps UEs than to 3.84Mcps UEs. A packet call rate gain is still seen for the 7.68Mcps system in comparison to the 3.84Mcps system. In this scenario, the higher packet call rate for 7.68Mcps UEs is due solely to the reduced scheduler blocking probability at the higher chip rate.

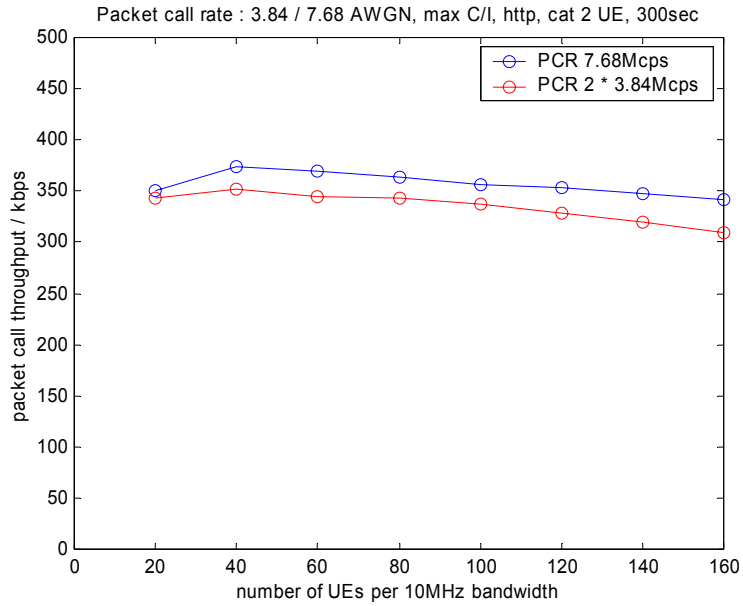

Figure 176 – Packet call rate for category 2 (1.2Mbps) HSDPA UEs with a max C/I scheduler in AWGN

In order to illustrate the packet call rate gains that are due solely to link level performance gains, it is possible to run the 3.84Mcps simulations using the 7.68Mcps link level performance curves (in this case, the effects of blocking probability and ability of the Node B to allocate more resource are removed from the simulation). Figure 177 shows packet call rate results using both 3.84Mcps and 7.68Mcps link level performance curves as inputs to the simulator : the simulator is run at the 3.84Mcps chiprate. These packet call rate results show a gain in packet call rate in channel PA3 that is solely due to the superior link level performance at 7.68Mcps. Note that there is only a very slight gain from use of the 7.68Mcps AWGN curves : this further illustrates that link level gains yield some system level packet call rate gains.

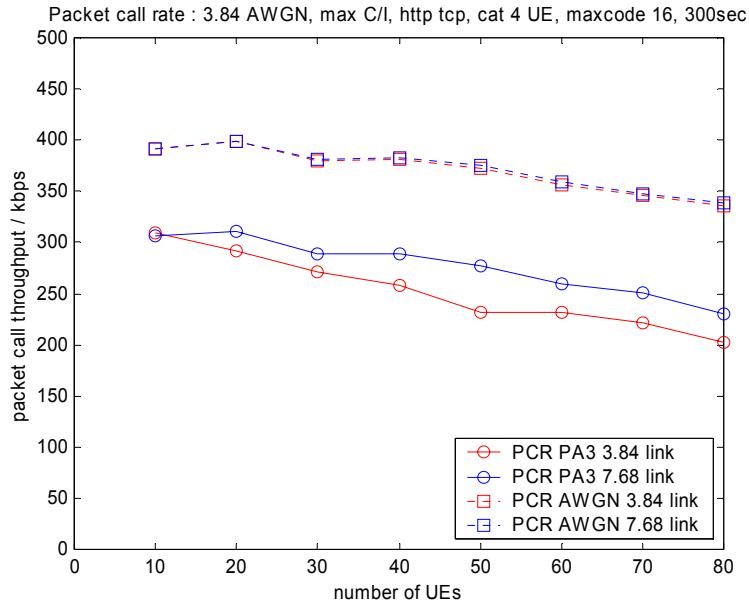

Figure 177 - Packet call rate results using 3.84Mcps link level results and 7.68Mcps link level results as input to the 3.84Mcps system simulation

5.3.2.5.2 Higher Number of UEs supported at 7.68Mcps

When a Round robin scheduler is employed, the number of UEs that can be supported by a single 7.68Mcps system is generally greater than the number that can be supported by two 3.84Mcps systems operating in parallel (when compared at the same mean packet call rate). This effect is more pronounced when the systems are not heavily loaded. This effect

may be seen in the mean packet call rate curves of section 5.3.2 and the packet call rate CDFs of section 5.3.2 (where more of the users achieve a higher packet call rate at any given total number of users, this is evident for both max C/I and Round robin schedulers).

When a Round robin scheduler is employed, as the load on the system increases, the mean packet call rate decreases due to the following effects :

- the blocking probability increases as the number of users increases (the packet call rates of high C/I UEs drop significantly as the Round robin scheduler starts to schedule lower C/I UEs during the packet calls of high C/I UEs).

- the age of CQI reports that are used by the scheduler increases as the number of UEs increases (recall that the CQI is returned on the HS-SICH and as the number of users increases, the number of HS-SCCH / HS-SICH allocations to a UE will decrease). This effect is important for pedestrian channels where the Node B attempts to track the fast fading of the channel.

Since the blocking probability is higher at 3.84Mcps than at 7.68Mcps, higher packet calls rates are seen at the higher chip rate. Once the blocking probability for 3.84Mcps and 7.68Mcps converges (towards unity when there is a large number of UEs present in the sector), the packet call rates for 3.84Mcps and 7.68Mcps converge.

The increase in number of users supported at a given mean packet call rate for a Round robin scheduler with the HTTP / TCP traffic model is shown in Table 72.

Table 72– Number of UEs supported for a given packet call rate for Round robin scheduler and HTTP / TCP traffic model

channel	comparison packet call rate / kbps	number of UEs in 1 7.68Mcps sector	number of UEs in 2 3.84Mcps sectors	increase in number of UEs (%)
AWGN	350	148	106	40
PA3	200	92	60	53
PB3	200	103	88	17
VA30	200	106	79	34
VA120	200	109	92	19
mixed	200	113	90	26

Note that the increase in number of UEs served at a given packet call rate is harder to quantify with the max C/I scheduler due to the “flatness” of the packet call rate curves with the max C/I scheduler (for the max C/I scheduler, the performance gain of 7.68Mcps is better seen by comparison of the packet call rate at a given number of UEs : section 5.3.2.4.1).

5.3.2.5.3 Over the air throughput

The TTI-based over the air throughput for two parallel 3.84Mcps is typically greater than that for 7.68Mcps at low loading. The code-based over the air throughput for 7.68Mcps is generally greater than or equal to that for 3.84Mcps.

A high TTI-based over the air throughput is achieved when a high proportion of the code resource within a TTI is used : this situation arises more frequently for a 3.84Mcps system due to the lower overall code resource available in a 3.84Mcps system.

As an example, consider category 4 UEs that experience a C/I such that they can transmit 24000 bits at rate 2/3 QPSK. In a 3.84Mcps system, a single UE offering this load would occupy all of the code resource within a TTI. In a 7.68Mcps system, two of these UEs would need to simultaneously offer this load to achieve the same over the air throughput (recall that the over the air throughput for a single 7.68Mcps TDD system is compared to the combined throughput of two parallel 3.84Mcps systems). It is less likely that two UEs will simultaneously offer load than that a single UE will offer load.

The higher over the air throughput at 3.84Mcps is thus an artifact of the definition of the TTI-based over the air throughput and is actually an indication that there is less resource available at 3.84Mcps than at 7.68Mcps.

5.3.2.5.4 Higher Cell Throughput at 7.68Mcps

The cell throughput of a 7.68Mcps cell is greater than the combined cell throughput of twin parallel 3.84 Mcps cells in channel types where 7.68Mcps exhibits a link level gain with respect to 3.84Mcps.

The increased cell throughput is most evident when the system is heavily loaded (when the system is lightly loaded, the cell throughput is limited by the offered load).

Table 73 compares the cell throughputs exhibited by a single 7.68Mcps system to the combined cell throughput for two parallel 3.84Mcps systems. The comparison is performed with 160 UEs serviced by the single 7.68Mcps system and 160 UEs serviced by two parallel 3.84Mcps systems. Results are shown for the HTTP / TCP traffic model and max C/I scheduler. Similar results are shown for the FTP / TCP traffic model in Table 74 with 40 UEs serviced by the single 7.68Mcps system and 40 UEs serviced by two parallel 3.84Mcps systems (40 UEs is considered to be a reasonable number of UEs at which the system is not overloaded with the FTP / TCP traffic model).

Table 73 – Cell throughput gains for 7.68Mcps wrt 3.84Mcps for the HTTP / TCP traffic model (160 UEs)

channel	7.68Mcps cell throughput (1 sector) / kbps	3.84Mcps cell throughput (2 sectors) / kbps	Cell throughput increase (%)
AWGN	2118	2125	0
PA3	2080	1926	8
PB3	2054	1965	5
VA30	1863	1815	3
VA120	1936	1803	7
mixed	2079	2035	2

Table 74 – Cell throughput gains for 7.68Mcps wrt 3.84Mcps for the FTP traffic model (40UEs)

channel	7.68Mcps cell throughput (1 sector) / kbps	3.84Mcps cell throughput (2 sectors) / kbps	Cell throughput increase (%)
AWGN	3303	3286	1
PA3	3045	2676	14
PB3	2982	2696	11
VA30	2514	2470	2
VA120	2583	2556	1
mixed	3035	2811	8

There are several reasons for the increased cell throughput at the higher chip rate :

- 7.68Mcps exhibits link level performance gains in some channels. This effect is most noticeable in channel PA3 (where there is a link level gain of approximately 2dB at an operating point of 10% BLER and there is a significant cell throughput gain).
- There are more UEs in high C/I conditions per sector at 7.68Mcps than at 3.84Mcps.
- The Node B is able to transmit more HS-SCCH at 7.68Mcps than at 3.84Mcps. There are thus more UEs with recent CQI information at the higher chip rate. In channels where the scheduler attempts to follow the fast fading profile of the channel (pedestrian channels), transmissions may be performed with a higher AMC level (the CQI derating parameter has a lesser effect on newer CQI reports : see section 5.3.2.2).

5.3.2.5.5 Lower Packet Delay at 7.68Mcps

Note that the packet delay results of sections 5.3.2.2 and 5.3.2.3 are mean packet delay results and refer to the delay between a packet arriving at the Node B and it being successfully acknowledged at the Node B (following transmission to the UE). The packet delay thus includes the buffering delay at the Node B. The round trip time (which impacts TCP slow start performance) cannot be derived directly from the results of sections 5.3.2.2 and 5.3.2.3 (however, this round trip time is inherently modeled in the system simulator).

The mean packet delays with the max C/I scheduler and 120 UEs per sector at 7.68Mcps and 120 UEs per two sectors at 3.84Mcps with the HTTP TCP traffic model are shown in Table 75.

Table 75 – Mean delay for 7.68Mcps wrt 3.84Mcps for the HTTP TCP traffic model (120 UEs) with the max C/I scheduler

channel	7.68Mcps mean delay / seconds	3.84Mcps mean delay / seconds	mean delay increase of 7.68Mcps wrt 3.84Mcps (%)
AWGN	0.15	0.24	-38
PA3	0.17	0.37	-54
PB3	0.16	0.25	-36
VA30	0.20	0.36	-44
VA120	0.17	0.34	-50
mixed	0.16	0.39	-59

Table 76 shows a similar comparison for the FTP traffic model with 30 UEs per sector at 7.68Mcps and 30 UEs per two sectors at 3.84Mcps with the FTP TCP traffic model.

Table 76 – Mean delay for 7.68Mcps wrt 3.84Mcps for the FTP TCP traffic model (120 UEs) with the max C/I scheduler

channel	7.68Mcps mean delay / seconds	3.84Mcps mean delay / seconds	mean delay increase of 7.68Mcps wrt 3.84Mcps (%)
AWGN	1.67	2.38	-30
PA3	3.42	7.78	-56
PB3	4.79	7.21	-34
VA30	8.73	18.28	-52
VA120	11.21	10.57	6
mixed	3.82	6.97	-45

The mean TCP packet delay seen at 7.68Mcps is significantly less than at 3.84Mcps. This reduced packet delay occurs due to the same reasons that the packet call rate is higher at 7.68Mcps than it is at 3.84Mcps (see section 5.3.2.5.1), namely :

- reduced blocking probability at 7.68Mcps compared to 3.84Mcps
- ability to allocate more resource to UEs in some channel conditions per TTI at 7.68Mcps
- improved link level performance at 7.68Mcps compared to 3.84Mcps

5.3.2.5.6 Limited Packet Call Rate for HTTP / TCP Traffic Model

The maximum packet call rate that is seen for any channel model with the HTTP / TCP traffic model is of the order of 400 kbps. The packet call rate CDFs indicate that few users achieve a mean packet call rate of greater than 1Mbps.

This limited packet call rate is due to modeling of the TCP slow start algorithm. When small web pages are downloaded according to the HTTP / TCP slow start traffic model, a significant proportion of the packet call can be attributed to the round trip times associated with TCP packets being sent from the internet server to the Node B. A high packet call rate will only be seen when the “slow start period” is completed; this will only occur for packet calls containing large amounts of data (note that TCP slow start is also modeled for the FTP traffic, but the packet call rates seen with this traffic model are greater due to the larger packet sizes).

It is to be expected packet call rates will increase with time as round trip times within the internet reduce and the sizes of web pages increase.

5.3.2.5.7 Outage Criteria

No specific criterion is applied to define UEs as being in outage : the system simulator attempts to service all UEs that are attached the centre cell of the 19-cell hexagonal grid.

When the max C/I scheduler is used, the results of sections 5.3.2.2 and 5.3.2.3 can be interpreted to include an outage criterion by use of the packet call rate CDFs. Users with a packet call rate that is less than a desired minimum can be considered to be in outage; packet call rate and delay curves can then be scaled to account for this outage (when users

are defined as being in outage, it is expected that the cell throughout will increase, but that this increase may be marginal with a max C/I scheduler).

Defining an outage criterion with the Round robin scheduler would increase the packet call rates and cell throughput results (the scheduler would schedule fewer low data rates users). The mean delay results would be decreased with an outage criterion applied.

5.3.2.5.8 MAC-hs Failure Rate in PA3

In channel PA3, the MAC-hs failure rate (the rate at which RLC retransmissions are required) is greater than the target rate of 10^{-4}. The higher than expected MAC-hs failure rate is due to the deep fades that are experienced in PA3. The scheduler may schedule UEs in a fade for a variety of reasons :

- the scheduler implemented in the simulation will always attempt to schedule a UE (the max C/I scheduler will schedule UEs with the best CQI reports, but these best UEs may still be in fades).

- the channel may change from being “non-faded” to being in a fade in the time between the CQI report and the actual transmission to the UE.

The scheduler also always schedules transmissions at a coding rate of greater than or equal to 1/12 (i.e. the maximum repetition factor used in rate matching is 4). Thus if the CQI report from a UE indicates very poor C/I, the scheduler may schedule that UE with a code rate (1/12) that is greater than the channel can support; the scheduler assumes that HARQ retransmissions will eventually lead to correct reception of the relevant transport block.

In order to reduce the MAC-hs failure rate, the maximum number of retransmissions at the Node B may be increased. Figure 178 to Figure 181 present results using the max C/I scheduler with the HTTP traffic model when the maximum number of retransmissions is increased to 6 (i.e. an initial transmission and up to 5 retransmissions).

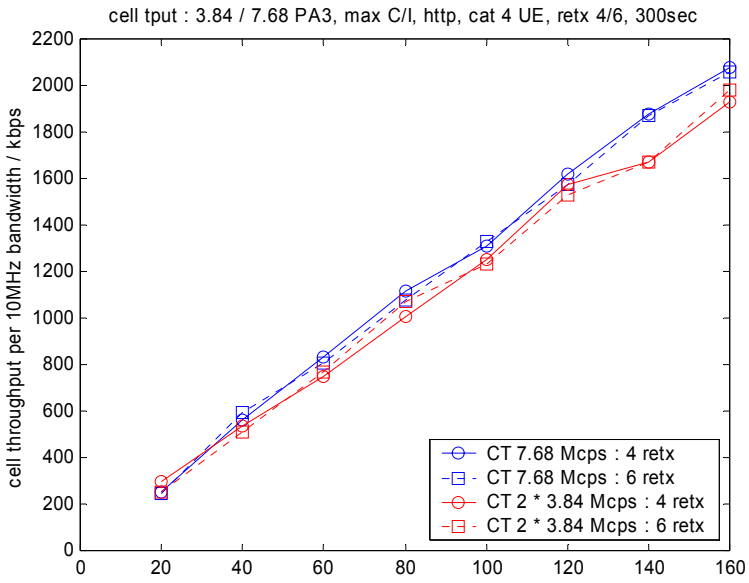

Figure 178 - PA3 : cell throughput with 4 and 6 max retransmissions

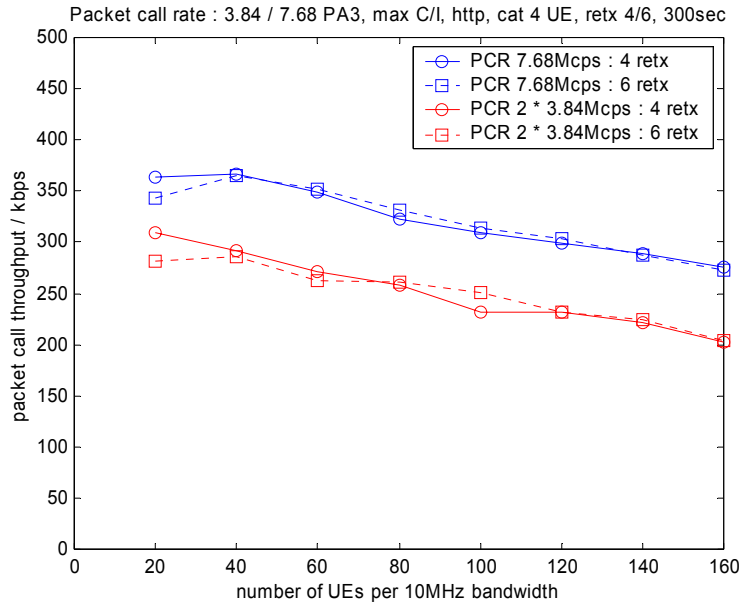

Figure 179 - PA3 : packet call rate with 4 and 6 max retransmissions

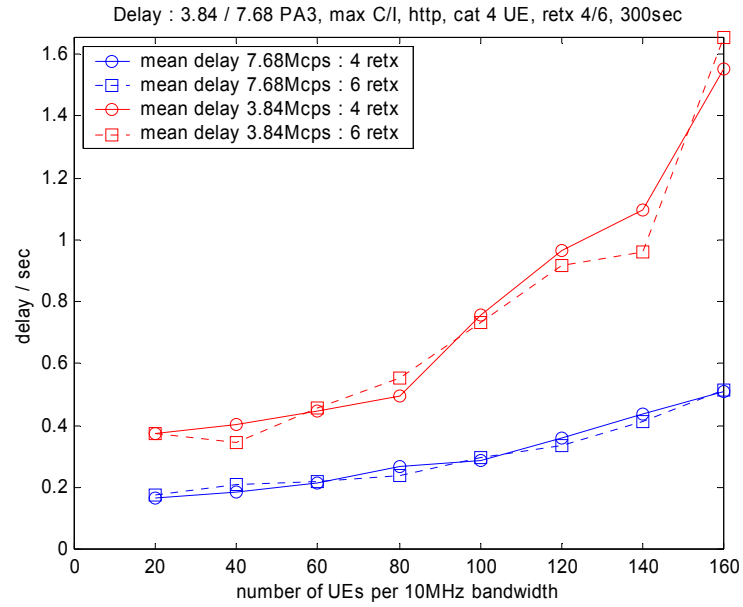

Figure 180 - PA3 : packet delay with 4 and 6 max retrnasmissions

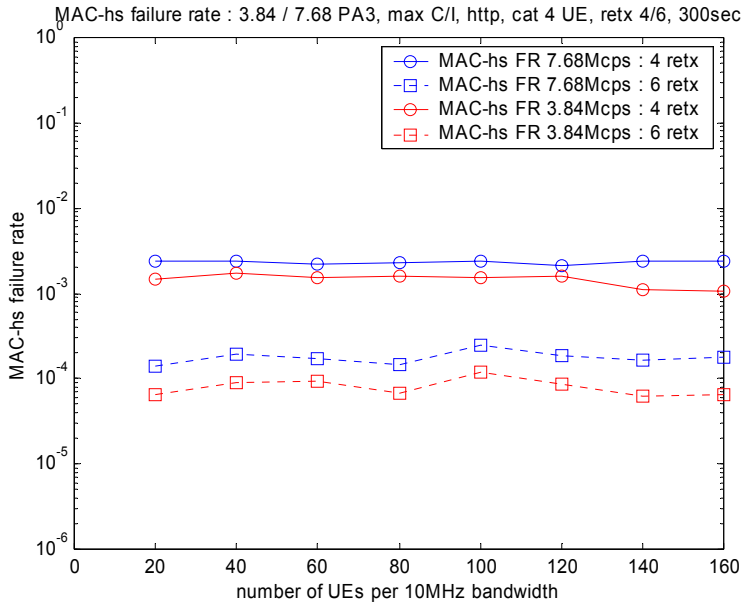

Figure 181 - PA3 : MAC-hs failure rates with 4 and 6 max retransmissions

These results show that the cell throughput, packet call rate and packet delay are not affected to a statistically significant extent by increasing the maximum number of retransmissions (note that an RLC re transmission is a rare event even when a maximum of 4 retransmissions are employed). However, increasing the maximum number of MAC-hs retransmissions to 6 reduces the MAC-hs failure rate to the target rate of 10^{-4}. Note that the MAC-hs failure rate at 7.68Mcps is slightly greater than that at 3.84Mcps. This is due to the steepness of the link level BLER curves at 7.68Mcps in relation to the 3.84Mcps curves (scheduling decisions are more "forgiving" at the lower chip rate due to the shallowness of the 3.84Mcps link level BLER curves).

These results illustrate that cell throughput, packet call rate and packet delay results are not significantly impacted when the maximum number of retransmissions is increased from 4 to 6, thus performance results obtained with 4 MAC-hs retransmissions may be used and it will be understood that the frequency of RLC retransmissions may be reduced simply by increasing the maximum number of MAC-hs retransmissions.

The MAC-hs failure rate results in the mixed channel model for FTP / TCP traffic and a max C/I scheduler are of interest (section 5.3.2.4.6). These results show a reduction of MAC-hs failure rate as the number of UEs increase. This result is due to the max C/I scheduler scheduling AWGN users in preference to PA3 users when there is a large population of users to schedule (the max C/I scheduler naturally does this since it prioritises scheduling of users that can transmit at a high AMC in preference to those in a low AMC : AWGN UEs are more likely to support a high modulation and channel coding rate than PA3 UEs). As expected, the Round robin scheduler does not show a decrease in MAC-hs failure rate with the mixed channel model : the scheduler is unable to schedule AWGN users in preference to PA3 users.

5.4 Link Budget

This section evaluates the impact of higher chip rate TDD systems on the link budget. The link budget of a 7.68 Mcps TDD system is compared to that of a 3.84 Mcps TDD system. The analysis focuses on a single timeslot and is performed in noise limited and interference limited environments for the downlink and uplink.

The path loss PL_X, of a system X, in the downlink is given as:

$$PL_X = P_{NB} + C - SF_X - N_X - \mathrm{E_b/N_0\ Target} + PG_X \qquad \mathrm{dB}$$

where, P_{NB} is the Node B transmit power in dBm and C is the fraction of code space used in dB. SF_X, N_X and PG_X are the spreading factor in dB, noise + interference in dBm and processing gain in dB respectively for system X. Note that the first three terms in the above equation correspond to the power per code used in the system X. Common factors that impact the path-loss such as antenna gain, feeder loss and receiver noise figure are assumed to be the same for all chip rate systems, thus the main difference between the systems is due to factors related to the difference in bandwidth.

In the uplink, the path loss of a system X is:

$$PL_X = P_{UE} - 10\times\mathbf{log}_{10}(NC) - N_X - \mathrm{E_b/N_0\ Target} + PG_X \qquad \mathrm{dB}$$

where, P_{UE} is the UE transmit power in dBm and NC is the number of codes used in the uplink.

In this analysis X=1 refers to 7.68 Mcps TDD system whilst X=2 refers to 3.84 Mcps TDD system. A common 8 kbps speech service is assumed for both systems, where the resources required in each system are summarized in Table 77 below [14]:

Table 77 : Resources for 8 kbps speech service.

TDD System	Downlink	Uplink
7.68 Mcps	SF32 × 1 code × 1 timeslot	SF32 × 1 code × 1 timeslot
3.84 Mcps	SF16 × 1 code × 1 timeslot	SF16 × 1 code × 1 timeslot

5.4.1 Noise Limited Environment

5.4.1.1 Downlink Link Budget

In the downlink, it is assumed that the maximum Node B transmit power and the fraction of code space used per timeslot in the network are the same for all systems. For the same service and E_b/N_0 target, the difference in path losses between two systems is:

$$PL_1 - PL_2 = (SF_2 - SF_1) + (PG_1 - PG_2) + (N_2 - N_1) \qquad \mathrm{dB}$$

For the same fraction of code space used, the power per code in the 3.84 Mcps TDD system is twice that of the 7.68 Mcps TDD system. However, the 7.68 Mcps TDD system has twice the processing gain per timeslot compared to that of a 3.84 Mcps TDD system, which offsets the loss in power per code. Hence, the difference in path losses between these two systems is dependent upon the noise and interference at the UE. Thermal noise power in the 7.68 Mcps TDD system is twice that of the 3.84 Mcps TDD system. Hence, in a noise limited environment, the 7.68 Mcps TDD system can only support 3 dB lower downlink path loss than that of a 3.84 Mcps TDD system. However this elementary analysis assumes that base station transmit power is equally divided between users, but if downlink power control is considered, the base station power is no longer constrained to be equally divided between all active users. In the case where full base station transmit power is dedicated to a single user in both systems, the increase in noise bandwidth in the 7.68Mcps system is offset by the improvement in processing gain, therefore the maximum downlink coverage can be considered to be the same for both systems.

5.4.1.2 Uplink Link Budget

In the uplink, it is assumed that the UE maximum power is the same for all systems. Since each system requires the same code resource for the 8 kbps service, the power per code is the same for all systems. For the same service and E_b/N_0 target, the difference in path losses between two systems is:

$$PL_1 - PL_2 = (PG_1 - PG_2) + (N_2 - N_1) \qquad \mathrm{dB}$$

The processing gain per timeslot in the 7.68 Mcps TDD system is twice that of the 3.84 Mcps TDD system. Since the thermal noise power in the 7.68 Mcps TDD system is twice that of the 3.84 Mcps TDD system, the uplink path loss supported by the two systems is identical.

5.4.2 Interference Limited Environment

5.4.2.1 Downlink Link Budget

In the downlink, it is assumed that the Node B transmit power and the fraction of code spaces used are the same in all systems.

In a system that is completely limited by the downlink interference level, the thermal noise floor of the system can be considered to be negligible, thus the dependence of maximum path loss upon receiver bandwidth is removed and the C/I ratio at the UE is only a function of the total base station transmit power. The 3dB processing gain improvement of the

7.68Mcps system over that of the 3.84Mcps results in 3dB lower power per user for the high chip rate system, which in turn results in a doubling of the number of users supported when compared to the 3.84Mcps system. Hence the link budgets in both systems are the same.

5.4.2.2 Uplink Link Budget

Similar to the evaluation in Section 5.4.1.2, for an interference limited environment, the difference in link budgets between two systems is dependent upon the interference and the processing gain of the systems. The interference of each system is evaluated using a Monte Carlo simulation with 1000 snap shots to give a statistically significant result. The simulation uses the parameters outlined in Annex B, where the network consists of 19 cells. However, in this section, each cell has a Node B using an omni directional antenna with a gain including feeder loss of 11 dB. The cell radius is reduced to 200 m to simulate an interference limited environment. The E_b/N_0 Target is 5.8 dB as suggested in [13] and Multiuser Detection is used in the simulation, which removes intra-cell interference. In the uplink, the interference power is evaluated at the Node B in the central cell.

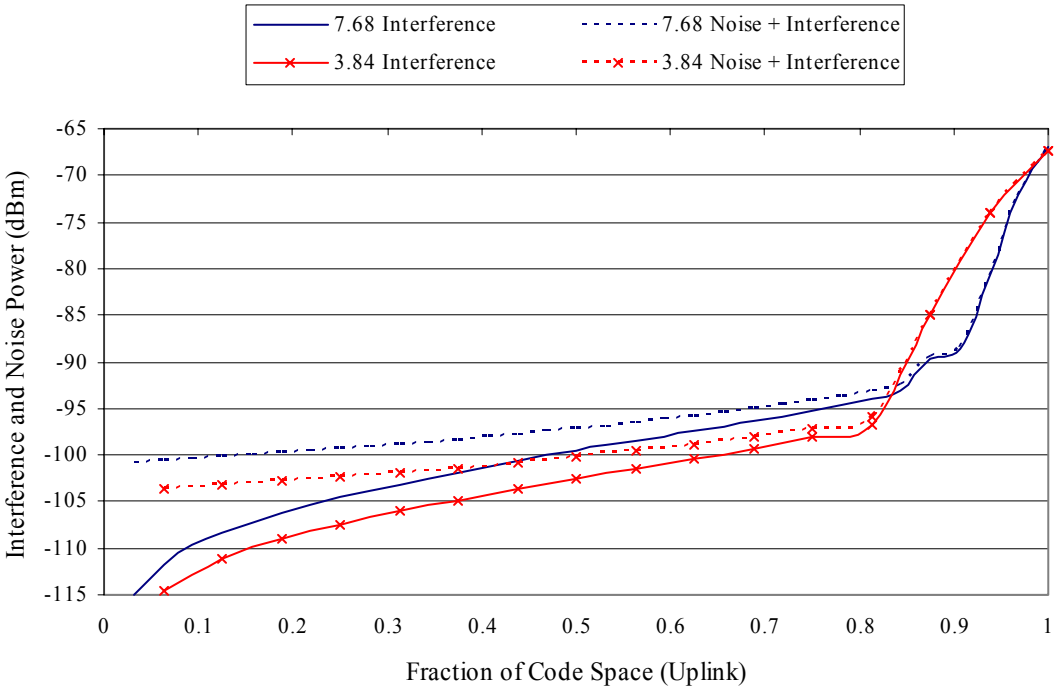

Figure 182: Uplink interference & noise (thermal noise + interference) power against code space fraction.

The simulation results are shown in Figure 182, which contains plots of the downlink average interference and noise (thermal noise + interference) power in dBm against the fraction of the code space used for each system. The pole capacity region when the fraction of code space used is greater than 0.8 is avoided and the interference limited environment is approximated by taking the results when the fraction of the code space used is between 0.6 and 0.8 (where the difference between interference and thermal noise is less than 3 dB). The average differences in interference and link budget are summarized in Table 78.

Table 78: Difference in Interference Power and Link Budget (dB) - Uplink

Systems Under Consideration	Difference in Interference Power (dB)	Difference in Path Loss (dB)
7.68 Mcps – 3.84 Mcps	2.89 dB	0.12 dB

Although each UE in the 7.68 Mcps TDD system requires less power per code compared to that of the 3.84 Mcps TDD system, the 7.68 Mcps TDD system can accommodate twice the number of UEs per timeslot giving 2.89 dB more uplink interference power compared to that of the 3.84 Mcps TDD system. The 7.68 Mcps TDD system has a small gain of 0.12 dB in uplink link budget over the 3.84 Mcps TDD system.

5.4.3 Conclusion

The link budget of the 7.68 Mcps TDD system is compared with that of the 3.84 Mcps TDD system in noise limited and interference limited environments.

For the noise limited case, the maximum supportable path losses in the downlink and uplink are found to be equivalent for both chip rates if the full base station transmit power is available to a single user in the downlink and the UE transmit powers for both systems are the same. In this situation the additional processing gain in the 7.68Mcps system compensates for the increase in the noise bandwidth.

In the interference limited case, the noise bandwidth of the system is not a limiting case in the downlink system therefore the 7.68Mcps system is able to use the additional processing gain to support a larger number of users than the 3.84Mcps system. Therefore, the downlink link budgets for both systems are the same. In the uplink, the interference statistics are a little more complex and a Monte Carlo analysis has shown that the interference on the uplink for the 7.68Mcps system shows a small statistical improvement in uplink efficiency which appears to be due to the increased processing gain reducing the influence of the probability that a single UE will dominate the inter-cell interference during any one snap shot.

The results are summarized in Table 79.

Table 79: Differences in Link Budget (dB).

Systems	Noise Limited		Interference Limited	
	Downlink	Uplink	Downlink	Uplink
7.68 Mcps – 3.84 Mcps	0 dB	0 dB	0 dB	0.12 dB

5.5 Complexity Analysis

5.5.1 UE Complexity

The significant functional blocks within the UE are shown in Figure 183. Not all of the functional blocks have complexities that vary significantly with the chip rate. The complexities of the following functional blocks do not vary significantly with chip rate:

- receiver transport channel processing (Turbo decoding, Viterbi decoding, de-interleaving, rate-matching etc.).
- transmit transport channel processing (Turbo and convolutional encoding, interleaving, rate-matching etc.).
- HSDPA (HARQ memory, additional transport channel processing elements, HS-SCCH and HS-SICH processing etc.).
- DSP, microcontroller, RAM and supporting interfaces.
- synchronization (since the 7.68Mcps PSC is simply a repetition encoded version of the 3.84Mcps SCH in the reference configuration)

The complexities of the following functional blocks vary with chip rate:

- modulator (spreading) and RRC filter
- channel estimation
- joint detector

For a 2Mbps UE (for example, a category 3 HSDPA UE), the complexities of receive transport channel processing, transmit transport channel processing, HSDPA, microcontroller and the joint detector are approximately equal and the complexity of any one of these elements dwarves the complexity of any other functional block.

This analysis thus concentrates on the complexity of the joint detector (section 5.5.1.1) which is assumed to account for 20% of UE complexity at the 3.84Mcps chip rate. The manner is which the complexities of less complex blocks varies with chip rate is considered in section 5.5.1.2.

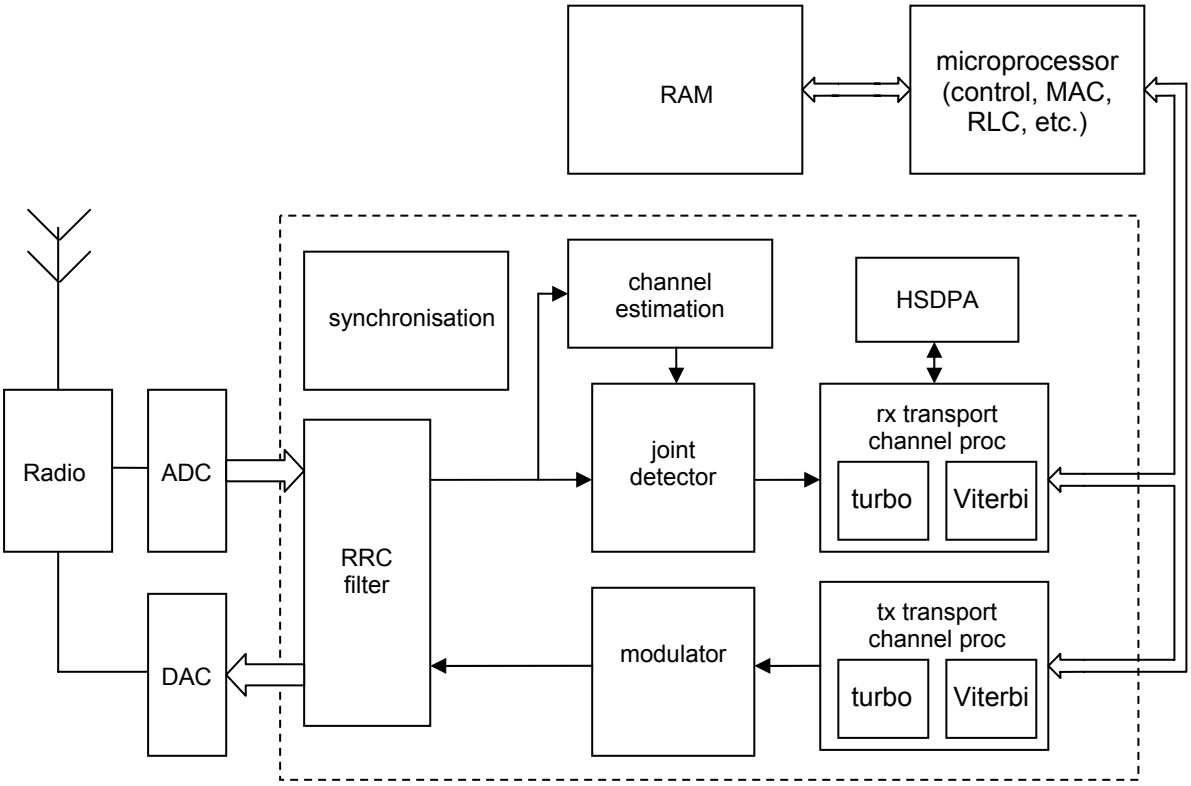

Figure 183 - Main UE architectural blocks

5.5.1.1 Joint Detector Complexity

Joint detection in the frequency domain is less complex than joint detection in the time domain [11] ([11] also describes an algorithm for performing joint detection in the frequency domain).

The complexity of the frequency domain joint detection algorithm in [11] applied to both 3.84Mcps and 7.68Mcps is analysed in Table 81 : the parameter values applied at 3.84Mcps and 7.68Mcps are detailed in Table 80.

Table 80 - Complexity parameter values

parameter	3.84Mcps value	7.68Mcps value
N = symbols / payload	69	69
Q = spreading factor	16	32
W = channel dispersion	57	114
K = users	16	32
D = FFT size	32	32
p^- = prelap symbols	3	3
p^+ = postlap symbols	5	5
L = payloads per burst	2	2
S = number of overlaps	6	6

Complexities in terms of real multiplications per timeslot are detailed in Table 81.

Table 81 – UE multiplication complexity at 3.84Mcps and 7.68Mcps

Operation	complexity / multiplications	3.84Mcps mults / timeslot	7.68Mcps mults / timeslot
B matrix calculation	$4K\left(2\sum_{q=1}^{Q} q + Q(W-Q-1)\right)$	58368	466944
FFT of **B** matrix $\mathbf{\Lambda} = \mathbf{F}_Q \widetilde{\mathbf{A}}$	$2KQD\log_2 D$	81920	327680
$\widetilde{\mathbf{A}}^H \widetilde{\mathbf{A}}$ matrix calculation	$4P\sum_{k=1}^{K} k - 2KP + 4K^2 \sum_{v=1}^{\lceil P/Q \rceil - 1} (P - vQ)$	167936	1361920
FFT of $\widetilde{\mathbf{A}}^H \widetilde{\mathbf{A}}$ matrix $\mathbf{\Sigma} = \mathbf{F}_K \widetilde{\mathbf{A}}^H \widetilde{\mathbf{A}}$	$2K^2 D\log_2 D$	81920	327680
Cholesky decomposition $\widetilde{\mathbf{L}}\widetilde{\mathbf{L}}^H = \mathbf{\Sigma}$	$4D\sum_{k=1}^{K-1} k(K-k) + 2D\sum_{k=1}^{K-1} k$	94720	732160
FFT of received samples $\mathbf{F}_Q \widetilde{\mathbf{r}}$	$2SQD\log_2 D$	30720	61440
Matched filtering $\widetilde{\mathbf{x}} = \mathbf{\Lambda}^H \cdot (\mathbf{F}_Q \widetilde{\mathbf{r}})$	$4SDKQ$	196608	786432
Forwards substitution $\widetilde{\mathbf{L}}\widetilde{\mathbf{y}} = \widetilde{\mathbf{x}}$	$4SD\sum_{k}^{K-1} k$	92160	380928
Backwards substitution $\widetilde{\mathbf{L}}^H \widetilde{\mathbf{d}} = \widetilde{\mathbf{y}}$	$4SD\sum_{k}^{K-1} k$	92160	380928
IFFT of symbol estimates $\hat{\mathbf{d}} = \mathbf{F}_K^{-1} \widetilde{\mathbf{d}}$	$2SKD\log_2 D$	30720	61440
Total		927232	4887552

Table 81 indicates that approximately 5 times more real multiplications per timeslot are required at 7.68Mcps than at 3.84Mcps. This complexity could be reduced by restricting the number of codes that the UE can simultaneously decode or the channel dispersion length that the UE joint detector can tolerate. Overall joint detector complexity can be derived when the number of downlink timeslots supported per frame is taken into account.

A category 1 3.84Mcps HSDPA TDD UE supports a maximum of 2 HS-DSCH timeslots per TTI and 16 HS-DSCH codes per timeslot. This UE thus supports 32 physical channels per TTI. HS-DSCH transport channel processing for a category 1 3.84Mcps HSDPA UE is thus dimensioned based on 32 physical channels per TTI. It is assumed that a category 1 HSDPA TDD UE would thus also be dimensioned based on support for 32 physical channels per TTI, thus a category 1 7.68Mcps HSDPA UE would support 1 HS-DSCH timeslot per TTI.

There is no restriction in terms of the number of HS-DSCH codes that a category 2 3.84Mcps TDD UE can decode. It is assumed that a category 2 7.68Mcps TDD UE is similarly unrestricted in terms of the number of timeslots that it can decode.

Accounting for the differing number of timeslots that a UE must decode at 3.84Mcps and 7.68Mcps, joint detector complexity for HS-DSCH category 1,3 and 5 UEs is approximately 2.6 times greater at the higher chip rate. Joint detector complexity for other HS-DSCH categories is approximately 5.3 times greater.

It is assumed that for non-HS-DSCH channels (e.g. DSCH, DCH), it is also reasonable for a UE to joint detect fewer timeslots per TTI. It is thus possible to implement a 2.4Mbps 7.68Mcps TDD UE where the joint detector is approximately 2.6 times as complex as at 3.84Mcps.

5.5.1.2 Complexity of other UE functional blocks

The complexity of the spreading and modulation, RRC filter and channel estimation functional blocks increases at the higher chip rate. As the complexity of these functional blocks is not significant at 3.84Mcps and remains insignificant at 7.68Mcps, this analysis merely indicates the manner in which the complexity of these functional blocks increases.

channel estimator

Channel estimation in the time domain may be implemented by forming the product $G^{*T} \cdot e$ where G is an $L \times L$ matrix consisting of elements of the midamble sequence from the set $\{\pm 1, \pm j\}$, e is an $L \times 1$ matrix consisting of received midamble samples. Channel estimation in the time domain thus consists of L^2 complex "swap and invert" operations (where L is the useful length of the midamble in chips). Channel estimation in the time domain may thus be four times as complex at 7.68Mcps than it is at 3.84Mcps, however the channel estimation operation does not involve multiplications and is thus not of significant complexity at either 3.84Mcps or 7.68Mcps. Efficient frequency domain channel estimation algorithms exist that have lower complexity than the time domain algorithm.

spreading / modulation

The spreading and modulation function may be implemented as a replication of pre-computed gain factors followed by a summation. The replication function has no significant complexity. Since there are twice as many chips per timeslot at 7.68Mcps compared to 3.84Mcps, there will be twice as many addition operations required in the summation operation at the higher chip rate. The complexity of the spreading / modulation operation is clearly not significant compared to that of other functions (such as joint detection, Turbo decoding etc.).

RRC filter

In TDD, a single RRC filter can be used for both transmission and reception. The length of the RRC filter impulse response is independent of chip rate. Since the filter coefficients of the RRC filter are fixed, it may be implemented using shift and add operations. Since there are twice as many chips per timeslot at 7.68Mcps as at 3.84Mcps, the complexity of a 7.68Mcps RRC filter is twice that of a 3.84Mcps RRC filter. However, the complexity of this filter is not significant in comparison to joint detector complexity, Turbo decoder complexity etc.

5.5.1.3 Complexity of decoding M=8 HS-SCCH

In the reference configuration, it is stated that a 7.68Mcps UE must be able to decode up to M=8 HS-SCCH compared to M=4 HS-SCCH at 3.84Mcps.

The HS-SCCH carries 65 bits (payload + tail bits) at 3.84Mcps and 67 bits (payload + tail bits) at 7.68Mcps. The HS-SCCH is convolutionally encoded with a constraint length 9 code. HS-SCCH decoding complexity is thus proportional to 4×65 at 3.84Mcps and 8×67 at 7.68Mcps.

This complexity is compared to the Turbo decoder complexity of a category 4 HSDPA UE: such a UE typically decodes 24000 turbo encoded bits in 15 timeslots (it is assumed that HS-SCCH is Viterbi decoded in a single timeslot). Assuming that the number of operations required to Turbo decode a data bit is approximately double that required to Viterbi decode a data bit (using the turbo and convolutional codes specified in [3]), HS-SCCH decoding complexity accounts for approximately 8% and 16% of FEC decoding complexity at 3.84Mcps and 7.68Mcps respectively.

Assuming that the ECC decoders account for approximately 20% of overall UE complexity, the requirement to decode M=8 rather than M=4 HS-SCCH increases UE complexity by less than 2%. System simulations do not show a clear performance benefit from decoding M=8 HS-SCCH and this additional complexity may be reduced by relaxing the number of HS-SCCH that the UE must decode without significantly impacting system performance.

5.5.1.4 Radio Complexity

The majority of the radio complexity is independent of the chip-rate used, as the analogue performance and power consumption is determined by the IF and RF frequencies. Two circuit elements where this assumption is not true are the PA and the analogue baseband filter.

The linearity requirement of a higher chip rate TDD PA would be greater than at 3.84Mcps. This linearity requirement would manifest itself as a reduction in UE output power or a reduction in PA manufacturing yield. The gain bandwidth product of the UE analogue baseband filter of a higher chip rate TDD UE will increase: the increased gain bandwidth product is readily achievable, but may result in greater UE power consumption than at 3.84Mcps. ADC and DAC components will have to operate at twice the speed at a higher chip rate compared to a 3.84Mcps TDD UE.

5.5.1.5 Overall UE Complexity Increase

It is feasible to implement a joint detector that is approximately 2.6 times more complex at 7.68Mcps than at 3.84Mcps. Other UE functional blocks have complexities that are either not significant (e.g channel estimation, spreading / modulation) or do not increase significantly as the chip rate is increased (transport channel processing, HSDPA, microcontrollers). Given that a 3.84Mcps joint detector accounts for approximately 20% of UE complexity at 3.84Mcps, a UE may be constructed with a complexity at 7.68Mcps which is approximately 33% greater than at 3.84Mcps.

5.5.2 UTRAN Complexity

This analysis compares the complexity of UTRAN serving 10MHz of spectrum at chip rates of 7.68Mcps and 3.84Mcps. It is assumed that a single 3.84Mcps Node B serves two contiguous 3.84Mcps frequencies that are denoted f_1 and f_2. At 3.84Mcps, the physical entity that services a single frequency is denoted a “cell card”. Thus the 3.84Mcps Node B consists of two cell cards (which could possibly be integrated onto a single circuit board according to implementation decisions). A deployment utilizing fewer 3.84Mcps Node Bs serving two frequencies (as per this analysis) is considered to be more efficient than a deployment using more 3.84Mcps Node Bs serving single frequencies: the deployment analysed minimizes hardware, cell site acquisition, cell site maintenance and backhaul provisioning costs. Figure 184 shows the implementation analysed at 3.84Mcps (the 3.84Mcps cells at both f_1 and f_2 share common cell sites) . Figure 185 shows the implementation analysed at 7.68Mcps.

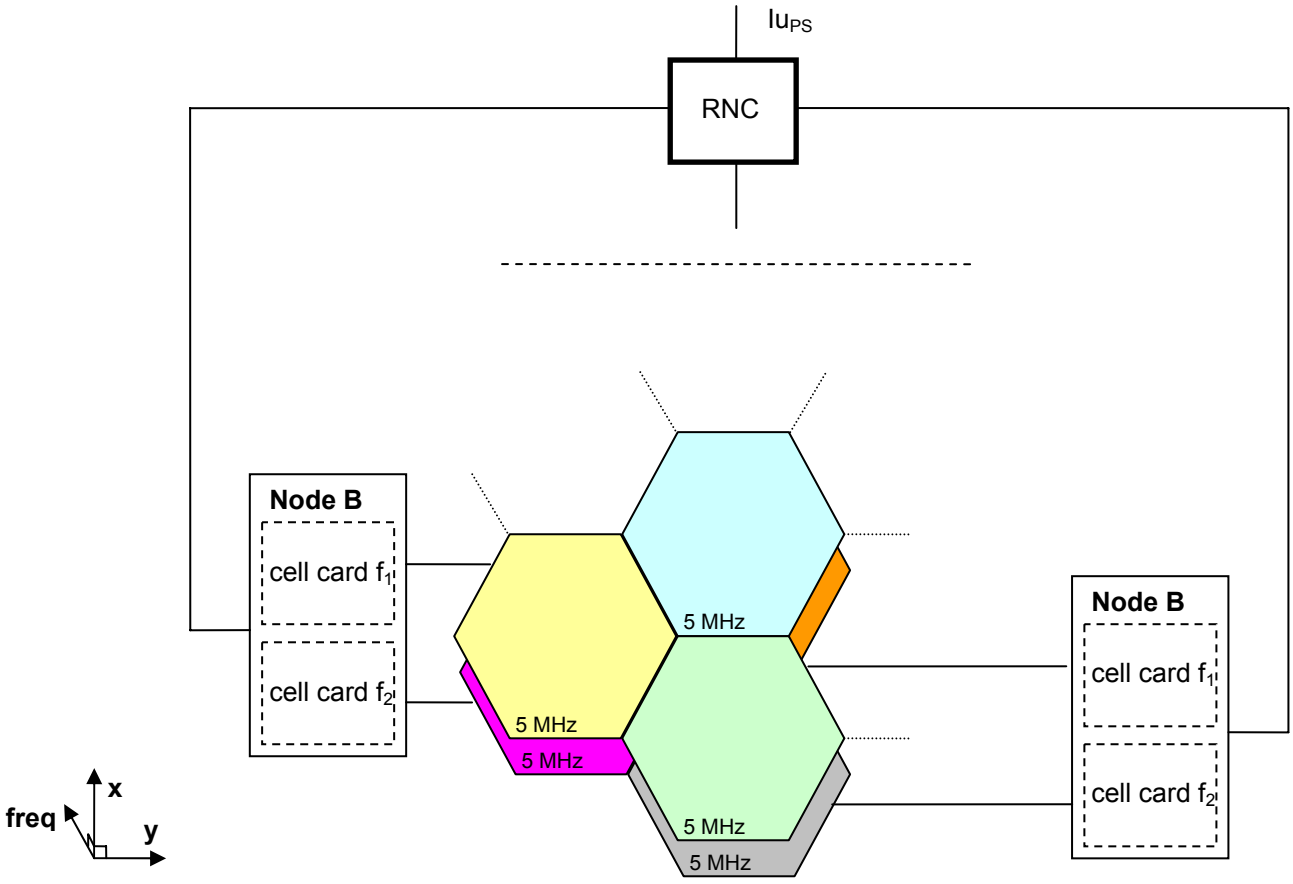

Figure 184 – Deployment of co-located cells (at frequencies f1 and f2) using multi-frequency 3.84Mcps Node Bs

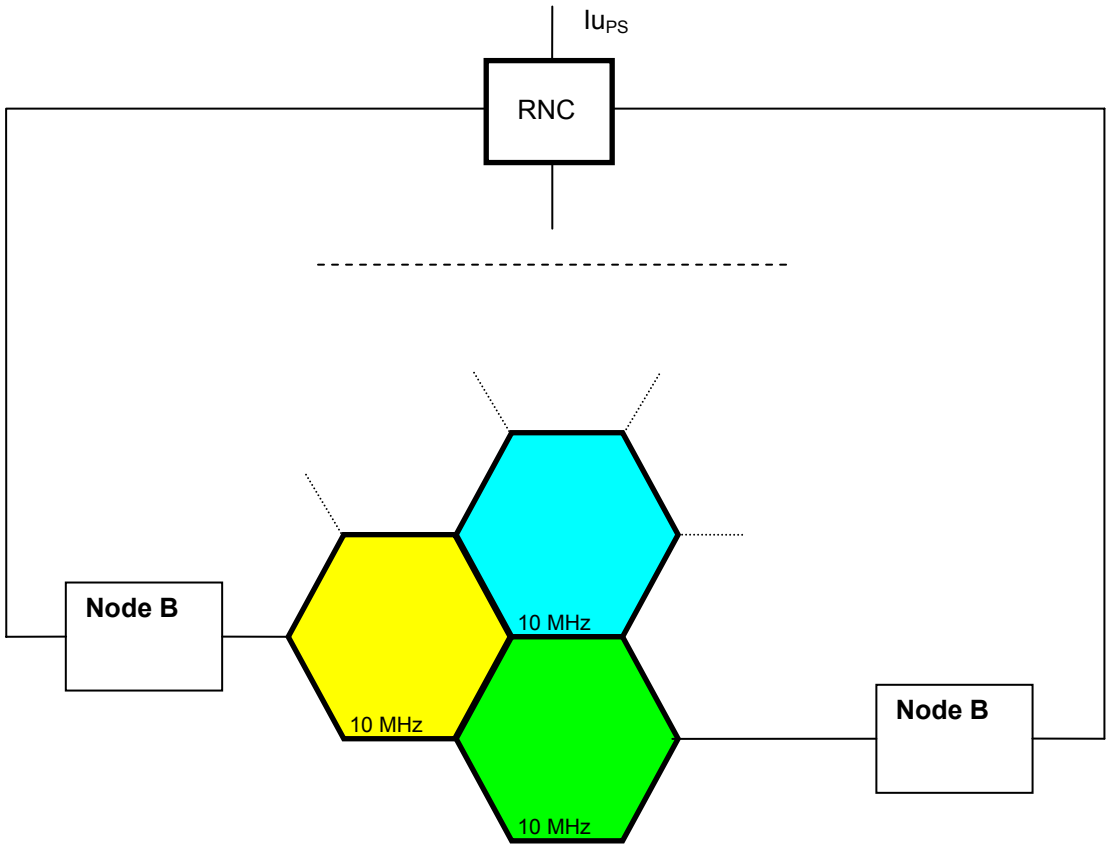

Figure 185 – 7.68Mcps deployment analysed

5.5.2.1 Node B Complexity

Figure 186 shows the high level functionality in the Node B required to service 10MHz of spectrum with a 7.68Mps TDD system, Figure 187 shows the high level functionality in the Node B required to service that spectrum with 3.84Mcps TDD. These figures show:

- a single joint detection / channel estimation function can serve 10MHz of spectrum at 7.68Mcps whereas two joint detection / channel estimation functions are required at 3.84Mcps.
- a single spreading / modulation function can support 10MHz of spectrum at 7.68Mcps whereas two such functions are required at 3.84Mcps
- the transport channel processing requirements in a 3.84Mcps Node B are comparable to those of a 7.68Mcps Node B (this aspect is considered further in the following text).
- the 3.84Mcps Node B requires channel separation stages to separate the output of the 3.84Mcps radio into sample streams for the cells at f_1 and f_2. Channel combination functionality is also required.

single 7.68Mcps Node B serving 10MHz

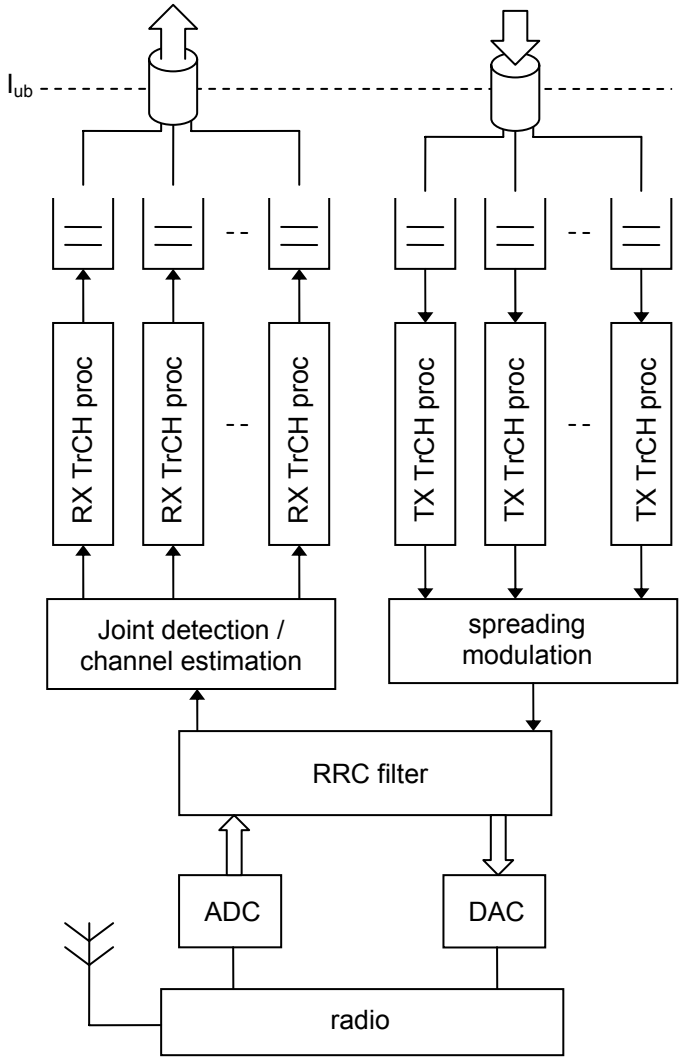

Figure 186 - High level Node B functionality required to service 10MHz of spectrum with 7.68Mcps TDD

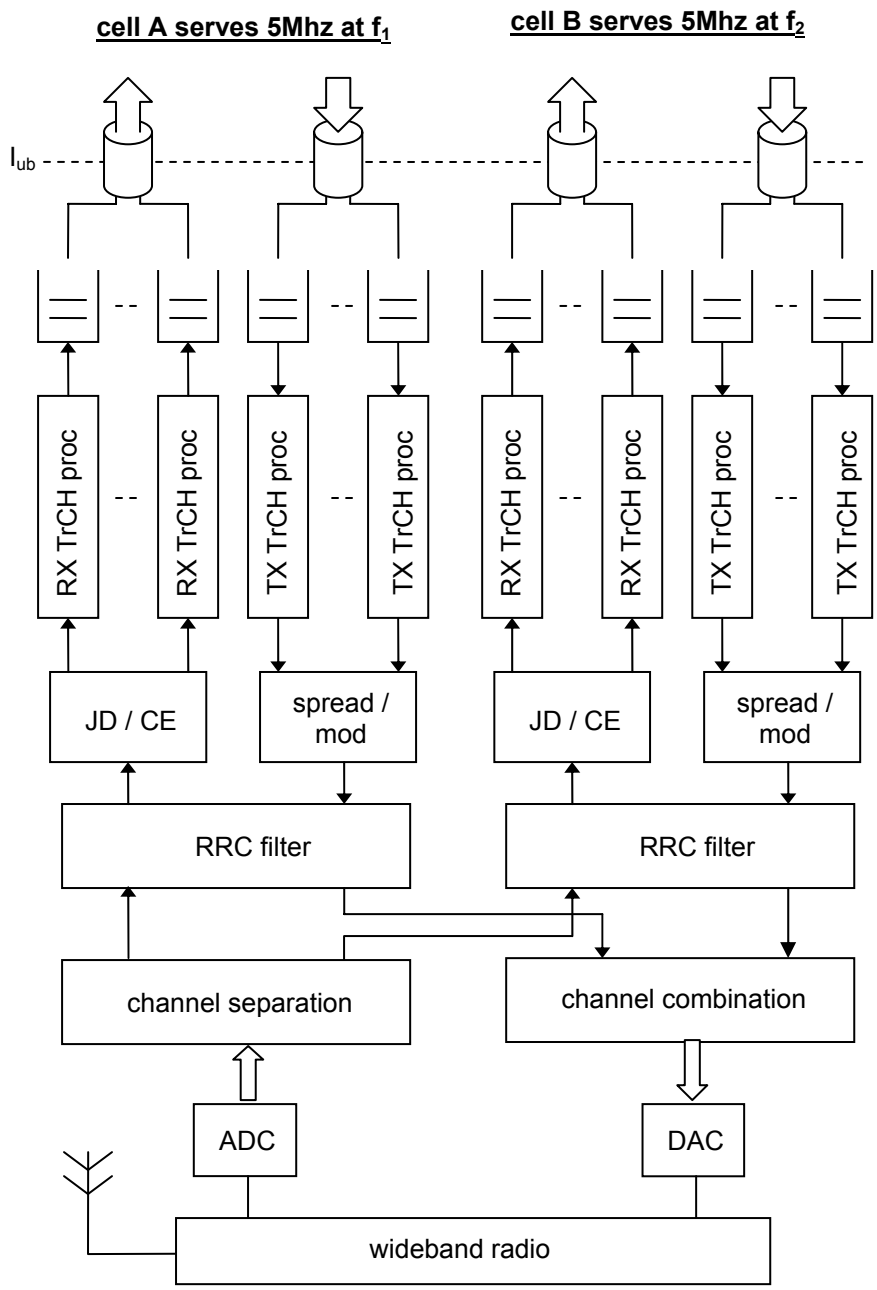

Figure 187 - High level Node B functionality required to service 10MHz of spectrum with 3.84Mcps TDD via two cells at frequencies f1 and f2

The complexity of the various functional blocks within the Node B is analysed below.

Joint detection / channel estimation

The Node B joint detection problem is similar to the UE problem, however the Node B must joint detect all UL-DPCH, PUSCH and HS-SICH timeslots. Section 5.5.1.1 shows that joint detector complexity at 7.68Mcps is approximately 5.3 times greater than at 3.84Mcps when all timeslots are joint detected. Furthermore, channel estimation is found to be four times as complex at the higher chip rate, though this complexity is not especially significant in comparison to the complexity of the joint detector.

A single 7.68Mcps Node B joint detector can service 10MHz of spectrum at 7.68Mcps, whereas two 3.84Mcps joint detectors are required to service 10MHz of spectrum at 3.84Mcps. The joint detection / channel estimation complexity of a 7.68Mcps Node B is thus approximately 2.6 times greater than that of a 3.84Mcps Node B (each Node B serving 10MHz of spectrum).

Spreading / Modulation

Spreading and modulation at the Node B is greatly simplified if the spreading operation and the operation of multiplication by gain factors are combined (such that the gain factors themselves are replicated). The remaining complexity in the spreading / modulation function then exists in summation of the codes.

In the 7.68Mcps Node B, up to 32 codes each of length 5120 chips must be summed. In the 3.84Mcps Node B (serving frequencies f_1 and f_2), $2 \times 16 = 32$ codes of length 2560 chips must be summed. The spreading / modulation complexity of the 7.68Mcps Node B is thus twice as great as for the 3.84Mcps Node B, though this complexity itself is comparatively small (the complexity consists of a set of additions).

RRC filter

Since two RRC filters are required in a 3.84Mcps Node B serving two frequencies and a single RRC filter operating at twice the rate is required for a 7.68Mcps Node B, the complexity of RRC filtering for the 7.68Mcps Node B is the same as that for the 3.84Mcps Node B serving two frequencies.

Transport channel processing

The complexity of the transport channel processing function is dependent on the cell throughput (as opposed to the number of UEs supported) if it is assumed that the transport channel processing functional resources can be efficiently switched between UE contexts in the Node B.

If the Node B is designed to support theoretical peak cell throughput, then the transport channel processing complexity of the 7.68Mcps Node B is identical to that of the 3.84Mcps Node B serving two frequencies.

If the Node B is designed to support a multiple of the mean cell throughput, then the transport channel processing complexity of the 7.68Mcps Node B is somewhat greater than that of the 3.84Mcps Node B serving two frequencies (by virtue of the higher cell throughput at the higher chip rate : section 5.3.2.5.4 indicates that the cell throughput at 7.68Mcps may be of the order of 10% greater at the higher chip rate).

Overall baseband processing complexity

The impact of increased joint detector complexity in the Node B is less than in the UE due to the increased transport channel processing requirements in the Node B. It is thus assumed that Node B baseband processing complexity will thus increase by approximately 25-30% at 7.68Mcps.

Buffering

The Node B needs to buffer data for the purposes of transmission and reception. This requirement is most clearly evident for the case of HSDPA where data must be ready for the Node B to transmit if the HSDPA scheduler decides to schedule a particular UE. The buffering requirement of a 7.68Mcps Node B is thus approximately 30-40% greater for a 7.68Mcps Node B than for a 3.84Mcps Node B serving two frequencies (section 5.3.2.5.2 indicates that of the order of 30-40% more UEs may be supported at a given packet call rate at 7.68Mcps compared to parallel 3.84Mcps cells).

HS-SCCH Encoding

The reference configuration states that a 7.68Mcps UE must decode up to M=8 HS-SCCH. UTRAN may however allocate each UE with an HS-SCCH set size of less than 8 (for example, UTRAN may allocate an HS-SCCH set size of 4 – matching the maximum number of HS-SCCH that the UE is required to decode). The reference configuration requirement that the UE must decode up to M=8 HS-SCCH thus has no UTRAN complexity implication.

Iub interface

If the I_{ub} interface is dimensioned according to mean cell throughput, the throughput requirement of FP on I_{ub} of a 7.68Mcps Node B is approximately 10% greater than that of a 3.84Mcps Node B..

The possible increase in I_{ub} capacity required to support FP traffic at the higher chip rate is somewhat counteracted by a reduction in NBAP traffic at the higher chip rate since only a single cell needs to be controlled by NBAP for a 7.68Mcps Node B, whereas two 3.84Mcps cells must be controlled for a 3.84Mcps Node B, furthermore there will be fewer inter-frequency handovers at 7.68Mcps.

Overall, there will be a minimal increase in I_{ub} throughput requirement at 7.68Mcps compared to 3.84Mcps.

Radio

The same wideband receiver may be used for a 7.68Mcps Node B and a 3.84Mcps Node B. The 3.84Mcps Node B however requires a channel separation function following the wideband receiver. Therefore, the 7.68Mcps radio function may be slightly less complex then the 3.84Mcps one.

The two 3.84Mcps carriers could be combined prior to the Node B power amplifier. Each 3.84Mcps carrier would be transmitted at the same power level as the 7.68Mcps carrier (noting that the spreading factor used at 7.68Mcps is double that at 3.84Mcps). The 3.84Mcps Node B would then require a wideband power amplifier with twice the output power of the 7.68Mcps Node B.

A 3.84Mcps Node B would typically use the same number of antennas as a 7.68Mcps Node B.

5.5.2.2 RNC Complexity

The following RNC complexity aspects are considered in this subsection : throughput, buffering / scheduling and interfaces.

Throughput

As the cell throughput at 7.68Mcps is approximately 10% greater than at 3.84Mcps (section 5.3.2.5.4), RNCs will have to support a higher mean data rate at the higher chip rate.

Buffering

Typically 30-40% more packet users can be supported at 7.68Mcps than at 3.84Mcps. The buffering requirements for USCH, HS-DSCH and DSCH data in the RNC will thus be proportionately greater at the higher chip rate.

RRM

Twice as many cells are supported at 3.84Mcps than at 7.68Mcps, thus twice as many RRM instances are required at 3.84Mcps than at 7.68Mcps.

Interfaces

The higher mean data rate that 7.68Mcps systems support leads to a requirement for slightly higher interface speeds on the I_{ub}, I_{ur} and I_{uPS} / I_{uCS} interfaces. These interfaces need to be approximately 10% faster at 7.68Mcps compared to 3.84Mcps.

5.5.2.3 UTRAN Complexity Summary

For a UTRAN that services a given spectral resource (for example, a UTRAN that services 2 3.84Mcps carriers or a single 7.68Mcps carrier), Node B baseband processing complexity at 7.68Mcps is approximately 30% greater than at 3.84Mcps; other aspects of Node B and RNC complexity are similar at 7.68Mcps and 3.84Mcps. Node B and RNC throughput, buffering and interfaces need to be dimensioned to support a 10% greater cell throughput and 30-40% more active users at 7.68Mcps.

5.5.3 Dual mode 3.84Mcps / 7.68Mcps UEs

The similarity of the higher chip rate reference configuration to 3.84Mcps allows functions implemented at the higher chip rate to be reused at 3.84Mcps. Thus, it is feasible to implement a 3.84Mcps / 7.68Mcps dual-mode TDD UE that is only slightly more complex than a single mode 7.68Mcps UE.

6 Feasibility

6.1 Coexistence with existing UTRA releases

6.1.1 TDD/TDD Coexistence

The co-existence of TDD systems using different chip rates on adjacent radio channels is studied in this section. The analysis comprises two elements, the first concentrates on the UE performance in terms of its radio parameters of adjacent channel selectivity and adjacent channel leakage ratio. The second element considers an elementary system deployment where macro 7.68Mcps and 3.84Mcps TDD systems occupy adjacent radio channels and quantifies the capacity reduction resulting as a consequence of the inter-system interference due to the aforementioned radio parameters.

The performance of the basestation radio has not been considered in this analysis because it is assumed the radio performance of the UE is the limiting factor in most system deployments. In addition, the two systems have been assumed to be slot synchronized such that both systems share common uplink and downlink timings. This assumption permits the uplink and downlink to be considered separately.

6.1.1.1 Radio Performance

The radio performance parameters assumed in the reference configuration are provided in section 4.2. The values put forward were derived from the existing radio performance specifications for 3.84Mcps TDD systems with additional constraints that were designed to minimize issues related to the coexistence of 3.84Mcps and 7.68Mcps systems deployed in adjacent channels. The rationale behind the choice of the parameters is discussed in the following sections.

6.1.1.2 Adjacent Channel Selectivity

The adjacent channel selectivity in the receiver is defined by the selectivity in the digital RRC filter. As the same normalized filter is to be used for both 7.68Mcps and 3.84Mcps chip-rates it can be expected that the selectivity of the 7.68Mcps UE for an adjacent 7.68Mcps signal offset by 10MHz will be the same as the selectivity of a 3.84Mcps UE for an adjacent 3.84Mcps signal offset by 5MHz.

Coexistence is affected by the case where different chip-rates are considered. By way of an example, the adjacent channel selectivity of an RRC filter with a roll-off factor of 0.22 is considered. A practical filter implementation of finite length and coefficient precision as detailed in Table 82.

Table 82 – RRC Filter Implementation

RRC Filter Implementation	Value	Unit
Length	10	Chips
Coefficient Precision	8	bits
Oversampling ratio	4	Samples/chip

A plot of the frequency response of this filter when used for a 7.68Mcps system is shown in Figure 188. For clarity, the two adjacent 3.84MHz channels have been highlighted. The selectivity of this filter for the first 7.68Mcps adjacent channel and the first two 3.84Mcps adjacent channels is given in Table 83. Note that the selectivity in this example filter is much higher than the minimum value specified in [8].

Table 83 – Selectivity of 7.68Mcps RRC Filter

Adjacent Channel Bandwidth	Adjacent Channel Offset	Selectivity
7.68MHz	10MHz	45dB
3.84MHz	7.5MHz	44dB
3.84MHz	12.5MHz	49dB

These results show that the example filter provides almost the same selectivity to the first adjacent channel 3.84Mcps signal as it does to the first adjacent channel 7.68Mcps. It can therefore be deduced that the coexistence of adjacent 7.68Mcps and 3.84Mcps systems will suffer the same downlink capacity degradations as two adjacent channel 3.84Mcps systems.

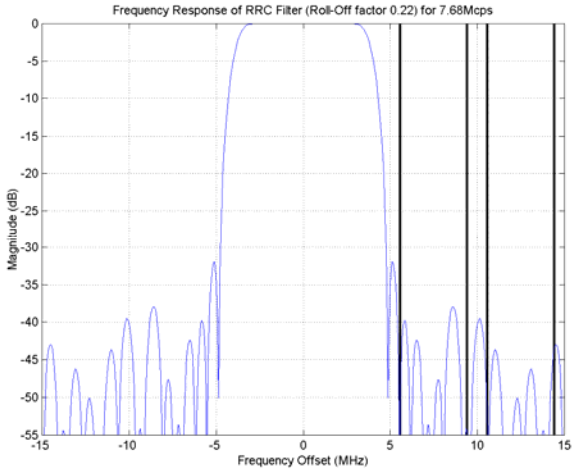

Figure 188 – Frequency Response of Example RRC Filter from 7.68Mcps System

6.1.1.3 Adjacent Channel Leakage Ratio

The performance of the UE transmitter is of paramount importance when considering the coexistence of adjacent 7.68Mcps and 3.84Mcps systems. Non-linear characteristics in the UE power amplifier spread the transmitted signal into adjacent channels. This spectral spreading is directly related the bandwidth of the transmitted signal, which results in the distortion products from a 7.68Mcps signal spreading further in absolute terms when compared to a 3.84Mcps signal. Figure 189 compares the output spectra from 3.84Mcps and 7.68Mcps signals when transmitted through the same power amplifier. For the purposes of this document the power amplifier has been simulated using a model based on [12] with a variable steepness parameter. This model describes the transfer characteristic of the amplifier by the following relation:

$$y(x) = \frac{L \cdot \mathrm{sgn}(x)}{\left[1 + \left(\frac{l}{|x|}\right)^{s}\right]^{1/s}}$$

The parameters used are listed in Table 84, and have been selected to give an output spectrum that closely corresponds with measurements made on real hardware operating at maximum output power. Despite the problems of this model reported in [12], it is well suited to comparing signals with different chip rates as the model is only used at a single power level.

Table 84 – Non-Linear Model Parameters

Parameter	Description	Value
l	Input limit level	1
L	Output limit level	1
s	Knee sharpness	20

The output spectrum obtained from this model for both chip-rates at the same output power is shown in Figure 189. Note that the 3.84Mcps chip rate signal has been shifted by 2.5MHz so that its upper band edge corresponds with the upper band edge of the 7.68Mcps signal and three adjacent 3.84Mcps bands are illustrated for comparison purposes.

It can be seen that the distortion products from the 7.68Mcps signal are spread across a larger frequency range than is the case for a 3.84Mcps signal. However it is interesting to note, that although the distortion products from a 3.84Mcps transmission decay quicker, the absolute power spectral density at the start of the first adjacent channel is higher than

the power spectral density from the 7.68Mcps transition. This is due to the increased spectral density of the 3.84Mcps transmission (same power concentrated in a narrower bandwidth).

The averaged adjacent power levels for the three adjacent 3.84Mcps channels indicated in Figure 189 are listed in Table 85.

Table 85 – Adjacent Channel Leakage Ratio for three adjacent channels with a 3.84MHz bandwidth

Chip Rate	ACLR 1	ACLR 2	ACLR 3
3.84Mcps	38.4 dB	56.8 dB	-
7.68Mcps	38.6 dB	47.3 dB	57.9 dB

The first point to note is that the adjacent channel leakage into the first the 3.84Mcps band is approximately equal for both chip rates, but the 7.68Mcps transmission results in a significantly higher power in the second adjacent channel (approx. 10dB).

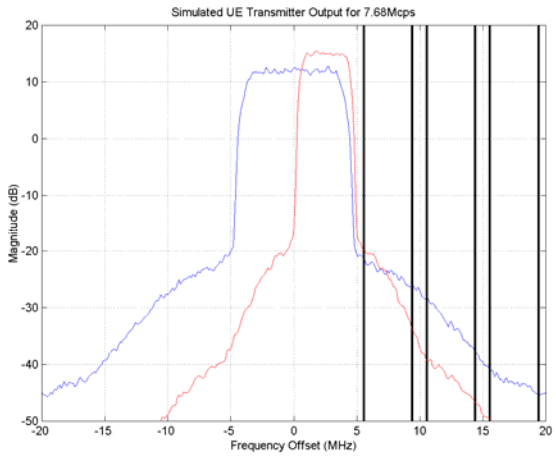

Figure 189 – Simulated UE Output Signal Showing ACLR Measurement bands

6.1.1.4 TDD/TDD Macro Coexistence (3.84Mcps TDD)

In order to assess the impact of the ACS and ACLR figures on adjacent systems a technique based on capacity reduction due to ACIR similar to the techniques used in [13] was used.

6.1.1.4.1 System Configuration

The system configuration is defined in Annex B, Table B.1, with the changes detailed in Table 86.

Table 86 – Parameters Changed in Table B.1

Parameter	Explanation/Assumption	Comments
Cellular layout	Hexagonal grid, 19-cell omni-directional	See Figure B.2 without sectors
Antenna horizontal pattern	Omni	
Site to site distance	1000m	suburban deployment
Propagation model	$L = 128.1 + 37.6\ Log_{10}(R)$	R in kilometers see [13]
BS antenna gain	11 dBi	
UE antenna gain	0 dBi	
UE noise figure	5 dB	
Thermal noise density	-174 dBm/Hz	
BS total Tx power	Up to 37 dBm	
BS noise figure	4 dB	
UE total transmit power	24dBm	
UE spatial distribution	Uniform random spatial distribution over system	
Frequency re-use	1	
Multi-User Detection	On	UL and DL

Both uplink and downlink timeslots from the adjacent systems are assumed to be time-synchronized. This assumption permits the uplink and downlink to be analyzed independently. In addition, only one timeslot was considered.

6.1.1.4.2 Uplink Capacity Reduction

For the uplink, the capacity is determined by the mean number of UEs in the system that results in a noise rise (interference level) of 6dB in the central cell. The source of this interference in the uplink is made up of intercell interference in the case of an isolated system and gives the reference capacity for the system. Several thousand Monte-Carlo snap-shots are required in order to obtain the necessary statistical significance. For the purposes of this simulation, the UL sensitivity and number users where selected such that the noise rise of 6dB was achieved with about 13 users per cell.

When the second system was added, the interference introduced by the ACLR of the UEs increases the noise rise observed in the first system, resulting in an overall reduction in the number of users that can be supported for a 6dB noise rise at the central cell. The basestations in the second system were situated at the cell borders of the first system, and as such represents the worst case condition as the probability of inter-system interference is higher.

Figure 190 shows the results of the capacity reduction simulated for differing values of UE ACLR. These results predict a slightly higher capacity reduction for the uplink in the TDD-TDD case in [13]. Further work may be required here to find a reason for the discrepancy, however, this work is considered beyond the scope of this study item. The results presented here indicate that the typical second-channel ACLR for the 7.68Mcps signal (47dB) will result in a small (~1%) capacity reduction.

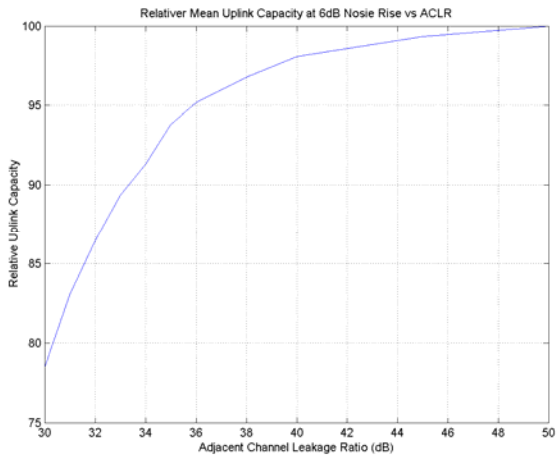

Figure 190 – Relative Uplink Capacity vs UE ACLR

6.1.1.4.3 Downlink Capacity Reduction

For the downlink, it is proposed in section 4.2.1 of this TR that the basestation ACLR figures for a 7.68Mcps basestation should not exceed those of a 3.84Mcps basestation. With this point accepted, it is clear that there is no additional interference caused by the transmission signal from a 7.68Mcps basestation over the interference from a 3.84Mcps basestation. It is therefore proposed only to study the impact of the UE ACS.

In section 6.1.1.2 of this TR, it was shown that there are no implementation issues associated with the filtering in 7.68Mcps UEs and the filtering is sufficient to provide the necessary ACS to operate with either 3.84Mcps or 7.68Mcps downlink transmissions in the adjacent channel. Therefore it is reasonable to assume that a 7.68Mcps UE is able to co-exist with both 7.68Mcps and 3.84Mcps adjacent systems with similar capacity losses as the commonly studied 3.84Mcps – 3.84Mcps case.

However, the adjacent channel selectivity is not only limited by the linear filtering capability of the UE, but is also influenced by the non-linear behaviour in the receiver. This is especially relevant at high levels of adjacent channel power. Simulations of the adjacent channel power present in the UE based on the simulation assumptions outlined in section 6.1.1.4.1 with worst-case geographical offset have been carried out and the cumulative distribution has been plotted in figure 191. This plot shows that for the Macro-Macro case there is a small probability (<2%) that the signal power will exceed -40dBm (note higher signals may be expected in microcell case). For these relatively high levels of adjacent channel powers, there is a danger that the ACS of the UE will become limited by the linearity of the receiver. This is especially important for 7.68Mcps adjacent channels as the wider modulation bandwidth means that the distortion levels in the second adjacent channel are higher than in the case of a 3.84Mcps signal.

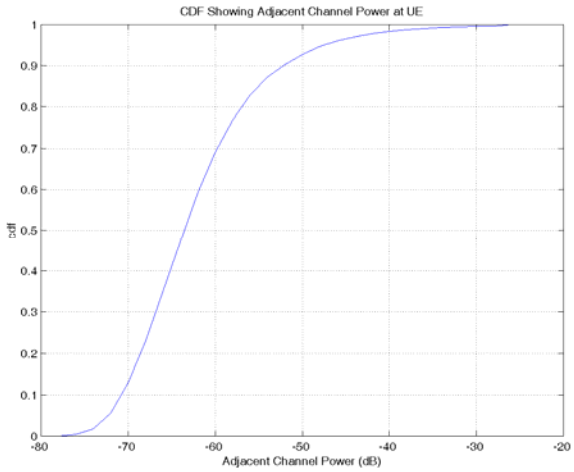

Figure 191 - CDF showing adjacent channel power at UE

The degradation of the second adjacent channel of a 7.68Mcps signal relative to the 3.84Mcps second adjacent channel is a strong function of the UE implementation. However, by using the relative 1st and 2nd ACLR figures from section

6.1.1.3 as a guide, it can be expected that provided the UE can maintain at least 33dB ACS for the first adjacent channel (for adjacent channels of both chip rates), then it is reasonable to assume that the second adjacent channel ACS will be close to 10dB better.

Simulations of the degradation in downlink capacity have been carried out according to the guidelines in [13] and a graph showing the capacity reduction is shown in figure 192. It can be seen, that for the assumed levels of 2nd adjacent channel ACS, the capacity loss is acceptably low (<1%).

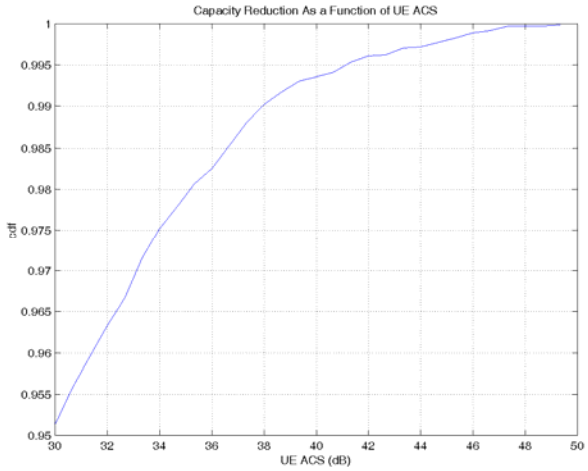

Figure 192 – Capacity Reduction as a function of UE ACS

6.1.1.4.4 Summary

It has been shown that the selectivity of an elementary RRC filter implementation in the UE is more than sufficient to permit 7.68Mcps systems to operate along side 3.84Mcps systems. This means that the coexistence of these systems in the downlink will be very similar to the 3.84Mcps to 3.84Mcps coexistence studies already documented in [13].

Analysis of the transmitted signal has shown that 7.68Mcps signal transmitted from the UE will not cause any additional inter-system interference into a 3.84Mcps system in the first adjacent channel over the interference caused by an adjacent 3.48Mcps system. However the 7.68Mcps will introduce a higher level of interference into the second adjacent channel.

To quantify the effect of this additional interference, uplink system simulations have been carried out that have determined the impact of UE ACLR on system capacity. These results have shown that the level of second adjacent channel power from a 7.68Mcps system will have minimal effect on the victim 3.84Mcps system.

The overall conclusion is that 7.68Mcps systems complying with the characteristics set out in section 4.2 can co-exist with 3.84Mcps with out any issues. Further more, simulations of the UE characteristics based closely on practical measurements confirm that it is feasible to implement 7.68Mcps UEs that can comply with these characteristics.

6.1.1.5 TDD/TDD Macro Coexistence (1.28Mcps TDD)

The capacity reduction of a lower chip rate TDD (1.28 Mcps) system that coexists with a higher chip rate TDD (7.68 Mcps) system is assessed for the uplink and downlink in a single timeslot. The system configuration defined in Section 6.1.1.4.1 and the assumptions laid out in TR25.945 [15] are used, where an 8 kbps speech service is assumed for both systems.

6.1.1.5.1 Uplink Capacity Reduction

The downlink capacity is defined as the average number of UEs per cell that will cause 95% of the UEs in the central cell to have an uplink C/I above a predefined threshold. Monte-Carlo simulations are performed to determine the uplink capacity for isolated 1.28 Mcps and 7.68 Mcps systems, which will act as the reference uplink capacities for each respective system.

The addition of a 7.68 Mcps system to a 1.28 Mcps system will introduce inter-system interference to the 1.28 Mcps system. As a result of this, less intra-system interference (inter-cell interference of the 1.28 Mcps system) can be tolerated by the UEs in the 1.28 Mcps system in order to maintain the uplink C/I threshold. This will reduce the downlink capacity of the 1.28 Mcps system. The base stations of the 7.68 Mcps system are located at the cell edges of the 1.28 Mcps system, where the 7.68 Mcps system is operating at the reference uplink capacity. This setup will cause the highest inter-system interference to the 1.28 Mcps system and will act as the worst case scenario. The uplink capacity (percentage of the reference uplink capacity) as a function of the UE ACLR for the 1.28 Mcps system coexisting with a 7.68 Mcps system is shown in Figure 193. Note that in this graph the UE ACLR represents the level of adjacent channel power falling in a 1.28MHz band adjacent to a 7.68Mcps transmitted signal.

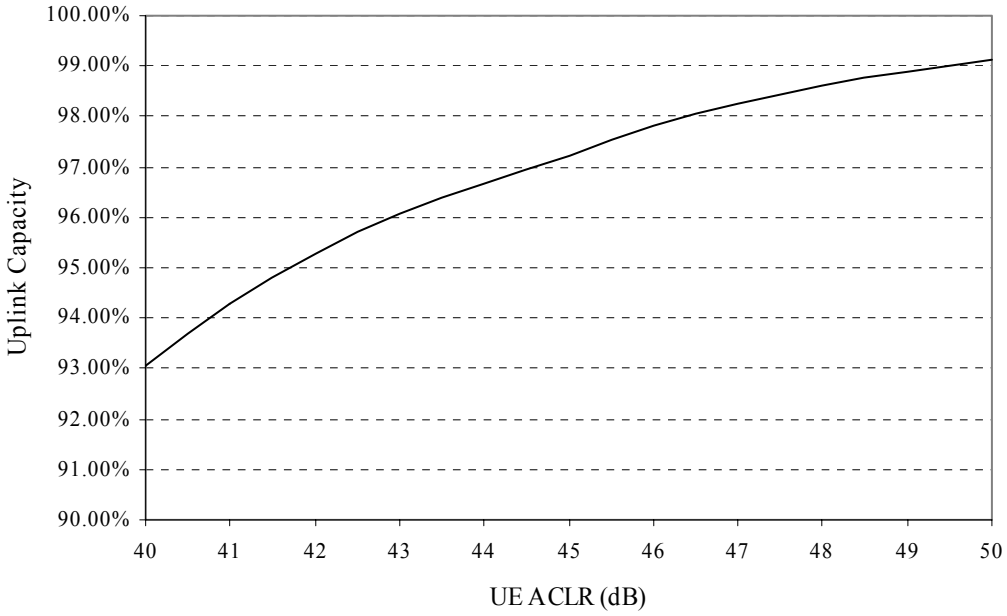

Figure 193 – Relative Uplink Capacity for a 1.28 Mcps TDD system vs. UE ACLR

In order to assess the typical ALCR from a 7.68Mcps transmission into adjacent 1.28MHz channels the same method as described in Section 6.1.1.3 is employed. The ACLR of six adjacent 1.28 MHz channels for the 7.68 Mcps systems are presented in Table 87.

Table 87 – Adjacent Channel Leakage Ratio for six adjacent channels with a 1.28 MHz bandwidth

Chip Rate	UE ACLR (dB)					
	1st	2nd	3rd	4th	5th	6th
7.68 Mcps	41.58	43.40	45.40	48.05	52.21	55.94

For a given UE transmit power the first 1.28 MHz adjacent channel leakage power for the 1.28 Mcps system, as described in TS 25.102, is 33 dB which is lower than that of the 7.68 Mcps system as shown in Table 87. Hence the 2nd ACLR is considered. The 2nd ACLR figure for the 1.28 Mcps as specified in TS 25.102 is 43 dB, which is in line with the 2nd ACLR (1.28 MHz bandwidth) figure for the 7.68 Mcps as shown in Table 87. It is therefore feasible to manufacture UEs for the 7.68 Mcps system that are able to meet the 1st and 2nd ACLR figures defined for 1.28 Mcps system. The results in Figure 193 show that the capacity reduction for the 2nd UE ACLR of 43.4 dB is small (about 4% of the reference uplink capacity).

6.1.1.5.2 Downlink Capacity Reduction

The downlink capacity is defined as the average number of UEs per cell that will cause 95% of the UEs in the central cell to have a downlink C/I above a predefined threshold. Monte-Carlo simulations are performed to determine the downlink capacities for isolated 1.28 Mcps and 7.68 Mcps TDD systems, which will act as the reference downlink capacities for each respective system.

The addition of a 7.68 Mcps system to a 1.28 Mcps system will introduce inter-system interference to the 1.28 Mcps system. As a result of this, less intra-system interference (inter-cell interference of the 1.28 Mcps system) can be tolerated by the UEs in the 1.28 Mcps system in order to maintain the downlik C/I threshold. This will reduce the downlink capacity of the 1.28 Mcps system. The base stations of the 7.68 Mcps system are located at the cell edges of the 1.28 Mcps system, where the 7.68 Mcps system is operating at reference downlink capacity. This setup will cause the highest inter-system interference to the 1.28 Mcps system and will act as the worst case scenario. The downlink capacity (percentage of the reference downlink capacity) as a function of the UE ACS for the 1.28 Mcps system coexisting with a 7.68 Mcps system is shown in Figure 194.

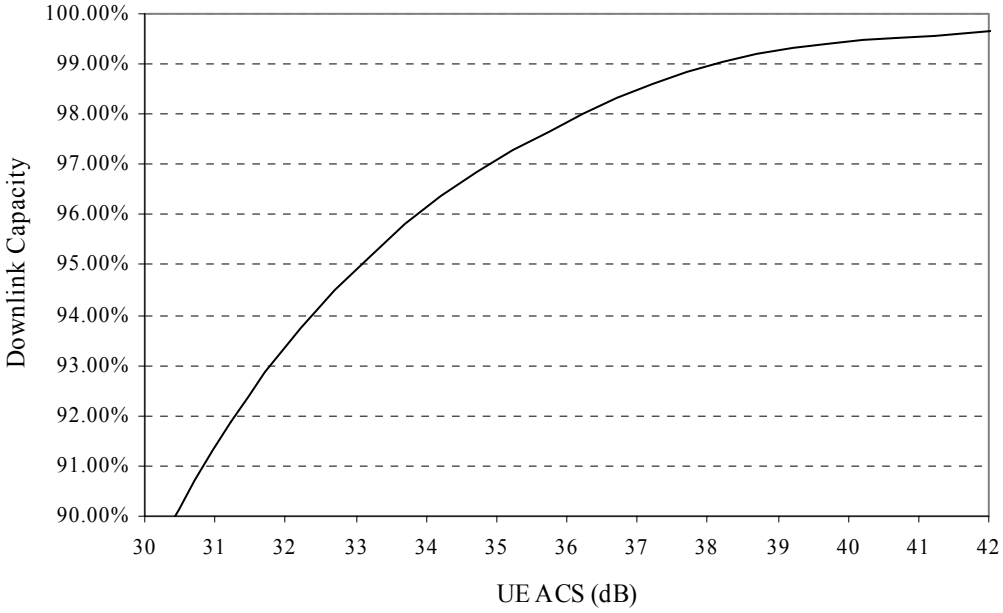

Figure 194 – Relative Downlink Capacity for 1.28 Mcps system vs. UE ACS

The UE ACS has two main contributing factors; selectivity in the UE which dominates at medium adjacent channel power levels and receiver front-end compression which dominates at higher adjacent power levels.

In the case of the 1.28 Mcps UE receiver, the selectivity part of the filter is assumed to be designed for an adjacent 1.28 Mcps carrier, in which case the task of rejecting a 7.68 Mcps adjacent channel signal is less demanding as less energy is immediately adjacent to the wanted signal. The results in Figure 194 show that the capacity loss for the existing 1.28 Mcps ACS of 33 dB is sufficient for the 1.28 Mcps TDD system to show minimal capacity loss (less than 5%).

In the case of the front-end induced distortion, the limiting case occurs when a 7.68 Mcps signal is adjacent to a wanted 1.28 Mcps signal. A proportion of the distortion created by the compression in the receiver front end will fall in band to the wanted signal. However as the figures in Table 87 show, the proportion of the distortion that falls in band is actually lower for the 7.68Mcps adjacent channel than it is for the equivalent 1.28Mcps adjacent channel case. Therefore a UE designed to operate with a 1.28 Mcps adjacent channel will also operate with a 7.68 Mcps adjacent channel.

6.1.1.5.3 Summary

It has been shown that the co-existence of 7.68 Mcps systems in spectrum immediately adjacent to 1.28 Mcps systems is possible, even in the worst case scenario, with minimum effect on the victim 1.28 Mcps system. No specification changes to the 1.28Mcps TDD system RF performance are required. The overall conclusion is that it is possible for 7.68Mcps TDD systems complying with the characteristics set out in Section 4.2 to co-exist with 1.28Mcps TDD without any issues.

6.1.2 TDD/FDD Coexistence

6.1.2.1 TDD / FDD Downlink

Current spectrum allocations have placed TDD spectrum well away from the FDD downlink spectrum, with large separations between the systems there are no modulation bandwidth specific co-existence issues foreseen. Hence it is reasonable to assume that co-existence between a 7.68Mcps system and a 3.84Mcps is identical and as such any further study is beyond the scope of this TR.

6.1.2.2 TDD Downlink / FDD Uplink

Current spectrum allocations allow for TDD systems to be placed in frequency bands adjacent to FDD uplink. In the case of TDD downlink transmissions interfering with FDD uplink receivers, a deterministic analysis of transmitter power, minimum coupling loss (which is a function of the co-existence scenario, eg co-siting or same geographic area) and receiver sensitivity leads to the values of Tx ACLR and Rx ACS that are required. Current specifications for the TDD transmitter [8] along with site-engineering solutions described in [13] are considered sufficient to offer the necessary protection between TDD and FDD. It is therefore proposed that the ACLR requirements set out in [8] for 3.84Mcps TDD should also apply to 7.68Mcps TDD.

6.1.2.3 TDD Uplink / FDD Uplink

For the FDD uplink, the reference system capacity without interference is first determined by the mean number of UEs in the system that results in a noise rise (interference level) of 6dB in the central cell. The source of this interference in the uplink is made up of both intracell and intercell interference. Several thousand Monte-Carlo snap-shots were run in order to obtain the statistical significance. Simulations assumptions were as set out in [13] for similar capacity analyses.

Once the reference (interference free) capacity had been determined, interference from the neighbouring TDD system was introduced. A spectrum arrangement consistent with the current IMT2000 allocations for FDD and TDD are assumed and that FDD uplink is immediately adjacent to TDD downlink. Note, in general terms, the TDD system may operate with fewer simultaneous uplink users but the level of interference generated by each cell that is visible to an external system can be quite high as a consequence of joint detection which removes intra-cell interference in the TDD system. The FDD system is assumed to be protected by the ACLR of the TDD system and a range of ACLR figures from 25 dB to 50dB have been evaluated. In addition to the ACLR, the uplink of the TDD system is assumed to be active for 7 out of the 15 timeslots which gives a further effective reduction in the total TDD interference of 3.3dB.

The capacity loss for the FDD system is then evaluated by comparing the number of users obtained for the 6dB noise rise for a given ACLR figure with the capacity of the reference case. The relative capacity obtained for a range of ACLR figures are plotted in figure 195.

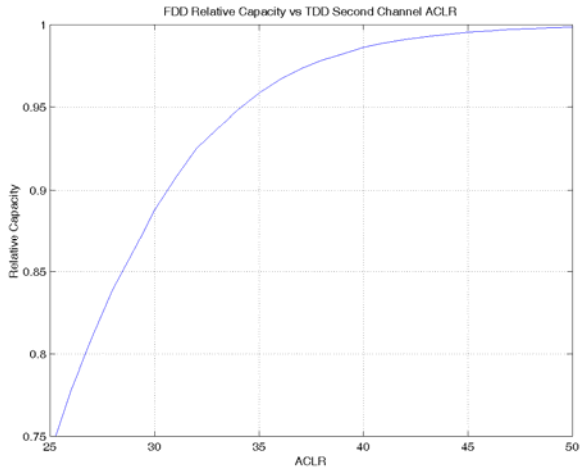

Figure 195 - FDD Uplink Relative Capacity vs TDD Adjacent Channel Leakage Ratio

The results show that the capacity reduction predicted is slightly higher than the FDD-FDD results in [13]. This is consistent with the use of joint detection in the TDD system creating higher interference levels into a co-existing system. However, the results presented here indicate that for the specified second-channel ACLR for the 7.68Mcps

signal (43dB/5MHz) will result in an acceptably small (<1%) capacity reduction. The relative difference between the capacity losses for the ACLR numbers for 3.84Mcps 2nd adjacent channel and 7.68Mcps 2nd adjacent channel given in section 6.1.1.3 is <0.25%.

6.1.2.4 Summary

Given the current spectrum allocations, co-existence between TDD and FDD downlink is not considered to present any modulation bandwidth specific issues, hence TDD/FDD co-existence results will apply both to 3.84Mcps and 7.68Mcps TDD.

The co-existence between TDD downlink and FDD uplink where these bands are in adjacent allocations can be handled with a combination of the current specifications for 3.84Mcps transmitters [8] and site engineering solutions [13].

For TDD uplink to FDD uplink, a statistical analysis has been carried out to assess the impact of the increased second adjacent channel power from a 7.68Mcps UE compared to a 3.84Mcps UE. It has been shown that the loss in FDD capacity due to a 7.68Mcps UE operating to the performance outlined in section 4.2.1 of this TR is less than 1%. Further more, comparing the capacity loss due to the second adjacent channel between realistic 3.84Mcps and 7.68Mcsp UEs, it was shown that the 7.68Mcps causes less than 0.25% additional capacity loss.

6.2 Use in diverse spectrum arrangements and allocations

A 7.68Mcps deployment requires a contiguous spectral allocation of 10MHz compared to the 5MHz spectral allocation required at 3.84Mcps. Spectrum for 7.68Mcps TDD may be allocated adjacent to spectrum for 3.84Mcps TDD.

A 7.68Mcps TDD system may be deployed either in geographies where at least 10MHz of contiguous TDD spectrum has been allocated to an operator or in future spectral allocations provided that contiguous 10MHz chunks of spectrum are allocated.

6.3 Mobility

6.3.1 Mobility Scenarios

A single mode higher chip rate UE can select, reselect or be handed over to another higher chip rate TDD cell.

A dual-mode (or multi-mode) higher chip rate UE can select, reselect or be handed over to another higher chip rate TDD cell or may be handed over to another mode (such as 3.84Mcps TDD, FDD or GSM). Furthermore, a dual-mode / multi-mode higher chip rate TDD UE that is being serviced by another mode (such as 3.84Mcps TDD, FDD or GSM) may reselect or be handed over to a higher chip rate TDD cell.

6.3.2 General

The decision (e.g. handover algorithms) and execution (e.g. handover signalling) phases of mobility procedures for higher chip rate TDD will be very similar to those for 3.84Mcps TDD and thus do not affect feasibility. The following subsections thus consider the issue of performing measurements for mobility procedures.

6.3.3 Intra higher chip rate TDD mobility

A single mode higher chip rate UE shall perform intra-frequency and inter-frequency measurements on other higher chip rate TDD cells in the same way as performed by a Release-5 3.84Mcps TDD UE. The time required to perform a measurement at the higher chip rate will be the same as at 3.84Mcps (noting that the timeslot structure of the higher chip rate TDD system is the same as that of 3.84Mcps TDD, the higher chip rate TDD UE will have to perform its internal operations, including measurements, within the same time constraints as a 3.84Mcps TDD UE).

6.3.4 Inter-frequency mobility to higher chip rate TDD

There are times (which can be controlled by the network for instance using compressed mode in FDD or by the network not allocating resource in TDD) at which Release 5 UEs can perform inter-frequency measurements on other frequencies. The list of inter-frequency measurements can be extended to include higher chip rate TDD frequencies. A UE capable of camping onto a higher chip rate cell will be capable of performing measurements on the higher chip rate

cell. A UE that is not capable of camping onto the higher chip rate cell need not perform measurements on higher chip rate TDD cells (such a UE will never perform a cell reselection to a higher chip rate TDD cell and UTRAN will never signal a handover to a higher chip rate TDD cell since UTRAN knows the capabilities of such a UE).

A Release 5 dual-mode 3.84 Mcps TDD / FDD UE may be signalled to measure up to 32 neighbour cells in the inter-frequency list. The UE must have the capability to make measurements on two other 3.84Mcps TDD frequencies and three FDD frequencies. If a higher chip rate TDD system is included, a dual-mode / multi-mode UE will still be required to measure up to 32 neighbour cells in the inter-frequency list. The multi-mode UE must have the capability to make measurements on two other 3.84Mcps TDD frequencies, three FDD frequencies and three higher chip rate TDD frequencies. Note that when more carrier frequencies are deployed by an operator, extra frequencies will have to be measured in the inter-frequency cell info list regardless of the UTRA mode applied to those frequencies (thus the requirement to measure additional frequencies is due to the allocation of more carrier frequencies and not due to an additional UTRA mode).

The time required to retune UE synthesizers to a different frequency will be significantly greater than the time required for front-end filters to be switched from a 3.84Mcps bandwidth to a higher chip rate bandwidth (i.e. the change of frequency has a greater impact on the front-end than the change of UTRA mode). It is thus likely that there will be an insignificant incremental time penalty incurred in making inter-frequency measurements at different chip rates compared to making inter-frequency measurements at the same chip rate.

6.3.5 Inter-RAT mobility to higher chip rate TDD

The issues surrounding mobility from RATs other than UTRA are the same as those surrounding inter-frequency mobility. A UE camped onto a non-UTRA RAT will make inter-RAT measurements according to an inter-RAT list that is signalled to the UE (e.g. in system information). The UE will only make inter-RAT measurements on the higher chip rate cell if it is capable operating at the higher TDD chip rate. The size of the inter-RAT measurement list will be the same as for Release 5, but the inter-RAT measurement list will include additional higher chip rate TDD frequencies that require measurement.

The higher chip rate TDD frame and timeslot structure is identical to that of 3.84Mcps TDD, thus inter-RAT issues relating to frame and timeslot structure for higher chip rate TDD are identical to those for 3.84Mcps TDD.

In many cases, a multi-RAT capable UE will have separate front-ends for each RAT. There is no fundamental reason why the time to make a measurement on a higher chip TDD cell should be different to the time required to make an FDD or 3.84Mcps TDD measurement.

6.3.6 Inter-frequency mobility from higher chip rate TDD

The issues regarding inter-frequency mobility from higher chip rate TDD are similar to the issues relating to mobility to higher chip rate TDD :

- a higher chip rate TDD UE will only make measurements on frequencies and on UTRA modes that it is capable of.
- the inter-frequency cell info list shall be the same size as for Release 5, but may include additional higher chip rate TDD frequencies to be measured (see section 6.3.4).
- the time to retune UE synthesizers to a different frequency is likely to be greater than the time required to switch higher chip rate TDD filters to another chip rate.

6.3.7 Inter-RAT mobility from higher chip rate TDD

The issues regarding inter-RAT mobility from higher chip rate TDD are similar to the issues relating to mobility to higher chip rate TDD.

6.4 Application to 3GPP system and services

A higher TDD chip rate can efficiently support voice, packet and broadcast services.

The main benefit of a higher TDD chip rate is for packet data services, where users will perceive higher packet call rates and reduced latencies compared to 3.84Mcps TDD. A higher TDD chip rate also allows for the support of higher peak rate data services.

6.5 Backward Compatibility

6.5.1 Operation of higher chip rate UEs in 3.84Mcps TDD infrastructure

It is clear that a UE that can only operate at the higher chip rate will not get service from a 3.84Mcps UTRAN. This situation is analogous to the case where DCS1800 only UEs do not get service from a GSM900 network.

Due to the similarity in the coding of the SCH, a dual mode (higher chip rate / 3.84Mcps TDD) UE is able to identify the chip rate and code group for a cell no matter whether the cell operates at 3.84Mcps or the higher chip rate. If, from the modulation of the SCH, the dual mode UE identifies that the cell operates at 3.84Mcps, it can reconfigure itself to operate at 3.84Mcps.

6.5.2 Operation in multiple frequency bands

In the case that higher chip rate TDD is implemented solely in one frequency band and 3.84Mcps TDD is implemented solely in another frequency band, there are no backwards compatibility issues : 3.84Mcps UEs are serviced in one band, higher chip rate UEs in the other band, dual mode UEs may be serviced in either band.

6.5.3 Operation of 3.84Mcps TDD UEs when higher chip rate UTRAN is deployed

When 3.84Mcps TDD carriers and higher chip rate TDD carriers are both deployed in the same band, 3.84Mcps UEs will not attempt to camp on to higher chip rate carriers since they :

1) are unlikely to correctly decode the code group for the higher chip rate cell

2) will be unable to correctly read system information and will thus reject the higher chip rate cell

These 3.84Mcps TDD UEs will then be able to camp on 3.84Mcps carriers in the same band.

6.5.4 Servicing of 3.84Mcps TDD UEs under higher chip rate UTRAN

Both 3.84Mcps TDD UEs and higher chip rate UEs can be serviced by a higher chip rate UTRAN when the higher chip rate UTRAN is dual mode. An example timeslot arrangement for dual mode higher chip rate UTRAN is given in Figure 196. In this arrangement, two separate chip rates can be accommodated in the same frame; the two chip rates may operate independently of one another. Each chip rate carries its own SCH and beacon function. 3.84Mcps TDD UEs will camp on the cell according to the 3.84Mcps TDD SCH and beacon. Higher chip rate UEs will camp on to the cell according to the higher chip rate TDD SCH and beacon. Dual mode UEs may be “handed over” between the timeslots within the frame. Additional higher layer modifications would be needed to support this configuration.

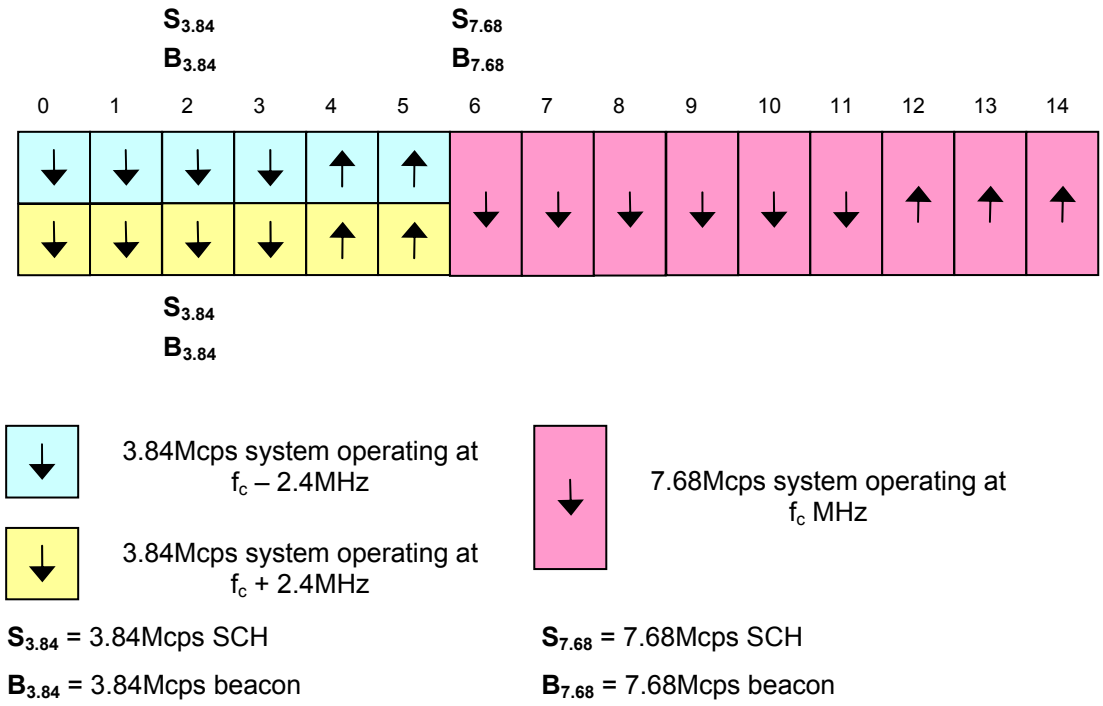

Figure 196 – frame structure allowing 3.84Mcps TDD and higher chip rate UEs to be serviced by a dual mode higher chip rate UTRAN

6.5.4 Operation of higher chip rate as an auxiliary downlink

Both 3.84Mcps TDD UEs and higher chip rate TDD UEs may be serviced when the higher chip rate TDD is used as an auxiliary downlink carrier. This operation is shown in Figure 197. 3.84Mcps TDD UEs are serviced by the 3.84Mcps carrier. Higher chip rate UEs can be serviced by the 3.84Mcps carrier (e.g. for uplink) and by the 7.68Mcps carrier (e.g. for downlink). The higher chip rate UE operates in a half-duplex mode.

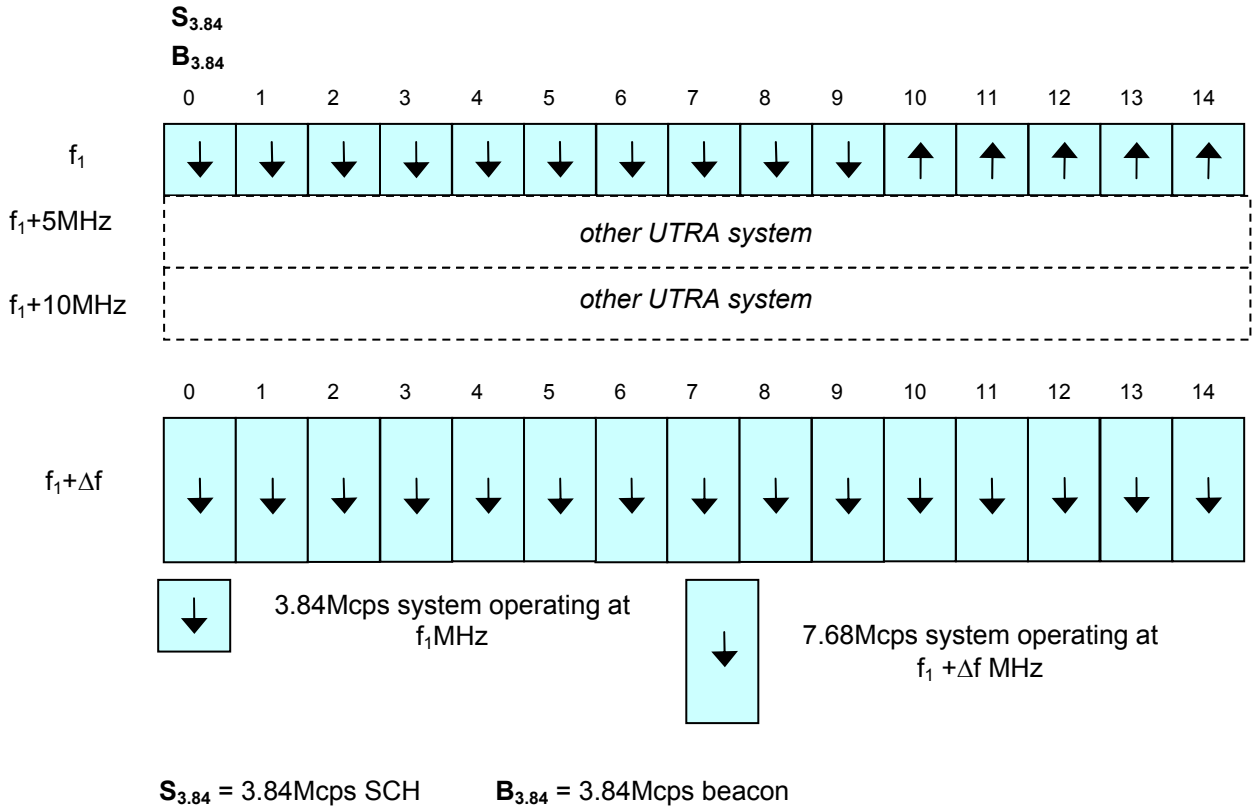

Figure 197 - Example operation of higher chip rate TDD as an auxiliary downlink

6.6 Impact on other working groups

Other than RAN1, the following working groups would be impacted by the introduction of a higher chip rate for TDD: RAN2, RAN3, RAN4 and T1. In this section, a summary of the impacts on each working group is provided. More details of the impact on other working groups may be derived from section 6.7.

Introduction of the higher chip rate for TDD would have the following impacts on 3GPP working groups:

RAN2

- requirement for editorial modifications to RAN2 specs indicating that sections applicable to 3.84Mcps TDD are also applicable to a higher TDD chip rate.
- modification of signalling to support a higher TDD chip rate (e.g. signalling of capability information, modification of HS-SCCH / HS-SICH signalling to accommodate a larger code space and greater maximum transport block size, modification of timing advance signalling to account for greater number of chips per unit time).
- definition of UE capability information for higher chip rate TDD.

RAN3

- requirement for editorial modifications to RAN3 specs indicating that sections applicable to 3.84Mcps TDD are also applicable to a higher TDD chip rate.
- modification of signalling to support a higher TDD chip rate (as per RAN2 impacts).

RAN4

- definition of UE and Node B transmitter and receiver characteristics (spectral masks, blocking characteristics, ACLR figures etc.).
- definition of performance requirements
- definition of Node B conformance tests
- update frequency bands to account for higher chip rate TDD

T1

- definition of UE conformance tests
- reference RABs and reference system configuration
- editorial alignments of higher chip rate TDD with 3.84Mcps TDD

6.7 Impact on Specifications

This section considers the changes that would be required to the 3GPP specifications in order to support the higher chip rate reference configuration.

The higher chip rate reference configuration has been chosen to have a minimal difference to 3.84Mcps TDD. The impact on some specifications is thus mainly editorial (e.g. changing text that reads "3.84Mcps TDD" to "3.84 / 7.68Mcps TDD").

The impacts on 3GPP core specifications are summarised in Table 88.

Table 88 – Impact on specifications

spec	title	impact	WG
25.201	Physical layer - general description	Text stating that there are 3 TDD options.	RAN1
25.221	Physical channels and mapping of transport channels onto physical channels (TDD)	• support of SF32 in uplink and downlink • definition of burst types for higher chip rate based on SF32 • transmission of TFCI / TPC at SF32 • construction of midambles • association between midambleand channelisation codes • definition of number of HS-SCCH associated with a UE	RAN1
25.222	Multiplexing and channel coding (TDD)	• coding of HS-SCCH to support signalling of greater range of codes and transport block size	RAN1
25.223	Spreading and modulation (TDD)	• definition of chip rate • channelisation code multipliers for SF32 • definition of scrambling codes • weight factor for SF32 • definition of synchronization codes	RAN1
25.224	Physical layer procedures (TDD)	• definition of number of timing advance bits • update to cell search procedure	RAN1
25.225	Physical layer; Measurements (TDD)	• update time difference measurement definitions (measurements should cover the same range in time at the higher chip rate).	RAN1
25.301	Radio Interface Protocol Architecture	• editorial modifications (that which is applicable to 3.84Mcps TDD is also applicable to higher chip rate TDD)	RAN2
25.302	Services provided by the physical layer	• 3.84Mcps TDD physical channel combinations are also applicable for higher chip rate TDD	RAN2

		• other editorial modifications (that which is applicable to 3.84Mcps TDD is also applicable to higher chip rate TDD)	
25.305	User Equipment (UE) positioning in Universal Terrestrial Radio Access Network (UTRAN); Stage 2	• editorial modifications (that which is applicable to 3.84Mcps TDD is also applicable to higher chip rate TDD)	RAN2
25.306	Radio Access capabilities definition	• extension of definition of physical channel parameters in DL / UL to higher chip rate TDD • capability flag to indicate support for higher chip rate TDD • definition of HSDPA UE categories and capabilities at the higher chip rate • other editorial modifications aligning higher chip rate TDD with 3.84Mcps TDD	RAN2
25.321	Medium Access Control (MAC) protocol specification	• HSDPA transport block size signalling to allow for higher capability UEs at the higher chip rate • control of RACH transmissions at the higher chip rate to align with 3.84Mcps • UL TFC selection at higher chip rate is aligned with 3.84Mcps.	RAN2
25.322	Radio Link Control (RLC) protocol specification	no impact	RAN2
25.323	Packet Data Convergence Protocol (PDCP) specification	no impact	RAN2
25.324	Broadcast/Multicast Control (BMC)	no impact	RAN2
25.331	Radio Resource Control (RRC) protocol specification	• RRC procedures and signalling for higher chip rate TDD to be aligned with 3.84Mcps TDD. The following specific areas require alignment: - power control procedures - RACH and access service class - timing advance procedures - use of SIB14 (uplink outer loop power control) • capability signalling extended to include higher chip rate • measurement capabilities extended to cover higher chip rate	RAN2
25.401	UTRAN overall description	• addition of higher chip rate TDD to UTRAN architecture • power control aligns with 3.84Mcps TDD • timing advance aligns with 3.84Mcps TDD	RAN3
25.413	UTRAN Iu interface RANAP signalling	no impact	RAN3
25.423	Iur interface Radio Network Subsystem Application Part (RNSAP) signalling	• power control aligns with 3.84Mcps TDD • timing advance aligns with 3.84Mcps TDD	RAN3
25.425	UTRAN Iur interface user plane protocols for CCH data streams	• Rx timing deviation (RACH) to be defined for higher chip rate TDD : should equal the timing deviation for 3.84Mcps TDD in terms of time.	RAN3
25.427	UTRAN Iur and Iub interface user plane protocols for DCH data streams	• Rx timing deviation measurement applied to higher chip rate TDD • timing advance procedure aligned with 3.84Mcps TDD • power control procedure aligned with 3.84Mcps TDD	RAN3
25.433	UTRAN Iub interface NBAP signalling	• editorial additions aligning higher chip rate TDD with 3.84Mcps TDD • extend channelisation code IE sizes to allow up to 32 channelisation codes to be signalled (e.g. allow channelisation codes up to 32 to be signalled in HS-	RAN3

		SCCH pool / set)	
25.435	UTRAN Iub interface user plane protocols for CCH data streams	• Rx timing deviation measurement applied to higher chip rate TDD • timing advance procedure aligned with 3.84Mcps TDD • power control procedure aligned with 3.84Mcps TDD	RAN3
25.102	User Equipment (UE) radio transmission and reception (TDD)	• transmitter characteristics (these are based on 3.84Mcps TDD characteristics: specifically, spectral masks and ACLR figures need to be amended for a higher chip rate) • receiver characteristics (these are based on 3.84Mcps TDD with adjacent channel selectivity, blocking characteristics and intermodulation characteristics amended for the higher chip rate) • performance requirements	RAN4
25.105	UTRA (BS) TDD: Radio transmission and reception	• update frequency bands where higher chip rate TDD may be applied • add channel spacing for higher chip rate TDD • transmitter characteristics (these are based on 3.84Mcps TDD characteristics: specifically, spectral masks and ACLR figures need to be amended for a higher chip rate) • receiver characteristics (these are based on 3.84Mcps TDD with adjacent channel selectivity, blocking characteristics and intermodulation characteristics amended for the higher chip rate) • performance requirements	RAN4
25.123	Requirements for support of radio resource management (TDD)	• requirements for measurements, timing advance, handover timing etc. for higher chip rate to be derived from 3.84Mcps TDD • measurement timing advance performance etc.	RAN4
25.133	Requirements for support of radio resource management (FDD)	• performance requirements for measurements of higher chip rate TDD cells • test definition for measurement of higher chip rate TDD cells	RAN4
25.142	Base Station (BS) conformance testing (TDD)	• addition of conformance tests for higher chip rate TDD. These should be derived from the existing 3.84Mcps TDD conformance tests.	RAN4
34.108	Common test environments for User Equipment (UE) conformance testing	• definition of supported channels and test frequencies for higher chip rate TDD • reference system configuration (based on 3.84Mcps TDD) • reference RABs (based on 3.84Mcps TDD)	T1
34.122	Terminal Conformance Specification; Radio Transmission and Reception (TDD)	• addition of conformance tests for higher chip rate TDD. These should be derived from the existing 3.84Mcps TDD conformance tests.	T1
34.123	User Equipment (UE) conformance specification; Part 1: Protocol conformance specification	• addition of conformance tests for higher chip rate TDD specific protocol aspects	T1
34.124	Electromagnetic compatibility (EMC) requirements for Mobile terminals and ancillary equipment	• editorial alignment of higher chip rate TDD with 3.84Mcps TDD • definition of narrow band response of receivers	RAN4

6.8 Signalling Impact

Signalling impacts of introducing a higher TDD chip rate are minimized when there is similarity between the higher TDD chip rate and 3.84Mcps TDD as per the approach taken in the higher chip rate TDD reference configuration. No requirements for new messages have been identified, however IEs of some existing messages may need to be extended to cover the higher chip rate. The main signalling impacts of a higher TDD chip rate identified in this study are:

- RRC signalling must be able to indicate UE capability for the higher TDD chip rate.
- RRC timing advance signalling for higher chip rate TDD needs to be modified compared to 3.84Mcps to cover a larger range in terms of number of chips (the same range in terms of time). The range of SFN-SFN observed time difference measurements may need to be similarly increased.
- RRC neighbour cell / measurement signalling needs to be modified to account for the potential need to make higher chip rate TDD measurements.
- RRC signalling needs to be modified to account for 32 channelisation codes in the downlink (e.g. PICH Info, PRACH channelisation code list IEs need to be extended to allow 32 channelisation codes).
- MAC-hs signalling on HS-SCCH and HS-SICH needs to be modified to allow for larger transport block sizes for maximum capability UEs.
- NBAP and RNSAP signalling needs to be aligned with above RRC signalling modifications.

6.9 Antenna Systems

Transmit diversity schemes that are applicable at 3.84Mcps are also applicable at a higher TDD chip rate.

6.10 Higher chip rates than 7.68Mcps

The following gains can be expected from a chip rate higher than 7.68Mcps (e.g. 15.36Mcps) :

- a superior ability to resolve multipath components would lead to further link level gains in some channel types.
- higher packet call rates and reduced packet delay due to a lower blocking probability at the higher chip rate.
- cell throughput gains due to superior link level performance and the larger pool of UEs that may be scheduled.

These gains will be achieved at the expense of increased UE complexity. The complexity of the UE joint detector does not scale linearly with chip rate (when the spreading factor is increased with the chip rate), thus the complexity of a 15.36Mcps (or even higher chip rate) TDD UE will be significantly greater than that of a 7.68Mcps UE.

Adaptation of the reference configuration directly to a chip rate higher than 7.68Mcps is considered to lead to a prohibitive rise in UE complexity at the current time. The approach adopted in the reference configuration (of increasing the spreading factor as the chip rate is increased) is scalable and allows higher chip rates to be adopted as chip manufacturing technology and / or processor technology improves.

7 Recommendations and Conclusions

In the study “Analysis of higher chip rates for UTRA TDD Evolution”, use of higher chip rates for TDD have been studied. The chip rate of 7.68Mcps has been studied in detail. The study considered a reference configuration at 7.68Mcps showing minimal changes from the 3.84Mcps UTRA TDD specifications. The following aspects of this system were considered:

- system and link level performance

- complexity
- link budget, coexistence and backwards compatibility
- mobility
- impact on working groups, specifications and signalling
- aspects related to 3GPP systems and services, antenna systems and higher chip rates than 7.68Mcps

Some specific aspects of antenna systems were not studied.

Simulation results presented in RAN1 have shown a significant performance improvement of the order of 30-40% for packet services when a chip rate of 7.68Mcps is adopted. The packet call rate increases by approximately 30-40% and packet delay decreases by approximately 30-40% at the higher chip rate. Alternatively, approximately 30-40% more users can be supported at the same packet call rate. These gains are witnessed over a range of channel models and for different traffic types (HTTP and FTP traffic types were studied, TCP was modelled). These gains are due to statistical multiplexing gains at 7.68Mcps (reduced blocking probability), the ability of the packet scheduler to allocate more resource to UEs at the higher chip rate and due to link level gains.

Simulation results for 12.2kbps DCH channels carrying voice traffic show an increase in capacity of the order of 10-15% across a range of channel types. The increased capacity at the higher chip rate is due to trunking efficiency gains (according to the Erlang-B model) and due to link level gains at the higher chip rate.

The gains stated above are the gains for a 7.68Mcps system over two independent 3.84Mcps system occupying the same bandwidth. Other methods of using the 10MHz bandwidth may be feasible, but are out of the scope of this study and have not been studied.

Link results have shown link level performance gains of 0-2dB at 7.68Mcps. These link level gains are particularly evident in channel PA3 and for high coding rates and modulations in other dispersive channels. The link level gains are due to the superior ability of the higher chip rate to resolve multipath components. These link level gains lead to cell throughput gains of the order of 5-10% for packet services in dispersive channels.

The complexity of a 7.68Mcps UE is approximately 33% greater than that of a 3.84Mcps UE for the same UE capability. Dual mode 3.84Mcps / 7.68Mcps TDD UEs are feasible. Node B baseband processing complexity is approximately 30% greater than at 3.84Mcps, though other aspects of Node B complexity are similar at 3.84Mcps and 7.68Mcps. Node B and RNC throughput, buffering and interfaces need to be dimensioned to support a greater cell throughput and more active users at 7.68Mcps.

The feasibility study shows that 7.68Mcps TDD can be designed to be backwards compatible with other UTRA modes (when a 7.68Mcps TDD UE also implements at least one of the other UTRA modes). Mobility of a UE between a 7.68Mcps UTRAN and UTRANs for other UTRA modes has been shown to be feasible.

Introduction of a higher TDD chip rate will have impacts on RAN working groups and specifications. The working groups that are principally affected are RAN1 and RAN4. By and large, it is only the TDD aspects of these working groups that are affected. The specifications controlled by these working groups are impacted in a substantive way. Specifications controlled by RAN2, RAN3 and T1 are impacted to a lesser extent. Some signalling impacts have been identified in the study (related to signalling of parameters of the 7.68Mcps TDD system – number of channelisation codes, timing advance quantization etc.).

Annex A (normative): Link Level Simulation Assumptions

A.1 Description of Bearer Services

Both circuit-switched speech/data and HSDPA-like packet-switched bearer services shall be evaluated.

A.1.1 Release 99/4 Type

A.1.1.1 Speech, 12.2 kbps

The normative reference measurement channels of 25.102 [8] annex A2.2 (DL) and 25.105 [9] annex A2.1 (UL) shall be used for simulation purposes. The spreading factors for both uplink and downlink are double those used for the 3.84Mcps system. Note that burst type 1 is used for both link directions for this service.

A.1.1.2 Circuit Switched Data, 384 kbps

The normative reference measurement channels of 25.102 [8] annex A2.5 (DL) and 25.105 [9] annex A2.4 (UL) shall be used for simulation purposes. The spreading factors for both uplink and downlink are double those used for the 3.84Mcps system. Note that burst type 2 is used for both link directions for this service.

A.1.2 Release 5 Type (HSDPA)

A set of fixed-rate reference channels are simulated for HSDPA. These results are generated in order to enable mapping of a short-term channel quality metric to a probability of HS-DSCH transport block failure within a dynamic system-level simulation.

Interpolation between these fixed-rate reference channels is used to infer the performances of other transport block sizes and resource allocations within the dynamic system model.

The six fixed-rate reference channels of Table A.1 are defined for HSDPA simulation.

The physical resource allocation is the same for all of the six channels and is equal to 8 timeslots per 10ms TTI, each containing 4 codes at SF 32.

The redundancy and constellation version, $X_{rv}=\{0,0,0,0\}$ is used for all reference channels.

Table A.1 – Fixed-Rate Reference Channels for HSDPA Link Simulation

Fixed Reference Channel ID	Modulation Type	Burst Type	Available bits across allocated physical channels	Transport Block Size	Approximate Code Rate
1	QPSK	2	8832	2912 bits	1/3
2	QPSK	2	8832	4384 bits	½
3	QPSK	2	8832	6592 bits	¾
4	16 QAM	2	17664	5856 bits	1/3
5	16 QAM	2	17664	8800 bits	½
6	16 QAM	2	17664	13184 bits	¾

A.2 Applicable Propagation Channels

Results shall be obtained in the following propagation channel types for all bearer services:-

- AWGN
- ITU Indoor to Outdoor Pedestrian A, 3kmph
- ITU Indoor to Outdoor Pedestrian B, 3kmph
- ITU Vehicular A, 30kmph
- ITU Vehicular A, 120kmph

[Editor's note : The applicability of ITU Vehicular B to CS services is FFS]

A.3 Deployment Specifics

The following deployment-specific parameters are assumed (Table A.2) :-

Table A.2 – Deployment Specific Parameters for Link Simulation

Parameter	Value	Comments
Carrier Frequency	2000 MHz	
Chip Rate	7.68 Mcps	
Tx Antenna Diversity at Node-B	OFF	
Tx Antenna Diversity at UE	OFF	
Rx Antenna Diversity at Node-B	ON	2 antennas
Rx Antenna Diversity at UE	OFF	
Midamble Allocation Scheme, DL	Common Midamble	
Midamble Allocation Scheme, UL	UE-specific	
Cell ID	0	Alternating scrambling code 0/1
Kcell, burst type 1	8	
Kcell, burst type 2	8	For the 7.68Mcps system burst type 2 uses a 512 chip midamble constructed using a 456-long base sequence. Kcell = 4 and 8 are applicable.

A.4 Transmitter Assumptions

Transport channel processing for all bearer services shall comply with 25.222 [3].

The transmit filter shall consist only of an RRC filter with two-sided bandwidth 7.68MHz and roll-off factor α=0.22.

A.5 Propagation Channel Simulation Assumptions

The channel is simulated at 2 times oversampling with respect to the chip rate.

Channel tap delay positions are quantised to the nearest integer ½ chip position.

A randomly selected delay of 0 or 1 "½ -chips" (both being equi-probable) shall be added to the entire channel impulse response in order to include the effects of sub-chip receiver timing offset.

Doppler shall conform to Jakes spectrum.

A.6 Assumptions on Interference

A.6.1 Intra-cell

A.6.1.1 Downlink

It is assumed for circuit switched services that a total of 16 codes at SF 32 are transmitted each DL timeslot from the Node-B. This number comprises all codes allocated to the user of interest and all intra-cell interferers. This is in line with the highest interference level test scenarios of 25.102 [8] for demodulation of DCH for the equivalent 3.84Mcps system.

For HSDPA services, a higher code space loading is assumed with 24 codes at SF32 being transmitted from the Node-B.

The mean power of all transmitted SF32 codes is assumed to be the same. This leads to the following (Table A.3):-

Table A.3 – Interference Characteristics for Downlink Simulation

Simulated Bearer	**Number of SF32 Codes Occupied by Bearer per Timeslot**	**Number of Interfering Codes at SF32 per Timeslot**	**DPCH or HS-PDSCH** $\frac{E_c}{I_{or}}$	$\frac{DPCH_0\_E_c}{I_{or}}$	$\frac{\sum DPCH_0\_E_c}{I_{or}}$
12.2 kbps Speech	2	14	-12.04 dB	-12.04 dB	-0.58 dB
384 kbps Data	8	8	-12.04 dB	-12.04 dB	-3.01 dB
HSDPA Reference Channels	4	20	-13.8 dB	-13.8 dB	-0.79 dB

A.6.1.2 Uplink

The following scenarios (Table A.4) are considered for the uplink simulations. As for the downlink these are in line with the highest interference level test scenarios of 25.105 [9] for demodulation of DCH for the equivalent 3.84Mcps system. One half of the code space is occupied in total, comprising the user of interest and all intra-cell interferers.

Table A.4 – Interference Characteristics for Uplink Simulation

Bearer	**Resource Occupied by Bearer**	**Number and SF of Interfering Codes per Slot**	**DPCH** $\frac{E_c}{I_{or}}$	$\frac{DPCH_0\_E_c}{I_{or}}$	$\frac{\sum DPCH_0\_E_c}{I_{or}}$
12.2 kbps Speech	1xSF16, 1 TS	14xSF32	-9.03 dB	-12.04 dB	-0.58 dB
384 kbps Data	1xSF4, 3 TS's	8xSF32	-3.01 dB	-12.04 dB	-3.01 dB

A.6.2 Inter-cell

All inter-cell interference (I_{oc}) is assumed to be AWGN-like in nature for both uplink and downlink.

A.7 Receiver Assumptions

The following parameters (Table A.5) of relevance to the receiver shall be used:-

Table A.5 – Receiver Parameters for Link Simulation

Parameter	Value	Comments
Receiver channelisation filter	RRC	Identical to Tx pulse shaping filter
Channel estimation	Realistic, based on midamble	Joint channel estimation using cyclic correlation
Detection	Advanced receiver (eg: MMSE Multi-User Detection)	Only intra-cell signals are jointly detected
Soft Metric for Channel Decoding	LLR	Log Likelihood Ratio
LLR Generation	Ideal	The exact theoretical LLR mapping given an SNR estimate
SNR estimation for LLR generation	Realistic	Based either on midamble or data
Turbo Decoding	Max Log MAP, 4 iterations	

A.8 Power Control

A.8.1 Downlink

For 12.2kbps speech and 384kbps circuit-switched data bearer services, closed inner-loop TPC-based power control is enabled. Outer-loop (quality-based) power control is disabled.

For the 12.2kbps speech and 384kbps data services TPC detection errors are generated randomly with probability n% where "n" is derived from the TPC reliability results of the corresponding uplink simulations at the same data rate and separately for each propagation channel type. For both 12.2kbps and 384kbps circuit switched services, n is the probability of TPC error at 1% UL DCH BLER.

TPC is neither simulated nor employed for HSDPA services. All HS-PDSCH are transmitted with the same power.

A.8.2 Uplink

All uplink channels utilise open-loop inner-loop power control as described within 25.331 [10] section 8.5.7. The delay between the most recent beacon measurement and the uplink transmission is assumed to be 4 timeslots.

Outer-loop power control is disabled.

A.9 HSDPA Services

The following assumptions apply specifically to the HSDPA bearer services:-

- Chase combining is assumed for all six fixed-rate reference channels. However, actual combining need not be simulated at the link level. It is assumed that the benefits of H-ARQ using Chase combining are incorporated within the system level simulation. Incremental redundancy is not simulated at the link or system level.
- There are no detection errors made on the ACK/NACK field of the HS-SICH
- There are no detection errors made on the HS-SCCH

A.10 Numerical Accuracy

Floating point accuracy is assumed throughout the simulation.

A.11 Output Metrics

Metrics are recorded during the simulations for each simulated propagation channel model in order to generate the following results of interest for the system level simulation activity.

A.11.1 Speech (12.2kbps) and Circuit Switched Data (384kbps) Bearer Services

1. Plots of mean $\frac{\hat{I}_{or}}{I_{oc}}$ versus DCH BLER

2. Plots of mean $\frac{\hat{I}_{or}}{I_{oc}}$ versus TFCI and TPC reliabilities

3. PDF of the Node-B and UE timeslot transmit powers when meeting 1% DCH BLER. These powers are expressed relative to I_{oc} and assume a mean pathloss of 0 dB.

4. Histogram of the short-term $\frac{\hat{I}_{or}}{I_{oc}}$ (averaged over each TTI transmission period) versus probability of transport block failure.

A.11.2 HSDPA Bearer Services

1. Plots of mean $\frac{\hat{I}_{or}}{I_{oc}}$ versus probability of HS-DSCH transport block failure for first-time transmissions.

2. Histogram of the short-term $\frac{\hat{I}_{or}}{I_{oc}}$ (averaged over each TTI transmission period – ie: 8 timeslots) versus probability of HS-DSCH transport block failure for first time transmissions.

Annex B (normative): System Level Simulation Assumptions

B.1 General

Given that system level simulation tools and platforms differ between companies, very detailed definition of system level simulation assumptions is not feasible. System level simulations may be performed in a dynamic manner or in a quasi-static manner. In either case, the link level simulation results from Annex A may be used as an input to the system level simulations.

This annex contains a set of basic assumptions and parameters allowing some harmonization of results.

B.2 System Level Parameters

B.2.1 Antenna Pattern

The antenna pattern used for each sector, is specified as :

$$A(\theta) = -\min\left[12\left(\frac{\theta}{\theta_{3\,dB}}\right)^2, A_m\right], \quad \text{where} \quad -180 \le \theta \le 180,$$

where min[ ] is the minimum function, θ_{3dB} is the 3dB beamwidth (corresponding to θ_{3dB} = 70 degrees) , and A_m= 20 dB is the maximum attenuation.

B.2.2 Antenna Orientation

The antenna bearing is defined as the angle between the main antenna lobe centre and a line directed due east given in degrees. The bearing angle increases in a clockwise direction. Figure B.1 shows an example of the 3-sector 120-degree center cell site, with Sector 1 bearing angle of 330 degrees. Figure B.2 shows the orientation of the center cell (target cell) hexagon and its three sectors corresponding to the antenna bearing orientation proposed for the simulations. The main antenna lobe centre directions each point to the sides of the hexagon. The main antenna lobe centre directions of the 18 surrounding cells shall be parallel to those of the centre cell. Figure B.2 also shows the orientation of the cells and sectors in the two tiers of cells surrounding the central cell.

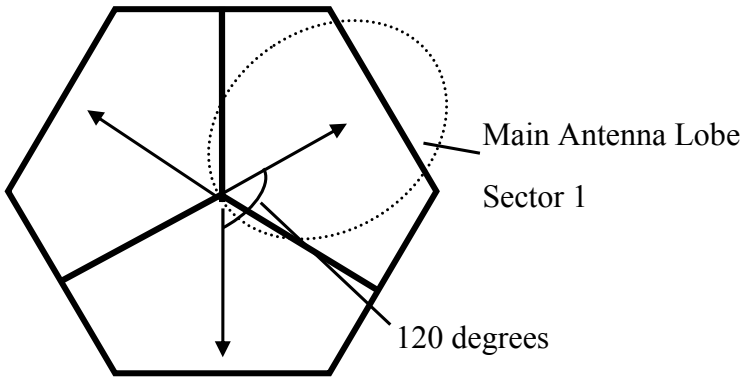

Figure B.1: Centre cell antenna bearing orientation diagram

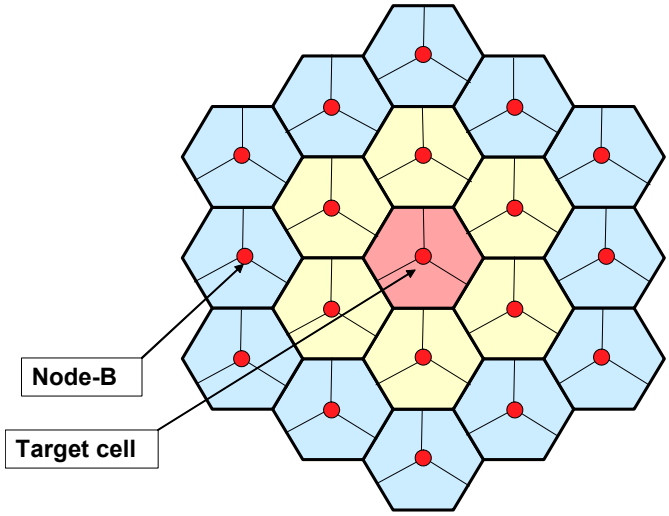

Figure B.2: Configuration of adjacent tiers of neighbouring cells, sectors, and Node-Bs

B.2.3 Common System Level Assumptions

The assumptions used in the system-level simulations that are common to Release 99/4 type and HSDPA type bearers are listed in Table B.1.

Table B.1 - Common system level simulation assumptions

Parameter	Explanation/Assumption	Comments
Cellular layout	Hexagonal grid, 3-sector sites	See Figure B.2
Antenna horizontal pattern	70 deg (-3 dB) with 20 dB front-to-back ratio	
Site to site distance	1000m	suburban deployment
Propagation model	$L = 128.1 + 37.6\ Log_{10}(R)$	R in kilometres
Slow fading	As modelled in UMTS 30.03, B 1.4.1.4	
Standard deviation of slow fading	8 dB	
Correlation between sectors	1.0	
Correlation between sites	0.5	
Correlation distance of slow fading	50 m	
BS antenna gain	14 dBi	
UE antenna gain	0 dBi	
UE noise figure	5 dB	
Thermal noise density	-174 dBm/Hz	
BS total Tx power	Up to 40 dBm	
BS noise figure	4 dB	
UE total transmit power	24dBm	
UE spatial distribution	Uniform random spatial distribution over elementary single cell hexagonal central Node-B	
Channel bandwidth	10MHz	
Frequency re-use	1	

It is assumed that the cells in the simulated configuration are synchronized such that all cells use the same timeslots for uplink and downlink and timeslot boundaries are synchronized in the network.

B.2.4 HSDPA specific simulation assumptions

The common system level assumptions of subclause 0 apply for HS-DSCH simulations. The system level assumptions that are specific to HS-DSCH channels are detailed in Table B.2.

Table B.2 - HS-DSCH specific system level simulation assumptions

Parameter	Explanation/Assumption	Comments
Power allocated to HS-DSCH in timeslot	100% of total cell power	
HSDPA TTI	10ms	
HARQ scheme	Chase combining	
Timeslot structure	according to Figure B.3.	
HS-SICH to HS-SCCH Node B turnaround	1 slot	
Feedback quality	Ideal	
HS-SCCH quality	Ideal	
CQI derivation	based on Ior_hat/Ioc in TTI	
Re-transmission priority	Maximum	
Scheduling	Proportional fair or round robin	
Maximum number of HARQ retransmissions	3	max 1 transmission and 3 re-transmissions per MAC-hs PDU

In the HS-DSCH system simulations, the scheduler shall schedule re-transmissions for UEs before it schedules initial transmissions to UEs. Re-transmissions are thus given the maximum priority by the scheduler.

The assumed frame structure for HSDPA related channels is shown in Figure B.3.

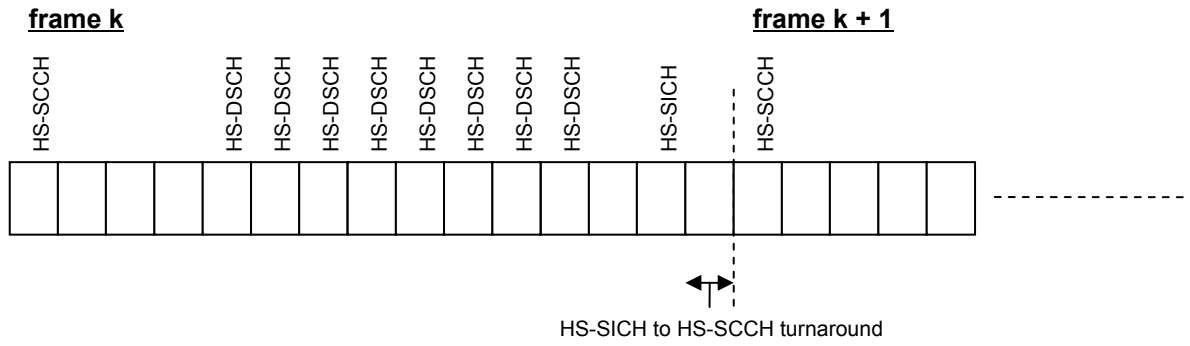

Figure B.3 - Frame structure for HS-DSCH system level simulations

B.2.4.1 Chase Combining assumptions

The Chase combining HARQ scheme shall be applied by the system simulator. A value $\hat{I}_{or}/I_{oc}\Big|_{comb}$ shall be maintained for each HARQ process of each UE in the system simulation. This value shall be reset to zero when the new data indicator bit is incremented for that UE. $\hat{I}_{or}/I_{oc}\Big|_{comb}$ shall be incremented by the amount $\hat{I}_{or}/I_{oc}\Big|_{inst}$ when there is a

(re)-transmission for that HARQ process (where $\left.\hat{I}_{or}/I_{oc}\right|_{inst}$ is an instantaneous value for the current TTI) . The probability of block error for the (re)-transmission is then read off the appropriate link level simulation curves for channel being simulated. This probability of block error is used to update the performance metrics.

Note that the method described here relates to symbol level Chase combining and allows the link level simulation results to be used to derive HARQ performance results.

B.2.4.2 CQI derivation assumptions

Following an HS-DSCH transmission, the system simulator shall derive a CQI for that UE based on the channel type, the $\left.\hat{I}_{or}/I_{oc}\right|_{inst}$ received by that UE, the link level simulation results and the BLER operating point for HS-DSCH. The system simulator shall base the MCS for retransmissions on the derived CQI value and may take account of the CQI value when scheduling UEs with HS-DSCH resources (according to the scheduler employed). For the purposes of scheduling, the system simulator may interpolate between the set of CQI values supported by the link level simulation results.

B.2.4.3 Size of allocations

The system simulator shall make HS-DSCH allocations with the code rates and modulations defined in Table A.8. The allocations shall span 8 timeslots. The number of codes in the allocation shall be an integer multiple of 2 (note that the link level results obtained in section A are derived using 4 code allocations, but are equally applicable to 2 code [and greater] allocations at the same code rate and modulation; at large transport block sizes, there is little variation in turbo decoder gain with transport block size). The performance of these allocations will be taken from the link level results as a function of code rate and modulation.

B.2.4.4 Scheduling Algorithms

Proportional fairness scheduling or round-robin scheduling may be applied. Other scheduling algorithms may be applied provided they are documented.

B.2.4.4.1 Proportional Fairness Scheduling

The proportional fairness (PF) scheduler shall be implemented as follows:

- At each time *n*, a priority function $P_i[n]$ is computed for each UE station *i*.
- The UE station *i* with the highest (largest) priority $P_i[n]$ is scheduled for the current time slot.

$P_i[n]$ is computed as follows:

$$P_i[n] = \frac{(DRR_i[n])^{\alpha}}{(T_i[n])^{\beta}}$$

where:

- n is the time (in TTIs)
- $DRR_i[n]$ is the data rate potentially achievable for UE station *i* at time *n* (computed using the CQI reported from the UE station). $DRR_i[n]$ is normalized to a 4 code, 8 timeslot allocation
- $T_i[n]$ is the average throughput served to this UE station up to time *n*
- α and β are indices used to control the scheduling fairness. The values normally used for simulation purposes here are $\alpha=\beta=1$. (Note that these two parameters can be varied to select a scheduling method anywhere between the two extremes of round-robin scheduling ($\alpha=0$, $\beta=1$) and maximum C/I scheduling ($\alpha=1$, $\beta=0$).)

$T_i[n]$ is computed as follows:

$$T_i[n] = \begin{cases} \lambda T_i[n-1] & \text{if MS } i \text{ was not scheduled at time } n\text{-1} \\ \lambda T_i[n-1] + (1-\lambda)\cdot N_i[n-1] & \text{if MS } i \text{ was scheduled } N_i[n\text{-1}] \text{ info bits at time } n\text{-1} \end{cases}$$

where $\lambda = 1 - \frac{10.0 \times 10^{-3}}{1.5}$, which corresponds to an IIR averaging time constant of 1.5 seconds.

Note that $N_i[n-1]$ is the number of information bits (payload bits) corresponding to an initial packet transmission occurring at TTI *n-1*. It is updated *only once* for the first transmission of a new packet since net throughput (goodput) is the quantity of interest.

B.2.4.4.2 Round Robin Scheduling

A round-robin (RR) scheduler is defined as a scheduler that cyclically allocates a TTI to each one of the UEs in order to transmit data signals without consideration of the packet quality (successful transmission or not) or the current channel quality (whether or not the UE is currently in a fade).

B.3 Traffic Models

B.3.1 Release 99 / 4 type bearers

Calls are created according to a Poisson process as a function of the system load in Erlangs. The call duration is exponentially distributed with a mean of 120 seconds.

B.3.2 Release 5 type bearers

The system level simulation for the higher chip rate reference configuration shall consider the traffic models detailed in the following subclauses (B.3.2.1 and B.3.2.2). Only system level simulations with homogenous traffic mixes shall be considered (all users in the simulation with have solely HTTP traffic or solely FTP traffic). There is no mixing of traffic types within a simulation.

The models in sections B.3.2.1 and B.3.2.2 assume that all UEs dropped are in an active packet session. A packet session consists of multiple packet calls (where "packet call" is defined in sections B.3.2.1 and B.3.2.2 for HTTP and FTP traffic respectively).

B.3.2.1 HTTP Traffic Model Characteristics

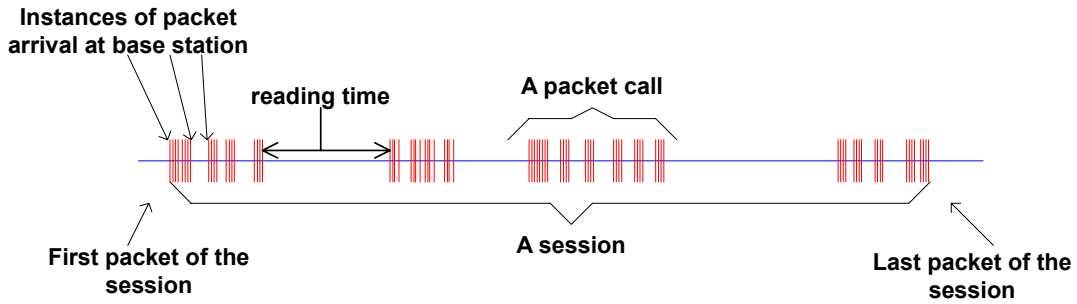

Figure B.4: Packet Trace of a Typical Web Browsing Session

Figure B.4 shows the packet trace of a typical web browsing session. The session is divided into ON/OFF periods representing web-page downloads and the intermediate reading times, where the web-page downloads are referred to as packet calls. These ON and OFF periods are a result of human interaction where the packet call represents a user's request for information and the reading time identifies the time required to digest the web-page.

As is well known, web-browsing traffic is self-similar. In other words, the traffic exhibits similar statistics on different timescales. Therefore, a packet call, like a packet session, is divided into ON/OFF periods as in Figure B.4. Unlike a packet session, the ON/OFF periods within a packet call are attributed to machine interaction rather than human interaction. A web-browser will begin serving a user's request by fetching the initial HTML page using an HTTP GET request. The retrieval of the initial page and each of the constituent *objects* is represented by ON period within the packet call while the parsing time and protocol overhead are represented by the OFF periods within a packet call. For simplicity, the term "page" will be used in this paper to refer to each packet call ON period.

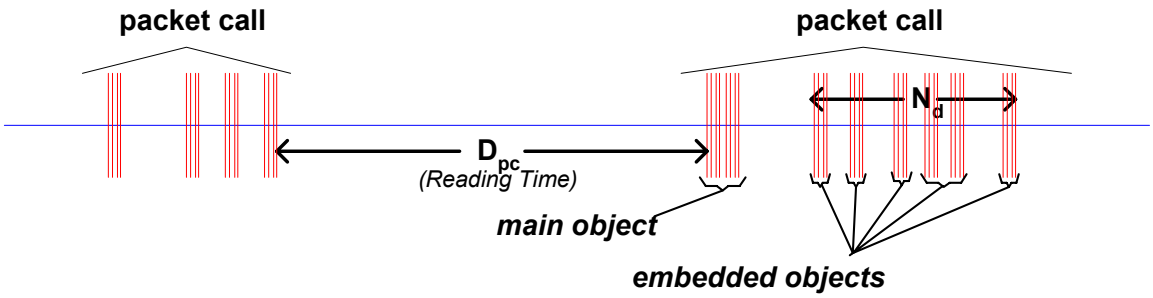

Figure B.5: Contents in a Packet Call

The parameters for the web browsing traffic are as follows:

- S_M: Size of the main object in a page
- S_E: Size of an embedded object in a page
- N_d: Number of embedded objects in a page
- D_{pc}: Reading time
- T_p: Parsing time for the main page

HTTP/1.1 persistent mode transfer is used to download the objects, which are located at the same server and the objects are transferred serially over a single TCP connection. The distributions of the parameters for the web browsing traffic model are described in Table B.3.

Table B.3: **HTTP Traffic Model Parameters**

Component	Distribution	Parameters	PDF
Main object size (S_M)	Truncated Lognormal	Mean = 10710 bytes Std. dev. = 25032 bytes Minimum = 100 bytes Maximum = 2 Mbytes	$f_x = \frac{1}{\sqrt{2\pi}\sigma x}\exp\left[\frac{-(\ln x-\mu)^2}{2\sigma^2}\right], x \geq 0$ $\sigma = 1.37, \mu = 8.35$
Embedded object size (S_E)	Truncated Lognormal	Mean = 7758 bytes Std. dev. = 126168 bytes Minimum = 50 bytes Maximum = 2 Mbytes	$f_x = \frac{1}{\sqrt{2\pi}\sigma x}\exp\left[\frac{-(\ln x-\mu)^2}{2\sigma^2}\right], x \geq 0$ $\sigma = 2.36, \mu = 6.17$
Number of embedded objects per page (N_d)	Truncated Pareto	Mean = 5.64 Max. = 53	$f_x = \frac{\alpha k^{\alpha}}{x^{\alpha+1}}, k \leq x < m$ $f_x = \left(\frac{k}{m}\right)^{\alpha}, x = m$ $\alpha = 1.1, k = 2, m = 55$ Note: Subtract k from the generated random value to obtain N_d
Reading time (D_{pc})	Exponential	Mean = 30 sec	$f_x = \lambda e^{-\lambda x}, x \geq 0$ $\lambda = 0.033$
Parsing time (T_p)	Exponential	Mean = 0.13 sec	$f_x = \lambda e^{-\lambda x}, x \geq 0$ $\lambda = 7.69$

B.3.2.2 FTP Traffic Model Characteristics

In FTP applications, a session consists of a sequence of file transfers, separated by *reading times*. The two main parameters of an FTP session are:

1. S : the size of a file to be transferred
2. D_{pc}: reading time, i.e., the time interval between end of download of the previous file and the user request for the next file.

The underlying transport protocol for FTP is TCP. The model of TCP connection described in Section B.3.2.1 will be used to model the FTP traffic. The packet trace of an FTP session is shown in Figure B.6.

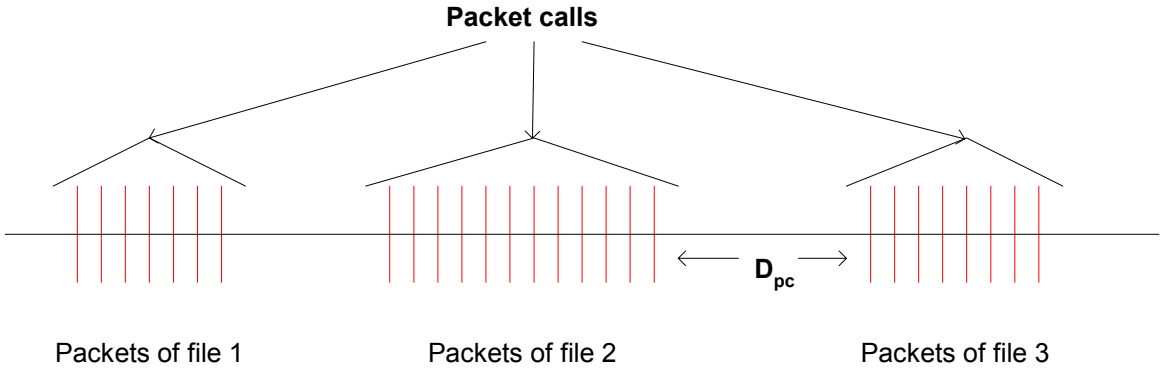

Figure B.6: Packet Trace in a Typical FTP Session

The parameters for the FTP application sessions are described in Table B.4.

Table B.4: FTP Traffic Model Parameters

Component	Distribution	Parameters	PDF
File size (S)	Truncated Lognormal	Mean = 2Mbytes Std. Dev. = 0.722 Mbytes Maximum = 5 Mbytes	$f_x = \frac{1}{\sqrt{2\pi}\sigma x}\exp\left[\frac{-(\ln x-\mu)^2}{2\sigma^2}\right], x \geq 0$ $\sigma = 0.35, \mu = 14.45$
Reading time (D_{pc})	Exponential	Mean = 180 sec.	$f_x = \lambda e^{-\lambda x}, x \geq 0$ $\lambda = 0.006$

Based on the results on packet size distribution, 76% of the files are transferred using an MTU of 1500 bytes and 24% of the files are transferred using an MTU of 576 bytes. For each file transfer a new TCP connection is used whose initial congestion window size is 1 segment (i.e. MTU).

B.3.3 Channel Models

Simulations shall be performed with a mix of channel models within the cell. When a mix of channel models are applied within a cell, UEs shall be randomly assigned channel types with the probabilities defined in Table B.5.

Table B.5 – Probability distribution for assignment of channel models

Channel	probability
AWGN	0.2
ITU Ped A : 3kmph	0.3
ITU Ped B : 3kmph	0.3
ITU Veh A : 30kmph	0.15
ITU Veh A : 120kmph	0.05

Simulations may also be performed with a homogeneous channel model for the entire cell (the channel model for each UE in the cell shall be the same). In this case, results shall be derived for the channels models defined in annex A.

B.4 Output Metrics

B.4.1 Release 99 / 4 type bearers

B.4.1.1 Definitions

B.4.1.1.1 Satisfied User

A satisfied user for a circuit switched service is defined as follows :

1. the user is not blocked when arriving onto the system
2. over both directions of the entire call together, $BLER > BLER_{threshold}$ for less than $x_1\%$ of the transport blocks.
3. the user's call is not dropped during the call. A call is dropped if, in either direction of a call, $BLER > BLER_{threshold}$ in every TTI for more than t_{drop} seconds

B.4.1.1.2 System Load

The system load is measure in [kbps/cell]

The system load v_{cs} is derived as follows :

$$v_{cs} = \omega_{cs} \times \text{user\_bitrate}$$

where ω_{cs} is the average number of (simultaneous) circuit switched users per cell, i.e. the offered load (Erlangs)

B.4.1.1.3 Cell Operating Load

The cell operating load is defined as the system load where there are exactly x_2 % satisfied users.

B.4.1.1.4 Parameters definitions

The default values for the parameters defined in subclause 0 are defined in Table B.6.

Table B.6 - Parameter values definitions for CS system simulations

Parameter	Name / description	Value
x_1	Bad quality probability threshold	$x_1\%$ = 5%
$BLER_{threshold}$	Block error rate threshold for DPCH	1%
t_{drop}	Dropping time-out, circuit switched	5 seconds
x_2	Threshold for ratio of satisfied users	$x_2\%$ = 98%

B.4.1.2 Performance Metrics for Release 99/4 type bearers

System level performance metrics should be derived using homogeneous bearer services (i.e. there should not be a mix of 12.2kbps and 384kbps bearer services in the cell). Performance metrics shall be collected for the centre cell only of the hexagonal grid of cells defined in subclause 0.

The following performance metrics are defined :

1. **Blocking probability** is the probability that a user is not allowed onto the system. Graphs of blocking probability against system load shall be plotted.

2. **Number of satisfied users** is defined as the number of satisfied users in a cell where a "satisfied user" is defined in subclause **Error! Reference source not found.** (this metric takes account of call blocking, call dropping and call quality). Graphs of number of satisfied users against system load shall be plotted.

The cell operating load may be stated as a summary of the performance.

B.4.2 Release 5 type bearers

The following statistics related to data traffic should be generated. Separate sets of statistics should be collected as the number of UEs per cell is varied.

The following statistics related to data traffic should be generated as system level simulation results.

1. **Average cell throughput [kbps/cell]** is used to study the network throughput performance, and is measured as

$$R = \frac{b}{3 \cdot T}$$

where b is the total number of correctly received data bits in all data UEs in the simulated system over the whole simulated time and T is the simulated time.

The average cell throughput is calculated for the centre cell site only (consisting of 3 sectors).

2. **Average packet call throughput [kbps]** for user *i* is defined as

$$R_{pktcall}(i) = \frac{1}{K}\sum_{k=1}^{K}\frac{\text{good bits in packet call k}}{(t_{end\_k} - t_{arrival\_k})}$$

where k denotes the k^{th} packet call from a group of K packet calls where the K packet calls can be for a given user i , $t_{arrival\_k}$ = time that first packet of packet call k arrives in queue, and t_{end_k} = time that last packet of packet k is received by the UE. Note for uncompleted packet calls, t_{end_k} is set to simulation end time. The mean, standard deviation, and distribution of this statistic are to be provided. The term "packet call" is defined in Figure B.5 for HTTP traffic and Figure B.6 for FTP traffic.

3. **The averaged packet delay per sector** is defined as the ratio of the accumulated delay for all packets for all UEs received by the sector and the total number of packets. The delay for an individual packet is defined as the time between when the packet enters the queue at the transmitter and the time when the packet is received

successfully by the UE. If a packet is not successfully delivered by the end of a run, its ending time is the end of the run.

4. **Number of satisfied users**
   A user is considered to be satisfied if an average of less than x_3 % of their MAC-hs PDUs cause an RLC retransmission due to the maximum number of HARQ retransmissions being exceeded.

Parameter values that shall be applied for the performance metrics of Release 5 type bearers are specified in Table B.7.

Table B.7 – Parameter values for performance metrics of Release 5 type bearers

Parameter	Name / description	Value
x_3	Threshold ratio of MAC-hs PDUs that cause an RLC retransmission	x_3 % = 0.01%

Annex C (informative):

Change History

Change history							
Date	**TSG #**	**TSG Doc.**	**CR**	**Rev**	**Subject/Comment**	**Old**	**New**
2002-10	RAN1#28 bis				Initial draft presented for discussion		0.0.0
2002-11	RAN1#29				Updated based on comments received in RAN1#28bis	0.0.0	0.0.1
2003-01	RAN1#30				Updated based on approved Tdocs in RAN1#29.	0.0.1	0.1.0
2003-02	RAN1#31				Updated based on approved Tdocs in RAN1#30	0.1.0	0.2.0
2003-02	RAN1#31				Updated based on approved Tdocs and comments in RAN1#31	0.2.0	0.2.1
2003-03	RAN#19				Version updated to v1.0.0 for presentation to RAN	v0.2.1	v1.0.0
2003-06	RAN1#32				Updated based on approved Tdocs in RAN1#32 and RAN4#27	v1.0.0	v1.0.1
2003-06	RAN1#32				Acceptance of changes	v1.0.1	v1.1.0
2003-06	RAN1#33				Version number updated after of v1.1.0 approval in RAN1	v1.1.0	v1.2.0
2003-09	RAN1#33				Updated based on approved Tdocs in RAN1#33	v1.2.0	v1.2.1
2003-10	RAN1#34	R1-031059			Text Proposal for HSDPA System Simulation Results for TR25.895	v1.2.1	v1.2.2
2003-10	RAN1#34	R1-031060			Link level results for Release 99 channels for higher chip rate TDD SI	v1.2.1	v1.2.2
2003-11	RAN1#35	R1-031287			Text Proposal on UE complexity for higher chip rate TDD SI	v1.2.2	v1.3.0
2003-11	RAN1#35	R1-031289			Text Proposal on UTRAN complexity for higher chip rate TDD SI	v1.2.2	v1.3.0
2003-11	RAN4#29	R4-031018			Coexistence with existing UTRA releases Text Proposal for TR 25.895	v1.3.0	v1.3.1
2004-02	RAN1#36	R1-040247			Corrections to TR25.895	v1.3.1	v1.3.2
2004-02	RAN4#30	R4-040062			UE Radio Complexity Aspects for Higher Chip Rate TDD SI	v1.3.1	v1.3.2
2004-02	RAN4#30	R4-040063			FDD/TDD Coexistence with existing UTRA releases - Text Proposal for TR 25.895 (with purely editorial corrections)	v1.3.1	v.1.3.2
2004-02	RAN4#30	R4-040065			Use of higher chip rate TDD in diverse spectrum arrangements and allocations	v1.3.1	v1.3.2
2004-05	RAN4#31	R4-040172			Corrections to TR25.895	v1.3.2	v1.3.3
2004-05	RAN4#31	R4-040174			Impact of Higher Chip Rate on Link Budget	v1.3.2	v1.3.3
2004-05	RAN4#31	R4-040346			TDD/TDD Macro Coexistence with Lower Chip Rate TDD Systems	v1.3.2	v1.3.3
2004-05	RAN1#37	R1-040640			Impact on specifications for higher chip rate TDD SI rev1	v1.3.2	v1.3.3
2004-05	RAN1#37	R1-040584			Link level results for Release 99 channels for higher chip rate TDD SI	v1.3.2	v1.3.3
2004-05	RAN1#37	R1-040585			Dual Mode UE Complexity Aspects of Higher Chip Rate TDD	v1.3.2	v1.3.3
2004-05	RAN1#37	R1-040586			Impact on other working groups for higher chip rate TDD SI	v1.3.2	v1.3.3
2004-05	RAN1#37	R1-040588			Signalling impact for higher chip rate TDD SI	v1.3.2	v1.3.3
2004-05	RAN1#37	R1-040589			Antenna Systems Aspects for Higher Chip Rate TDD SI	v1.3.2	v1.3.3
2004-05	RAN1#37	R1-040590			Feasibility of higher TDD chip rates than 7.68Mcps	v1.3.2	v1.3.3
2004-08	RAN1#38				Document number incremented for presentation to RAN1#38	v1.3.3	v1.3.4
2004-08	RAN1#38				V1.3.4 approved and version number incremented to v1.4.0	v1.3.4	v1.4.0
2004-08	RAN1#38	R1-041027			System Simulation Results for Release 99 type bearers for TR25.895	v1.4.0	v1.4.1
2004-08	RAN1#38	R1-041043			Application to 3GPP systems are services	v1.4.0	v1.4.1
2004-08	RAN1#38	R1-041044			Text proposal for conclusion to TR25.895	v1.4.0	v1.4.1
2004-09	RAN#25	RP-040361			Document number updated for approval of TR by RAN	v1.4.1	v2.0.0